THE PETROLOGY OF OLIVINE-RICH BASALTIC

ROCKS, NUANETSI, RHODESIA.

by

BRIAN G. JAMIESON, B.Sc.

Thesis presented for the Degree of Doctor of Philosophy

of the University of Edinburgh in the Faculty of Science.

1969

ABSTRACT

The Karroo volcanic succession in the Nuanetsi Igneous Province of southeastern Rhodesia is 22,000 - 26,000 feet thick. The lowest 6,500 feet of this succession comprises the Olivine-rich Group - a distinctive series of tholeiitic lavas and hypabyssal intrusions which are rich in olivine and which frequently have glassy groundmasses. Preliminary chemical analyses of these basalts, limburgites and picrites indicated (a) that these rocks were rich in K_2O and certain trace elements and (b) that the relationship between the Olivine-rich Group and the overlying low-MgO Upper Basalts was not a direct one involving the fractionation of the phenocryst phases found in the lavas.

A mineralogical study indicates that the rare, magnesian (En_{90-80}), orthopyroxene phenocrysts, which occur in half the rocks examined, and the rare, magnesian (Fo_{92-78}), olivine megacrysts are an inherited assemblage. This is supported by a consideration of the bulk compositions of the 56 rocks analysed in this study and possible phase relations in a natural basaltic system. It is suggested that this inherited phenocryst assemblage may have crystallised under 7-10 kb. pressure. However, the compositional variation displayed by the suite of rocks cannot be fully accounted for by this proposed fractional crystallisation event alone.

The whole-rock chemical analyses confirm the high-MgO nature of the rocks and that they contain normative hy. It is concluded that this picritic character was an inherent feature of the magmas and does not reflect near-surface accumulation of olivine phenocrysts in more evolved tholeiitic magmas, cf. Hawaiian picrites. Only limited low-

pressure differentiation by crystal-liquid fractionation appears to have taken place and the effects of this are largely restricted to the hypabyssal holocrystalline picrites.

The richness of K and the associated elements P, Ti, Ba, Sr, Rb and Zr is confirmed by the whole-rock analyses. There is also an intriguing, and statistically highly significant, sympathetic relationship between MgO and K and associated elements.

The degrees of enrichment of K and associated elements in these high-MgO tholeiites and possible enrichment processes are discussed at considerable length. It is proposed that the fractionation of eclogite from primary magmas at pressures of c. 40 kb. may account for the high enrichment levels and the sympathetic relationship with MgO.

Finally, a tentative polybaric evolutionary model for the Nuanetsi high-MgO magmas is proposed. The main features are, (a) the fractionation of eclogite at high pressure - c. 40 kb. (b) the fractionation of harzburgite in the pressure range 7-10 kb. and (c) rapid ascent to the surface from c. 30 km. depth accompanied by a minimum of crystal-liquid fractionation, and hence differentiation.

CONTENTS

CHAPTER 1

INTRODUCTION

The geographical and geological settings of the Nuanetsi olivine-rich tholeiites are described and the main objectives of the research project are defined.

The Nuanetsi Igneous Province

The Nuanetsi Igneous Province is situated in the extreme south-east of Rhodesia (see Fig. 1). The geology of this area was studied in considerable detail by members of the Research Institute of African Geology, University of Leeds, during the period 1956 - 1959. The combined results of this work were published in 1965 (Cox et al).

The general geology of the Nuanetsi Igneous Province and the surrounding area is given in Fig. 1. Karroo sediments, frequently less than 500' thick, unconformably overlie the gneissose Basement Complex. Overlying these sediments is a thick series of late - Karroo basic and acidic lavas; the maximum thickness of this volcanic series has been estimated at 22,000 - 26,000 ft. (Cox et al, 1965, p.85). The lavas have been intruded by a number of ring complexes and a large granophyric sheet - the Main Granophyre.

Whole-rock Rb/Sr age determinations by Manton (1968) indicate that the rhyolitic lavas, which occur in the upper parts of the volcanic succession, were erupted 206 ± 13 m. yrs. ago, i.e. during the very late Triassic. Granites from the ring complexes gave ages of 177 ± 7 m. yrs., i.e. early Jurassic.

The two main structural elements of the Nuanetsi Igneous Province

FIGURE 1

General geology of the Nuanetsi Igneous Province and
surrounding areas.

The area included in the main figure is stippled
in the inset figure.

(after Cox et al, 1965, Fig. 1).

N

20 MI.

Fort Victoria

Triangle

Nuanetsi R.

Lundi R.

Bubye R.

MATEKE - SABI MONOCLINE

Nuanetsi

TULI SYNCLINE

NUANETSI SYNCLINE

Beitbridge

Messina

Limpopo R.

LEBOMBO MONOCLINE

Sabi R.

A
A
A

A

Zambia

Rhodesia

Botswana

Mozambique

South Africa

Lesotho
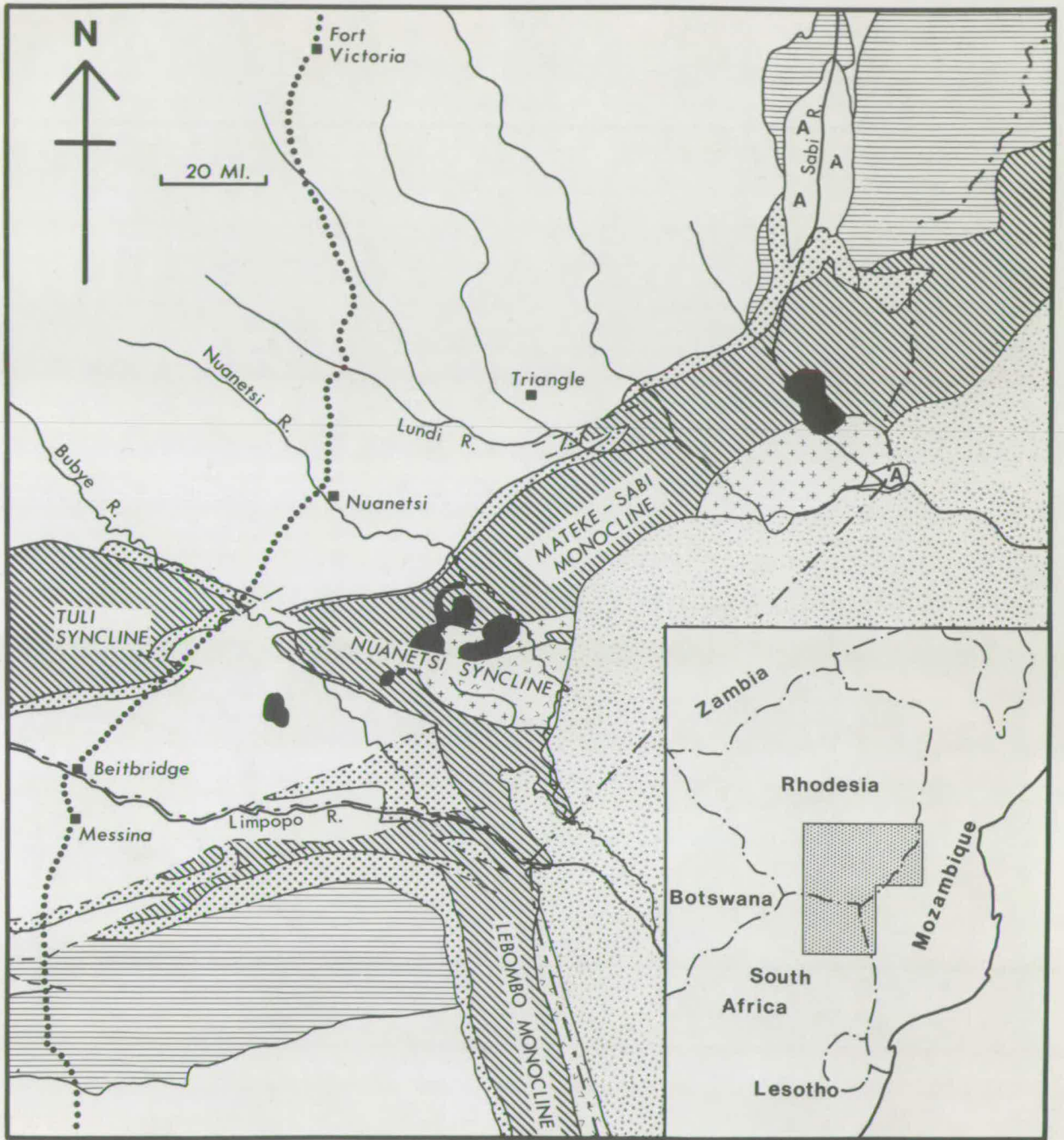
KEY

CRETACEOUS

RING COMPLEXES

MAIN GRANOPHYRE

RHYOLITE

BASALT

KARROO IGNEOUS ROCKS

KARROO SEDIMENTS

WATERBERG, UMKONDO

BASEMENT

A   ALLUVIUM

FAULT

ROAD

INTERNATIONAL BOUNDARY

I

are the Mateke-Sabi monocline and the Nuanetsi syncline.   The latter
feature is up to 35 miles wide - judging by present-day outcrop
patterns.   Cox et al (1965) considered that deformation of this syncline
was contemporaneous with much of the volcanic and intrusive igneous
activity.

On a broader scale, the Nuanetsi Igneous Province is a part of
the huge late and post-Karroo magmatic event, the results of which are
preserved in many areas of southern Africa.   The main expression of
this event was volcanic and from the Nuanetsi area the outcrop of lavas
continues in a north-easterly direction towards Mozambique and Malawi
and southwards into the Lebombo monocline of Mozambique, Swaziland and
the Republic of South Africa.   Outcrop in a westerly direction is
discontinuous, through the shallow Tuli Syncline, to Botswana.   Cox
et al (1967, Fig. 1) have illustrated all the significant outcrops of
Karroo lavas in southern Africa.   General accounts of Karroo volcanicity
have been given by du Toit (1954) and Haughton (1963).

The Volcanic Succession

The volcanic succession of the Nuanetsi syncline was divided by
Cox et al (1965) into 3 units.   They are, in stratigraphic order :

	feet
Rhyolites, with subordinate basalts	5,500
Upper Basalts, tholeiitic and essentially olivine-free	10,000
Olivine-rich Group	6,500

The figures are estimates of the maximum thickness each unit attains
in the Nuanetsi syncline.   No rhyolites are exposed in the Mateke-Sabi
monocline.   However, this may simply be a result of the overlap by the
post-Karroo sediments - the Malvernia Beds.   The approximate boundary

between the lower Olivine-rich Group and the Upper Basalts is shown in
Fig. 2.   In general, the Olivine-rich Group is restricted to the
northern and southern limbs of the Nuanetsi syncline and the Mateke-
Sabi monocline.   Because of the stratigraphic level exposed, in the
east, and the westerly overlap by the Upper Basalts, in the west, few
olivine-rich rocks have been recorded in the axial parts of the syncline.

A detailed petrological study of the Olivine-rich Group is the
subject of the current research.

The Olivine-rich Group

(i) Previous research

Lightfoot (1938) described a reconnaissance geological trip to
the area between the Nuanetsi and Lundi Rivers in south-east Rhodesia.
He recorded the occurrence of coarse-grained picrite - 'olivine gabbro' -
at the base of the volcanic succession and presented a chemical analysis
of the rock.   The analysis is given in Table 1.   The picrite was
collected from 'a small escarpment' and Lightfoot observed that 'the
composition and non-vesicular character of the rock combined with its
coarse grain is more suggestive of a basic sill'.   On the basis of this
description and the analysis (Table 1) it is certain that this specimen
came from what is now known as the Beacon sill.

Cox et al (1965) established the areal distribution of the Olivine-
rich Group (see Fig. 2).   On petrographic grounds they divided the rocks
into limburgites, with abundant glass and no feldspar, olivine basalts
and picrite-basalts which are frequently glassy, and picrites.   The latter
are relatively coarse-grained and are holocrystalline.   They are especially
common in the Beacon - Gomakwe area and were thought to represent
hypabyssal intrusions, both sills and dykes, closely associated with the

<u>Geology of the Nuanetsi Igneous Province.</u>

Localities referred to in the text and in Appendix
A are shown.

KEY
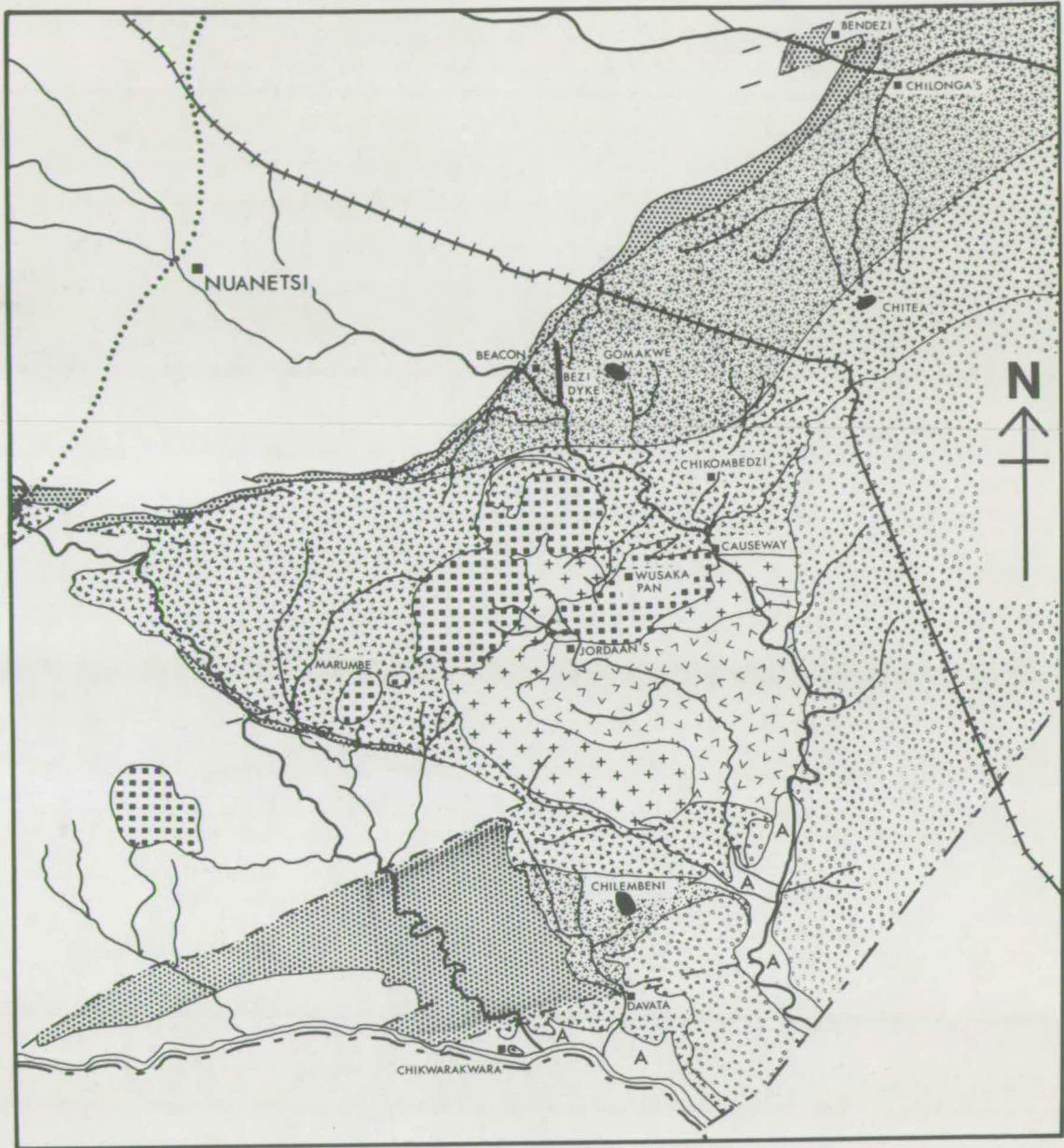
`A`	ALLUVIUM		RING COMPLEXES			KARROO SEDIMENTS
	CRETACEOUS		MAIN GRANOPHYRE			BASEMENT
			INTRUSIVE PICRITES, ETC	KARROO		
·····	ROAD		RHYOLITES	IGNEOUS		FAULT
┼┼┼┼	RAILWAY		UPPER BASALTS	ROCKS		10 MI.
·–·–·	INTERNATIONAL BOUNDARY		OLIVINE – RICH GROUP			

2

lavas.   Many of these holocrystalline rocks were found to contain
alkali feldspar in addition to plagioclase.   Seven new chemical analyses
were carried out.   These are given in Tables 1 and 2.   The C.I.P.W.
norms of the analyses (Table 3) show varying amounts of _hy_ - the rocks
are, therefore, tholeiitic as defined by Yoder and Tilley (1962) and
Tilley and Muir (1967).

Both Cox _et al_ (1965) and Monkman (1961) pointed out that the
rocks of the Olivine-rich Group, despite an overall thoroughly basic
character, had relatively high contents of SiO_2, K_2O, TiO_2, P_2O_5, Ba,
Sr and Zr.   Monkman carried out a further 5 partial analyses - for
K_2O, Na_2O and TiO_2 - which confirmed that the contents of K_2O and TiO_2
and the K/Na ratio of the olivine-rich rocks are higher than in most
basic rocks.   He compared the geochemistry of the Nuanetsi rocks with
that of the volcanic rocks of the Birunga - Bufumbira area of S.W.
Uganda and the Congo which have been described by Holmes (1950) and
Higazy (1954).

In a complementary manner, Cox _et al_ (1965) contrasted the
geochemistry of the Nuanetsi - northern Lebombo basic rocks (both the
olivine-rich types and the overlying Upper Basalts) with the geochemistry
of the Karroo dolerites and lavas of South Africa and Lesotho.   The
basic rocks of these two southern areas, although broadly contemporaneous
with the Nuanetsi volcanic rocks, have much lower contents of K_2O, TiO_2
and P_2O_5 and a higher Al_2O_3 content.

Since the current research was started Cox _et al_ (1967) have
published a paper which emphasises the contrasting geochemical aspects
of Karroo basic lavas in southern Africa.   Two geochemical provinces
were defined, the Nuanetsi basic rocks belonging to the northern province
which is characterised by high K_2O, TiO_2, P_2O_5, Ba, Sr and Zr.

TABLE 1

LITERATURE ANALYSES

Wt.%	LM 428	LM 432	LM 434	KC 37	LM 593	KC 42	C 888	L
SiO_2	49.11	48.98	49.61	49.58	43.89	44.97	46.59	45.00
TiO_2	2.99	3.34	3.54	2.87	1.54	1.48	2.83	2.06
Al_2O_3	9.39	7.74	11.28	9.17	5.51	5.74	5.89	5.13
Fe_2O_3	1.83	3.75	2.13	2.47	6.50	3.45	3.54	3.52
FeO	7.90	6.53	10.11	8.49	7.32	10.18	8.31	10.35
MnO	0.14	0.13	0.18	0.15	0.17	0.18	0.16	0.17
MgO	12.84	15.52	7.67	14.82	25.53	24.15	21.00	23.06
CaO	7.18	6.44	9.66	7.36	4.51	6.26	5.79	6.64
Na_2O	2.31	1.40	2.37	2.07	0.81	0.91	1.37	1.06
K_2O	1.42	2.44	1.83	1.98	0.59	0.75	1.97	1.60
P_2O_5	0.83	0.54	0.52	0.52	0.28	0.23	0.46	0.15
H_2O^+	3.59	2.36	0.80	0.52	2.77	0.87	1.76	1.25
H_2O^-	0.62	0.91	0.42	0.18	0.56	0.29	0.10	0.19
Cr_2O_3	-	-	-	-	-	-	0.19	-
NiO	-	-	-	-	-	-	-	0.14
S	-	-	-	-	-	-	-	0.08
CO_2	-	-	-	-	-	0.50	-	-
Total	100.15	100.08	100.12	100.18	99.98	99.96	99.96	100.40

Key to analyses presented below Table 3.

TABLE 2

LITERATURE ANALYSES

ppm.	LM 434
Ba	700
Be	10
Co	45
Cr	—
Ga	30
Ge	30
La	100
Li	5
Mo	3
Nb	50
Ni	300
Pb	25
Sc	10
Sr	700
Ta	300
V	300
Y	60
Zr	450

All analyses by optical spectrograph.

Key to analysis presented below Table 3.

TABLE 3

C.I.P.W. NORMS OF LITERATURE ANALYSES

Wt.%	LM 428	LM 432	LM 434	KC 37	LM 593	KC 42	C 888	L
or	8.35	14.47	10.57	11.69	3.34	4.45	11.7	9.6
ab	19.40	12.06	19.92	17.30	6.82	7.86	11.5	9.1
an	11.13	7.51	15.02	10.01	9.73	9.17	4.7	4.6
di	15.09	16.40	23.77	18.16	8.30	14.58	16.9	22.1
hy	28.10	30.55	17.64	18.65	31.03	21.56	18.1	5.9
ol	3.64	2.91	0.97	13.40	24.33	32.57	24.2	39.4
mt	2.55	5.33	3.01	3.47	9.49	5.10	5.1	5.2
il	5.61	6.37	6.68	5.46	2.88	2.89	5.3	4.0
ap	2.02	1.34	1.34	1.34	0.67	0.34	1.0	0.4
cc	-	-	-	-	-	0.50	-	-
H_2O	-	-	-	-	3.33	1.16	1.9	1.4

KEY to Analyses in Tables 1 - 3.

LM 428 :   Limburgite, (Cox et al, 1965, Table 9)

LM 432 :   Limburgite, (Cox et al, 1965, Table 9)

LM 434 :   Olivine basalt, erroneously described as limburgite by
                      Cox et al.(1965, Table 9)

LM 593 :   Picrite, (Cox et al, 1965, Table 12)

KC 37 :   Limburgite, (Cox et al, 1965, Table 9)

KC 42 :   Picrite, (Cox et al, 1965, Table 12)

C 888 :   Picrite, (Cox et al, 1965, Table 12)

L   :   Olivine Gabbro, (Lightfoot, 1938, p.195)

Cox et al (1965) considered the petrogenesis of the Nuanetsi volcanic succession. With the aid of an addition-subtraction variation diagram these authors were able to demonstrate convincingly that low-pressure crystal-liquid fractionation of one parental magma could not account for the recorded compositional variation of the basic rocks - from the limburgites and basalts of the Olivine-rich Group to the olivine-poor and Q normative basalts which are typical of the Upper Basalts. They stated :

> 'It must be concluded that whatever the Tholeiitic Series /of lavas7 represents, it does not represent a crystallisation-differentiation trend caused entirely by the separation or concentration of the minerals actually present in the lavas.' (Cox et al, 1965, p. 208).

The relationship between the olivine-rich and olivine-free Nuanetsi lavas, therefore, differs from the direct relationship observed between the picritic and olivine-free basalts of Hawaii - the picrites representing olivine basalt magma which has become enriched in cumulus olivine; the olivine-free basalts representing residual liquid magmas (Macdonald, 1944; Muir et al, 1957; Powers, 1955).

Of the possible causes of variation of the basaltic compositions which were considered by Cox et al, varying degrees of mantle partial melting was thought to be the most likely factor. The voluminous Upper Basalts were taken to be the normal products of partial melting of an ultrabasic mantle and it was proposed that the lavas of the Olivine-rich Group were the result of more complete fusion of the mantle.

Eclogite fractionation at elevated pressures and zone-refining (Harris, 1957) were suggested as possible causal factors of the observed

high contents of K_2O and certain trace elements.

To summarise, previous research has established in the Nuanetsi Igneous Province:

(a) the occurrence of an Olivine-rich group of lavas and minor intrusions, of maximum thickness 6,500', in the lower parts of the Karroo volcanic succession of Nuanetsi,

(b) that the rocks are frequently glassy, may contain no feldspar and contain up to 50% olivine (generally 15 - 30%),

and preliminary chemical analyses indicate :

(c) that the rocks of the Olivine-rich Group are rich in hy and contain relatively high contents of K_2O, TiO_2, P_2O_5 and possibly Ba, Sr and Zr and have a high K/Na ratio,

(d) that the relationship between the Olivine-rich Group and the overlying thick Upper Basalts is not a direct one which involves the fractionation of the phenocryst phases found in the lavas.

(ii) Current research

In view of the implications of the two features indicated by the existing analyses, it was decided that the primary objectives of the current research should be an investigation of :

(a) the apparently unusual geochemistry of the olivine-rich rocks,

(b) the status and history of the magmas from which the olivine-rich rocks crystallised.

It was considered that a detailed petrochemical study of the Olivine-rich Group, supplemented by petrographic and mineralogical studies should elucidate the significance of these features.

On a more general scale, it was hoped that the results of the current research might have some bearing on the origin and evolution of basic magmas in general and our knowledge and understanding of the Karroo volcanic event.

Fieldwork was carried out during the period July - October, 1964 and consisted of collecting samples of the entire Nuanetsi volcanic succession. Thin sections of 300 specimens were examined in the laboratory and 71 of these were selected for chemical analysis; selection being on the basis of freshness and sampling the range of petrographic types.

Plan of the Thesis

The text consists of the presentation of data, the interpretation and discussion of the data and conclusions. Only data which are relevant to the primary objectives of the research are included in the text. Other analytical data are given in Appendix C; all methods of analysis are described in Appendix B and descriptions of the analysed specimens are given in Appendix A.

CHAPTER 2

PETROGRAPHY AND ROCK CLASSIFICATION

The salient petrographic features of the Nuanetsi olivine-
rich lavas are described.   The classification scheme which is adopted
is based on the phenocryst assemblages and the nature of the groundmass
phases.   The use of the rock name 'limburgite' is discussed.

Main Petrographic Features

As Cox et al (1965, pp. 130-138) have already outlined the
petrography of the Olivine-rich Group, only those features which
characterise the Group are described below.

(i) Olivine content

A high modal content of olivine is a conspicuous feature of
these rocks.   Modal analysis of 41 specimens, which are thought to be
from lava flows, indicates the average content of olivine phenocrysts
is 21% by volume - the range being 5 - 39%.   In addition, small
amounts (2-7%) of olivine have been identified in the groundmass of
the more coarse-grained specimens and are probably present in most
of the rocks.

(ii) Abundance of glass

Many of the olivine-rich rocks contain a high proportion of
glass.   Rocks which contain only olivine, an ore phase and clino-
pyroxene have previously been termed 'limburgites'.   The use of this
term is discussed below.

Examination of some 150 thin sections has shown that there is
a continuous spectrum from limburgitic lavas, with no feldspar,

through glassy basalts, with abundant glass and small amounts of
skeletal or dendritic plagioclase, to basalts with abundant plagioclase
laths and interstitial glass in the groundmass.

Approximately 25% of the specimens from the Olivine-rich Group
are relatively coarse-grained holocrystalline rocks.   Although some of
these specimens have higher contents of modal olivine than the lavas
they do have the same distinctive chemical features and are taken to
be their hypabyssal equivalents.   Furthermore, some of the holocrystal-
line specimens were collected from obvious intrusive bodies -
especially sills.

(iii) Crystal habit and form

Cox et al (1965, p.131 and Figs. 36 and 37) have drawn attention
to, and illustrated, the occurrence of embayed, skeletal and dendritic
crystals in the lavas.   However, current research has established
that the best development of skeletal and dendritic crystals is
restricted to a few lavas and rarely do all the crystalline species
in one specimen display such habit.   Nevertheless, the ore phase very
frequently occurs as a series of sub-parallel, elongate, bladed crystals.
These have been described as combs by Cox et al (1965, p.133) and are
illustrated in Plates 1 and 13.   The combs are interpreted as cross-
sections of lamellar branches of large dendritic crystals.

In many of the glassy basalts plagioclase occurs as skeletal
or dendritic crystals (Plates 1 and 18).   Clinopyroxene dendrites and
larger, skeletal crystals are less common but occur in many limburgites
and glassy basalts (Plates 3, 4 and 14).

Although olivine phenocrysts are frequently euhedral -
subhedral, some of the phenocrysts in a number of specimens are embayed

and somewhat skeletal (Plates 5 and 18). However, the acicular skeletal crystals with axial cavities, which have been described by Drever and Johnston (1957) and Clarke (1968) from natural rocks and by Kopecký and Voldán (1959) from melting experiments on natural rocks, have not been found.

There is, therefore, an increasing tendency to skeletal and even dendritic habit in the series :

<div style="text-align: center;">olivine → clinopyroxene → plagioclase → ore.</div>

(iv) Orthopyroxene phenocrysts

The occasional occurrence of large orthorpyroxene phenocrysts is a striking feature of many of the rocks. The characteristics of these phenocrysts are their large size, euhedral – subhedral habit and invariable rim of clinopyroxene.

The occurrence of these phenocrysts was referred to briefly by Cox et al (1965, p.132) but Rogers (1925) appears to have been first to record them. In a description of the Karroo limburgitic lavas of the Zoutpansberg area of South Africa, which is situated across the Limpopo River from Nuanetsi, he states (p.48) :

'... but some (olivines) are enclosed in large (3 mm. wide and more than that in length) crystals of enstatite which have a colourless monoclinic pyroxene along the margin.'

Current research has shown that at least 60% of the olivine-rich lavas contain small amounts of these highly distinctive ortho-pyroxene phenocrysts. Thin sections of the orthopyroxene-bearing rocks frequently contain only 1-5 phenocrysts (ca. 1% by volume) and only 5 specimens contain more than 1% orthopyroxene phenocrysts. Of these, only 2, N-88 and N-117 with 21% and 6% respectively, contain

more than 4%.

The orthopyroxene phenocrysts, which are up to 10 mm in length, are generally larger than any other phenocrysts in the rocks (Plates 6-11). Composite clusters of 2-4 orthopyroxene crystals have been commonly observed (Plates 7 and 8).

The rim of clinopyroxene can be up to 3 mm but is generally less. In some specimens the rim is composed of a large number of granular crystals which appear to be replacing the orthopyroxene. In others the clinopyroxene is continuous around the orthopyroxene and all parts of the clinopyroxene are in optical continuity (Plates 9 and 10). Again, however, the clinopyroxene appears to be replacing the ortho-pyroxene. In some specimens only a small core of orthopyroxene remains inside a broad rim of clinopyroxene which may have euhedral (clino-pyroxene) habit (Plates 9, 10 and 11). Polysynthetic twinning of the clinopyroxene is common. In a few specimens there is a concentration of small rounded olivine crystals around the orthopyroxene and these have been partially included within the clinopyroxene rim (Plate 11).

An interesting, and probably significant, feature is that these orthopyroxene phenocrysts are almost completely absent in the holo-crystalline picritic rocks - only 3 examples have been found in thin sections of some 40 rocks. However, some of the picrites do contain smaller orthopyroxene crystals which lack all the distinctive features which are described above. In contrast, neither phenocrysts nor groundmass crystals of orthopyroxene without the characteristic clino-pyroxene rim have been found in the Nuanetsi lavas.

It is appreciated that many investigators would describe these phenocrysts as 'xenocrysts'. However, the author feels strongly that

until it can be shown that the crystals are indeed foreign material and not related to the development of the basic magma at depth they should be described as phenocrysts.

In a discussion of the mineralogy of the rocks (Chapter 3) it will be demonstrated that the orthopyroxene phenocrysts could not have been in equilibrium with a liquid phase and the olivine and clino-pyroxene phenocrysts of the rocks.

(v) Olivine nodules

One nodular aggregate of large olivine crystals was found (in N-160). The maximum dimension of the nodule was ca. 35 mm.

In several other lava specimens, notably N-356 (Plate 12), a few exceptionally large and euhedral olivine crystals contrasted sharply in size and habit with the more abundant olivine phenocrysts. These differences immediately led one to suspect that the large crystals, or megacrysts, were of a different and earlier generation.

(vi) Alteration

In many rocks both the phenocryst and the groundmass olivine are somewhat altered. The most common products are a red iddingsitic material and ore - both hematite and magnetite. Less common is a pale-green - yellow - colourless serpentinous material which occurs to the exclusion of the iddingsitic material. This serpentinous alteration is more penetrative and olivines in some rocks (not analysed) are completely pseudomorphed.

In an attempt to offset the chemical effects of this olivine alteration, the analysed contents of Fe_2O_3 and FeO have been adjusted in some specimens (see Chapter 4).

The Term 'Limburgite'.

In one respect 'limburgite' is not an entirely appropriate name for the Nuanetsi feldspar-free glassy rocks. All the analysed rocks contain hy in the C.I.P.W. norm and it is implicit in several standard references that limburgites are critically undersaturated with respect to SiO_2 and, therefore, contain ne in the norm, e.g. Turner and Verhoogen (1960) and Williams et al (1954). Furthermore, Holmes (1920) defines limburgite as being chemically equivalent to nepheline basalt, with glass in place of nepheline.

However, the name was first used by Rosenbusch (1872) on a strictly mineralogical basis to describe rocks from the Kaiserstuhl complex, West Germany. Rosenbusch (1908) defines the essential features of limburgites as the presence of olivine, augite (often of two generations) and a brown glass. The rock chemistry was not a factor in this definition.

Mennell (1910, p.140) appears to be first to have applied the term 'limburgite' to rocks in southern Africa. He described a rock from the Zoutpansberg area of South Africa as being very similar to the Kaiserstuhl limburgites. In the same area Rogers (1925) recorded abundant glassy Karroo volcanic rocks which he named limburgites. The name is also found in du Toit's (1954) description of the Karroo volcanic succession of the Zoutpansberg area and the northern part of the Lebombo monocline.

North of the Limpopo River Lightfoot (1938, p.198) and Swift et al (1953, p.37) used the name 'limburgite' to describe Karroo rocks in the country around the Sabi River, and Cox et al (1965) have employed the name extensively in describing the Nuanetsi volcanic succession.

Therefore, on grounds of priority and because of established local usage, the term 'limburgite' has been retained in the current study as a name for the feldspar-free, glassy, tholeiitic lavas.

Rock Classification

Within the range of olivine-rich rocks examined during the current research the following groupings can be distinguished on petrographic grounds :

(a) 1 - phenocryst limburgites, containing phenocrysts of olivine in a groundmass of glass, microphenocrysts of clino-pyroxene which are frequently skeletal, and dendritic ore (Plates 13 and 14).

(b) 2 - phenocryst limburgites, which contain phenocrysts of olivine and clinopyroxene in a groundmass of glass and ore, the ore commonly being dendritic. The clinopyroxene phenocrysts are generally smaller than the olivine phenocrysts (Plates 15 and 16). However, a small number of rocks contain euhedral clinopyroxene phenocrysts and olivine phenocrysts of similar dimensions (Plate 17).

(c) 1 - phenocryst glassy olivine basalts, which contain olivine phenocrysts in a groundmass of glass, dendritic and normal ore crystals, skeletal and dendritic plagioclase and clinopyroxene (Plate 18).

(d) 2 - phenocryst glassy olivine basalts, which are similar to the 1- phenocryst glassy basalts but also contain clino-pyroxene as a phenocryst phase.

(e) 1 - phenocryst olivine basalts, which differ from the 1- phenocryst glassy basalts in their smaller content of

glass and the presence of well-formed euhedral - subhedral laths of plagioclase.

(f) 2 - phenocryst olivine basalts, which are similar to the 1- phenocryst olivine basalts but contain, in addition, clinopyroxene phenocrysts.

(g) 3 - phenocryst olivine basalts, which contain phenocrysts of olivine, clinopyroxene and plagioclase in an intersertal groundmass. This type of basalt is rare.

(h) Picrites, which are holocrystalline and relatively coarse-grained. In most specimens no clear distinction between phenocrysts and groundmass crystals can be made. As mentioned above, this group is considered to be the hypabyssal equivalent of the lavas.

In order to be consistent with a previous classification scheme (Monkman, 1961, p.44) and generally accepted usage in other provinces, e.g. Hawaii, olivine basalts rich in modal olivine are termed picrite-basalts. Hence we have 1 and 2- phenocryst glassy picrite-basalt and 1 and 2- phenocryst picrite-basalt. The division between olivine and picrite-basalt is 25% modal olivine, in contrast to the 15% division adopted by Macdonald (1949). In a similar manner, holocrystalline rocks with less than 25% olivine are termed picrodolerites.

In the case of one picritic body, the Beacon sill, modal analyses of samples collected at different levels (Table 4) clearly indicate that sorting of olivine crystals has occurred.

Since there appears to be a continuous spectrum of types from 1- phenocryst limburgites to 3- phenocryst olivine basalts, the classi-fication scheme is sometimes difficult to apply and, because the

TABLE 4

BEACON SILL PICRITE

Vol.%	N-21	N-22	N-23
Olivine	29	38	42
Clinopyroxene	27	25	32
Alkali Feldspar			19
	38	35	
Plagioclase			3
Ore	6	2	3
Apatite	1	tr.	1
MgO (wt.%)	15.6	20.3	23.0

criteria used in the classification are somewhat subjective, differences between members of adjacent groups may be marginal. However, there are clear differences between, for example, groups (a) and (c) and groups (b) and (d).

The classification scheme is summarised in Table 5 and Table 6 shows the distribution in the various groups of the 56 specimens analysed in the current study.

The scheme is easy to use - requiring only a thin section examination - and, being based on the order of appearance of crystalline phases it is related to possible low pressure fractionation events. Cox et al (1967) have used an essentially similar scheme to sub-divide Karroo basic lavas from different areas of Rhodesia.

The petrographic criteria which are used in the scheme clearly result from the relationship between phase equilibria in the appropriate natural basaltic system and the bulk composition and temperature of the lavas immediately prior to eruption. It is implicit in the observed petrographic groupings that the order of the appearance of the silicate crystalline phases was :

olivine then clinopyroxene then plagioclase.

The large orthopyroxene phenocrysts occur in all the groups of lavas. They are, however, rare in the picrites. The presence or absence of these phenocrysts cannot be rationally related to any other petrographic feature. These observations are consistent with the belief that the phenocrysts are not the products of low pressure crystallisation - an argument developed in a discussion of the mineralogy of the rocks (Chapter 3).

TABLE 5

ROCK CLASSIFICATION SCHEME

		Groundmass		
		Glass	Glass and skeletal plagioclase	Plagioclase laths and glass
Phenocryst assemblage	Olivine	1-phenocryst limburgite	1-phenocryst glassy olivine basalt and picrite-basalt	1- phenocryst olivine basalt and picrite basalt
	Olivine + clinopyroxene	2-phenocryst limburgite	2-phenocryst glassy olivine basalt and picrite-basalt	2- phenocryst olivine basalt and picrite basalt
	Olivine + clinopyroxene + plagioclase			3- phenocryst olivine basalt

Note : (i) clinopyroxene is also present in the groundmass of all types

(ii) olivine basalt $<$ 25% modal olivine $<$ picrite basalt.

(iii) picrites and picrodolerites are holocrystalline, relatively coarse-grained rocks.

(iv) picrodolerite $<$ 25% modal olivine $<$ picrite.

TABLE 6

PETROGRAPHIC TYPES

Groups	No. of Specimens
1 - phenocryst limburgite	9
2 - phenocryst limburgite	10
1 - phenocryst glassy olivine basalt and picrite-basalt	10
2 - phenocryst glassy olivine basalt and picrite-basalt	7
1 - phenocryst olivine basalt	6
2 - phenocryst olivine basalt	3
3 - phenocryst basalt	2
Picrite and picrodolerite	9

CHAPTER 3

MINERALOGY

The compositions of mafic phenocryst and groundmass phases in several limburgites, basalts and picrites have been determined. These are reported and discussed in this chapter.

The Mg : Fe ratios of these phases indicate that the rare, large orthopyroxene phenocrysts are unlikely to have been in equilibrium with the clinopyroxene and olivine phenocrysts and groundmass crystals present in the rocks. However, the orthopyroxene phenocrysts and the rare nodular olivine aggregates and megacrysts could constitute an equilibrium assemblage. On this basis a distinction is made between a relict orthopyroxene-olivine assemblage inherited from an elevated pressure crystallisation event and the common low pressure assemblage olivine - clinopyroxene - ore - plagioclase - very rare orthopyroxene.

The clinopyroxene rim around the orthopyroxene phenocrysts is considered to be an overgrowth and not the product of reaction between orthopyroxene and liquid.

Olivine

Olivines from 2 picrites, N-22 and N-27, were separated, purified and analysed by X-ray spectrographic techniques (see Appendix B). The results are presented in Table 7. According to the nomenclature of Deer et al (1962a, p.22, Fig. 11) both are chrysotile.

Electron microprobe analyses of the rare, large olivines, or megacrysts, and olivine phenocrysts were carried out in one limburgite (N-356, illustrated in Plate 12) and one glassy olivine basalt (N-117). These results are given in Table 8. It is clear that the megacrysts

TABLE 7

OLIVINE ANALYSES

Wt.%	N-22 OLIV	N-27 OLIV
SiO_2	39.2	38.5
TiO_2	0.15	0.27
Al_2O_3	0.11	0.26
Fe_2O_3	0.7	3.5
FeO	19.8	17.9
MnO	0.27	0.26
MgO	39.4	38.0
CaO	0.27	0.33
H_2O	0.06	0.44
Total	100.0	99.5

p.p.m.		
Cr	100	-
Ni	2120	2100

Formula	Fo_{78}	Fo_{80} *

---

* - adjustment made to Fe^{+++} / Fe^{++} before

formula calculated.

TABLE 8

OLIVINE MICROPROBE ANALYSES

(a) Megacrysts

Wt.%	N - 76 I			N - 356 I		N - 356 II		
	Core	Core	Margin	Core	Margin	Core	Margin	Margin
FeO T	12.9	15.3	20.2	14.1	18.9	8.3	17.1	21.0
MgO	44.7	42.4	39.3	44.5	37.0	50.5	44.1	41.8
CaO	0.22	0.28	0.27	0.25	0.24	0.27	0.57	0.28
Formula	Fo_{86}	Fo_{83}	Fo_{78}	Fo_{85}	Fo_{78}	Fo_{92}	Fo_{82}	Fo_{78}

(b) Small phenocrysts and groundmass crystals

Wt.%	N-76 Groundmass	N-356 Phenocryst
FeO T	22.7	22.4
MgO	37.0	32.7
CaO	0.33	0.32
Formula	Fo_{74}	Fo_{72}

are significantly more forsterite-rich than the phenocrysts.

Figure 3, which shows the intensity of Fe radiation during a traverse of olivine crystals, shows that both phenocrysts and megacrysts are regularly and normally zoned from core to margin.

This analytical work was supplemented by X-ray diffraction determinations of the composition of olivine concentrates from several specimens. The methods employed are described in Appendix B; the results are presented in Table 9. Again it is clear that the olivine which constitutes the nodule in the glassy olivine basalt N-160 is considerably more forsteritic than the olivine phenocrysts. With the olivine concentrate from N-356 the determinative technique of Jackson (1960) consistently produced a split olivine (062) peak. This is taken to indicate 2 discrete olivine compositions - a result of the compositional difference between the rare megacrysts and the more common phenocrysts.

The compositions of N-22 OLIV and N-27 OLIV determined by the diffraction method are in good agreement with the chemical analyses (Table 7).

Orthopyroxene

Orthopyroxene phenocrysts were separated from 3 basalts, N-88, N-117 and N-313. This last basalt was not analysed. Satisfactory final purification ($>$ 99%) could not be achieved in the cases of N-117 and N-313 and contamination by clinopyroxene was estimated by point-counting to be 5% and 2.5% respectively. When electron microprobe analyses of the clinopyroxene rims were available appropriate adjustments were made to these orthopyroxene X-ray spectrographic analyses.

The analyses, adjusted where necessary, are presented in Table 10 and Fig. 4. The pyroxenes are enstatite and bronzite according to the nomenclature used by Deer et al (1962b, p.28, Fig. 10).

FIGURE 3

Olivine zoning.

Electron microprobe scan for Fe radiation across olivine phenocrysts in N-117 and N-356.

3

a

b

Olivine

FeO

wt
percent

FeO

30

20

10

30

20

10

0.1 mm.
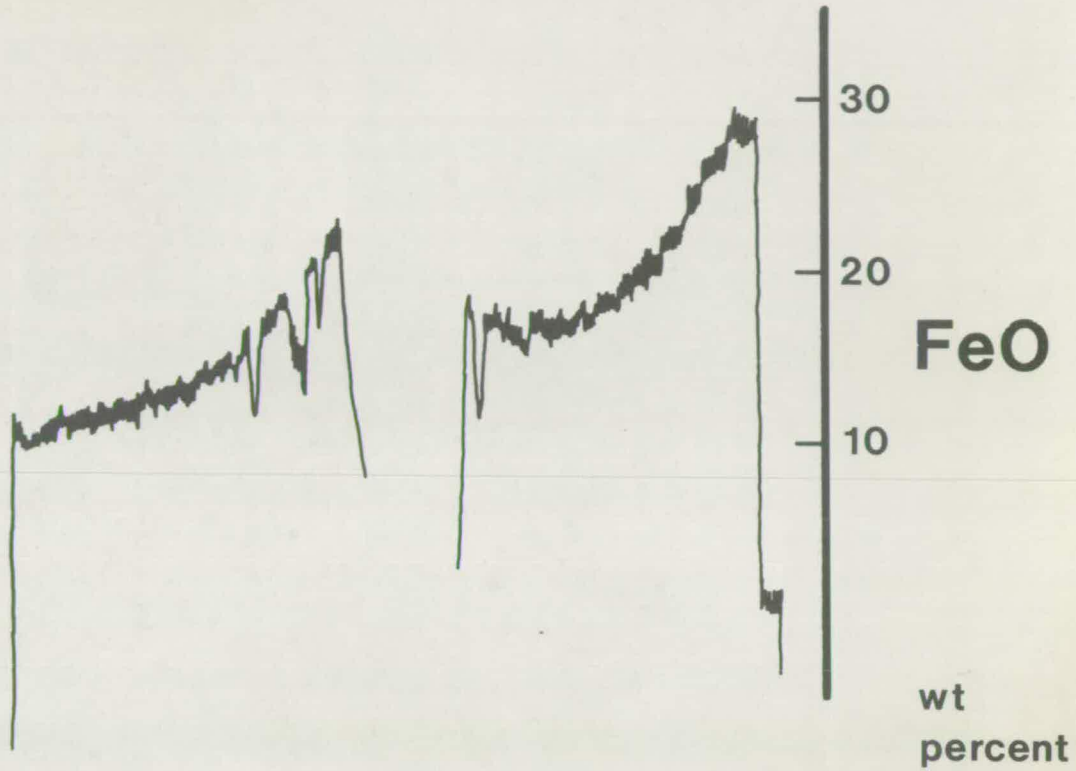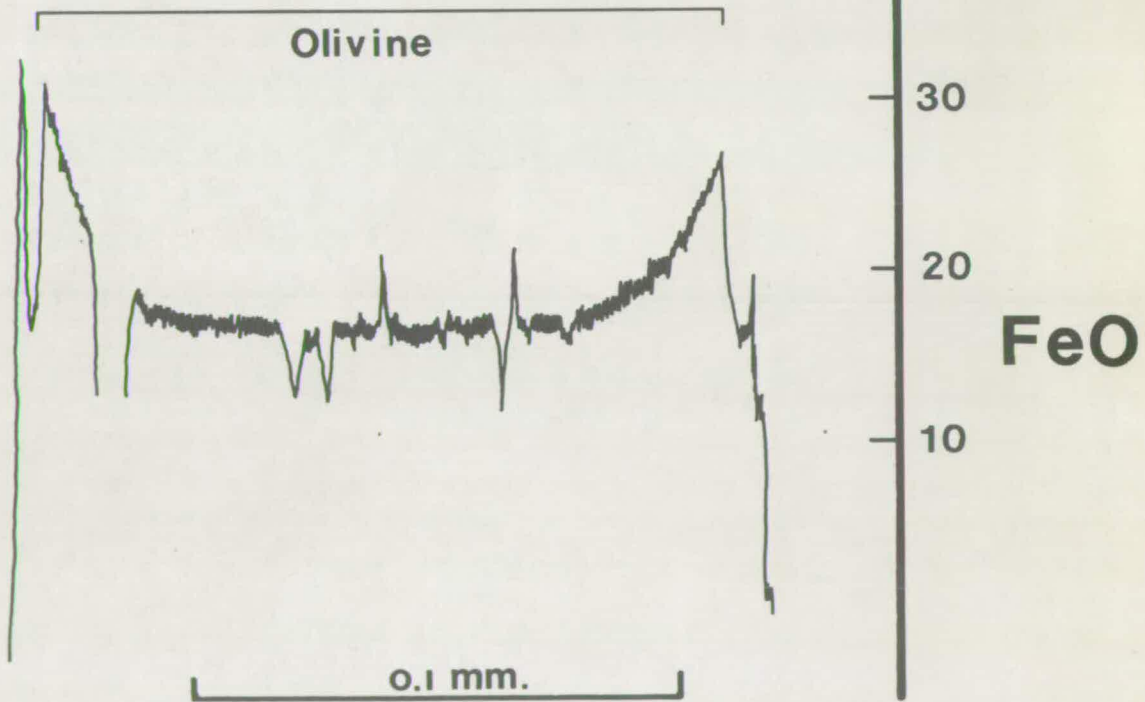
TABLE 9

OLIVINE COMPOSITIONS

		Fo mol %
Picrites	N-21	76
	N-22	78
	N-27	78
	N-41	77
	N-90	83
	N-95	75
Limburgites	N-55	73
	N-60	77
	N-356	86 and 78
Olivine nodule	N-160 nod	87

Figures given are the means of determinations given by the two diffraction methods described in Appendix B.   The individual determinations are given in Table B-11.

TABLE 10

ORTHOPYROXENE ANALYSES

Wt.%	N-88 OPX	N-117 OPX	N-313 OPX
SiO_2	55.4	54.3	54.5
TiO_2	0.35	0.51	0.30
Al_2O_3	1.66	1.44	1.49
Fe_2O_3	0.64	0.6	0.3
FeO	6.39	10.8	10.0
MnO	0.13	0.20	0.19
MgO	32.9	28.5	29.6
CaO	1.50	2.60	2.50
Na_2O	0.14	0.13	-
K_2O	0.02	0.03	-
Total	99.1	99.1	98.9

p.p.m.	N-88 OPX	N-117 OPX	N-313 OPX
Cr	3110	2340	3060
Cu	33	39	-
Ni	1727	1158	1292
Zn	97	126	120
Formula	$En_{89.6}$	$En_{81.8}$	$En_{83.6}$

Cations per 6 Oxygens *		N-88 OPX	N-117 OPX	N-313 OPX
	X + Y	2.03	2.00	2.01
	Z	1.99	2.00	2.00

* - calculated according to the scheme of Hess (1949)

Electron microprobe analyses were carried out on orthopyroxene phenocrysts in 2 basalts, N-88 and N-117, and 1 limburgite, N-76. Table 11 and Fig. 4 give the results.

An electron microprobe traverse (Fig. 5) across an orthopyroxene phenocryst revealed that there is not continuous compositional zoning but, instead, there is a sharp change near the phenocryst margins to a more Ca-rich and Fe-rich composition.

One rock (N-90, a picrite) contained 4% orthopyroxene which lacked the distinctive characters of the large orthopyroxene phenocrysts in the lavas. The composition of this orthopyroxene was determined by an X-ray diffraction technique (Appendix B). The results of this determination (Table 12) show this orthopyroxene to be more Fe-rich than the phenocrysts.

Clinopyroxene

Clinopyroxenes from 3 different modes of occurrence were investigated.

Firstly, clinopyroxenes from 6 picrites (N-22, N-23, N-27, N-41, N-90 and N-95) and a 2-phenocryst limburgite (N-60) were separated, purified and analysed by the X-ray spectrographic technique (Appendix B).

The analyses are presented in Table 13 and Fig. 6. The compositions are all very similar and according to the nomenclature of Poldervaart and Hess (1951, p.474) are, with the exception of N-95 CPX, endiopside but lie close to the endiopside-augite boundary.

Secondly, because attempts to separate and purify groundmass and phenocryst clinopyroxene from 1 and 2 - phenocryst lavas were generally unsuccessful, groundmass clinopyroxenes in two 1- phenocryst rocks (N-76 and N-356) were analysed using the electron microprobe.

TABLE 11

ORTHOPYROXENE MICROPROBE ANALYSES

Wt. %	N - 76 I			N - 76 II		
	Core	Core	Core	Margin	Margin	Margin
Al_2O_3	0.6	0.8	1.0	0.6	1.9	1.4
FeO T	7.1	7.3	7.1	9.6	8.9	7.7
MgO	31.7	31.8	31.7	28.8	28.5	31.7
CaO	1.7	1.8	1.7	3.0	2.9	1.9
Total*	96.1	97.1	96.5	96.5	95.3	98.4
Formula	En_{89}	En_{89}	En_{89}	En_{84}	En_{85}	En_{88}

Wt.%	N - 88			N-356
	Core	Core	Margin	Core
Al_2O_3	1.3	1.6	0.8	1.1
FeO T	7.2	7.4	8.8	7.9
MgO	31.6	31.4	29.9	31.4
CaO	1.5	1.7	2.7	1.1
Total*	96.4	96.9	97.0	97.8
Formula	En_{89}	En_{88}	En_{84}	En_{87}

* - totals calculated assuming an ideal metasilicate formula,
i.e. $AlAlO_3$, $FeSiO_3$, $MgSiO_3$ and $CaSiO_3$.

FIGURE 4

Orthopyroxene compositions.

● : separated and analysed orthopyroxenes.

+ : electron microprobe analyses.

The location of the main figure is indicated by stippling in the Di - Hd - En - Fs quadrilateral.

Compositions are expressed in mol. %.
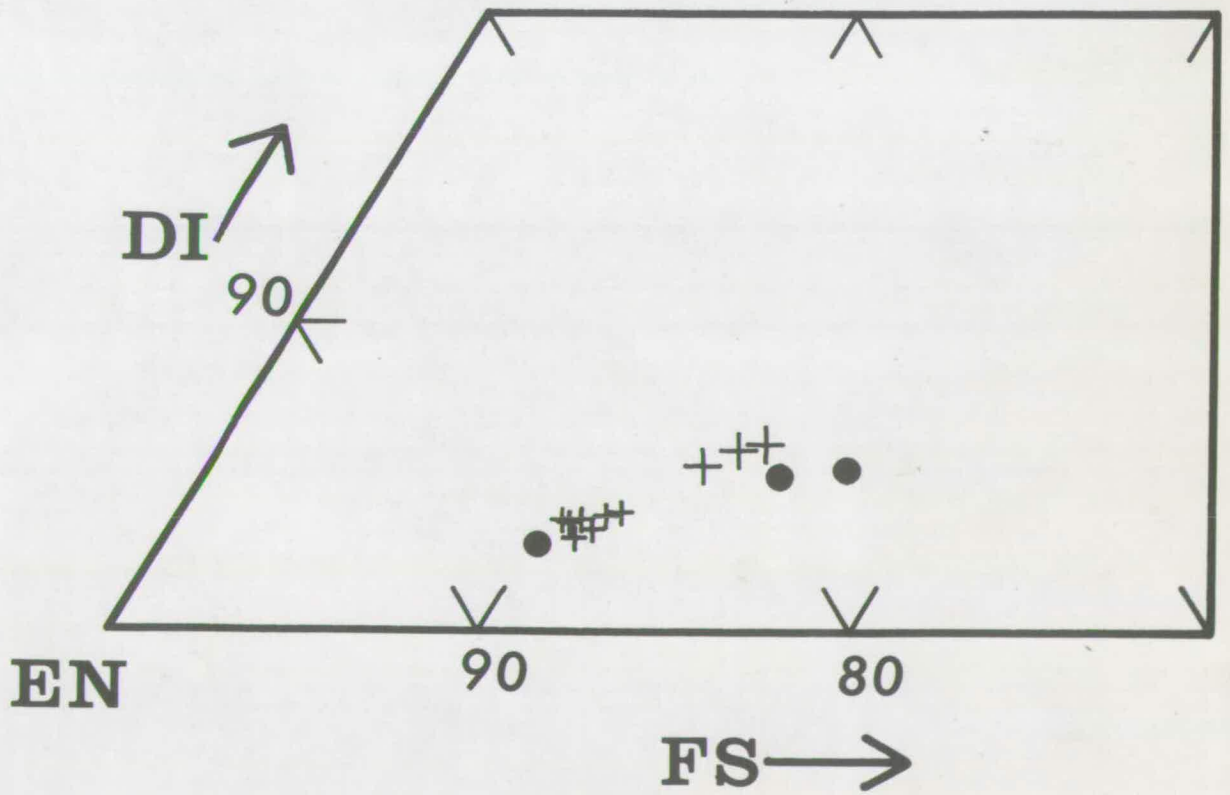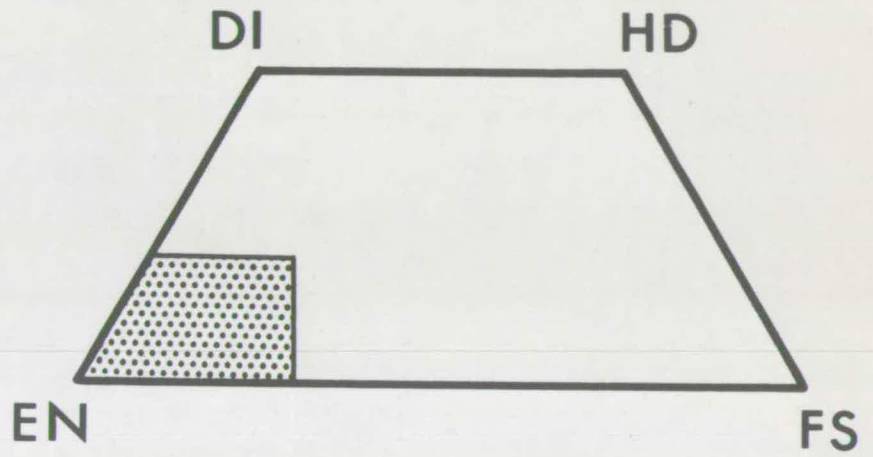
DI HD

EN FS

DI

90

EN

90 80

FS →

FIGURE 5

Orthopyroxene zoning.

    Chart record of electron microprobe scan across
orthopyroxene phenocryst in N-88;   Fe and Ca radiation
being counted simultaneously.

FeO

wt
percent

Core

Margin

Margin

CaO

0.1 mm.
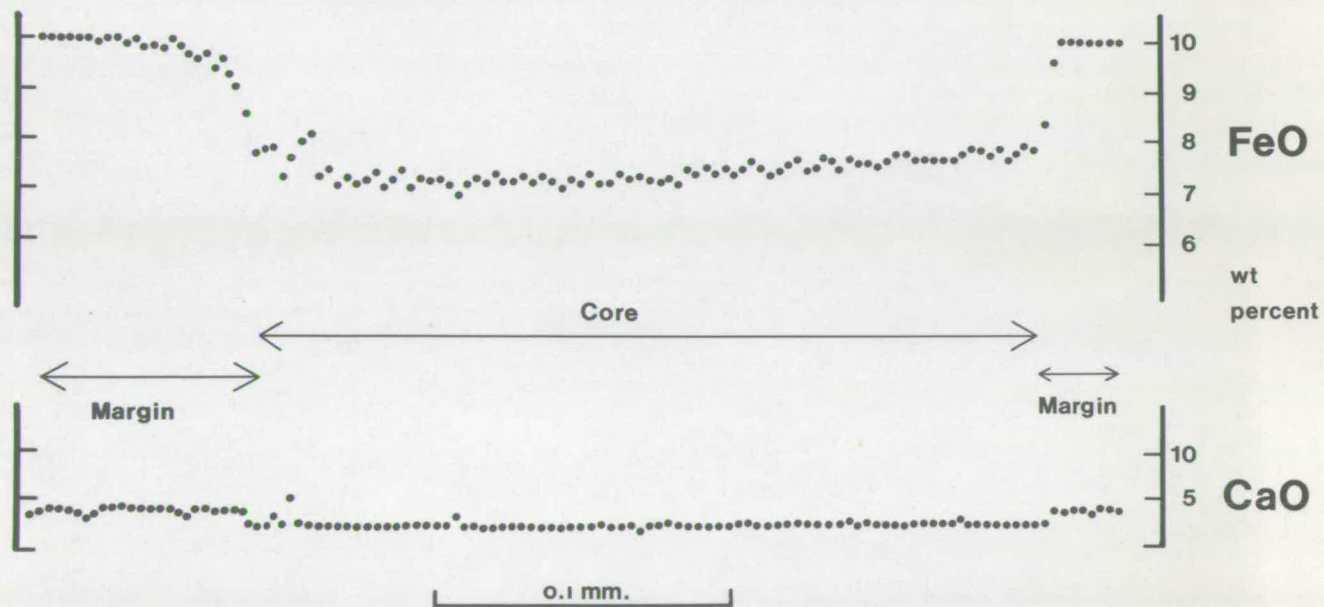
TABLE 12

ORTHOPYROXENE DATA

N-90 OPX

Al_2O_3 wt. %   1.1

En mol %   82

TABLE 13

CLINOPYROXENE ANALYSES

Wt.%	N-22 CPX	N-23 CPX	N-27 CPX	N-41 CPX	N-60 CPX	N-90 CPX	N-95 CPX
SiO_2	52.5	52.4	52.6	52.6	52.5	52.6	51.8
TiO_2	1.31	1.16	1.29	1.33	1.37	1.16	1.27
Al_2O_3	1.75	1.64	1.61	1.78	1.78	1.82	2.42
Fe_2O_3	0.77	0.72	0.84	1.78	0.73	0.84	1.26
FeO	5.21	5.26	4.93	4.61	4.95	4.80	5.80
MnO	0.12	0.14	0.13	0.14	0.13	0.13	0.15
MgO	17.5	17.8	18.0	17.4	17.6	18.9	17.0
CaO	20.6	20.0	20.1	19.6	20.6	19.6	19.3
Na_2O	0.36	0.35	0.32	0.36	0.35	0.28	-
K_2O	0.06	0.07	0.05	0.11	0.03	0.03	-
Total	100.2	99.5	99.9	99.7	100.0	100.2	99.0

p.p.m.							
Cr	3925	4425	4425	3650	4300	4305	4140
Ni	490	530	560	465	525	555	490
Zn	56	50	58	55	57	58	61
Zr	56	48	36	97	48	38	36

		N-22	N-23	N-27	N-41	N-60	N-90	N-95
	Ca	41.6	40.6	40.6	41.4	41.6	39.0	40.0
Formula	Mg	49.1	50.0	50.6	50.0	49.5	52.4	49.0
	Fe^o	9.3	9.4	8.9	9.5	9.0	8.6	11.0
Cations per 6	W + X + Y	2.02	2.02	2.02	2.00	2.02	2.03	1.98
Oxygens*	Z	1.98	1.98	1.99	1.99	1.99	1.98	2.00

Fe^o - Fe^{++} + Fe^{+++} + Mn

* - calculated according to the scheme of Hess (1949)

FIGURE 6

Clinopyroxene compositions.

● : separated and analysed clinopyroxenes.

+ : electron microprobe analyses of groundmass
clinopyroxenes.

O : electron microprobe analyses of clinopyroxene
rims around orthopyroxene phenocrysts.

The location of the main figure is indicated by

stippling in the Di - Hd - En - Fs quadrilateral.
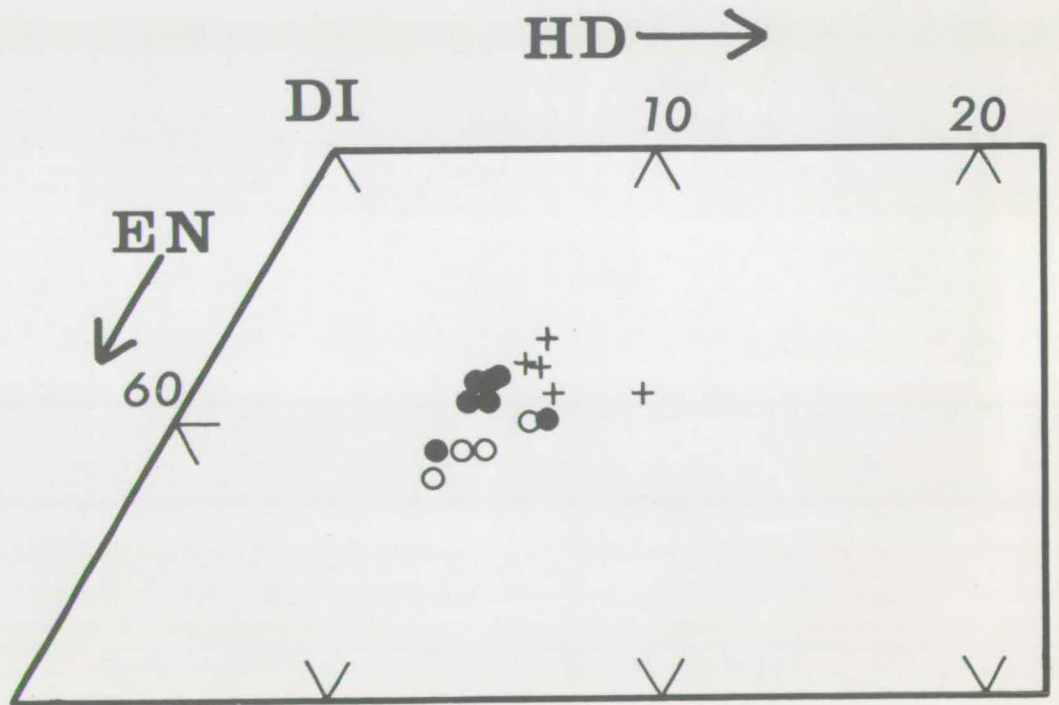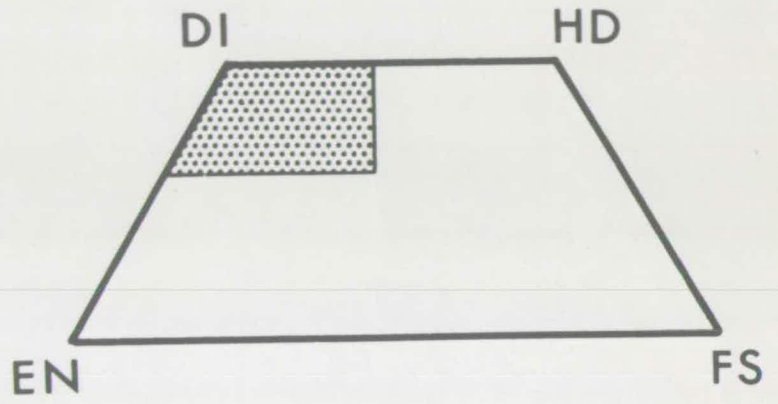
Compositions are expressed in mol. %.

These results are presented in Table 14a and plotted in Fig. 6. All the compositions are augite according to the nomenclature of Poldervaart and Hess (1951). When compared with the clinopyroxenes from the picrites and the 2- phenocryst limburgite N-60 they have marginally lower Mg : Fe ratios. This is almost certainly due to the relatively later crystallisation of these small groundmass crystals and is entirely consistent with the assumption that the picrites are the hypabyssal equivalents of the lavas.

Finally, the clinopyroxene phase which occurs as a rim surrounding the large orthopyroxene phenocrysts was analysed by electron microprobe in 3 specimens (N-76, N-88 and N-356). The results are presented in Table 14b and Fig. 6. The compositions are very similar to those of the analysed bulk clinopyroxene phases. In view of the different analytical techniques employed it is not clear whether the apparent lower Ca contents of the clinopyroxene rims is a significant feature. The formation of the clinopyroxene rims is discussed below.

Other Minerals

No work was undertaken on any other minerals. Alkali feldspar is relatively abundant in many picrites and von Knorring and Cox (1961) have recorded a new Ti (Mg, Fe) oxide mineral - kennedyite - in a picritic rock. Although an electron microprobe study of the feldspars and ore phases would certainly be a valuable mineralogical contribution, these phases are considered to be a reflection of, and not the cause of, the unusual petrological features of the rocks.

Mineral Equilibria

(i) Clinopyroxene - orthopyroxene

Despite several limitations, for example see O'Hara and Mercy

TABLE 14

CLINOPYROXENE MICROPROBE ANALYSES

(a) Groundmass crystals

Wt.%	N-76 I	N-76 II	N-76 III	N-76 IV	N-356
Al_2O_3	2.1	2.6	2.6	2.3	1.9
FeO T	6.3	6.2	5.5	8.5	6.6
MgO	16.8	16.3	16.9	15.9	16.8
CaO	20.8	20.8	20.5	20.0	19.9
Total*	98.6	97.7	97.2	98.9	97.0

Formula		N-76 I	N-76 II	N-76 III	N-76 IV	N-356
	Ca	42	43	42	41	41
	Mg	48	47	48	45	48
	Fe	10	10	10	14	11

(b) Rims around orthopyroxene

Wt.%	N-76 I	N-76 II	N-88	N-356
Al_2O_3	0.7	1.6	3.0	1.7
FeO T	5.6	6.0	6.8	5.8
MgO	18.9	18.2	16.9	17.7
CaO	19.0	19.2	19.3	19.6
Total*	97.4	97.6	97.6	96.9

Formula		N-76 I	N-76 II	N-88	N-356
	Ca	38	39	40	39
	Mg	53	51	49	52
	Fe	9	10	11	10

* - totals calculated assuming an ideal metasilicate formula, i.e. $AlAlO_3$, $FeSiO_3$, $MgSiO_3$ and $CaSiO_3$.

(1963, pp. 307-309), the distribution coefficient of Fe and Mg between coexisting pyroxene pairs, $K_{D\ (Mg:Fe)}$, has been used as a possible indicator of equilibrium and non-equilibrium assemblages.   As defined by Kretz (1961 and 1963)

$$K_{D\ (Mg:Fe)} = \frac{Xopx\ .\ 1\ -\ Xcpx}{1\ -\ Xopx\ .\ Xcpx}$$

where Xopx and Xcpx are the mole fractions of Mg in each pyroxene phase. Distribution coefficients are given in Table 15, the Mg : Fe ratios having been abstracted from Tables 10,11,13,14.

$K_{D\ (Mg:Fe)}$ for the pyroxene pair in the picrite N-90 is within the range of values recorded from igneous environments - 0.65 - 0.86 (Kretz, 1963, p. 777).   This distribution pattern suggests that the pyroxenes attained their compositions in equilibrium with each other and a liquid phase.   This is, of course, consistent with the petrography of the rock which offers no evidence of non-equilibrium.

In contrast the compositions of coexisting pyroxenes in the limburgites N-76 and N-356, as determined by electron microprobe, give values of $K_{D\ (Mg:Fe)}$ (Table 15) which are well outside the range of distribution coefficients recorded from supposed igneous equilibrium assemblages.

Although no further analyses of coexisting pyroxene pairs are available, it is instructive to consider the average and the range of Mg : Fe ratios in the remaining analysed pyroxenes.   These ratios are presented both in tabular form (Table 15) and graphically (Fig. 7). The possible orientation of the tie-line between the coexisting pyroxenes of N-90 has been added to Fig. 7.   Because of the restricted compositional ranges of both pyroxenes this treatment is not unreasonable and the data indicate that, in general, the Mg : Fe ratios of the orthopyroxene

TABLE 15

PYROXENE DISTRIBUTION COEFFICIENTS

Sample	X cpx	X opx	K_D (Mg:Fe)
N-90	85.8	82	0.75
N-76	83 *	89 *	1.65
N-356	81 *	87 *	1.57
All	85 - 76 mean of 11 - 83	90 - 82 mean of 3 - 86	1.0

* - since Fe_2O_3 content is not given by electron

microprobe analysis, FeO T has been used in

the calculation of X cpx and X opx.

FIGURE 7

Possible clinopyroxene - orthopyroxene equilibria.

- ● : separated and analysed pyroxenes.
- □ : electron microprobe analyses of orthopyroxene
      phenocrysts and groundmass clinopyroxenes.
- ○ : electron microprobe analyses of clinopyroxene
      rims round orthopyroxene phenocrysts.

The tie-line between co-existing pyroxenes in N-90
is based on a full analysis of the clinopyroxene and the
M/F ratio of the orthopyroxene.

Compositions are expressed in atomic %.
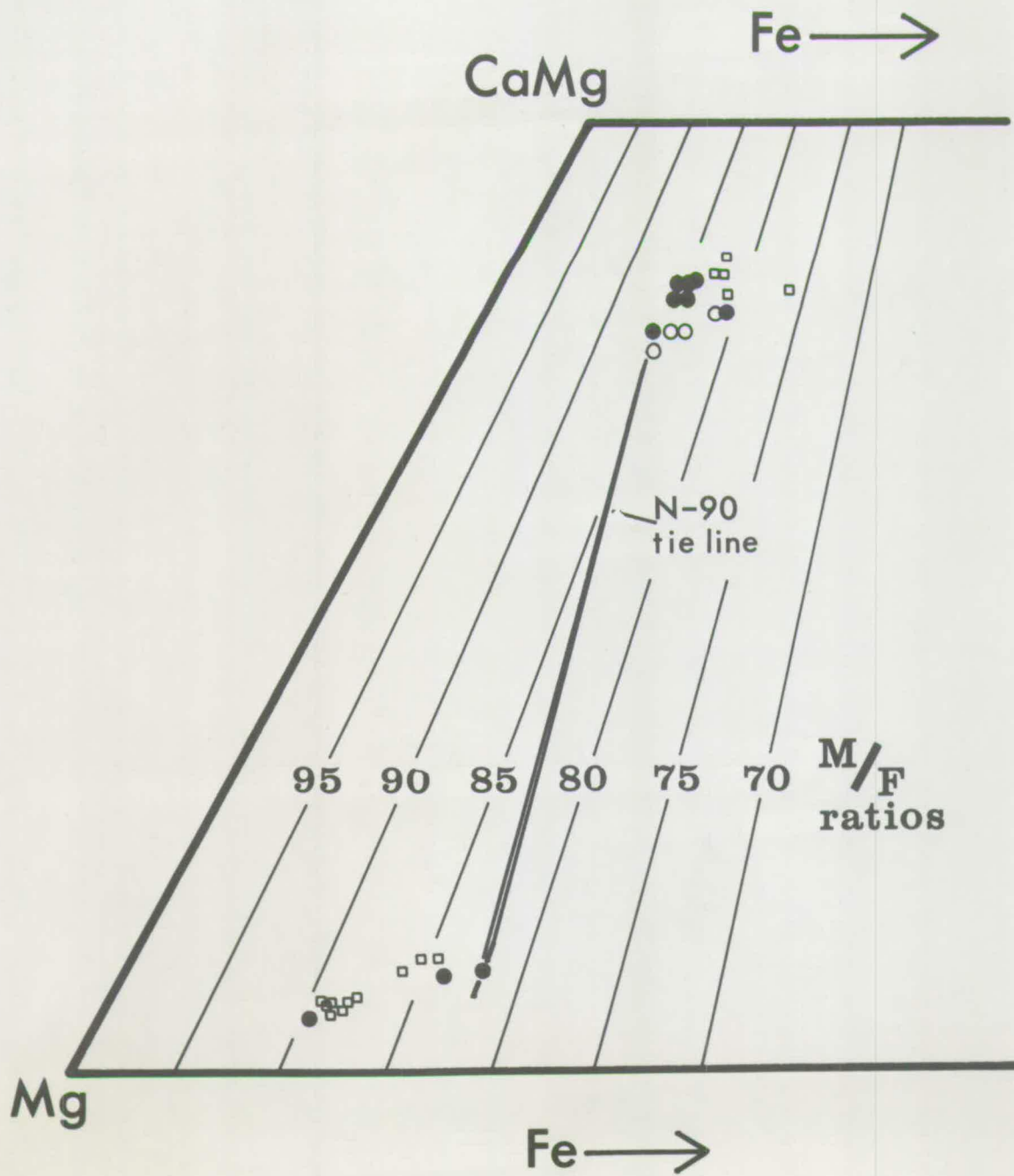
phenocrysts are too high to give values of $K_{D (Mg:Fe)} < 1$. This implies that the orthopyroxene phenocrysts and the clinopyroxenes of the rocks do not constitute an equilibrium assemblage.

(ii) Olivine - orthopyroxene

Bowen and Schairer (1935), Ramberg and De Vore (1951) and O'Hara (1963) have noted that in most magnesian (Mg : Fe $>$ 60) igneous equilibrium assemblages the Mg : Fe ratios of olivine and orthopyroxene are either close to unity or the olivine is relatively more magnesian. The data of O'Hara (1963, Figs. 1 and 2) indicate that only in one mode of occurrence - peridotite nodules in kimberlite - is olivine commonly enriched in Fe relative to coexisting orthopyroxene. This distribution of Fe between Mg-rich olivine and orthopyroxene is, of course, contrary to that between olivine and Ca-poor clinopyroxene determined by Bowen and Schairer (1935) in the system $MgO - FeO - SiO_2$ - at equilibrium the synthetic olivine was enriched in Fe relative to the Ca-poor clinopyroxene.

In the case of N-90 OLIV (Mg : Fe = 83) and N-90 OPX (Mg : Fe = 82) the distribution of Fe between the two phases suggests one is dealing with an equilibrium igneous assemblage.

Figure 8 gives the range of orthopyroxene compositions from 4 lavas, the range of compositions recorded in olivines in picrites and as lava phenocrysts, and the range of compositions of olivine megacrysts. Tie-lines connect the compositions of the phases in a limburgite (N-356). A consideration of these tie-lines and the general range of compositions in Fig. 8 suggests that, if the observations of Ramberg and De Vore (1951) and O'Hara (1963) do apply to these rocks, only the olivine megacrysts can constitute an equilibrium assemblage with the orthopyroxene

FIGURE 8

Possible orthopyroxene - olivine equilibria.

The ranges of measured compositions of olivine megacrysts, phenocrysts and groundmass crystals and the range of orthopyroxene compositions are shown in terms of the M/F ratio.

The compositions of olivines and orthopyroxenes in N-356 are also indicated. The tie-line marked ? is considered not to represent an equilibrium assemblage (see text).
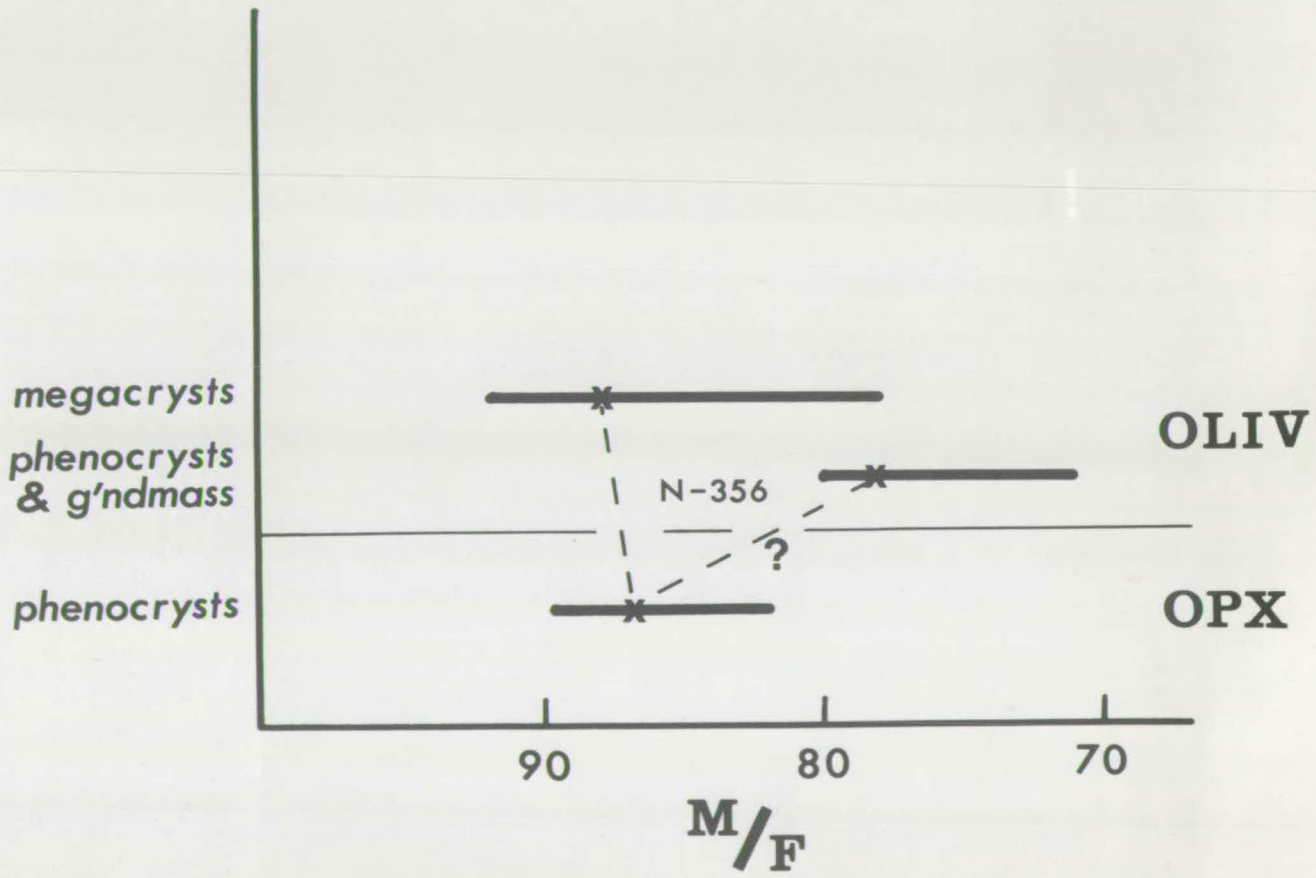
phenocrysts - the other olivines in the rocks are relatively too Fe-rich.

(iii) Conclusions

The mafic mineral assemblage olivine - orthopyroxene - clinopyroxene, which is recorded in one picrite, N-90, appears to represent an equilibrium assemblage.

The large orthopyroxene phenocrysts are unlikely to have been in equilibrium with the clinopyroxene and olivine present in the rocks but could constitute an equilibrium assemblage with the rare olivine megacrysts. The first observation regarding the orthopyroxene phenocrysts is, of course, strongly supported by petrographic features, by the apparent haphazard distribution of orthopyroxene phenocrysts in the rocks, and also by phase equilibrium considerations (see Chapter 5).

These conclusions lead the author to recognise two distinct mafic mineral assemblages :

(a) a low pressure olivine - clinopyroxene - very rare orthopyroxene assemblage; olivine and clinopyroxene occurring both as phenocrysts and groundmass crystals.

(b) an olivine - orthopyroxene phenocryst assemblage, characterised by higher Mg : Fe ratios, which is considered to have been inherited from an elevated pressure crystallisation event. As such this relict assemblage constitutes valuable evidence regarding the development of the basic magmas at depth.

The Olivine - Orthopyroxene Phenocryst Assemblage.

The Al_2O_3 content of Al_2O_3-saturated pyroxenes and the mutual solubility of coexisting pyroxenes are two parameters which have been

widely used in attempts to estimate the T and P of equilibration of mafic mineral assemblages. References to the relevant literature are given by O'Hara (1967). Using data from both synthetic and natural assemblages, O'Hara produced a provisional P-T grid (Fig. 12-4) which utilises these parameters. However, as there is no evidence that the olivine mega-crysts and orthopyroxene phenocrysts ever coexisted with a Ca-rich pyroxene or an Al_2O_3-rich phase, these parameters cannot be used as a guide to the depth of crystallisation of this assemblage.

Phase equilibrium considerations have proved to be more useful in assessing the P and T of equilibration (see Chapter 5). After the relationship between the bulk compositions of the rocks, the mineral assemblage and phase relations in natural and synthetic systems at elevated pressure had been fully explored (Chapter 5) it was concluded that the olivine - orthopyroxene assemblage, if cognate, must be inherited from depths exceeding 10 km.

Figure 5 demonstrates a sharp compositional change near the edge of an orthopyroxene phenocryst. This change may indicate that after the initial, main growth further crystallisation took place under different pressure conditions, that the final crystallisation occurred in a magmatic liquid with a different composition, or a combination of both factors.

Clinopyroxene Rims

Figure 6 and Table 15 demonstrate that the clinopyroxene rims around the orthopyroxene phenocrysts have compositions which closely match the other clinopyroxene phases in the rocks. This feature suggests that the rims are simply overgrowths of the normal, low pressure clinopyroxene of the lavas and are not the products of reaction between

orthopyroxene and the magmatic liquid.   In those specimens where the
orthopyroxene appears, superficially, to have been replaced by clino-
pyroxene it is considered that the resorption took place prior to the
overgrowth of clinopyroxene.   Once shielded by clinopyroxene rims
the non-equilibrium orthopyroxene phenocrysts would clearly be preserved
from further magmatic resorption.

It is interesting to note that, on the basis of an electron
microprobe examination, Muir and Long (1965) have demonstrated that
clinopyroxene jackets around (equilibrium) hypersthene phenocrysts in
two Hawaiian lavas have the same compositions as the groundmass clino-
pyroxene phase.   Muir and Long conclude that the clinopyroxene jacket
is a parellel growth effect.

The concentration of olivine crystals around some of the ortho-
pyroxene phenocrysts (Plate 11) is further evidence of resorption of
the phenocrysts.   During resorption the liquid phase surrounding the
orthopyroxene must have been relatively enriched in Mg^{++}, Fe^{++} and
SiO_4^{4+} ions and ionic lattices and, if olivine was a precipitating phase,
a concentration of olivine would occur around the orthopyroxene
phenocrysts.   Since these small olivine crystals are partly enclosed
within the clinopyroxene rims this feature is consistent with the
relatively late growth proposed, above, for the rim.

CHAPTER 4

PETROCHEMISTRY

Chemical analyses and C.I.P.W. norms of 47 limburgites and basalts and 9 picrites are presented.

The overall high-magnesian character of the rocks is confirmed by average MgO contents of 15.1% in the lavas and 19.1% in the picrites. Since few rocks with MgO contents in the range 8-10% have been found, it appears that the olivine-rich lavas form a group which is not only stratigraphically but also compositionally distinct from the voluminous low-MgO, Upper Basalts.

The contents of K and the associated elements Ti, P, Ba, Rb, Sr and Zr are high throughout the range of rock compositions - confirming the earlier observations of Monkman (1961) and Cox et al (1965). These elements behave as a strongly coherent group.

A positive correlation between K and associated elements and MgO and a negative correlation between K_2O and Na_2O are noted. These features are considered to be the most significant geochemical aspects of the variation within this picritic suite.

The chemistry of the olivine-rich rocks is compared with that of other tholeiites.

Chemical Analyses

    (i) The data.

Analyses of 47 basalts and limburgites and 9 picrites are presented in Tables 16 and 17 respectively. Short descriptions of the analysed specimens, including modal analyses and localities, are

TABLE 16

CHEMICAL ANALYSES OF LAVAS

Wt.%	N-1	N-5	N-13	N-15	N-26	N-34	N-35	N-37	N-40
SiO_2	49.9	48.2	45.1	48.7	49.5	48.4	48.6	50.5	49.6
TiO_2	3.10	3.04	2.56	2.16	3.30	3.14	3.26	2.94	2.66
Al_2O_3	8.24	10.1	5.61	10.4	8.35	7.34	7.19	8.68	8.93
Fe_2O_3	3.0*	4.2*	7.3*	2.9	2.3	2.9	2.5	1.8	1.7
FeO	7.86*	8.26*	5.00*	9.25	8.34	7.82	8.05	9.76	9.86
MnO	0.11	0.15	0.13	0.16	0.14	0.12	0.12	0.15	0.16
MgO	15.0	12.5	23.3	13.4	15.4	16.3	15.8	15.3	15.7
CaO	7.13	8.54	5.25	8.45	7.26	6.57	6.56	7.68	8.21
Na_2O	1.42	1.97	0.98	2.01	1.57	1.30	1.89	1.74	1.13
K_2O	2.52	1.87	1.72	0.78	2.50	2.92	1.80	1.52	1.62
P_2O_5	0.50	0.44	0.41	0.32	0.47	0.48	0.52	0.33	0.47
H_2O	0.90	0.42	2.23	1.53	0.54	3.21	3.47	0.66	0.81
Total	99.7	99.7	99.6	100.1	99.7	100.5	99.8	101.1	100.9
F/M	41.9	49.4	33.6	47.7	41.0	38.6	40.0	43.1	42.5

p.p.m.

	N-1	N-5	N-13	N-15	N-26	N-34	N-35	N-37	N-40
Ba	1235	830	925	420	1165	1250	1320	650	570
Cr	965°	680	1130	770	990	1190	1130	970	920
Cu	38	-	44	-	-	-	-	-	-
La	62	-	53	-	-	-	60	-	-
Nb	24	-	18	-	-	-	24	-	-
Ni	730	588	1380	710	750	813	794	725	675
Pb	< 20	-	< 20	-	-	-	< 20	-	-
Rb	45	30	32	28	51	75	70	23	18
Sr	1237	946	931	625	1191	1200	1295	907	666
V	230°	-	-	-	-	-	-	-	-
Zn	108	-	113	-	-	-	97	-	-
Zr	380	245	342	205	450	445	454	290	275

* - values subsequently adjusted

o - spectrophotometric determination

$$F/M = \frac{Fe_2O_3 + FeO}{Fe_2O_3 + FeO + MgO}$$

TABLE 16 (continued)

CHEMICAL ANALYSES OF LAVAS

Wt.%	N-55	N-60	N-72	N-76	N-79	N-84	N-88	N-89	N-91
SiO_2	48.1	45.7	48.6	47.6	49.3	50.4	49.3	50.2	49.6
TiO_2	2.85	2.89	2.90	2.60	2.74	1.82	1.71	1.24	2.70
Al_2O_3	8.98	6.11	7.27	6.52	9.41	11.5	5.77	15.1	10.0
Fe_2O_3	3.6*	4.0*	3.2*	4.7*	1.7	1.6	7.0*	2.2	2.2
FeO	7.79*	8.07*	7.78*	6.48*	9.65	9.97	4.18*	8.13	9.03
MnO	0.15	0.15	0.14	0.14	0.15	0.16	0.15	0.15	0.15
MgO	14.4	21.3	16.4	19.0	13.6	11.1	20.7	8.26	12.7
CaO	7.83	4.85	7.24	5.94	8.28	8.63	5.87	10.5	8.12
Na_2O	1.45	1.10	1.35	0.98	1.83	2.19	0.91	2.58	1.78
K_2O	1.90	1.83	2.19	2.08	1.25	0.52	0.78	0.64	1.56
P_2O_5	0.47	0.46	0.52	0.46	0.38	0.24	0.26	0.19	0.39
H_2O	1.62	2.68	1.46	2.86	1.02	1.25	3.06	1.06	1.38
Total	99.1	99.1	99.1	99.4	99.3	99.4	99.7	100.3	99.6
F/M	43.9	35.8	40.1	36.3	45.4	51.2	34.7	55.4	46.9
p.p.m.									
Ba	565	1335	960	960	865	300	325	320	750
Cr	900	1240	1110	1130	920	780	1526°	198°	580
Cu	-	62	-	-	-	-	45	39	-
La	-	53	-	-	-	-	75	20	-
Nb	-	18	-	-	-	-	12		
Ni	660	1235	850	1108	635	390	1105	220	596
Pb	-	-	-	-	-	-	< 20	-	-
Rb	36	36	35	36	17	18	25	9	31
Sr	819	996	1083	884	978	354	444	359	833
V	-	-	-	-	-	-	180°	210°	-
Zn	-	110	-	-	-	-	106	89	-
Zr	280	370	400	346	285	130	188	130	310

* - values subsequently adjusted

o - spectrophotometric determination

$$\frac{F}{M} - \frac{Fe_2O_3 + FeO}{Fe_2O_3 + FeO + MgO}$$

TABLE 16 (continued)

CHEMICAL ANALYSES OF LAVAS

Wt.%	N-100	N-102	N-105	N-113	N-117	N-126	N-133	N-135	N-149
SiO_2	48.6	50.4	49.3	49.2	49.5	49.3	47.2	47.9	48.4
TiO_2	3.10	2.64	2.58	2.48	2.31	2.73	2.55	2.78	2.71
Al_2O_3	10.4	10.0	8.51	9.06	9.08	9.00	6.34	7.83	8.88
Fe_2O_3	6.5*	4.1*	2.1	2.8	2.6	2.5	4.4*	7.0*	2.3
FeO	6.0*	7.36*	8.87	8.70	7.91	9.38	7.30*	4.63*	9.99
MnO	0.16	0.15	0.14	0.14	0.14	0.15	0.09	0.11	0.13
MgO	10.9	12.8	15.1	14.1	14.9	13.5	19.6	16.8	15.3
CaO	8.75	8.11	7.60	7.90	7.27	8.01	6.55	7.07	8.40
Na_2O	1.97	1.88	1.55	1.82	1.53	1.78	1.08	1.39	1.60
K_2O	1.90	1.59	1.48	0.73	1.53	1.34	2.01	2.46	0.90
P_2O_5	0.46	0.39	0.42	0.36	0.35	0.42	0.45	0.47	0.34
H_2O	0.36	0.30	1.29	2.31	2.39	1.43	1.96	2.48	0.96
Total	99.1	99.7	98.9	99.6	99.5	99.5	99.5	100.9	99.9
F/M	52.6	46.8	42.0	45.0	43.5	46.9	36.8	39.9	48.0

p.p.m.

	N-100	N-102	N-105	N-113	N-117	N-126	N-133	N-135	N-149
Ba	910	740	640	615	600	640	1040	990	600
Cr	660	820	1100	1000	910	760	1321°	1010	940
Cu	93	-	-	-	74	-	65	-	-
La	61	-	-	-	18	-	73	-	-
Nb	20	-	-	-	18	-	16	-	-
Ni	912	431	730	700	748	644	1055	901	730
Pb	< 20	-	-	-	-	-	-	-	-
Rb	39	32	30	53	27	28	39	40	19
Sr	1008	819	795	777	695	822	1077	1015	665
V	-	-	-	-	220°	-	180°	-	-
Zn	102	-	-	-	98	-	104	-	-
Zr	360	285	280	325	275	305	353	350	280

* - values subsequently adjusted

o - spectrophotometric determination

$$F/M - \frac{Fe_2O_3 + FeO}{Fe_2O_3 + FeO + MgO}$$

TABLE 16 (continued)

CHEMICAL ANALYSES OF LAVAS

Wt.%	N-160	N-187	N-190	N-225	N-231	N-245	N-355	N-356	N-357	N-361
SiO_2	48.7	48.6	48.9	48.6	48.8	49.8	48.9	49.6	50.7	48.9
TiO_2	2.73	2.75	3.23	2.22	2.46	1.62	2.72	2.54	2.53	1.49
Al_2O_3	8.71	9.39	7.79	9.42	7.77	13.3	8.06	7.99	10.3	10.5
Fe_2O_3	2.1	5.4*	1.8	2.1	2.6	2.3	2.3	2.6*	2.7	2.7
FeO	9.16	7.27*	8.36	11.7	8.49	8.94	9.78	7.39*	8.31	9.15
MnO	0.15	0.16	0.13	0.18	0.14	0.16	0.17	0.13	0.16	0.17
MgO	15.0	11.2	15.2	13.7	17.6	9.65	14.4	16.9	12.6	13.9
CaO	7.69	9.76	6.74	8.69	6.46	9.36	8.74	5.62	7.61	8.65
Na_2O	1.80	1.67	1.64	1.64	1.29	2.59	1.65	1.44	2.06	2.16
K_2O	1.08	1.26	2.12	0.20	1.38	0.76	1.27	2.78	1.74	0.73
P_2O_5	0.44	0.39	0.56	0.23	0.36	0.29	0.44	0.36	0.45	0.21
H_2O	1.90	2.08	3.00	1.42	2.16	1.36	1.09	1.94	0.53	1.20
Total	99.5	99.9	99.5	100.1	99.5	100.1	99.5	99.3	99.7	99.8
F/M	43.0	52.5	40.1	50.2	38.6	53.7	45.8	37.0	46.3	46.1
p.p.m.										
Ba	570	595	1105	175	580	656	748	1540	867	460
Cr	930	790	1140	680	1040	730	1020	870	890	1090
Cu	-	-	-	-	-	-	-	-	94	-
La	-	-	-	-	-	-	-	-	47	-
Nb	-	-	-	-	-	-	-	-	30	-
Ni	734	460	775	704	904	296	540	962	570	545
Pb	-	-	-	-	-	-	-	-	-	-
Rb	27	16	81	6	34	11	26	53	34	21
Sr	800	683	1107	354	667	676	792	1146	855	658
V	-	-	-	-	-	-	-	-	-	-
Zn	-	-	-	-	-	-	-	-	90	-
Zr	275	280	365	140	260	148	246	363	310	165

* - values subsequently adjusted

o - spectrophotometric determination

$$F/M - \frac{Fe_2O_3 + FeO}{Fe_2O_3 + FeO + MgO}$$

TABLE 16 (continued)

CHEMICAL ANALYSES OF LAVAS

Wt.%	N-399	N-400	N-405	N-406	N-440	N-442	N-462	N-517	N-519	KC-204
SiO_2	48.7	47.8	49.2	48.9	48.2	50.2	48.4	47.6	49.9	49.7
TiO_2	2.85	2.50	2.80	2.83	2.80	3.17	2.54	2.94	2.83	3.18
Al_2O_3	8.36	6.93	9.65	9.64	6.60	9.04	7.74	7.29	11.4	7.77
Fe_2O_3	2.1	6.1*	2.2	1.9	4.8*	2.3	3.5*	7.5*	3.0	2.8*
FeO	9.39	5.4*	10.1	10.2	6.27*	8.27	7.27*	3.76*	9.74	7.94*
MnO	0.15	0.14	0.17	0.17	0.14	0.14	0.14	0.14	0.16	0.14
MgO	15.7	18.1	13.0	13.2	19.0	13.8	17.7	17.0	10.4	16.5
CaO	7.97	5.88	8.60	8.62	5.75	7.47	6.16	6.61	9.72	6.69
Na_2O	1.70	1.32	1.81	1.83	1.20	1.49	1.23	1.40	1.97	1.45
K_2O	0.84	2.22	1.25	1.32	1.83	2.12	2.10	2.17	0.80	2.47
P_2O_5	0.41	0.48	0.40	0.37	0.47	0.55	0.42	0.49	0.33	0.56
H_2O	1.70	2.38	0.86	0.81	2.60	1.65	2.21	2.54	0.94	0.46
Total	99.9	99.3	100.0	99.8	99.7	100.2	99.4	99.4	101.2	99.7
F/M	42.2	38.1	48.6	47.6	36.3	43.3	37.6	38.7	55.1	39.1

p.p.m.

	N-399	N-400	N-405	N-406	N-440	N-442	N-462	N-517	N-519	KC-204
Ba	440	1180	700	610	1050	1082	1040	1060	460	940
Cr	960	750	550	650	1180	970	1200	1010	650	925
Cu	79	-	-	104	-	-	-	-	-	-
La	22	-	-	39	-	-	-	-	-	-
Nb	19	-	-	24	-	-	-	-	-	-
Ni	780	1026	540	565	1093	663	1295	911	338	835
Pb	-	-	-	-	-	-	-	-	-	-
Rb	22	45	26	24	29	40	46	31	17	40
Sr	704	1056	743	731	1135	1113	921	1109	597	1105
V	-	-	-	-	-	-	-	-	-	-
Zn	107	-	-	100	-	-	-	-	-	-
Zr	265	325	275	265	320	395	330	400	250	395

* - values subsequently adjusted

o - spectrophotometric determination

$$F/M = \frac{Fe_2O_3 + FeO}{Fe_2O_3 + FeO + MgO}$$

TABLE 17

CHEMICAL ANALYSES OF PICRITES

Wt.%	N-21	N-22	N-23	N-27	N-41	N-90	N-95	N-163	N-364
SiO_2	48.5	47.6	46.1	46.3	47.6	46.4	47.5	49.3	49.5
TiO_2	3.62	2.62	2.20	2.88	3.54	1.79	2.53	2.12	1.51
Al_2O_3	6.98	5.83	4.35	6.22	6.65	4.87	7.46	9.09	9.52
Fe_2O_3	4.2*	3.4*	3.1*	3.0	5.0*	2.7	4.4*	3.4*	2.6
FeO	7.02*	8.40*	9.80*	8.80	6.32*	8.60	7.74*	8.64*	9.78
MnO	0.15	0.15	0.17	0.15	0.15	0.16	0.16	0.16	0.17
MgO	15.6	20.3	23.0	20.7	17.4	26.8	17.0	14.9	16.4
CaO	7.18	6.05	7.11	5.75	7.07	4.46	8.13	8.65	6.83
Na_2O	1.53	1.09	0.84	1.09	1.39	0.90	1.52	1.55	1.72
K_2O	2.46	1.99	1.34	2.12	2.20	1.20	1.06	0.62	0.52
P_2O_5	0.54	0.42	0.33	0.46	0.51	0.35	0.37	0.23	0.19
H_2O	1.15	1.48	0.91	1.55	1.31	1.26	1.45	0.94	1.58
Total	98.9	99.3	99.3	99.0	99.1	99.5	99.3	99.6.	100.3
F/M	42.3	36.4	35.9	36.3	38.8	29.7	41.3	44.5	43.1
p.p.m.									
Ba	880	760	540	860	960	605	380	155	230
Cr	860	1265	1245	1252°	820	1175	960	780	690
Cu	-	-	-	78	-	-	-	-	-
La	-	-	-	86	-	-	-	-	-
Nb	-	-	-	20	-	-	-	-	-
Ni	760	1145	1290	1145	800	1470	830	703	812
Pb	-	-	-	-	-	-	-	-	-
Rb	43	30	22	37	46	26	18	11	11
Sr	1130	945	775	1000	1240	655	690	440	275
V	-	-	-	200°	-	-	-	-	-
Zn	-	-	-	110	-	-	-	-	-
Zr	430	370	220	380	390	220	220	165	130

* - values subsequently adjusted

o - spectrophotometric determination

$$F/M - \frac{Fe_2O_3 + FeO}{Fe_2O_3 + FeO + MgO}$$

given in Appendix A.

The analyses were carried out by a combination of X-ray spectrographic and rapid chemical techniques.   Details of the analytical methods and the crushing and grinding procedure are given in Appendix B.

Because the olivine in some of the rocks is somewhat altered (see Chapter 3) the appropriate values of Fe_2O_3 and FeO in Tables 16 and 17 were adjusted before the calculation of C.I.P.W. norms and other parameters.   This was done for rocks which, in thin section, showed signs of alteration by adjusting the determined values of Fe_2O_3 and FeO so that the ratio $Fe^{+++}/ Fe^{+++} + Fe^{++}$ equalled 0.18 - this being the value calculated from the Fe_2O_3 and FeO contents of the 30 rocks in which no alteration was detected.   This adjustment to a predetermined ratio is justified by the apparent lack of a rational relationship between $Fe^{+++} / Fe^{+++} + Fe^{++}$ and the other components in the 30 unaltered rocks.

C.I.P.W. norms for the analysed rocks are presented in Tables 18 and 19.   Without exception they contain <u>hy</u> and by definition are tholeiitic.

(ii) <u>Average analyses</u>.

The data of Tables 16 - 19 are summarised in Tables 20 and 21. Table 20 gives both the concentration range of each major oxide and trace element in the lavas and picrites and the mean values. Similarly Table 21 gives the range of normative constituents in the two groups of rocks and C.I.P.W. norms of the two mean analyses.

The most striking features in these Tables are the high content of MgO in all the rocks and the high content of K_2O, both in absolute

TABLE 18

C.I.P.W. NORMS OF LAVAS

Wt.%	N-1	N-5	N-13	N-15	N-26	N-34	N-35	N-37
z	0.1	0.1	0.1	0.1	0.1	0.1	0.1	0.1
or	15.0	11.1	10.4	4.7	14.9	17.7	11.0	8.9
ab	12.1	16.8	8.5	17.2	13.4	11.3	16.5	14.6
an	8.8	13.3	5.9	17.3	8.4	5.7	6.0	11.3
di	19.0	21.4	14.4	18.6	19.8	20.0	19.4	19.6
hy	25.6	12.1	15.3	24.0	20.2	20.0	25.2	26.4
ol	9.0	14.7	35.6	8.9	12.3	13.9	10.1	9.9
mt	3.1	3.5	3.7	4.3	3.4	4.3	3.8	2.6
ct	0.2	0.2	0.3	0.2	0.2	0.3	0.3	0.2
il	5.9	5.8	5.0	4.2	6.3	6.1	6.4	5.5
ap	1.2	1.1	1.0	0.8	1.1	1.2	1.3	0.8

Wt.%	N-40	N-55	N-60	N-72	N-76	N-79	N-84	N-88
z	0.1	0.1	0.1	0.1	0.1	0.1	0.0	0.0
or	9.5	11.5	11.2	13.2	12.7	7.5	3.1	4.8
ab	9.5	12.6	9.6	11.7	8.6	15.7	18.9	8.0
an	14.5	12.7	6.5	7.5	7.5	14.0	20.4	9.7
di	18.6	19.2	12.3	20.7	16.0	20.4	17.6	14.9
hy	29.8	22.8	22.5	23.2	28.7	25.0	31.8	47.2
ol	9.3	11.0	27.3	13.4	16.8	8.5	1.7	7.9
mt	2.5	3.3	3.5	3.1	3.2	2.5	2.4	3.2
ct	0.2	0.2	0.3	0.3	0.3	0.2	0.2	0.3
il	5.0	5.5	5.7	5.6	5.1	5.3	3.5	3.4
ap	1.1	1.1	1.1	1.3	1.1	0.9	0.6	0.6

Calculated on a H_2O-free basis.

TABLE 18 (continued)

C.I.P.W. NORMS OF LAVAS

Wt.%	N-89	N-91	N-100	N-102	N-105	N-113	N-117	N-126
z	0.0	0.1	0.1	0.1	0.1	0.1	0.1	0.1
or	3.8	9.4	11.4	9.5	8.9	4.4	9.3	8.1
ab	22.0	15.3	16.9	16.0	13.4	15.8	13.3	15.3
an	27.9	14.9	14.1	14.2	12.1	14.8	13.7	12.8
di	19.0	18.9	21.8	19.1	18.9	18.5	16.7	20.0
hy	16.6	27.1	16.5	27.1	29.8	34.4	33.0	28.3
ol	4.6	4.9	8.5	4.7	7.4	2.1	4.5	5.4
mt	3.2	3.2	3.5	3.2	3.1	4.2	3.9	3.7
ct	0.0	0.1	0.1	0.2	0.2	0.2	0.2	0.2
il	2.4	5.2	6.0	5.0	5.0	4.8	4.5	5.3
ap	0.5	0.9	1.1	0.9	1.0	0.9	0.9	1.0

Wt.%	N-133	N-135	N-149	N-160	N-187	N-190	N-225	N-231
z	0.1	0.1	0.1	0.1	0.1	0.1	0.0	0.1
or	12.1	14.8	5.4	6.5	7.6	12.9	1.2	8.4
ab	9.3	12.0	13.6	15.6	14.5	14.3	14.0	11.2
an	6.7	8.0	14.5	12.8	14.7	7.8	18.0	11.6
di	18.9	19.7	20.3	18.7	26.1	18.4	19.5	15.0
hy	20.5	15.1	25.2	27.4	23.9	26.5	32.7	35.0
ol	22.7	20.4	11.3	9.3	3.1	9.2	6.6	9.1
mt	3.4	3.2	3.4	3.1	3.6	2.7	3.1	3.9
ct	0.3	0.2	0.2	0.2	0.2	0.3	0.2	0.2
il	5.0	5.4	5.2	5.3	5.3	6.3	4.3	4.8
ap	1.1	1.1	0.8	1.1	0.9	1.4	0.6	0.9

Calculated on a H_2O-free basis.

TABLE 18 (continued)

C.I.P.W. NORMS OF LAVAS

Wt.%	N-245	N-355	N-356	N-357	N-361	N-399	N-400	N-405
Z	0.0	0.1	0.1	0.1	0.0	0.1	0.1	0.1
or	4.5	7.6	16.8	10.3	4.4	5.0	13.4	7.4
ab	22.1	14.1	12.5	17.3	18.5	14.6	11.5	15.4
an	22.7	11.0	7.3	13.8	17.0	12.9	6.6	14.6
di	18.2	24.2	15.2	17.1	20.2	19.7	16.3	20.8
hy	18.3	23.9	24.0	27.5	18.2	28.7	23.3	24.3
ol	6.9	9.2	15.2	3.7	14.2	9.3	19.1	7.8
mt	3.4	3.4	2.9	3.9	4.0	3.1	3.3	3.2
ct	0.2	0.2	0.2	0.2	0.2	0.2	0.2	0.1
il	3.1	5.2	4.9	4.8	2.9	5.5	4.9	5.4
ap	0.7	1.1	0.9	1.1	0.5	1.0	1.2	1.0

Wt.%	N-406	N-440	N-442	N-462	N-517	N-519	KC-204
Q	-	-	-	-	-	0.9	-
Z	0.1	0.1	0.1	0.1	0.1	0.1	0.1
or	7.9	11.1	12.7	12.7	13.3	4.7	14.7
ab	15.6	10.5	12.8	10.7	12.3	16.5	12.3
an	14.3	7.4	11.9	9.6	7.4	19.8	7.4
di	21.3	15.1	17.7	15.2	18.6	21.0	17.8
hy	20.8	31.1	32.0	27.2	21.1	26.5	24.5
ol	10.8	14.7	2.0	15.2	16.9	-	12.5
mt	2.8	3.1	3.4	3.1	3.2	4.3	3.1
ct	0.1	0.3	0.2	0.3	0.2	0.1	0.2
il	5.4	5.5	6.1	5.0	5.8	5.3	6.1
ap	0.9	1.2	1.3	1.0	1.2	0.8	1.3

Calculated on a H_2O-free basis.

TABLE 19

C.I.P.W. NORMS OF PICRITES

Wt.%	N-21	N-22	N-23	N-27	N-41	N-90	N-95	N-163	N-364
Z	0.1	0.1	0.1	0.1	0.1	0.1	0.1	0.0	0.0
or	14.8	12.0	8.0	12.8	13.3	7.2	6.4	3.7	3.1
ab	13.2	9.4	7.2	9.4	12.0	7.7	13.1	13.2	14.7
an	5.0	5.2	4.2	5.9	5.5	5.8	10.6	16.2	16.9
di	22.1	18.1	23.5	16.1	21.5	11.5	22.5	20.7	12.9
hy	21.5	23.0	16.4	18.9	18.2	23.6	20.8	31.2	35.0
ol	11.7	22.5	31.7	25.4	17.8	36.4	17.1	7.0	10.0
mt	3.2	3.4	3.7	4.4	3.3	3.2	3.4	3.1	3.8
ct	0.2	0.3	0.3	0.3	0.2	0.3	0.2	0.2	0.2
il	7.0	5.1	4.2	5.6	6.9	3.5	4.9	4.1	2.9
ap	1.3	1.0	0.8	1.1	1.2	0.8	0.9	0.6	0.5

Calculated on a H_2O-free basis.

TABLE 20

SUMMARY OF CHEMICAL ANALYSES

Wt.%	47 Basalts and Limburgites Range	Mean	Anhydrous Mean	9 Picrites Range	Mean	Anhydrous Mean
SiO_2	45.1 - 50.7	48.9	49.7	46.1 - 49.5	47.6	48.2
TiO_2	1.24 - 3.26	2.64	2.68	1.51 - 3.62	2.53	2.56
Al_2O_3	5.61 - 15.1	8.77	8.91	4.35 - 9.52	6.77	6.86
Fe_2O_3	1.6 - 7.5	2.0*	2.0*	2.6 - 5.0	2.4*	2.4*
FeO	3.76 - 11.7	10.2*	10.5*	6.32 - 9.80	9.38*	9.50*
MnO	0.09 - 0.18	0.15	0.15	0.15 - 0.17	0.16	0.16
MgO	8.26 - 23.3	15.1	15.3	14.9 - 26.8	19.1	19.4
CaO	4.85 - 10.5	7.56	7.68	4.46 - 8.65	6.80	6.90
Na_2O	0.91 - 2.59	1.62	1.64	0.84 - 1.72	1.29	1.31
K_2O	0.20 - 2.92	1.58	1.61	0.52 - 2.46	1.50	1.52
P_2O_5	0.19 - 0.55	0.41	0.42	0.19 - 0.54	0.38	0.39
H_2O	0.30 - 3.47	1.63	-	0.91 - 1.58	1.29	-

p.p.m.						
Ba	175 - 1540	795	795	155 - 960	597	597
Cr	198 - 1526	929	929	690 - 1265	1005	1005
Ni	220 - 1380	752	752	703 - 1470	995	995
Rb	9 - 81	33	33	11 - 46	27	27
Sr	275 - 1240	859	859	275 - 1240	795	795
Zr	130 - 454	300	300	130 - 430	281	281

* - adjusted values.

TABLE 21

SUMMARY OF C.I.P.W. NORMS

| Wt.% | 47 Lavas | | 9 Picrites | |
	Range	Mean	Range	Mean
Q	0.0 - 0.9	0.0	-	-
Z	0.0 - 0.1	0.1	0.0 - 0.1	0.1
or	1.2 - 17.7	9.5	3.1 - 14.8	9.0
ab	3.1 - 22.1	13.8	7.2 - 14.7	11.1
an	7.8 - 22.7	12.0	4.2 - 16.9	8.4
di	14.4 - 26.1	18.4	11.5 - 23.5	18.6
hy	12.1 - 47.2	24.2	16.4 - 35.0	24.4
ol	0.0 - 35.6	13.2	7.0 - 36.4	19.1
mt	2.4 - 4.3	2.9	3.1 - 4.4	3.5
ct	0.0 - 0.3	0.2	0.2 - 0.3	0.2
il	2.4 - 6.4	5.1	2.9 - 6.9	4.9
ap	0.5 - 1.3	1.0	0.5 - 1.3	0.9

terms and relative to Na_2O. The trace elements Ba, Sr, and Zr are also exceptionally high for such basic (MgO-rich) compositions. These chemical aspects are described in more detail below.

The considerable excess of hy over ol in the norms of the lavas is a reflection of the high SiO_2 content and there is a marked contrast between contents of normative and modal olivine - compare Table 17 and petrographic data given in Chapter 2.

(iii) Variation

Table 22 is a correlation matrix which gives the correlation coefficients (r) between the 16 chemical variables in the 47 olivine-rich lavas.

Chayes (1960; 1962) has emphasised that correlation coefficients between variables in an array of variables which have a constant sum (100 in the present case) must be treated with caution. The main restriction imposed by the constant sum factor is that negative correlations between variables which make a significant contribution to the total variance of the array tend to be enhanced. This is because a real increase in the concentration of one oxide variable causes an apparent decrease in the concentration of all the remaining oxide and element variables. Before assessing the correlation matrix (Table 22) it is, therefore, advisable to examine the contribution each variable makes to the total variance of the 47 member array.

The standard deviations (σ) and variances (σ^2) of each oxide and trace element are presented in Table 23. One variable (MgO) contributes more than half the total variance of the array and 5 variables (MgO, Al_2O_3, CaO, SiO_2 and Fe_2O_3 T) make up more than 95% of the total variance. These findings are, in general terms, similar to those

TABLE 22

CORRELATION MATRIX

	SiO_2	TiO_2	Al_2O_3	Fe_2O_3T	MnO	MgO	CaO	Na_2O	K_2O	P_2O_5	Rb	Sr	Ba	Zr	Cr	Ni
SiO_2	1.00															
TiO_2	-0.19	1.00														
Al_2O_3	+0.45	-0.51	1.00													
Fe_2O_3T	-0.38	-0.09	+0.14	1.00												
MnO	+0.18	-0.36	+0.49	+0.51	1.00											
MgO	-0.52	+0.23	-0.92	-0.19	-0.50	1.00										
CaO	+0.34	-0.33	+0.86	+0.42	+0.55	-0.91	1.00									
Na_2O	+0.42	-0.38	+0.90	+0.14	+0.45	-0.88	+0.78	1.00								
K_2O	-0.17	+0.65	-0.54	-0.57	-0.63	+0.43	-0.63	-0.53	1.00							
P_2O_5	-0.22	+0.84	-0.58	-0.37	-0.50	+0.38	-0.51	-0.49	+0.80	1.00						
Rb	+0.02	+0.57	-0.48	-0.51	-0.55	+0.36	-0.56	-0.30	+0.71	+0.68	1.00					
Sr	-0.20	+0.75	-0.55	-0.48	-0.65	+0.40	-0.59	-0.38	+0.88	+0.83	+0.74	1.00				
Ba	-0.22	+0.61	-0.53	-0.50	-0.61	+0.45	-0.66	-0.41	+0.88	+0.73	+0.74	+0.92	1.00			
Zr	-0.20	+0.82	-0.62	-0.45	-0.62	+0.45	-0.60	-0.50	+0.85	+0.86	+0.76	+0.91	+0.84	1.00		
Cr	-0.21	+0.22	-0.80	-0.26	-0.48	+0.79	-0.72	-0.69	+0.34	+0.37	+0.43	+0.39	+0.37	+0.42	1.00	
Ni	-0.56	+0.28	-0.85	-0.18	-0.48	+0.91	-0.89	-0.82	+0.49	+0.41	+0.40	+0.45	+0.51	+0.50	+0.69	1.00

TABLE 23

ANALYSIS OF VARIANCE

	Standard Deviation (σ)	Variance (σ^2)	% of Total Variance
SiO_2	0.983	0.97	5.7
TiO_2	0.462	0.21	1.3
Al_2O_3	1.80	3.25	19.2
Fe_2O_3 T	0.798	0.64	3.8
MnO	0.0164	*	*
MgO	3.12	9.77	57.7
CaO	1.22	1.49	8.8
Na_2O	0.378	0.14	0.8
K_2O	0.653	0.43	2.5
P_2O_5	0.0927	0.01	*
Rb	0.0015	*	*
Sr	0.023	*	*
Ba	0.031	*	*
Zr	0.0080	*	*
Cr	0.023	*	*
Ni	0.025	*	*

Concentrations of oxides and trace elements calculated on a wt. % basis.

* - insignificant.

reported by Chayes (1964) in a survey of variance-covariance in analyses of calc-alkaline basalt - andesite - dacite suites. However, Chayes found that SiO_2, not MgO, made the dominant contribution to the total variance - the range being 37 - 76% of σ^2 Total, and that SiO_2, together with Al_2O_3, CaO, FeO, Fe_2O_3 and MgO - which individually contributed 3-9% - accounted, on average, for more than 97% of the total variance.

From the reasoning developed by Chayes (1960, pp. 4185-4188) it is clear that, as a result of the constant sum factor, at least 2 of the correlation coefficients between the variable with the dominant variance (MgO) and variables with smaller but significant variance (Al_2O_3, CaO, SiO_2 and Fe_2O_3 T) are likely to be strongly negative. The expected value of the correlation coefficients resulting from the constant sum factor can be estimated from the following equation, several assumptions being made :

$$E\ (r_{1j}) \ = \ \frac{\sigma_1}{\sigma_{c(1 - M')}}$$

Variable 1 is MgO and variables j = 2 - 5 are Al_2O_3, CaO, SiO_2 and Fe_2O_3 T, σ c is the mean standard deviation of variables j = 2 - 5 and M' is the reduced number of variables, i.e. 5. The equation and the assumptions made are given by Chayes (1962, p.442).

Substituting in this equation it was found that a correlation coefficient of -0.65 could result between MgO and the other significant variables solely because of the constant sum factor. The negative correlations between MgO and SiO_2, Al_2O_3 and CaO are, therefore, not as high as the values of r indicate.

Correlation between the variable of dominant variance (MgO) and

the components which make very small contributions to the total variance
of the array of variables (Na_2O, K_2O, P_2O_5, TiO_2 and trace elements) is
virtually unaffected by the constant sum factor and the correlation
coefficients in Table 22 can be accepted without reservation.

Certainly the most interesting aspects of Table 22, and, perhaps,
also the most genetically significant aspects are :

(a) that all correlation coefficients between pairs in the
     group of components MgO, TiO_2, K_2O, P_2O_5, Rb, Sr, Ba,
     Zr, Cr and Ni are positive.

(b) the totally contrasting behaviour of K_2O and Na_2O.

The above analysis of variance has demonstrated that as a simple
index of variation for the Nuanetsi olivine-rich lavas, the MgO content
is an obvious choice.   From a petrological standpoint the use of MgO
as a variation index is also sound since any crystal-liquid processes
during the development of the Nuanetsi MgO-rich magmas must have
involved mafic mineral assemblages with high MgO contents.   Table 24,
therefore, qualitatively summarises the covariance between MgO and the
other components - the appropriate modification being made in the
case of CaO, Al_2O_3, SiO_2 and Fe_2O_3 T.   Because of the constant sum
factor one is not dealing with independent variables and quantitative
assessment of the correlation coefficients is difficult.   However,
Student t tests are not inappropriate in the case of correlation
between MgO and TiO_2, K_2O, P_2O_5 and the trace elements.   These tests
indicate that r values of 0.36 and 0.45 are significant at the 99%
and 99.9% levels respectively.

Figures 9 - 11 are variation diagrams in which MgO is plotted
against SiO_2, Na_2O and K_2O.   This has been done to illustrate graphically

TABLE 24

CORRELATION WITH MgO

Insignificant	Significant		Very Significant	
	+	-	+	-
SiO_2	TiO_2	Al_2O_3	K_2O	Na_2O
Fe_2O_3 T		CaO	P_2O_5	MnO
			Rb	
			Sr	
			Ba	
			Zr	
			Cr	
			Ni	

FIGURE 9

MgO v. SiO$_2$ variation diagram.

     ● : basalts and limburgites - 44 in number.

     □ : picrites - 9.

     ○ : lavas enriched in cumulus olivine - 2.

     △ : lava enriched in cumulus orthopyroxene - 1.

     Control lines from typical magnesian olivine

(c. Fo$_{85}$), full lines, and orthopyroxene (c. En$_{90}$),

broken lines, have been added to this variation diagram.
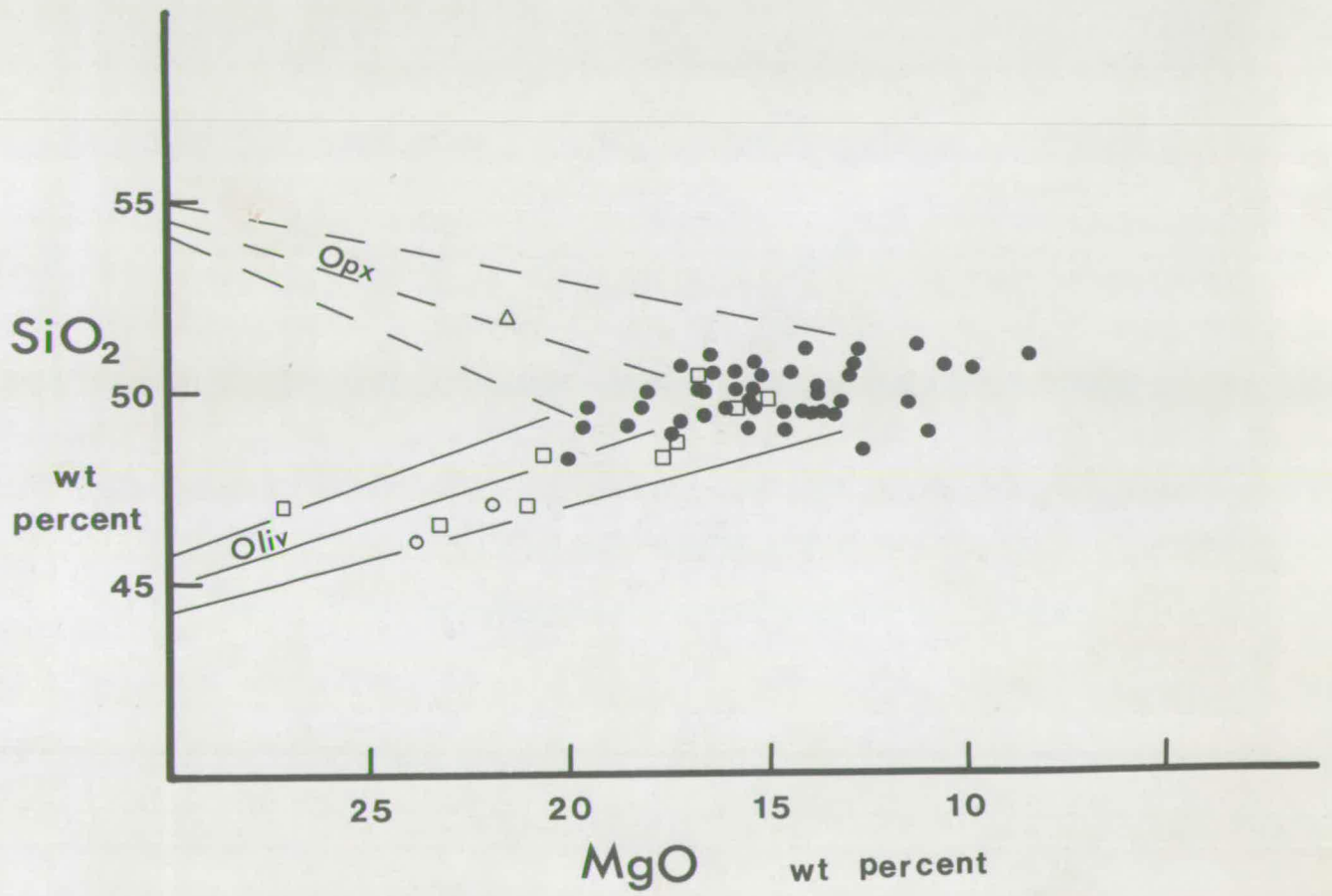
FIGURE 10

MgO v. Na$_2$O variation diagram

Key as for Figure 9.

Control lines from magnesian olivine (full lines)

and orthopyroxene (broken lines) have again been added.
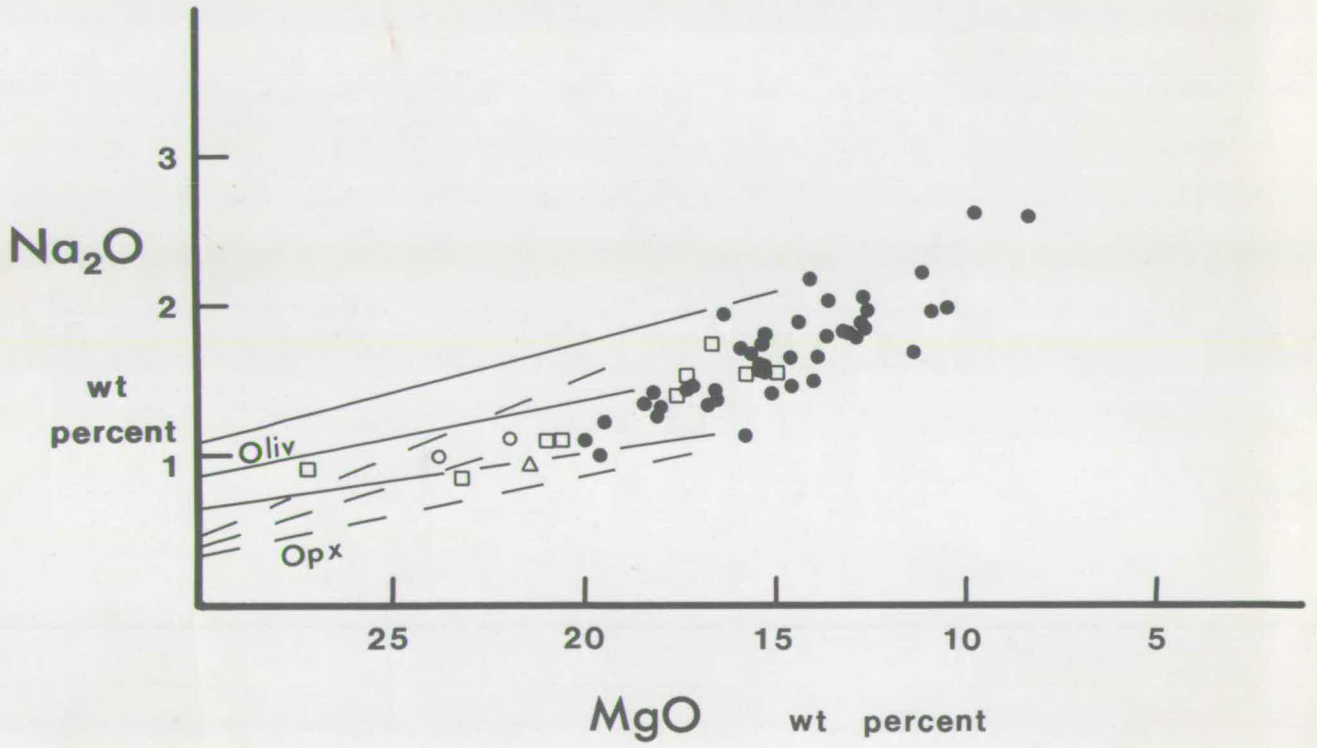
FIGURE 11

MgO v. K_2O variation diagram

Key as for Figure 9.

Olivine and orthopyroxene control lines have again been added.
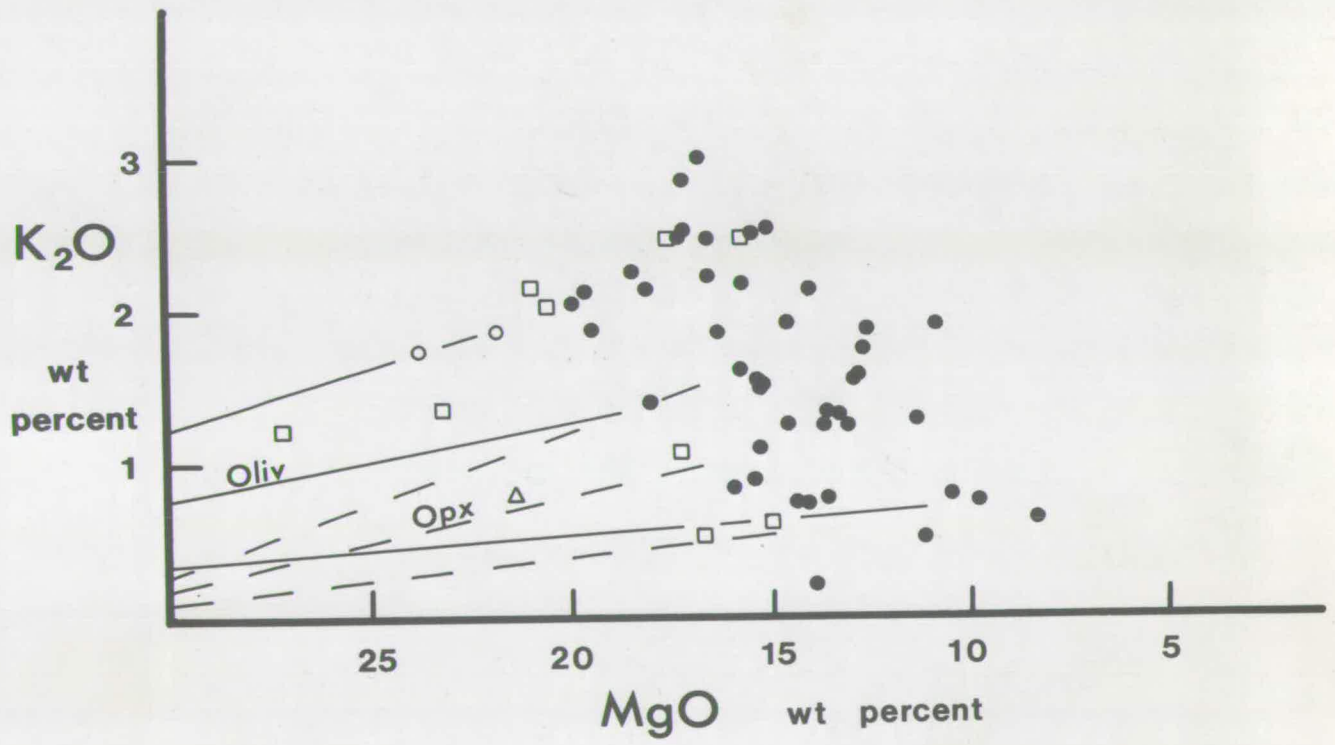
very significant and insignificant correlations, and to demonstrate possible relationships between the lavas and the picrites - the 9 picrite analyses have also been plotted in these Figures.

The olivine and orthopyroxene control lines in Figs. 9 - 11 are lines which radiate from the plotted positions of a typical forsteritic olivine - say Fo_{85}, and that of an enstatite-rich orthopyroxene - say En_{90}. Three lavas which were suspected, on petrographic grounds, of being cumulus-enriched - N-13 and N-60 in olivine phenocrysts and N-88 in inherited orthopyroxene phenocrysts - are plotted in Figs. 9 - 11 with a distinctive ornament.

The relationship between the control lines and the rock composi-tions is clearly consistent with earlier proposals that the picrites are the hypabyssal analogues of the lavas and that they tend to display varying degrees of enrichment in cumulus olivine. Furthermore, two of the lavas (N-13, N-60) do appear to have experienced significant enrichment in cumulus olivine phenocrysts and one lava (N-88), which contains 21% orthopyroxene phenocrysts, has had its bulk composition significantly modified by orthopyroxene accumulation - a process which must have taken place at elevated pressures (see Chapters 3 and 5). These conclusions are not solely based on the evidence of Figs. 9 - 11. Variation diagrams in which MgO is plotted against other chemical components display similar features.

One aspect of the average analyses in Table 20 is apparently anomalous with respect to the olivine-enrichment mechanism proposed above - the K_2O/Na_2O ratio of the picrites is higher than that determined in the basalts and limburgites. However, the picrites analysed are mainly from the Beacon - Gomakwe area of the Nuanetsi syncline northern

limb. The lavas, and hence also the picrites, of this area are somewhat more K_2O-rich than the Olivine-rich Group lavas from other areas of the province.   The apparent anomaly is, therefore, considered to be the result of a sampling bias and in Table 20, picrites, which are dominantly from a relatively restricted area, are compared with basalts and limburgites with a much wider areal distribution.

From this assessment of the variation of rock compositions using MgO as a variation index it is concluded that the major or primary compositional variation is that shown by the 44 lava compositions.   The compositions of the picrites and the remaining three lavas can be related to the major variation trend through simple processes of crystal sorting - these processes being the cause of the minor or secondary element of the total compositional variation.

Only the overt aspects of the compositional variation have been considered above.   In the following Chapters the variation is examined in more detail - using transformed variables in Chapter 6 and from the standpoint of phase relations, known and estimated, in natural and synthetic systems in Chapter 5.

Potassium and Associated Elements

Potassium is largely rejected by the major silicate phases of any probable 3 or 4- phase peridotite assemblage in the zone of magma generation in the upper mantle (Griffin and Murthy, 1968a and b; Harris, 1957; Oxburgh, 1964).   Although relevant data are sparse, this is probably also true of P, Rb, Sr, Ba, Zr, Pb, Th, U and the rare earth elements. Ringwood (1966) proposed the term 'incompatible elements' for this group.   However, the term 'K and associated elements' is preferred by the present author since it avoids the genetic implications

of the term 'incompatible elements'.

Because of the chemical discrimination by the major silicate phases, K and associated elements are likely to be concentrated in the initial liquid formed on the partial melting of mantle peridotite and should remain in the residual liquid during any subsequent fractional crystallisation.   This aspect of the minor and trace element geochemistry of basalts was fully appreciated by Harris (1957).

The enrichment level of K and associated elements in basalts has been an important aspect of the arguments developed in several publications dealing with the origin of basalts, viz. Harris (1957); Engel et al (1965), Green and Ringwood (1967), Gast (1968) and O'Hara (1968a).

The mean of the 47 lava analyses (Table 20) is reproduced in Table 25 along with the average composition of 182 olivine tholeiites as compiled by Manson (1967) and Prinz (1967).   Comparison of these average analyses, despite the limited number of trace element data included in the general average, confirms the conclusions of Monkman (1961), Cox et al (1965) and Cox et al (1967) that the Nuanetsi olivine-rich rocks are greatly enriched in K_2O, P_2O_5, TiO_2, Ba, Sr and Zr in relation to other basalts.

Correlation coefficients between K_2O, P_2O_5, Ba, Rb, Sr, and Zr which are given in Table 22 are reproduced in Table 26. Correlations with TiO_2 are also given and these demonstrate that Ti can also be considered as an element which is associated with K in these rocks.   In fact, although Ti is not excluded by the major minerals of peridotite (Mercy and O'Hara, 1967), on the basis of its geochemical behaviour this element has frequently been considered as one of the 'incompatible elements', e.g., by Green and Ringwood (1967).

TABLE 25

AVERAGE THOLEIITIC ANALYSES

Wt.%	1	2	3
SiO_2	49.7	49.0	45.92
TiO_2	2.68	1.7	1.02
Al_2O_3	8.91	15.6	10.66
Fe_2O_3	2.0*	2.6	2.98
FeO	10.5*	8.8	8.17
MnO	0.15	0.17	0.18
MgO	15.3	8.5	19.56
CaO	7.68	10.4	9.47
Na_2O	1.64	2.3	1.34
K_2O	1.61	0.6	0.14
P_2O_5	0.42	0.23	0.12

p.p.m.			
Ba	795	215	59
Cr	929	218	1040
Ni	752	130	695
Rb	33	18	2.4
Sr	859	350	170
Zr	300	91	68

1 - 47 Nuanetsi lavas (from Table 20).

2 - 182 olivine tholeiites (Manson, 1967, Table VI, no. 8 and Prinz, 1967, Table II, no. 2).

3 - 48 Baffin Island - West Greenland lavas (D.B. Clarke, personal communication).

* - adjusted value.

TABLE 26

CORRELATION MATRIX

	K_2O	P_2O_5	TiO_2	Ba	Rb	Sr	Zr
K_2O	1.00						
P_2O_5	+0.80	1.00					
TiO_2	+0.65	+0.84	1.00				
Ba	+0.88	+0.73	+0.61	1.00			
Rb	+0.71	+0.68	+0.57	+0.74	1.00		
Sr	+0.88	+0.83	+0.75	+0.92	+0.74	1.00	
Zr	+0.85	+0.86	+0.82	+0.84	+0.76	+0.91	1.00

Level of significance — 99% when r = 0.36

99.9% when r = 0.45

Because the oxides K_2O, P_2O_5 and TiO_2 and trace elements Ba, Rb, Sr and Zr together contribute less than 5% of the total variance of the closed array of compositions, and because all the correlations between these variables are positive, the constant sum restrictions do not apply and the significance of the correlations can be assessed by the Student t test.   These highly significant correlation coefficients clearly demonstrate that in addition to being relatively abundant, K and the associated elements P, Ti, Ba, Rb, Sr and Zr behave as a geochemically coherent group in the Nuanetsi olivine-rich lavas.

Content of MgO

Average MgO contents of 15.1% in the lavas and 19.1% in the picrites convincingly confirm the overall picritic character of the Olivine-rich Group.

It is pertinent at this stage to consider the status of this picritic character in the broader context of the complete Nuanetsi volcanic succession.   The relationship between the picritic Olivine-rich Group and the thicker sequence of olivine-poor Upper Basalts is of particular interest.   This aspect of the picritic compositions is best demonstrated by a histogram which gives the frequency distribution of MgO contents in all available Nuanetsi basaltic analyses (Fig. 12). Most of the data in this histogram are from Tables 1, 16, 17 and C-3. Further analyses were taken from Cox et al (1967, Table 1), Cox et al (1965, Table 31).   All the analyses were recalculated on an anhydrous basis.

There is clearly a bimodal distribution in Fig. 12.   However, because the olivine-rich rocks have been relatively oversampled as a

FIGURE 12

Frequency distribution of MgO determinations in
basaltic rocks from the Nuanetsi Igneous Province.

Upper Basalts

MgO   wt percent
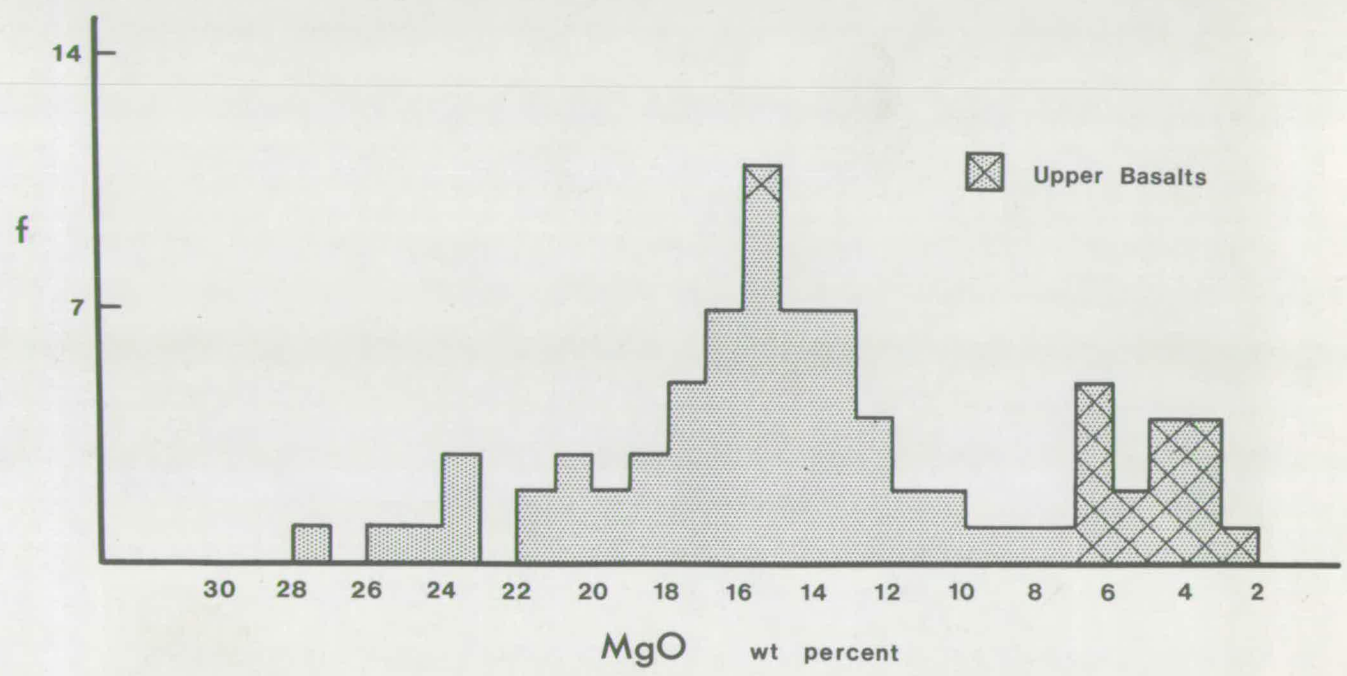
result of the current research, no significance can be attached to the actual sizes of the two modes. A proportional representation of the many olivine-poor and olivine-free basalts which have been collected and examined, but not analysed, in the current research would greatly enhance the numbers of MgO contents in the 2-7% range.

A deliberate effort was made to over-represent in the samples selected for analysis lavas which had olivine contents intermediate between the typical olivine-rich types and the olivine-poor Upper Basalts. Specimens N-89, N-100, N-245 and N-519 are examples of this intermediate type; they have MgO contents in the range 8-11%. Because of this bias in favour of lavas with intermediate olivine contents (9-15%) in Fig. 12, it is confidently concluded that lavas with intermediate olivine contents, or MgO contents in the range 7-10%, are relatively rare in the succession of basic lavas. The olivine-rich lavas are, therefore, not only stratigraphically but also compositionally distinct from the thick succession of Upper Basalts.

This is a further piece of evidence which suggests that the olivine-rich lavas are unlikely to have a direct genetic relationship with the Upper Basalts. As is mentioned in Chapter 1, this aspect of the volcanic succession was noted by Cox et al (1965) on the basis of an addition-subtraction variation diagram. It is further discussed in Chapter 5.

Comparison with other Suites

The analyses presented in Table 25 clearly demonstrate that the average of the Nuanetsi olivine-rich lavas is, in two respects, in marked contrast to the average of a general compilation of olivine tholeiite analyses, viz.

(a) the content of MgO, and Cr and Ni.

      (b)   the content of K and the associated elements Ti, P,

          Ba, Rb, Sr and Zr.

Combinations of high MgO, Cr and Ni with extremely high contents

of K and associated elements are found in the mafic members of the

K-rich volcanic provinces of Leucite Hills, Wyoming (Carmichael, 1967),

the Western Rift in S.W. Uganda (Holmes, 1950; Higazy, 1954) and West

Kimberley, Australia (Wade and Prider, 1940) and occasionally in the

Italian Quaternary volcanic province (J.D. Appleton, personal communi-

cation).   In contrast to the Nuanetsi lavas, however, these suites

are characterised by the occurrence, often in abundance, of the silica-

undersaturated minerals leucite, kalsilite, melilite and phlogopite.

Nevertheless the Nuanetsi lavas do provide a compositional link

between these extreme compositions and more common basalts which are

characterised by an excess of Na over K and have compositions which

generally conform to the mean tholeiite in Table 25.

Finally, attention is drawn to the occurrence of a suite of

Tertiary picritic tholeiite lavas in Baffin Island, Canada and the

adjacent parts of West Greenland (Clarke, 1968). The average of 48

analyses is given in Table 25 to demonstrate that the overall picritic

character of a thick succession of lavas is a feature which is not

exclusive to the Nuanetsi Igneous Province - in fact the Baffin

Island - West Greenland lavas are considerably more MgO-rich than

their Nuanetsi counterparts. However, with respect to K and associated

elements the contrast between the two suites is total.

CHAPTER 5

PHASE EQUILIBRIUM ASPECTS

In this chapter the lava analyses are considered as composition points in a pseudo-quaternary natural basaltic system. Geometrical projections within this equilibrium tetrahedron allow an assessment of the positions of the rock compositions relative to mineral composition points and to the probable location of phase boundaries.

On the basis of such projected phase diagrams, the inherited nature of the large orthopyroxene phenocrysts is again demonstrated and the primitive picritic character of the Olivine-rich Group is confirmed.

The genesis of the olivine megacryst - orthopyroxene phenocryst assemblage is considered and, in the light of known and estimated pressure-induced changes to phase relations in analogous natural and synthetic systems, it is concluded that this bimineralic assemblage could have crystallised from these compositions in the depth range of 22 - 30 km.

However, all aspects of the compositional variation of the lavas - in particular the sympathetic relationship between MgO and K_2O - cannot be the result of the fractionation of this harzburgite (olivine + orthopyroxene) assemblage alone. It is concluded, therefore, that there must be yet another factor in the evolutionary history of the Nuanetsi olivine-rich magmas.

Data Reduction and Projection Scheme

Chemical, mineralogical and textural features of basic igneous rocks have been extensively described with reference to phase relations in synthetic systems such as $CaMgSi_2O_6 - Mg_2SiO_4 - CaAl_2Si_2O_8 - SiO_2$

and the bounding ternary faces, for example, by Bowen (1914 and 1928) and by Osborn and Tait (1952).   In general there is a similarity between phase assemblages and crystallisation behaviour in the synthetic and natural systems.   However, since only 4 of the 12 major and minor oxides in basic rocks are included in the synthetic system, the similarity between the crystallisation of synthetic melts and basic magma should not be overstressed.

Experimental studies on natural basic rocks, carried out over the last decade, have led towards an understanding of crystallisation behaviour in a complex natural system.   From the results of these experiments it has been possible to estimate the essential features of the phase relations in a natural basic system with its 12 major and minor oxide components.   It should also be possible to describe and predict, with some measure of success, the crystallisation histories of analysed rocks, the melting relations of which have not been determined, by relating the bulk compositions to these phase relations.

The graphical presentation of phase relations in a 12 component system does, however, present considerable geometrical problems and two methods of data reduction have been adopted in recent attempts to draw natural phase diagrams :

(a) A norm-based method   - Coombs (1963), Muir and Tilley (1964, Fig. 6) and O'Hara (1965, Figs. 2 and 3), by considering only normative diopside, plagioclase, olivine and quartz, or nepheline, have reduced the analyses of tholeiitic and other basalts to 4 components and after carrying out geometrical projections within this tetrahedron, have constructed partial natural phase diagrams.   In general,

70 - 90%, by weight, of the rock bulk compositions is included in this scheme.

(b) An oxide-based method. - By considering chemical affinities between cations in basic magmas, O'Hara (1968a) has devised a scheme which allows 10 of the major and minor oxides of basic rocks to be expressed in terms of 4 components. These components are analogous to Al_2O_3, CaO, MgO and SiO_2 but have been labelled R_2O_3, XO, YO, ZO_2 to avoid confusion with the synthetic system. This nomenclature is a modification of the A - C - M - S labelling scheme used by O'Hara. This data reduction method is described in full by O'Hara (1968a, Fig. 4).

This latter data reduction scheme has been adopted in the current investigation since it has already been tested (O'Hara, 1968a; Jamieson, in press) and it appears to have the following advantages over the normative selection method :

(a) Although co-ordinates are calculated on a weight percent basis, the calculation, for example, of all FeO, MnO and MgO as YO avoids the distortion brought about by varying Fe/Mg ratios in the normative scheme.

(b) Since almost all the major minerals of basic and ultrabasic rocks have composition points in the system R_2O_3-XO-YO-ZO_2, e.g. diopside is XO.YO.$2ZO_2$, a large number of convenient projection points and planes are available within the tetrahedron. The comprehensive nature of this scheme allows a wide range of basic and ultrabasic rock compositions to be handled, for example, types over-saturated and under-saturated in silica can be represented on the same diagram.

As described by O'Hara (1968a, Fig. 4) a computer program has
been written to calculate the co-ordinates of analyses in the R_2O_3-XO-
YO-ZO_2 tetrahedron and in various sub-projections within the tetrahedron.
Co-ordinates of up to 12 sub-projections are printed out and the user
can select those most appropriate to his needs.

In the present study the following three sub-projections are
used :

(a) a projection to, or from, the clinopyroxene composition
point, XO.YO.$2ZO_2$, into the plane YO - R_2O_3 - XO.ZO_2.

(b) a projection to, or from, the olivine composition point,
$2YO.ZO_2$, into the plane R_2O_3 - XO.ZO_2 - YO.ZO_2.

(c) a projection to, or from, the orthopyroxene composition
point, YO.ZO_2, into the plane $2YO.ZO_2$ - $2XO.3ZO_2$ - $2R_2O_3$.
$3ZO_2$.

The analysed Nuanetsi picrites, limburgites and basalts are
presented in these projections in Figs. 13-15 respectively. The phase
boundaries projected in these natural phase diagrams are those on the
boundary of the primary phase volume of the mineral which is the
projection point, i.e. olivine, clinopyroxene or orthopyroxene. They
have been drawn on the basis of the projected composition points and
the atmospheric pressure melting relations of some 30 basalts. Most
of the melting relations were determined in the Geophysical Laboratory,
Washington, D.C., and they have been reported regularly by Tilley, Yoder
and Schairer in the Annual Report of the Director during the period
1963-68. These phase boundaries have already been used by O'Hara
(1968a) and Jamieson (in press) to describe and predict basalt crystal-
lisation behaviour at low pressure.

FIGURE 13

A projection from $XO.YO.2ZO_2$ (Clinopyroxene) into the plane $XO.R_2O_3 - YO - ZO_2$ of phase relations and Nuanetsi rock compositions.

The projected phase relations, at atmospheric pressure, on the boundary of the clinopyroxene primary phase volume have been taken from O'Hara (1968a, Fig. 6).

The fields labelled OLIV, PLAG, and OPX correspond to the loci of liquid compositions in the equilibria Oliv + Cpx + Liq, Plag + Cpx + Liq and Opx + Cpx + Liq on the surface of the clinopyroxene primary phase volume.

The projected data points are as follows :

● : basalts and limburgites - 44 in number
□ : picrites - 9
○ : lavas enriched in cumulus olivine - 2
△ : lava enriched in cumulus orthopyroxene - 1.

The compositions are expressed in weight %.
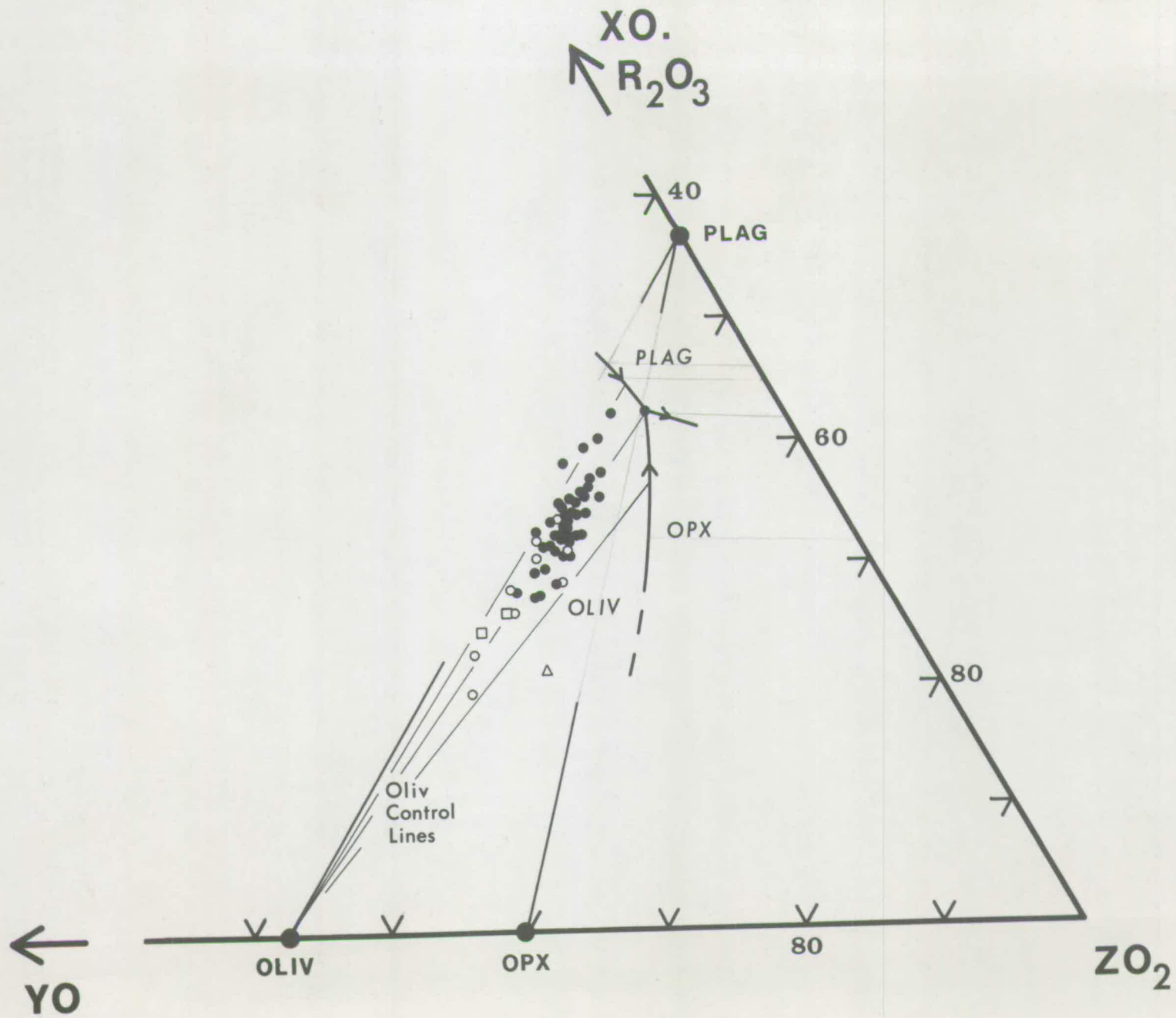
FIGURE 14

A projection from $2YO.ZO_2$ (Olivine) into the plane
R_2O_3 - $XO.ZO_2$ - $YO.ZO_2$ of phase relations and Nuanetsi
rock compositions.

The projected phase relations, at atmospheric
pressure, on the surface of the olivine primary phase
volume have been taken from O'Hara (1968a, Fig. 4).

The fields labelled PLAG, CPX and OPX correspond
to the loci of liquid compositions in the equilibria Plag +
Oliv + Liq, Cpx + Oliv + Liq and Opx + Oliv + Liq on the
surface of the primary phase volume of olivine.

The intersection of the olivine - plagioclase join
with the projection plane - the olivine - plagioclase
piercing point - is shown.

The projected data points are as follows :

● : basalts and limburgites - 44 in number.
□ : picrites - 9.
○ : lavas enriched in cumulus olivine - 2.
△ : lava enriched in cumulus orthopyroxene - 1.

The compositions are expressed in weight %.

PLAG

Oliv - Plag p.p.

CPX

OPX

R_2O_3

60

80

$XO.ZO_2$

CPX

60

80

OPX

$YO.ZO_2$

14
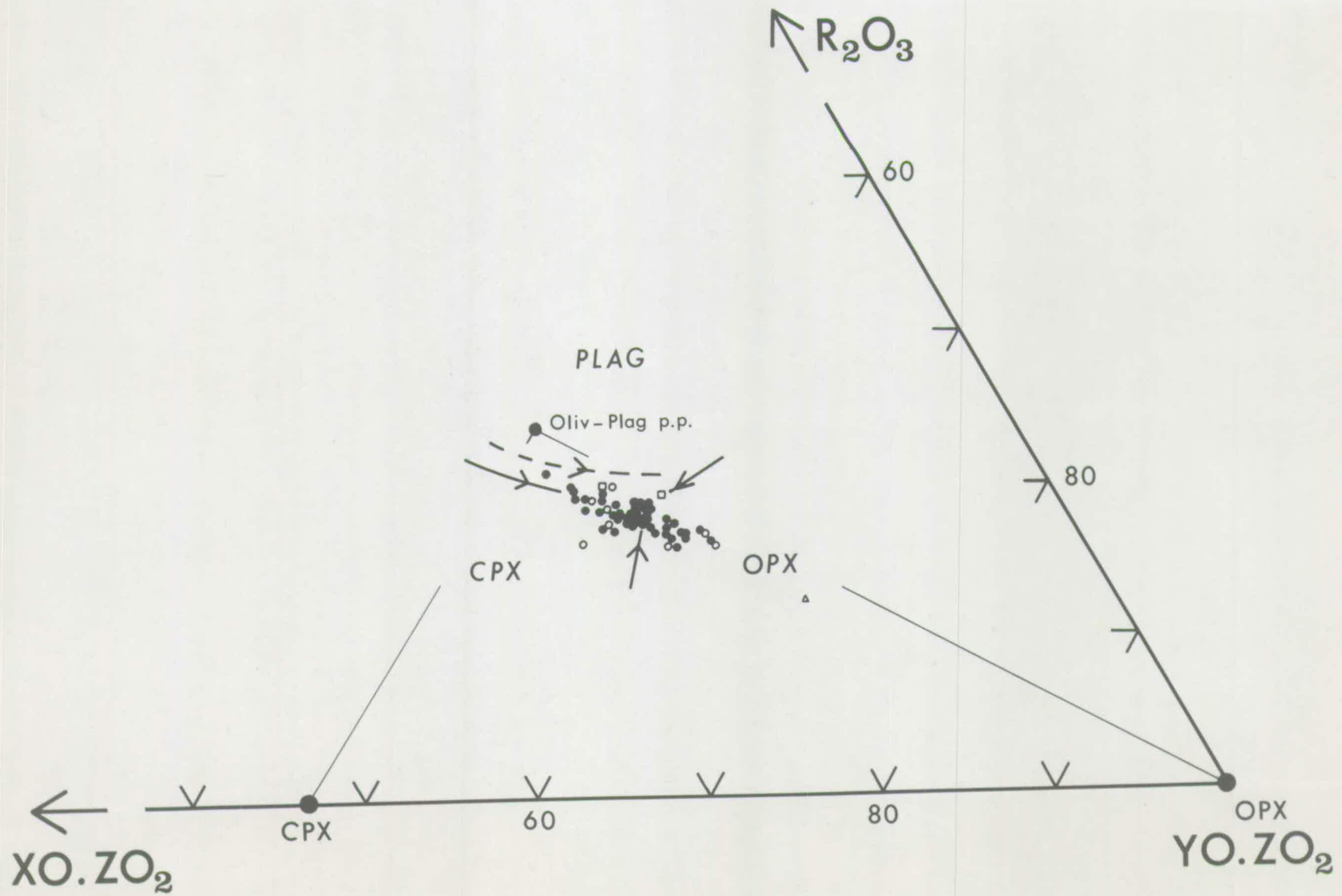
FIGURE 15

A projection from $YO.ZO_2$ (Orthopyroxene) into the plane
$2R_2O_3.3ZO_2 - 2XO.3ZO_2 - 2YO.ZO_2$ of phase relations and
Nuanetsi rock compositions.

The projected phase relations, at atmospheric pressure,
on the boundary of the orthopyroxene primary phase volume
have been taken from O'Hara (1968a, Fig. 5).

The field labelled OLIV, PLAG and CPX correspond to
the loci of liquid compositions in the equilibria Oliv + Opx +
Liq, Plag + Opx + Liq and Cpx + Opx + Liq on the surface of
the orthopyroxene primary phase volume.

The projected data points are as follows :

● : basalts and limburgites - 44 in number.
□ : picrites - 9.
○ : lavas enriched in cumulus olivine - 2.
△ : lava enriched in cumulus orthopyroxene - 1.

The compositions are expressed in weight %.
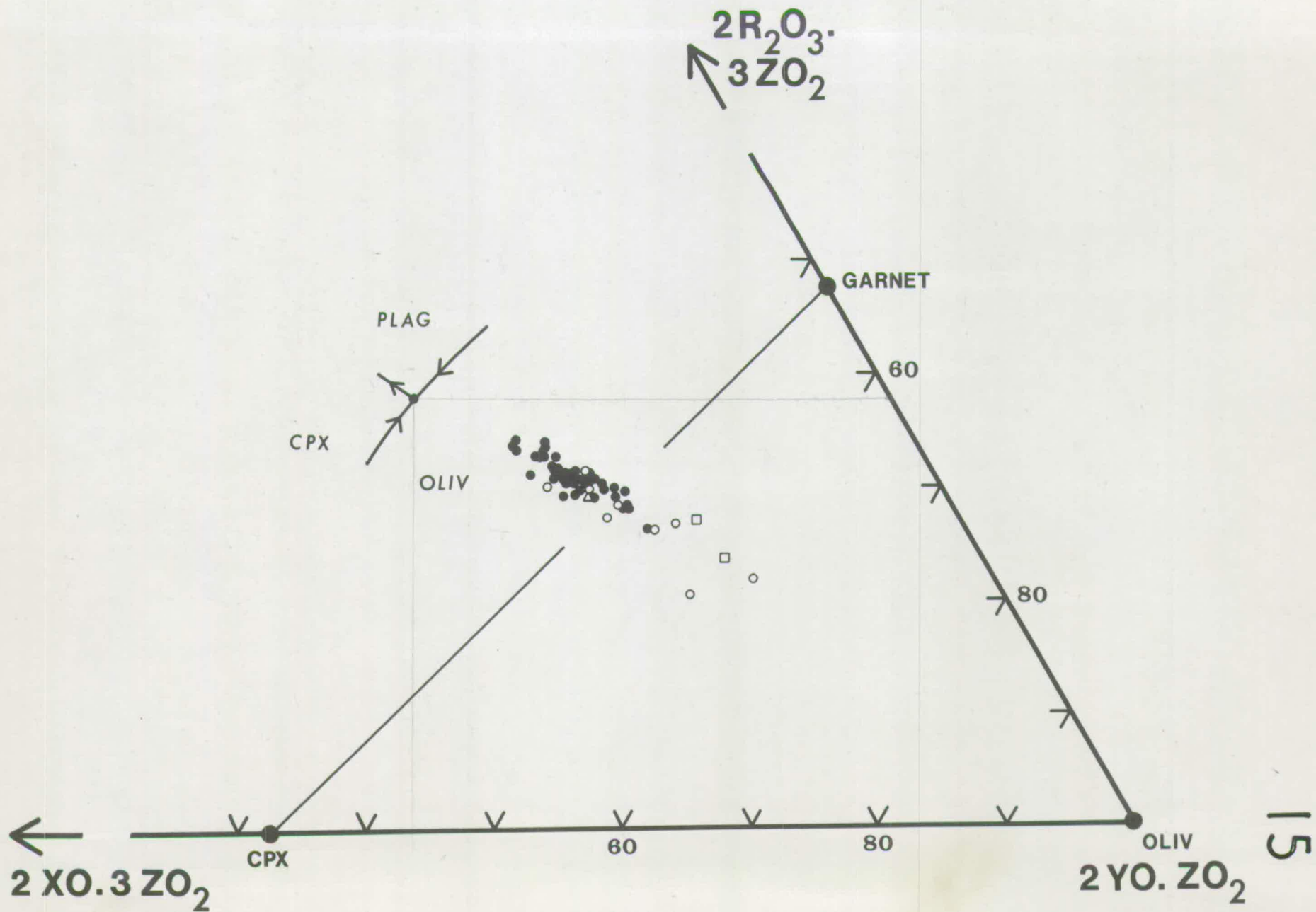
Since the melted basalts were mainly from Hawaii it is likely that these phase boundaries give only a general indication of the position of the Nuanetsi phase boundaries. Experience with these diagrams has led one to expect a shift in the location of some boundaries as the content of minor elements, K_2O, TiO_2 and trace elements varies from province to province. Nevertheless, although these natural phase diagrams must be used with caution, when taken together they do demonstrate that all the Nuanetsi composition points lie within the olivine primary phase volume.

Picritic Character

It has been argued previously, on the basis of variation diagrams, especially K_2O v. MgO (Cox et al, 1965), and on the basis of an MgO- gap (Chapter 4), that the Olivine-rich Group is unlikely to represent magmas of Upper Basalt composition enriched in cumulus olivine - in contrast to the accepted origin of the relatively rare Hawaiian picrite basalts, see, for example, Murata and Richter (1966 a and b). The clinopyroxene projection (Fig. 13) shows that the lava compositions form a roughly linear trend which is oblique to olivine control lines. The compositions of these lavas could not, therefore, have resulted from the accumulation of olivine in any low-MgO tholeiitic magma.

The picritic character of the Nuanetsi Olivine-rich Group is, therefore, an inherent feature of the rocks. They must have crystallised from magmas which had compositions which were primitive, i.e. poorly evolved, in terms of possible fractionation under conditions of, and the phase relations appropriate to, pressures close to one atmosphere.

The occurrence of this thick series of lavas and hypabyssal rocks

which have apparently undergone very limited low pressure fractionation
is attributed to relatively fast ascent of the magmas through the low
pressure regime of the continental crust, say the upper 15 km. Evidence
of some low-pressure olivine accumulation within the Group, especially
in the hypabyssal rocks, has, of course, been presented in Chapters 2
and 4.

Low Pressure Crystallisation

On the basis of the petrography and mineralogy of lavas it has
previously been argued (Chapter 2) that the order of appearance of phases
during the final crystallisation of the rocks was :

Olivine - Clinopyroxene - Plagioclase - possibly Orthopyroxene

Evidence for the late appearance of orthopyroxene was mainly
negative but the phase was recorded in one holocrystalline picrite. The
large orthopyroxene phenocrysts with their clinopyroxene rims were
considered to be relicts of an earlier crystallisation event (Chapter 3).

The order of crystallisation proposed above is not entirely
consistent with the natural phase diagrams (Figs. 13 - 15). The location
of phase boundaries in Fig. 14 implies that the liquidus phase, olivine,
should be joined by plagioclase before clinopyroxene in some of the
compositions. Since the phenocryst assemblage olivine + plagioclase
has not been recorded, not even in the rocks which project into the
olivine + plagioclase + liquid area of Fig. 14, it is concluded that,
for the Nuanetsi compositions, the boundary between the olivine +
plagioclase + liquid and olivine + clinopyroxene + liquid fields in Fig.
14 should be moved up the diagram as indicated.

One feature of the data reduction and projection schemes adopted
is that the phase boundaries in the olivine projection (Fig. 14) appear

to be sensitive to the overall minor oxide and element content of the projected rock compositions. For example, Fig. 16 shows that the phase boundaries for the Hawaiian lavas are considerably removed from the analogous boundaries in the synthetic system Al_2O_3 - CaO - MgO - SiO_2, and Clarke (1968) has shown that the phase boundaries for the Baffin Bay Tertiary basalts - a series with very low contents of alkali oxides, TiO_2, P_2O_5 and trace elements - must lie between the synthetic and established Hawaiian phase boundaries.

Such shifts in the position of phase boundaries are, in general, likely to have two components - an apparent movement due to the method of distribution of oxides inherent in the data reduction scheme and a real movement which actually reflects the changing bulk compositions of the rocks in the poly-component natural system.

The clinopyroxene and olivine projections (Figs. 13 and 14) indicate that orthopyroxene should be the third phase to crystallise, after olivine and clinopyroxene, in almost 33% of the rocks. This is not confirmed by the petrographic evidence. Two explanations of this apparent anomaly are, firstly, that the orthopyroxene primary phase volume in the Nuanetsi natural basaltic system is more restricted than that in the Hawaiian case and, secondly, that the orthopyroxene expected to crystallise is occult in clinopyroxene$_{ss}$ until a relatively late stage of the crystallisation is reached.

The large orthopyroxene phenocrysts are unlikely to be the missing pyroxenes. Considerations of Fe/Mg ratios apart (Chpater 3), the large size of these phenocrysts suggests an early, rather than late, commencement of crystallisation. Furthermore, the distribution in Figs. 17 and 18 of composition points which represent rocks containing these orthopyroxene

FIGURE 16

$2YO.ZO_2$ (Olivine) projection showing changes in the positions of phase boundaries.

See caption to Figure 14 for a general description of this projection.

The phase boundaries between the Cpx + Oliv + Liq, Opx + Oliv + Liq and Plag + Oliv + Liq fields on the boundary of the olivine primary phase volume are as follows:

Syn   : in the synthetic system Al_2O_3 - CaO - MgO - SiO_2 (O'Hara and Schairer, unpublished data).

BB   : tholeiitic basalts of the Baffin Bay area (Clarke, 1968).

Haw   : Hawaiian tholeiites (O'Hara (1968a) and Jamieson (in press).

Nu   : Nuanetsi (see text).
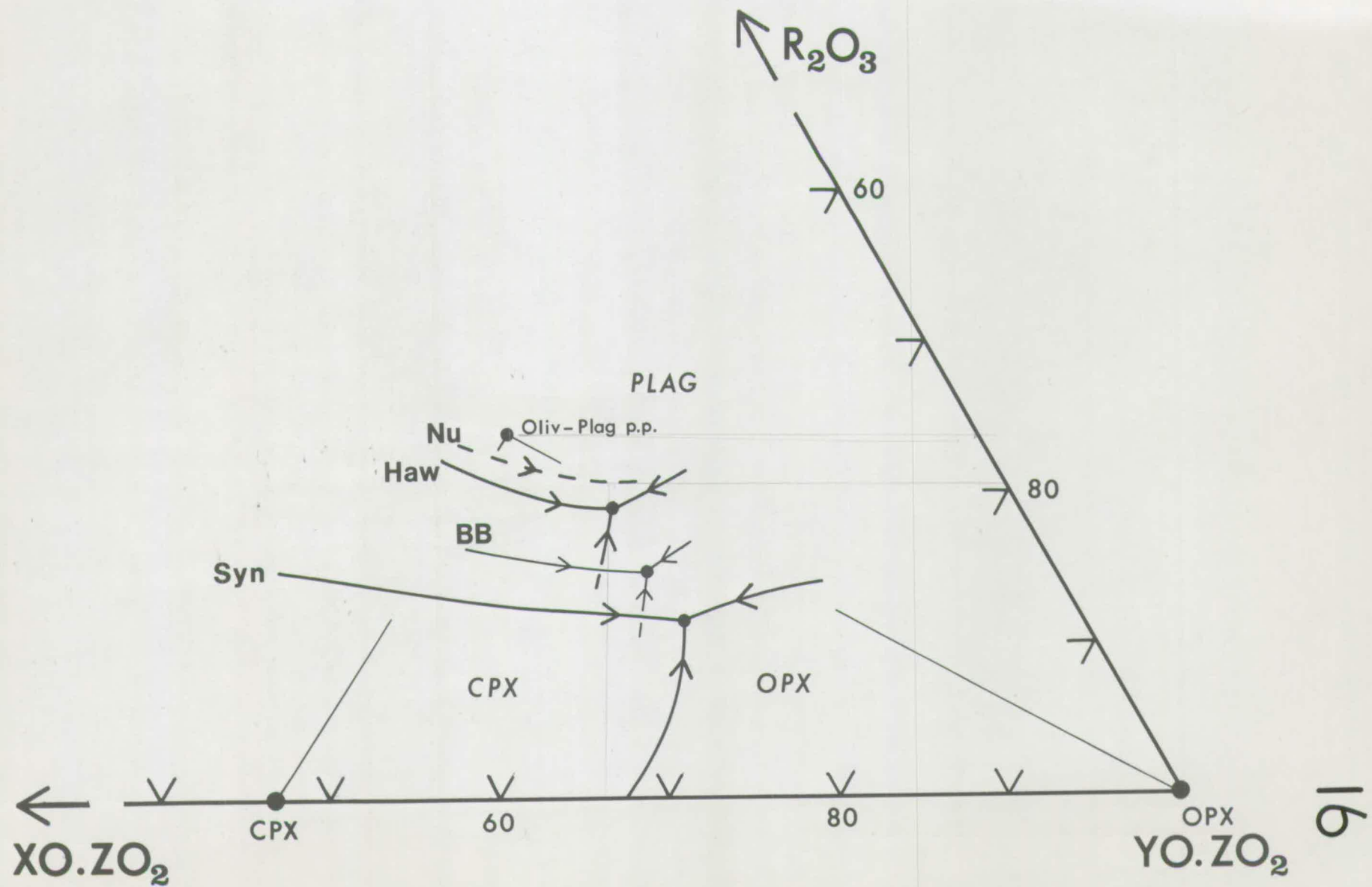
FIGURE 17

XO.YO.2ZO$_2$ (Clinopyroxene) projection showing the distribution of orthopyroxene phenocrysts in the Nuanetsi olivine-rich lavas.

See caption to Figure 13 for a general description of this projection.

The data points are as follows :

● :   lavas which contain orthopyroxene phenocrysts
○ :   lavas which do not contain orthopyroxene phenocrysts.

FIGURE 18

$2YO.ZO_2$ (Olivine) projection showing the distribution
of orthopyroxene phenocrysts in the Nuanetsi olivine-
rich lavas.

See caption to Figure 14 for a general
description of this projection.

The data points are as follows :

● : lavas which contain orthopyroxene phenocrysts

○ : lavas which do not contain orthopyroxene
phenocrysts.

R_2O_3

60

80

PLAG

Oliv–Plag p.p.

CPX

OPX

XO.ZO₂

CPX

60

80

OPX

YO.ZO₂

$\overline{8}$
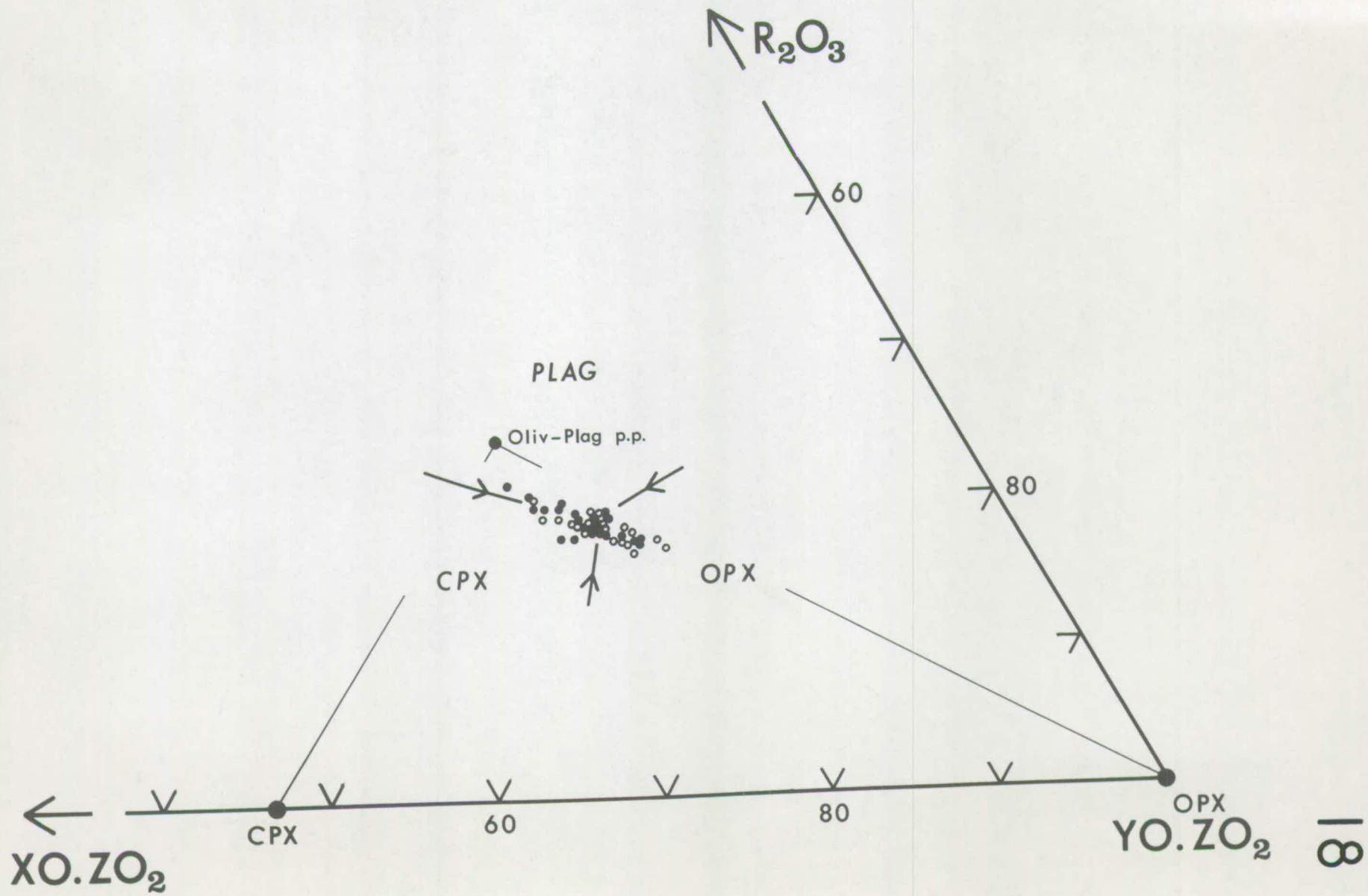
phenocrysts cannot be rationally related to any likely configuration of the atmospheric phase boundaries. This provides further support for the interpretation of the large orthopyroxene phenocrysts as the products of a crystallisation event at elevated pressures.

Atmospheric pressure phase relations in natural phase diagrams, therefore, confirm the inherited nature of the orthopyroxene phenocrysts and the observed low pressure phenocryst assemblages are broadly consistent with the relation between the rock composition points and the phase relations in these natural phase diagrams. However, more definitive phase diagrams for the Nuanetsi province cannot be drawn until the melting relations of a number of the rocks are determined.

Phase Relations at Elevated Pressures

Experimental determinations in synthetic and natural systems at various elevated pressures up to 40 kb. have given an insight into the general features of the phase relations which control the partial melting of ultrabasic mantle material and any subsequent equilibrium or fractional crystallisation of the partial melt, i.e. the primary magma.

Of considerable relevance to the development of the Nuanetsi picritic magmas at elevated pressure is the demonstration that the primary phase volume of orthopyroxene expands progressively with pressure increase in the range 0 - 15 kb., there being concomitant contractions of the olivine and plagioclase primary phase volumes.

Even before high pressure experimental work commenced, petrographic evidence had led several investigators to propose that the "... crystallisation of hypersthene is favoured over olivine at great depth (great pressure)." (Yoder and Tilley, 1962, p.410).

Vogt (1921) and Holmes and Harwood (1932) appear to have been amongst the first to make such proposals. Yoder and Tilley (1962, pp. 410-413) give a review of the proposals and illustrate tentative phase relations in the systems $Di - Fo - SiO_2$ and $An - Fo - SiO_2$ at 10 kb. assuming the En primary phase area has increased at the expense of the Fo area.

In synthetic systems the expansion of the primary phase volume of orthopyroxene is implicit in the demonstration, by Boyd, England and Davis (1964), that protoenstatite and enstatite melt congruently at pressures in excess of $2 - 5$ kb. Yoder (1964), in the join $Fo - Ab$ at 9 kb., and Kushiro (1964), in the system $Di - Fo - SiO_2$ at 20 kb., provide clear evidence of the expansion of the orthopyroxene primary phase volume. Yoder, however, at that time attributed the appearance of liquidus orthopyroxene in the join $Fo - Ab$ to metastable crystal- lisation. Further confirmation was provided by Kushiro (1965) in systems involving the plagioclase end members - $Fo - CaAl_2SiO_6 - SiO_2$ (at 20 kb.) and $Fo - Ne - SiO_2$ (at 10 and 20 kb.).

In natural basaltic systems the results of Tilley and Yoder (1964) and Green and Ringwood (1964) demonstrate analogous changes. The olivine tholeiite and picrite compositions investigated by Green and Ringwood have olivine as liquidus phase at atmospheric pressure but between $10 - 20$ kb. pressure orthopyroxene becomes the liquidus phase. The olivine tholeiite (K 1921) studied by Tilley and Yoder has olivine as liquidus phase at one atmosphere (Tilley, Yoder and Schairer, 1963) but no olivine was recorded in the 20 kb. crystallisation history. The primary phase volume of olivine must, therefore, have contracted with increasing pressure.

Using these initial results in natural systems, and subsequent
results from the Geophysical Laboratory, Washington, D.C., the Department
of Geophysics and Geochemistry, A.N.U., Canberra and the Institute of
Geophysics and Planetary Physics, U.C.L.A., California, O'Hara constructed
diagrams which show the phase relations for natural basic and ultrabasic
compositions at various pressures in the range 0 - 30 kb. (1968a, Figs.
4 - 6).   O'Hara was encouraged to find that these results, produced
by different workers using a variety of techniques, were, in general,
mutually consistent.

The main features of the projected phase diagrams drawn by O'Hara
are, with pressure increase :

(a)   the continuous contraction of the olivine primary phase
      volume

(b)   the expansion of the clinopyroxene and orthopyroxene
      primary phase volumes, especially the latter, in the
      range 0 - 20 kb.

(c)   the expansion of a garnet primary phase volume, at the
      expense of all the other volumes at pressures in excess
      of 20 - 25 kb.

For details of the pressure-induced changes on the phase
equilibria in natural basic and ultrabasic systems the reader is
referred to O'Hara (1968a).

Genesis of the Olivine-Orthopyroxene Assemblage.

The natural phase diagrams constructed by O'Hara (1968a) were
produced by using the same data reduction and projection scheme as has
been adopted in this study.   It has been possible, therefore, to

transfer the 10 kb. phase boundaries directly from O'Hara's Figs. 4 - 6
to the various projections of Nuanetsi composition points.   This has
been done in Figs. 19 and 20.

These Figs., and the orthopyroxene projection (not shown)
indicate that at 10 kb. almost all the composition points lie in, or
close to, the olivine + orthopyroxene + liquid surface, some distance
from the intersection of this surface with the clinopyroxene primary
phase volume.   Olivine and orthopyroxene would be the first two phases
to crystallise from these compositions at 10 kb. pressure.   Therefore,
the relation between the composition points and the likely form of the
10 kb. phase boundaries is clearly consistent with the rare olivine-
orthopyroxene megacryst, phenocryst assemblage (identified in Chapter 3)
being the product of early crystallisation at ca. 10 kb.

On the basis of all the available experimental data, in particular
the results of Green and Ringwood (1967), O'Hara (1968a) has estimated
that at a pressure around 8 - 10 kb. the orthopyroxene primary phase
volume must penetrate the plane of critical silica - undersaturation -
clinopyroxene - plagioclase - olivine.   Above this pressure hypersthene-
normative compositions can, by fractionating olivine and orthopyroxene,
produce nepheline-normative residual liquids.

The absence of nepheline-normative basalts in the Nuanetsi
sucesssion could be taken as evidence that the crystallisation of the
olivine-orthopyroxene assemblage took place at pressures less than
those needed to cross this plane, i.e. at pressures less than 8 - 10 kb.
A different, but valid interpretation, however, is that only limited
fractionation of olivine and orthopyroxene took place and as a result
no extreme diversification of magma compositions occurred during this

FIGURE 19

XO.YO.2ZO$_2$ (Clinopyroxene) projection showing Nuanetsi rock compositions and possible phase relations at 10 kb. pressure.

See caption to Figure 13 for a general description of this projection.

Phase relations at 10 kb. pressure on the surface of the clinopyroxene primary phase volume have been taken from O'Hara (1968a, Fig. 6A). These are shown by full lines. Broken lines represent the phase boundaries at 1 atmosphere – taken from Figure 13.

The fields labelled SP, PLAG, OLIV and OPX correspond to the loci of liquid compositions in the equilibria Spinel + Cpx + Liq, Plag + Cpx + Liq, Oliv + Cpx + Liq and Opx + Cpx + Liq on the surface of the primary phase volume of clinopyroxene at 10 kb. pressure.

The key to the projected data points is as in the captions to Figures 13 – 15.
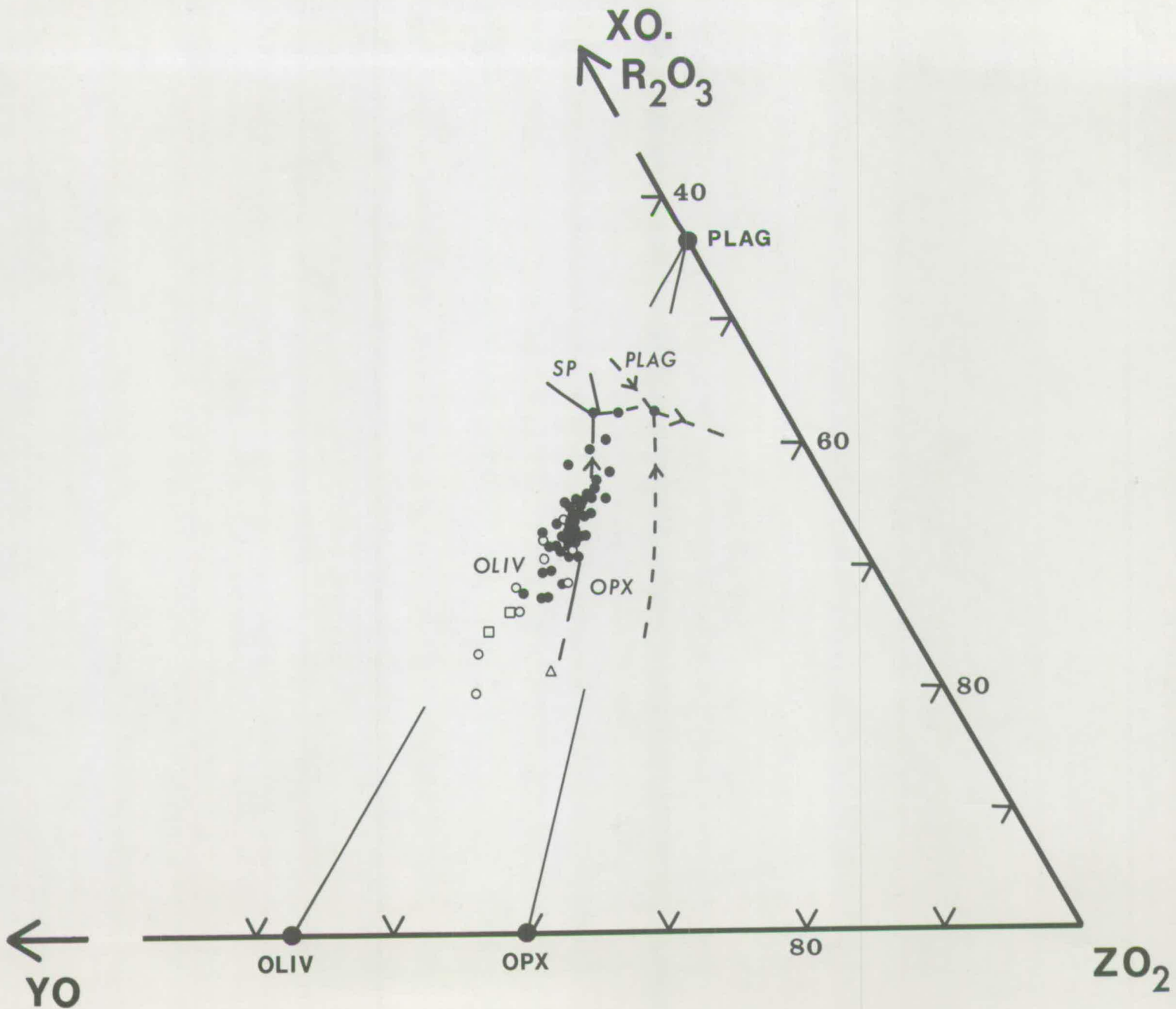
FIGURE 20

2YO.ZO$_2$ (Olivine) projection showing Nuanetsi rock
compositions and possible phase relations at 10 kb.
pressure.

See caption to Figure 14 for a general description
of this projection.

Phase relations at 10 kb. pressure on the surface
of the olivine primary phase volume have been taken from
O'Hara (1968a, Fig. 4A).   These are shown by full lines.
Broken lines represent the phase relations at 1 atmosphere -
taken from Figure 14.

The fields labelled SP, PLAG, OPX and CPX
correspond to the loci of liquid compositions in the
equilibria Spinel + Oliv + Liq, Plag + Oliv + Liq, Opx +
Oliv + Liq and Cpx + Oliv + Liq on the surface of the
olivine primary phase volume at 10 kb. pressure.

The key to the projected data points is as in the
captions to Figure 13 - 15.
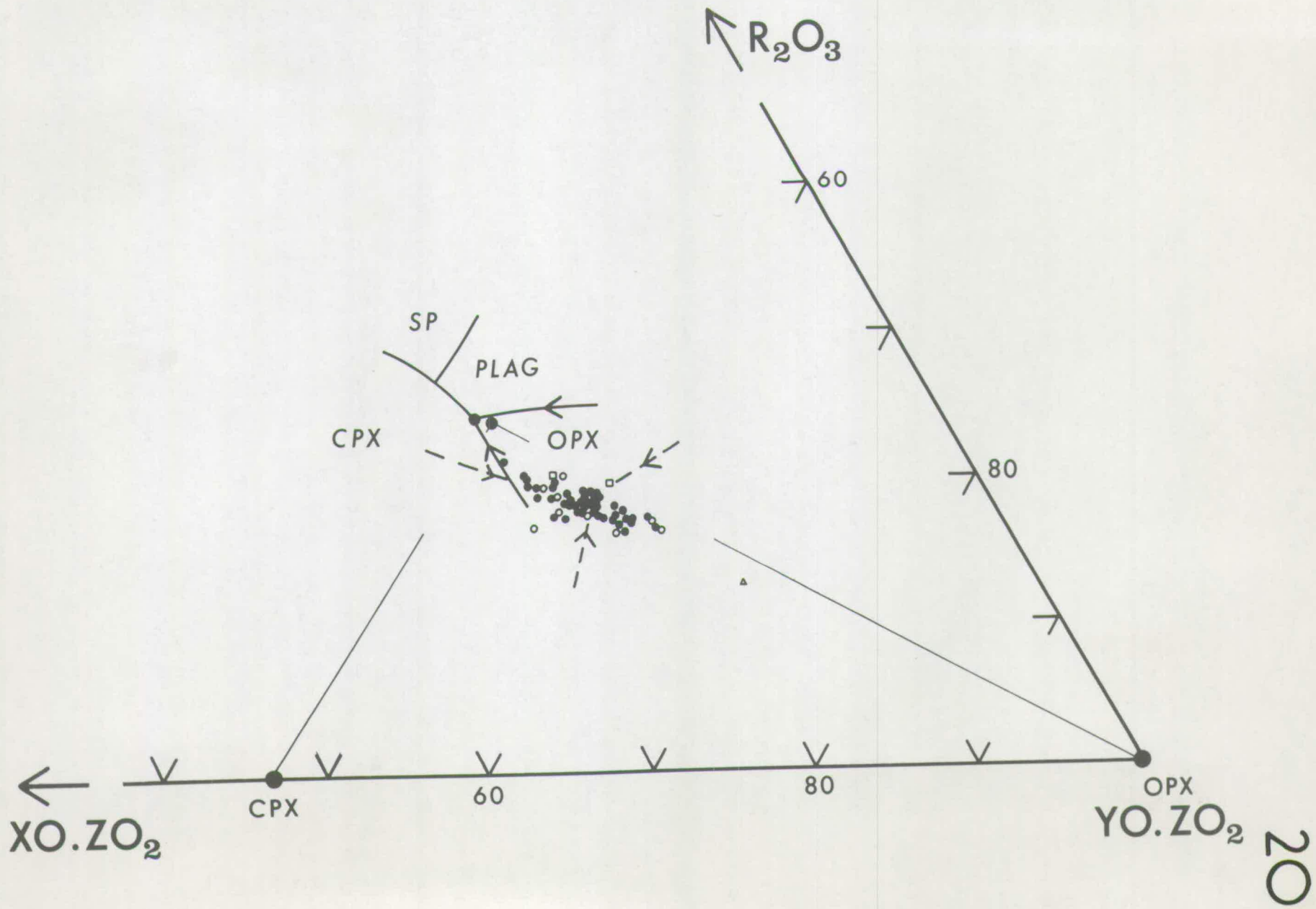
stage of the magmatic development.

The relatively low contents of Al_2O_3 in the Nuanetsi orthopyroxenes – 1.5 – 1.7% – is also suggestive of crystallisation at relatively modest pressures; compare Al_2O_3 contents of 4.9 and 5.4% in orthopyroxenes from the assemblage olivine + orthopyroxene + glass generated at 9 kb. and 1270 – 1290°C in an olivine tholeiite by Green and Ringwood (1967, Table 9). However, in the absence of an Al_2O_3-rich coexisting phase, such comparisons are difficult. The assemblages generated by Green and Ringwood may represent a greater degree of crystallisation.

The abundance of orthopyroxene phenocrysts in one specimen – N-88 with 21% orthopyroxene – at first suggested that orthopyroxene alone was the precipitating phase during this elevated pressure event. However, as has been pointed out by O'Hara (1968a) this is a remote possibility in any magma which is the partial melt of an olivine-rich peridotite. Because the primary phase volume of olivine appears to expand continuously with pressure decrease, all ascending magmas are likely to remain in equilibrium with olivine and to precipitate olivine at all stages of development, unless olivine has a reaction relationship with the liquid – a situation which is realised at pressures of less than 2 – 5 kb. with the onset of the familiar reaction :

$$\text{olivine} + \text{liquid} \longrightarrow \text{orthopyroxene.}$$
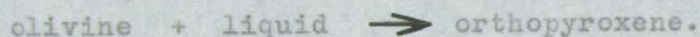
Because of this objection to the crystallisation of orthopyroxene alone, selective, or differential fractionation must be involved to account for the abundance of phenocrysts in the picrite – basalt, N-88.

Taking all the above evidence together, it is concluded that the olivine-orthopyroxene megacryst and phenocryst assemblage bears witness to the imperfect fractional crystallisation of harzburgite from the

ascending Nuanetsi picritic magmas at depths of 22 - 30 km. (7 - 9 kb.)
The primitive picritic compositions of the rocks, discussed above, and
the preservation of the harzburgitic assemblage imply that, subsequent
to the proposed harzburgite fractionation event, little differentiation
took place. Relatively rapid ascent of the magmas from depths as great
as 30 km. is, therefore indicated.

The role played by intermediate pressure harzburgite fractionation
in diversifying the magma compositions is discussed below.

Compositional Variation

Used as variation diagrams, Figs 13 - 15 demonstrate that olivine
and orthopyroxene may have exercised considerable control over the
variation of rock compositions. The phase equilibrium aspects of
Figs. 19 and 20 appear to be perfectly consistent with a petrogenetic
scheme which assumes parental or primary picritic magma, of near constant
composition, was supplied at depths of 22 - 30 km. and that harzburgite
fractionation at this depth, together with some low pressure olivine
fractionation, were responsible for the diversification of the initial
magma composition.

However, such an interpretation is not consistent with all the
available evidence. An assessment of the analytical data reveals that
K and associated elements reach their highest concentration at the
basic end of the trend of composition points in Fig. 19 - the reader
may recall the intriguing sympathetic relationship between K and
associated elements and MgO. This is demonstrated in Fig. 21, a
clinopyroxene projection with the K_2O/Na_2O ratios of the rocks added.
The concentrations of P_2O_5, Ba, Rb, Sr and Zr in the rocks display
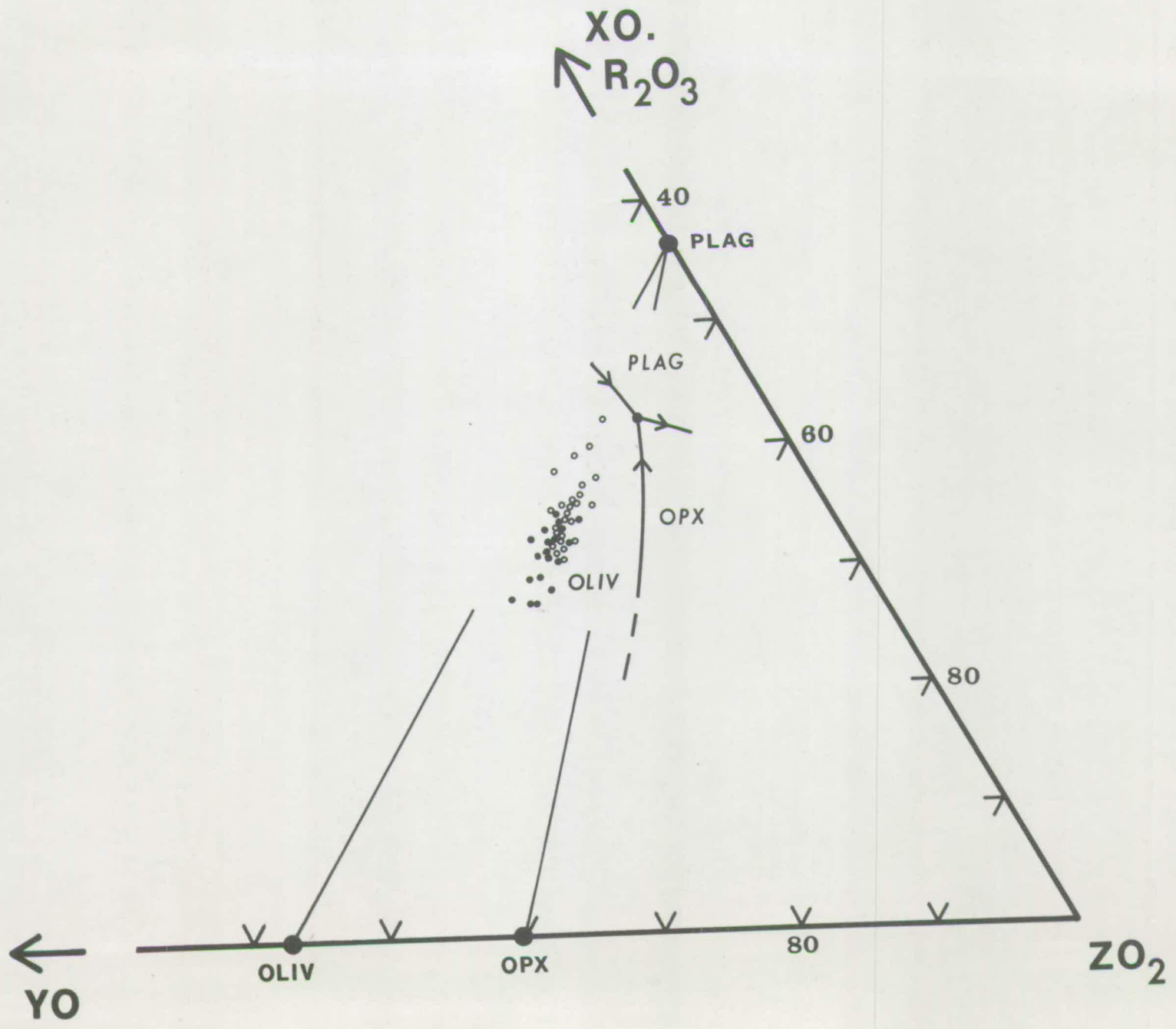similar distribution patterns in this projection.

FIGURE 21

XO.YO.2ZO$_2$ (Clinopyroxene) projection showing the K$_2$O/Na$_2$O
ratios of the Nuanetsi olivine-rich lavas.

See caption to Figure 13 for a general description
of this projection.

The data points are as follows :

● : lava with K$_2$O/Na$_2$O ratio > 1.

○ : lava with K$_2$O/Na$_2$O ratio < 1.

Such a systematic relationship clearly could not result from the fractionation of harzburgite alone. It follows, therefore, that, either the magmas were not of constant composition prior to the onset of the proposed harzburgite fractionation at c. 10 kb. pressure but were already differentiated in a rational manner, or a further differentiation mechanism, for example, the fractionation of a further crystalline phase, occurred between the intermediate pressure fractionation of harzburgite and the low pressure fractionation of olivine, or during either of these fractionation events.

In the following two Chapters this interesting aspect of the compositional variation is considered in detail and several causal mechanisms are proposed and critically discussed.

CHAPTER 6

STATISTICAL ANALYSIS

The standard statistical technique of principal component analysis has been applied to the chemical analyses of the Nuanetsi olivine-rich lavas. From the results of this treatment three variation diagrams have been constructed - by plotting the first and second transformed variables, the first and third transformed variables and the second and third transformed variables. Once selected mineral analyses are added, these diagrams provide convincing evidence supporting the proposal that the fractionation of olivine and orthopyroxene has exercised considerable control on the bulk compositional variation of the lavas. The statistical analysis also confirms that the progressive changes in the concentrations of MgO and K and associated elements is an important element of the overall variation. Although specific conclusions cannot be drawn from the transformed variable variation diagrams, they do show that this latter aspect of the variation may be the result of the fractionation of bimineralic eclogite, phlogopitic mica or amphibole.

Principal Component Analysis

(i)   General

Principal component analysis is a standard statistical technique which detects the main elements or components of variation in an array of data containing m members (e.g. chemical analyses);   each member containing n variables (e.g. oxides).   Each member of such an array of data can be considered as a point in n-dimensional space   -   the

position of the point being defined by n co-ordinates (e.g. oxide

concentration values) along n axes (e.g. oxide axes).

In a principal component analysis such a n-dimensional cloud of

m points is statistically assessed - using a computer - and new,

or transformed, linear axes are calculated.   The first, or major,

transformed axis, by definition accounts for the maximum possible

variation within the cloud of points - for example, in a 3-dimensional

analogy, the first transformed axis in a cigar-shaped cloud of data

points would be close to the major axis of the cloud.

The second, and subsequent, transformed axes account for increasingly

smaller proportions of the total variation.   The transformed axes are all

mutually perpendicular.

The orientation of the transformed axes relative to the original

(oxide) axes is given by eigenvectors.   These eigenvectors are the

cosines of the angles between a transformed axis and each of the original

axes - in n-dimensional space.   Each transformed axis has its

characteristic set of n eigenvectors.   A large eigenvector for one

variable (say, MgO) means that that transformed axis has an orientation

in n-dimensions which is, amongst other things, close to the MgO axis.

Following similar reasoning it is obvious that a small eigenvector

indicates that the transformed axis is close to being perpendicular to

the oxide axis.

It is important to appreciate that this is purely a statistical

analysis and that the number of significant components of the overall

variation, or transformed axes, which are detected bears no direct

relation to the number and nature of the individual events or processes

(e.g. crystal-liquid fractionation events) which have combined to

produce the total variation.   In general, the number of significant components of variation will greatly exceed the number of individual events causing variation.

The transformed variable of each member (chemical analysis) of the m member array is the co-ordinate of each of the data points on a transformed axis.   Transformed variables are calculated by summing the products of each original variable (oxide) times the eigenvector of that variable (oxide) for the appropriate transformed axis.

In summary, the principal component analysis identifies the main linear elements (transformed axes) of the total variation in an array of data and produces co-ordinates of (transformed variables) each member of the array along each of the transformed axes.

For a more rigorous description of principal component analysis the reader is referred to Kendall (1957) and Cooley and Lohnes (1962). Le Maitre (1968) has used this technique in a petrochemical context.

(ii)   Current Application

Because rectilinear, triangular and projected tetrahedral variation diagrams all involve the selection or the combination of some components dissimilar rock and mineral compositions can appear similar, in terms of the variation diagram being used.   Misleading interpretations can be the result of a slavish adherence to the apparent relationship between rock compositions in such diagrams.

In general, therefore, a principal component analysis of the variation displayed by an array of rock compositions is advised since all the chemical variables can be included, without any combination, in this procedure.

It was demonstrated in Chapter 5 that one aspect of the variation of the bulk composition of the Nuanetsi olivine-rich rocks - the sympathetic relationship between MgO and K and associated elements - is not apparent in the projected phase diagrams (Figs. 13 - 15). Therefore, the application of a principal component analysis to this array of chemical data is especially pertinent.

A computerised principal component analysis was carried out on an array of 47 analyses of Nuanetsi basalts and limburgites. Dr. R.F. Cheeney, Grant Institute of Geology, kindly wrote the necessary program.

Table 27 gives the variance and eigenvectors of each of the three most significant linear elements, or transformed axes, of the bulk composition variation of the 47 chemical analyses. The sum of the variances indicates that 84% of the total variation can be expressed in terms of three transformed axes.

Bearing in mind that the eigenvectors are the cosines of the angles between the transformed axes and the original axes, it is obvious that the first transformed axis (TA_1) is not close to any single oxide or trace element axis but has a rather similar orientation (eigenvector) relative to all the original axes. The TA_1 eigenvectors of TiO_2, MgO, K_2O, P_2O_5, Rb, Sr, Ba, Cr and Ni are very similar - in the range -0.22 to -0.29. This indicates that the sympathetic relationship between these elements and oxides is an important factor in the principal component of variation (TA_1), which accounts for 57% of the total variation and confirms that this sympathetic relationship is statistically very significant.

Of the original axes, SiO_2, Fe_2O_3T and MgO are closest to TA_2 and, if these components are sufficiently abundant in the original

TABLE 27

EIGENVECTORS OF PRINCIPAL COMPONENTS

Variance		SiO_2	TiO_2	Al_2O_3	Fe_2O_3T	MnO	MgO	CaO	Na_2O
1	57%	0.12	-0.22	0.28	0.15	0.24	-0.26	0.29	0.25
2	17%	-0.31	-0.22	-0.26	0.26	0.07	0.36	-0.19	-0.30
3	9%	-0.48	0.43	-0.05	0.58	0.20	-0.11	0.19	-0.01

continued

Variance		K_2O	P_2O_5	Rb	Sr	Ba	Zr	Cr	Ni
1	57%	-0.28	-0.27	-0.25	-0.28	-0.28	-0.29	-0.23	-0.26
2	17%	-0.22	-0.21	-0.23	-0.25	-0.21	-0.21	0.25	0.31
3	9%	0.01	0.23	-0.11	0.10	0.02	0.14	-0.24	-0.04

analyses, they are likely to make the largest contributions to the co-ordinate, or transformed variable (TV), of each analysis on TA_2. Similarly, TiO_2 and Fe_2O_3T will tend to make the dominant contributions to co-ordinates on TA_3.

Once the principal components or major transformed axes, have been calculated, the transformed variables of each chemical analysis are calculated. The end-members of the transformed variables on each of the 3 transformed axes are given in Table 28.

Transformed Variable Variation Diagrams

Since 84% of the total variation displayed by the array of 47 chemical analyses can be represented in a 3-dimensional diagram, the mutually perpendicular axes of which are the 3 principal transformed axes, a set of 3 rectilinear variation diagrams is a convenient graphical representation of the variation trend. Figures 22 - 24 are such variation diagrams, TV_1 of each rock composition being plotted against TV_2, then TV_1 against TV_3 and, finally, TV_2 against TV_3.

In addition to the 47 lava analyses, selected analysed rocks and minerals have been added to these diagrams. Transformed variables for these minerals were calculated by summing the products of each oxide and trace element value times the appropriate eigenvector. These additional analyses have been added to the diagrams in order to assess the importance of crystal-liquid fractionation in the generation of the trend of lava bulk composition variation.

In Figs. 22-24 the alignment of the variation trend and the relative positions of the mineral composition points are consistent

TABLE 28

RANGE OF TRANSFORMED VARIABLES

TV_1

N-60 . . . . N-89

3.47 . . . . 13.06

TV_2

N-89 . . . . N-60

-17.06 . . . . -6.19

TV_3

N-88 . . . . N-225

-18.18 . . . . -14.13

FIGURE 22

TV$_1$ v. TV$_2$ transformed variable variation diagram.

● : represents Nuanetsi olivine-rich lavas -
47 in number.

☐ : represents selected minerals which are coded
as follows -

OLIV   - join between 2 magnesian olivines
OPX   - join between 2 magnesian orthopyroxenes
Amph   - amphibole (Aoki and Kushiro, 1968)
Phlog A - phlogopite (Aoki and Kushiro, 1968)
Phlog C - phlogopite (Carmichael, 1967)
Ecl Y   - eclogite (Yoder and Tilley, 1962)
Ecl S   - eclogite (Saggerson, 1968)
Gnt   - garnet separated from eclogite - Ecl Y
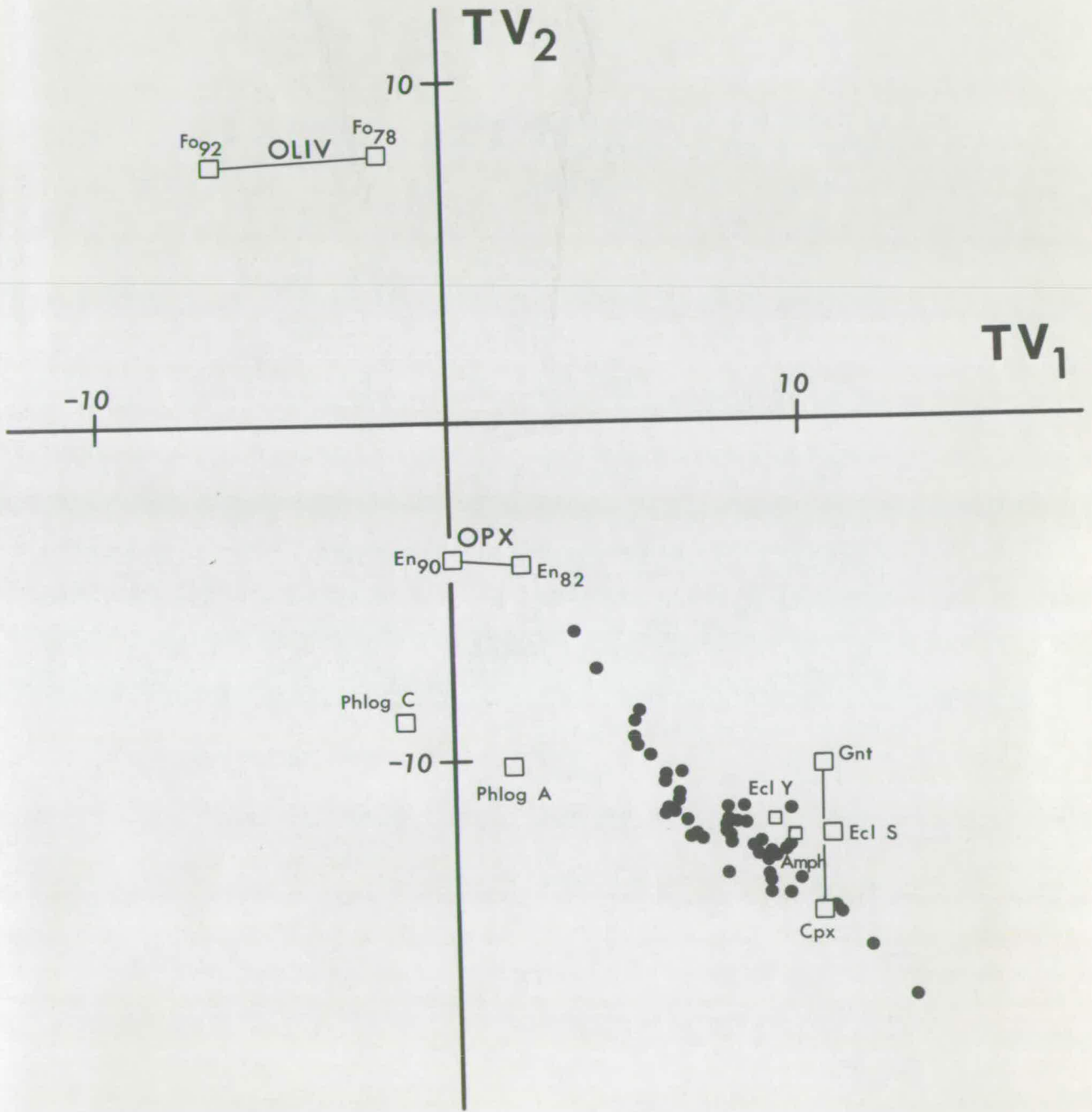Cpx   - clinopyroxene separated from eclogite Ecl Y.

TV$_2$

10

Fo$_{92}$ OLIV Fo$_{78}$

TV$_1$

10

−10

OPX

En$_{90}$ En$_{82}$

Phlog C

−10 Phlog A

Gnt

Ecl Y

Ecl S

Amph

Cpx

FIGURE 23

TV_1 v. TV_3 transformed variable variation diagram

Key as in caption to Figure 22.

TV$_3$ TV$_1$

-10   10

Fo$_{78}$

-10

OLIV

Amph

Gnt

Phlog A

Ecl S

Fo$_{92}$

Ecl Y   Cpx

-20

Phlog C   En$_{82}$

OPX

En$_{90}$
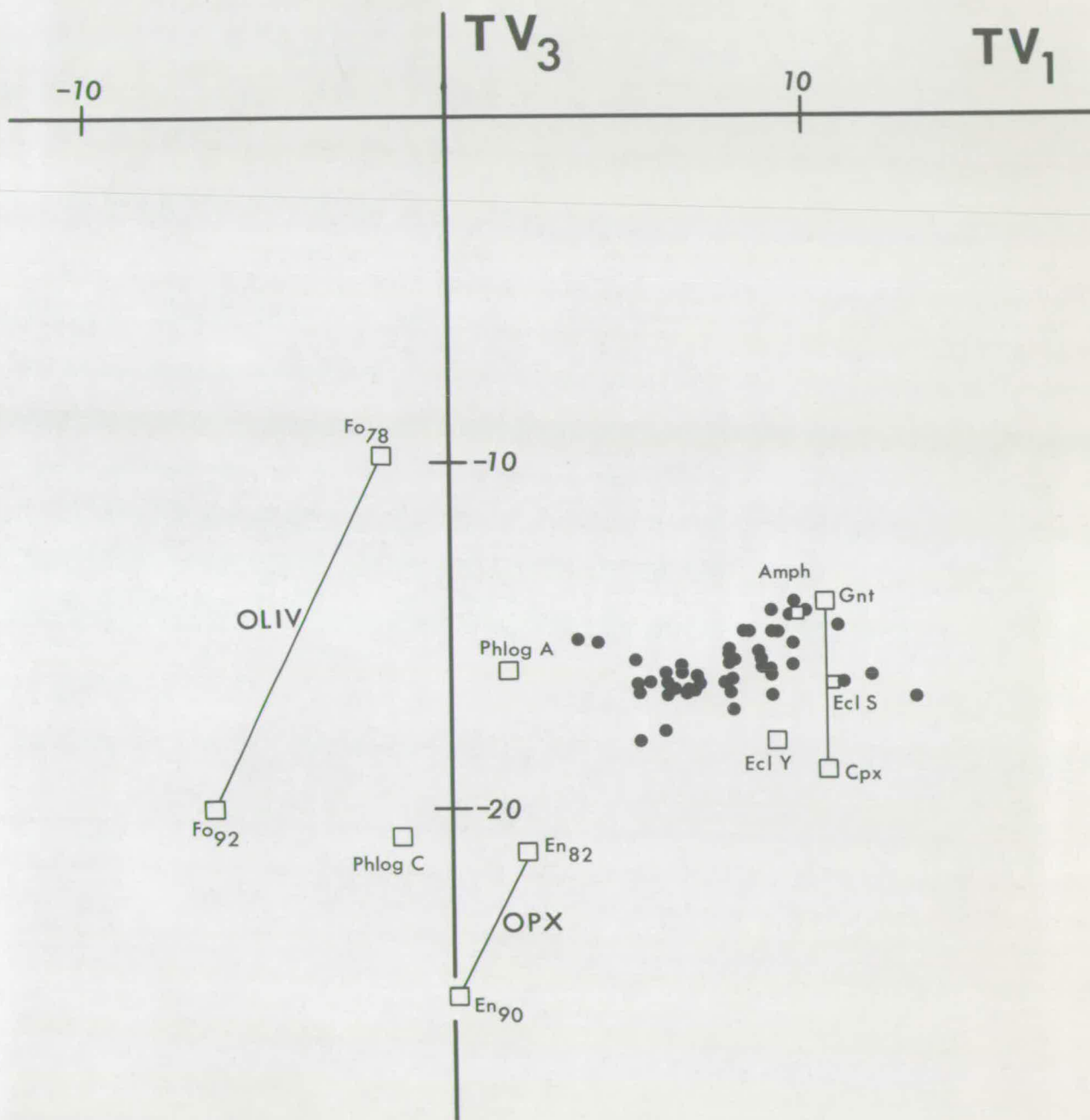
FIGURE 24

TV_2 v. TV_3 transformed variable variation diagram

Key as in caption to Figure 22.

TV$_2$

10

TV$_3$

Fo$_{92}$ OLIV   Fo$_{78}$

-20   -10

En$_{90}$ OPX   En$_{82}$

Phlog C

Phlog A

Gnt

Ecl Y

Amph

Ecl S

10

Cpx
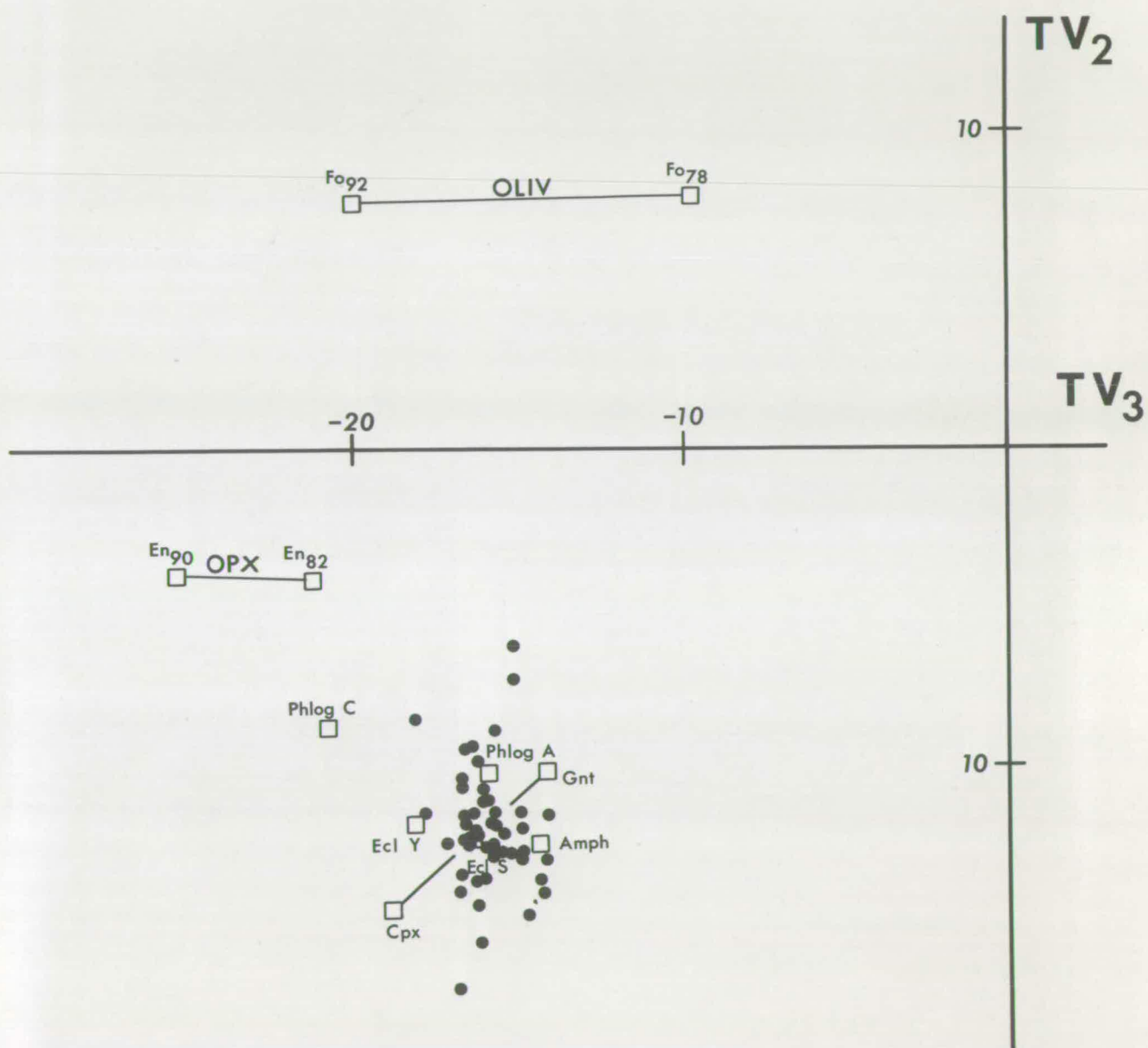
with the proposed fractionation of olivine and orthopyroxene (at
intermediate pressure) and olivine (at low pressure).   This mineralogical
control on the variation trend is most obvious in Fig. 22 - a diagram
which presents 75% of the total variation - but is also shown in the
other diagrams (Figs. 23 and 24).

The orthopyroxenes which have been plotted in these figures are
from the basalts N-88 and N-117 and have compositions of En_{90} and En_{82}
respectively.   One of the olivines is from the picrite N-22 and has
the composition Fo_{78}, the other olivine analysis, which gives a
composition of Fo_{92}, was taken from Deer et al (1962a, Table 2, no. 5).

In an attempt to understand more completely the behaviour of K
and associated elements in the Nuanetsi olivine-rich lavas, composition
points representing 2 eclogite nodules in basalt (Saggerson, 1968,
Table 2, no. 9, and Yoder and Tilley, 1962, Table 41, no. 1) and the
garnet and clinopyroxene separated from one of these nodules - from
Salt Lake Crater, Oahu, Hawaii (Yoder and Tilley, 1962, Table 41, nos.
2 and 3) - have been added to Figs. 22-24.   O'Hara and Yoder (1967)
and O'Hara (1968a) have proposed that the high pressure fractionation
of bimineralic eclogite from primary and primitive basic magmas plays
an important role in determining the concentration level and K and
associated elements in basalts erupted at the Earth's surface.

The K-bearing mafic phases phlogopite and amphibole are also
relevant to this aspect of the variation trend.   Accordingly
composition points representing one amphibole (Aoki and Kushiro, 1968,
Table 4, no. 1) and two phlogopites (Carmichael, 1967, Table 6; and
Aoki and Kushiro, 1968, Table 4, no. 2) have also been added to the
variation diagrams (Figs. 22-24).   The amphibole and the phlogopite

reported by Aoki and Kushiro occur in nodular inclusions in the Dreiser Weiher alkali basalts and tuffs, West Germany. The phlogopite analysis given by Carmichael is the average of 12 individual analyses of phlogopites in the K-rich lavas and plugs in the Leucite Hills, Wyoming.

Since the composition points of phlogopite plot in Figs. 22-24 at the same end of the variation trend as two established fractionating crystalline phases - olivine and orthopyroxene - these variation diagrams are considered to be, in general terms, consistent with the hypothesis that the fractionation of phlogopite was a further cause of differentiation in the evolution of the lavas. This possibility is examined in more detail in the following Chapter.

The viability of eclogite fractionation as an alternative K-enrichment process is difficult to assess in terms of the information presented in the transformed variable variation diagrams. The stability relations of eclogite imply that fractionation of this assemblage must be a high pressure event - occurring at pressures in excess of 20 - 25 kb. Any variation trend produced by such high pressure fractionation would be modified by subsequent fractionation - for example, the proposed olivine + orthopyroxene fractionation at intermediate pressure. Nevertheless the general position of eclogite composition points at the low-K_2O and low K_2O/Na_2O end of the trend of lava composition points is broadly consistent with eclogite fractionation being a significant differentiation mechanism. As with phlogopite fractionation, further aspects of eclogite fractionation will be considered in the following chapter.

Figures 22 - 24 show that, although the amphibole composition point is not positioned at an extremity of the variation trend,

intratelluric fractionation of this phase should be considered as a possible differentiation factor leading to the observed variation of K and associated elements in the trend.   Fractionation of olivine and/or orthopyroxene _after_ a period of amphibole fractionation would tend to produce the relationship between the lava composition points and the amphibole composition point in Fig. 22.

The limitations of transformed variable variation diagrams (Figs. 22-24) in this situation should be fully appreciated. Because the compositional variation displayed by these rocks is likely to be the result of, perhaps, 2 or 3 fractionation events, the diagrams are not competent to specifically identify each fractionating assemblage. By considering bulk compositions alone there is unlikely to be an unique solution to the relation between rock and mineral composition points and minerals other than those plotted in Figs. 22 - 24 could, apparently, be equally suitable as fractionating phases. Therefore, to further investigate the distribution of K and associated elements in the Nuanetsi olivine-rich lavas, all petrological and chemical aspects of the possible fractionating assemblages must be considered. This is done in Chapter 8, along with an assessment of other mechanisms leading to K-enrichment.

In conclusion, this statistical treatment of the variation of the lava bulk compositions has confirmed conclusions made in Chapter 5 on the basis of natural phase diagrams which have finite compositional limits and are, therefore, more restricted.   The control of olivine and orthopyroxene on the variation trend is again clearly demonstrated. On the grounds of bulk composition alone, the fractionation of phlogopitic mica, eclogite or amphibole are shown by the transformed

variable variation diagrams to be possible causes of the rational

distribution of K and associated elements in the variation trend.

CHAPTER 7

POTASSIUM AND ASSOCIATED ELEMENTS

- ENRICHMENT LEVELS

Estimates are made of the enrichment factors of K and associated elements, relative to the average upper mantle composition, which are displayed by the Nuanetsi olivine-rich lavas.

General

Reference has previously been made to the probable distribution of K, and the associated elements P, Rb, Sr, Ba, Zr, Th, U and R.E.E., in the upper mantle (Chapter 4). Largely rejected by the major silicate phases of peridotite, these elements may be principally held in trace amounts of amphibole (Lambert and Wyllie, 1968; Oxburgh, 1964) or mica (Kushiro et al, 1967; Yoder and Kushiro, 1969), apatite and zircon.

The geochemical behaviour of Ti was also described in Chapter 4. Although significant amounts of Ti are held in the major silicate phases, in basic rocks this element tends to vary sympathetically with K and associated elements and, on these grounds, it has been considered as a member of this distinctive group, for example, by Green and Ringwood (1967).

Because of this very limited incorporation in the major mafic silicate phases, K and associated elements will passively build up in the residual liquid during the fractionation of basic magmas.

The concentration of K and associated elements in basic rocks and magmas, and its implications, were fully considered in recent

publications by Engel et al (1965), Green and Ringwood (1967) and O'Hara (1968a). By using the concentration levels of this group of elements as a type of fractionation index, Engel et al (1965) proposed that the deep oceanic tholeiites, with their characteristic low contents of K and associated elements, represent an upper mantle primary magma - a proposition which is, however, open to strong criticism, see for example O'Hara (1968b).

Levels of Enrichment

In Chapter 4 the content of K and its associated elements in the Nuanetsi olivine-rich rocks was shown to be high relative to the average values in olivine tholeiites. The enrichment of these elements is particularly marked when the overall picritic character of the lavas is taken into consideration - the average content of MgO being 15.3%.

Before discussing possible causes of the enrichment of K and associated elements in the Nuanetsi olivine-rich rocks, a semi-quantitative estimate was made of the enrichment levels which these rocks display relative to the average mantle composition. These enrichment factors are presented in Table 29, column 3. The derivation of these factors is described below.

In Table 29 the contents of SiO_2, Al_2O_3, Fe_2O_3 T, MnO, MgO, CaO, Na_2O, Cr, Ni, TiO_2 and P_2O_5 in the average mantle peridotite composition (column 1) are the values in the average composition of garnet lherzolite nodules in kimberlite (Ito and Kennedy, 1967, Table 1, no. 3). O'Hara and Mercy (1963) have argued that these 4-phase peridotite nodules are pieces of the upper mantle which have suffered a minimum of primary magma extraction and that they are the best available chemical and mineralogical sample of the peridotite in the upper parts

TABLE 29

ENRICHMENT FACTORS IN LAVAS

	Average Mantle Peridotite	Nuanetsi Olivine-rich Lavas	E	Deep Oceanic Tholeiites	E
SiO_2	45.6	49.7	1.1	49.94	
Al_2O_3	2.6	8.91	3.4	17.25	
Fe_2O_3 T	7.9	12.5	1.6	9.67	
MnO	0.13	0.15	1.2	0.17	not
MgO	41.4	15.3	0.37	7.28	applicable
CaO	1.90	7.68	4.0	11.86	
Na_2O	0.19	1.64	8.6	2.76	
Cr	3100	929	0.30	297	
Ni	1950	752	0.39	97	
K_2O	0.014	1.61	115	0.16	11
TiO_2	0.2	2.69	13	1.51	7.6
P_2O_5	0.03	0.42	14	0.16	5.3
Rb	0.25	33	132	1.2	4.8
Sr	15	859	57	130	8.7
Ba	3.9	795	202	14	3.6
Zr	12	300	25	95	7.9

Oxides in wt.% ; trace elements in p.p.m.

Enrichment factor (E) = Conc. of component in basalt/
Conc. of component in average
mantle.

of the Earth's mantle. The average composition of garnet lherzolite is, unfortunately, based on only 4 analyses. However, the enrichment factors for the major oxides and Cr and Ni are not of critical importance in this discussion and the enrichment factors for TiO_2 and P_2O_5 can be checked by an independent method - see below.

The value of K_2O reported by Ito and Kennedy in the average garnet lherzolite in kimberlite - 0.12% - is not used in Table 29. A small amount of contamination of the K_2O-poor nodules by the volatile-rich and K_2O-rich host kimberlitic fluid would greatly alter the original content of K_2O. Some contamination is indicated by the occurrence of secondary serpentine and phlogopite - a primary phase in kimberlite - in garnet lherzolite nodules (Holmes, 1936; Nixon et al, 1963; Ito and Kennedy, 1967).

The contents of K_2O, Rb and Sr used in Table 29 for the average mantle peridotite are from a recent theoretical estimate of the absolute abundance and distribution of these elements in the Earth (Hurley, 1968 a and b). The data presented by Hurley (1968b) have been modified in this study by assuming that these elements are absent from the Earth's core.

As there have been no recent estimates of Ba and Zr in the mantle, the figures in Table 29 for these elements in the average mantle peridotite have been based on the chondritic Earth model. Chondritic abundances of 4 p.p.m. Ba and 10 p.p.m. Zr are indicated by Taylor (1964b, Table 1) and by the data of Schmitt et al (1964) respectively. The figure for Zr is a revision of earlier estimates which indicated an average chondritic content of 35 p.p.m. (Taylor, 1964b, Table 1). The mantle average values in Table 29 were derived from the chondritic mean values by assuming that both elements are absent from the Earth's core

and that 33% of the Earth's total Ba and 1.6% of the Zr are in the crust - these proportions have been estimated by Taylor (1964b).

The enrichment factor (E), relative to the average mantle peridotite, is given for each oxide and trace element in the Nuanetsi lavas in Table 29, column 3. These figures highlight the contrast between the geochemistry in basic rocks of K and associated elements on the one hand - the 'incompatible elements' of Ringwood (1966) - and, on the other hand, the remaining 'compatible' oxides and elements which have enrichment factors in the range 0.30 - 8.6.

The net chemical results of the processes involved in the generation of the Nuanetsi olivine-rich basalts from the upper mantle are :

(a) Substantial increases in Al, Ca and Na.

(b) Equivalent decreases in Mg, Cr and Ni.

(c) Enormous increases in the concentration of K and associated elements.

The processes which brought about these chemical changes must include partial melting and crystal-liquid fractionation and may also include contamination by both mantle and crustal material.

Since the enrichment factors for K and associated elements in the Nuanetsi basalts from the basis of the semi-quantitative discussion of enrichment processes which follows, it is desirable that there should be independent confirmation of their accuracy. The average analysis of a small number of deep oceanic tholeiites (Engel et al, 1965; Tatsumoto et al, 1965), presented in Table 29, offers an opportunity for such a check.

Assuming that K and associated elements are characterised by highly incompatible behaviour, i.e. distribution coefficients between

liquid and solid are in excess of 10, the liquid formed on the partial melting of peridotite will contain almost all the K and associated elements in the liquid-solid system. The initial enrichment factors, therefore, depend on the degree of melting. Subsequent enhancement of these initial enrichment factors will be brought about by crystal-liquid fractionation and will be directly related to the degree of fractionation. In such a closed-system melting-fractionation scheme O'Hara (1968a) has estimated that the lowest enrichment factors likely to be recorded in common basalt types at the surface is 8. This assumes advanced partial melting - 20% - and the minimum of fractionation which is consistent with the degrees of bulk compositional evolution displayed by basalts at the surface.

The deep oceanic tholeiites have very low contents of K and associated elements yet are well-evolved in terms of 'compatible' elements (O'Hara, 1968b). It is tempting, therefore, to consider that the evolution of these basalts represents a close approach to the limiting conditions envisaged by O'Hara and it is appropriate to calculate enrichment factors for K and associated elements, relative to the assumed average mantle composition, for the average deep oceanic tholeiite (Table 29, column 5), and to compare these with the optimum minimum figure of 8.

The general agreement between the enrichment factors for the deep oceanic tholeiite average and the value of 8 predicted by O'Hara's model suggests that the average values of K and associated elements in mantle peridotite which are used in Table 29 are acceptable estimates of the real values. It follows, therefore, that the Nuanetsi enrichment factors (Table 29, column 3) are reasonably accurate.

There is an indication in the data in Table 29 that the average mantle Ba content of 3.9 p.p.m. is too high. A value of 1.8 p.p.m. is necessary to raise the deep oceanic tholeiite enrichment factor to 8. If adopted, this downward revision of the mantle Ba content would raise the Nuanetsi enrichment factor from the high value of 202 to the extraordinary value of 455.

The occurrence of very high K and associated enrichment levels in lavas which have also been shown to have primitive picritic compositions (Chapter 5) emphasises the independence, or decoupling, of these elements from the major oxide composition of basalts. Although Harris (1957) drew attention to the likelihood of such behaviour, it is only in recent years that there has been widespread appreciation of its significance and implications, for example, in publications by Ringwood (1966), Green and Ringwood (1967), Gast (1968), Griffin and Murthy (1968b) and O'Hara (1968a).

Available chemical analyses indicate that deep oceanic tholeiites with low or primitive contents of K and associated elements – but evolved major oxide compositions – and the Nuanetsi olivine-rich tholeiites which have high or evolved contents of K and associated elements represent the end-members of a spectrum of contents of these elements in tholeiitic basalts.

The independence of K and associated elements from the major oxide composition in tholeiitic basalts is also shown by the wide range of K_2O contents displayed by average tholeiitic analyses which have the same MgO content, i.e. the same degree of evolution (Jamieson and Clarke, in preparation).

Processes leading to the enrichment of K and associated elements in tholeiites, in general, and in the Nuanetsi lavas, in particular, are discussed in the following Chapter.

CHAPTER 8

POTASSIUM AND ASSOCIATED ELEMENTS
- ENRICHMENT PROCESSES

Several enrichment processes of K and associated elements are critically discussed. The significance of these processes is assessed both from a general standpoint and in the specific context of the Nuanetsi olivine-rich rocks.

Of the processes considered mantle wall-rock reaction and the high pressure fractionation of eclogite from picritic primary magmas seem to be the most plausible. Both of these are clearly deep-seated processes; they are also rather speculative. It is difficult, therefore, to choose objectively between them. However, the compositions of the olivine-rich rocks suggest that any eclogite fractionation during the evolution of the magmas must have taken place under very high pressures - c. 40 kb. Existing experimental evidence indicates that one possible, and intriguing, result of eclogite fractionation under such pressures - which correspond to depths of 120 - 140 km. - may be an enrichment of both K_2O and MgO in residual liquids.

Because of this possible mechanism for simultaneously generating the recorded MgO - K_2O relationship, the author proposes a petrogenetic model for these rocks which incorporates the fractionation of eclogite at 40 kb. pressure as an important enrichment process of K and associated elements.

Introduction

Before discussing the merits of various petrological processes it is pertinent to restate concisely the main features of the distribution of K and associated elements in the Nuanetsi olivine-rich lavas :

(a) The mean contents of K and associated elements in 47 lavas are very high. Enrichment relative to the average mantle composition ranges from 13 times to 202 times.

(b) There are highly significant sympathetic relationships between each member of the K and associated group of elements and Mg.

These chemical aspects of the rocks may, or may not, be related.

The reader may recall (from Chapter 1) that Cox et al (1967) demonstrated that the high levels of K and associated elements recorded in the Nuanetsi olivine-rich rocks are also found, to a lesser degree, in all the Karroo basic rocks of Rhodesia. It was this distinctive geochemical character which Cox et al used as a criterion to divide the Karroo basic rocks of Southern Africa into 2 provinces — the Northern province having high K, Ti, P, Ba, Sr and Zr, the Southern province with contents of these elements which are lower and which closely conform with the tholeiitic average.

The processes leading to the marked enrichment in the Nuanetsi olivine-rich rocks appear, therefore, to have operated, albeit on a lesser scale, in the generation of the Nuanetsi Upper Basalts and the basalts of adjacent areas in Rhodesia. Therefore, an acceptable hypothesis must not be specific only to the Nuanetsi olivine-rich rocks.

The following processes, which potentially could lead to the enrichment of K and associated elements in basic magmas, are now discussed.

    (a)   Chemical inhomogeneity in the mantle.

    (b)   Partial melting of the mantle.

    (c)   Mantle contamination or wall-rock reaction.

    (d)   Crystal-liquid fractionation.

    (e)   Crustal contamination or wall-rock reaction.

    (f)   Volatile transfer, etc.

Mantle Inhomogeneity

(i)   Vertical

Any hypothesis based on a model upper mantle which is chemically and mineralogically homogeneous is likely to be an oversimplification. The mineral assemblage at the beginning of melting varies with depth because of P- and T- dependent solid-solution effects. The stabilities of mica and amphibole, possible trace constituents, are critically dependent on P, T and volatile content (Kushiro et al, 1967; Lambert and Wyllie, 1968; Yoder and Kushiro, 1969). Therefore, we can expect small, but possibly significant, changes in the distribution coefficients of elements between solid and liquid. For example, Dickinson and Hatherton (1967) have considered that a sympathetic relationship between the K_2O content of andesites and the depth of seismic activity in the Benioff zone is a result of distribution coefficients between solid peridotite and magma varying with pressure.

The absolute abundances and distribution in the crust and the mantle of the radioactive heat-producing elements K, U and Th is still a matter of discussion, cf. Taylor (1964a), Hurley (1968b) and Shaw

(1968). However, there is widespread agreement that the equivalence of oceanic and continental heat-flow implies that the heat-producing elements in the oceanic mantle are almost totally concentrated in the upper 400 - 700 km. (see, for example, Von Herzen (1967) and Shaw (1968)).

This proposed upwards concentration is not, however, consistent with the enrichment factors relative to _average_ mantle peridotite which are shown by deep oceanic tholeiites (Table 29). Average mantle contents of 0.015 p.p.m. U and 0.054 p.p.m. Th (Hurley, 1968b) and the average contents in 6 deep oceanic tholeiites of 0.09 p.p.m. U and 0.17 p.p.m. Th (Tatsumoto, 1966) give enrichment factors of 6 and 3.2 respectively - the figure for K is 11 (Table 29). As has been pointed out these values are generally consistent with 20% partial melting of this average mantle peridotite at pressures of 25 - 35 kb. and a simple fractionation scheme involving the removal of olivine only from the primary magma.

The contents of K, U and Th in deep oceanic tholeiites, therefore, place a severe restriction on the concentration of these elements in the zone of magma generation of the upper mantle. Values in excess of the postulated average mantle concentrations cannot be reconciled with the contents in these basalts. If the data for U and Th in Table 29 are correct, either the model of O'Hara (1968b) is wrong, or the upwards concentration of K, U and Th in the upper mantle is much less marked than has been assumed. The latter is a strong possibility, especially if the principal means of heat-transfer in the upper mantle is convection rather than conduction.

In conclusion, it is considered that the variations in the concentration of K and associated elements which are recorded in basalts are unlikely to be the direct result of the mantle being

vertically inhomogenous with respect to these elements. Any downward depletion of K and associated elements is unlikely to be marked in the upper 150 km. - the part of the mantle which has been considered to be the zone of magma generation by O'Hara and Yoder, (1967). Furthermore, the absolute abundances of K, U and Th in deep oceanic tholeiites do, in fact, cast doubts on the proposed marked concentration of these elements in the upper-most mantle.

(ii) Lateral

Reference has been made above to the widely accepted hypothesis that the sub-oceanic upper mantle must be greatly enriched in heat producing elements relative to the sub-continental upper mantle. Such a geochemical distribution would cause striking inhomogeneity with respect to these elements in the zone of magma generation - i.e. down to 150 km. depth.

Although the data for trace elements are sparse, there seems to be a very close petrochemical similarity between oceanic and continental basalts. The average analyses of tholeiitic basalts from these two environments, which were calculated by Manson (1967), are reproduced in Table 30. As has been pointed out by Engel et al (1965), the continental average analysis contains more K_2O than its oceanic counterpart. However, MgO is lower and SiO_2 is higher in the continental average and it is concluded that the greater part of these small differences is due to the higher degree of evolution, or differentiation, displayed by continental basalts - a reflection, perhaps, of a slower passage through the continental crust to the Earth's surface.

Data compiled by Wood (1968, Table 33) show that 10 continental

TABLE 30

THOLEIITIC AVERAGES

	282 Oceanic Tholeiites	946 Continental Tholeiites
SiO_2	49.3	51.5
TiO_2	2.4	1.2
Al_2O_3	14.6	16.3
Fe_2O_3	3.2	2.8
FeO	8.5	7.9
MnO	0.17	0.17
MgO	7.4	5.9
CaO	10.6	9.8
Na_2O	2.2	2.5
K_2O	0.53	0.86
P_2O_5	0.26	0.21

Data from Manson (1967, Table IV)

TABLE 31

ENRICHMENT OF K, Rb, Sr AND Ba

IN PERIDOTITE PARTIAL MELTS

	Spinel Lherzolite			Garnet Lherzolite		Hbl. Lherzolite	
Degree of melting %	1.2	4.8	10.8	5	10	5	10
	Kl/Ko	Kl/Ko	Kl/Ko	Kl/Ko	Kl/Ko	Kl/Ko	Kl/Ko
K	23	15	9	18	10	16	10
Rb	36	19	9	16	9	18	10
Sr	17	13	9	17	9	15	10
Ba	27	17	9	18	9	13	10

Kl/Ko - concentration in the liquid/concentration in the unmelted peridotite.

Data from Gast (1968, Figs. 9 and 11) for spinel lherzolite; from Griffin and Murthy (1968b, Tables 9, 10 and 13) for garnet and hornblende lherzolites.

By adopting the contents of K and associated elements in selected mafic minerals Gast (1968) and Griffin and Murthy (1968b) calculated possible distribution coefficients for K and associated elements and considered the behaviour of these elements during the partial melting of various model peridotitic assemblages.   Data from these theoretical studies which give the relative enrichment of K and associated elements in the liquid phase after various small degrees of partial melting are given in Table 31.

While the actual values in Table 31 clearly depend on the distribution coefficients adopted, it is obvious that, with distribution coefficients in the range 10 - 100 increased melting can only effect a dilution of these elements in the primary magmas.

Thus degrees of melting of mantle peridotite in the realistic range of 5% - 33% can endow primary magmas with enrichment factors for K and associated elements which could, ideally, range from 20 - 3. Both Harris (1967) and O'Hara (1968a) have drawn attention to the importance of partial melting as an enrichment factor.

The effect of varying the degree of partial melting will be much less marked for the major oxide bulk composition of primary magmas.   The results of Ito and Kennedy (1967) indicate that, with increased melting, in the range 5% - 33% the primary picritic magma, which is produced at 30 kb. from a garnet lherzolite mantle, will be progressively enriched in ol and hy - olivine and orthopyroxene being the residual solid phases when this composition is partially melted at 30 kb.   If subjected only to the simplest fractionation scheme of O'Hara (1968a) - polybaric fractionation of olivine - all such magmas would be erupted as basalts.   These basalts would display small but significant variations of major oxide bulk composition but

a considerable range of enrichment factors of K and associated elements.

Thus the partial melting of the upper mantle peridotite must be an important enrichment factor of K and associated elements in basalts and variations in the degree of partial melting are a very efficient method for varying enrichment factors.

The relative compositional differences between the average Kilauea and Mauna Loa basalts are interpreted as reflecting different degrees of partial melting (Table 32). No low pressure fractionation scheme, which is plausible in terms of the recorded appearance of crystalline phases, can account for the major oxide composition and the relative concentrations of K and associated elements.

In the case of the Nuanetsi olivine-rich tholeiites, however, there is little support for the superficially attractive hypothesis that the peculiar geochemistry of the rocks is largely the result of unusually small, but variable, degrees of partial melting of mantle peridotite. Firstly, it is difficult to envisage the thick and voluminous succession of olivine-rich basalts (Chapter 1) being the result of unusually small degrees of partial melting. The thick nature of the succession and the evidence of relatively rapid ascent of the magmas (Chapter 5) indicate a vigorous magmatic event which implies an abundance of magma in the zone of generation and in the conduits leading to the surface. Secondly, the sympathetic relationship between MgO and K and associated elements (Chapters 4 and 6) is just the reverse of that expected if the variation of enrichment values within the suite of rocks was to be the result of variable degrees of partial melting in the mantle. Increased melting of garnet lherzolite at 30 kb. produces primary magmas which are more picritic and which have lower enrichment values of K and associated elements.

TABLE 32

KILAUEA AND MAUNA LOA THOLEIITES

	SiO_2*	MgO*	K_2O*	P_2O_5*	Ba	Sr	Zr
Kilauea	49.96%	8.39%	0.54%	0.30%	184	652	202
Mauna Loa	51.11%	8.79%	0.38%	0.24%	59	481	144

* - from Macdonald and Katsura (1964, Table 9,
nos. 6 and 7). Trace elements in p.p.m.,
from Prinz (1967, Table IV).

Mantle Wall-Rock Reaction

Harris (1957) proposed that the industrial metal purification process of zone-refining might be relevant to the genesis of K-rich mafic lavas. In the geological analogy Harris envisaged a body of magma (solid + liquid), surrounded by hot wall-rock, ascending by a process of solution of mantle peridotite, at the top, and precipitation of a peridotitic assemblage, in the lower parts of the magma body. The proportions of silicate phases melted and precipitated was controlled by the phase relations appropriate to the prevailing P and T. During such a process K and associated elements, with liquid/solid distribution coefficients > 1, would be readily incorporated in the melt but the silicate precipitate would be almost free of these elements. Hence the magma would become enriched in these elements although the major oxide bulk composition changed very little.

In 1967 Green and Ringwood formulated a more generalised version of the zone-refining hypothesis. Their wall-rock reaction process has much wider application and it was considered by Green and Ringwood that all alkali basalts and some tholeiites had their K and associated element enrichment factors enhanced by this process. Described as 'solution of low-melting components from the wall-rock and their incorporation into the magma' (Green and Ringwood, 1967, p.175), the process is essentially an attempt to achieve equilibrium between the magma and the relatively unaltered wall-rock through which it is passing. It is important to realise that this process is not haphazard but is controlled by distribution coefficients and the rather obscure phase relations which control the initial stages of the partial melting of peridotite - stage 1 (O'Hara, 1968a). The magma composition produced after extensive wall-rock reaction would be

similar to that produced by small amounts - ∼ 3% - of partial melting of peridotite.

The author accepts the principle of mantle wall-rock reaction but finds it very difficult to assess the importance of the process. The following two pertinent observations have recently been made with regard to this process :

(a) '... although it might work reasonably well for the first batch of magma to ascend through a conduit, it is difficult to envisage it working with equal or increased efficiency for succeeding batches ...' (O'Hara, 1968a, p.117).

(b) '... the opportunity for enrichment will decrease rapidly as small conduits (10 - 100 cm.) coalesce into larger channels.' (Gast, 1968, p.1081).

These observations are considered by the author to be very reasonable. They imply that reaction between peridotite wall-rock and magma may be, in general, of limited importance as a factor giving rise to enrichment in K and associated elements. However, the Nuanetsi olivine-rich tholeiites display enrichment factors of these elements which are exceptionally high when compared with those of other tholeiitic rocks. To account for this geochemical feature one can invoke either an extremely unusual process or a common process, normally of limited importance, which has operated with unusual efficiency in the particular case.

The efficiency of any reaction process between magma and wall-rock must increase as temperature increases in the zone of magma generation and, in particular, its immediate surrounds. Reaction will

also be encouraged if the contacts between magma and the wall-rock are penetrative and diffuse. Maximum enhancement of K and associated elements might, therefore, be expected to occur by this process if there was a thermal high of exceptionally large volume in the upper mantle. Under these circumstances there might be a minimal temperature contrast between magma and the wall-rock peridotite for a considerable distance away from the zone of magma generation and the coalescing of small magma droplets, conduits and other bodies might occur at a relatively late stage in the evolution of the magma. The occurrence of an unusually large thermal high in the mantle is not inconsistent with the voluminous nature of the volcanic products - both the Olivine-rich Group and the Upper Basalts - in the Nuanetsi Province.

Unusually efficient reaction between magma and peridotite wall-rock resulting from exceptional physical conditions in the mantle does, therefore, seem to be a possible cause of the high contents of K and associated elements in the Nuanetsi olivine-rich tholeiites. It is difficult, however, to envisage how this process can account for the observed sympathetic relationship between MgO and K and associated elements. Nevertheless, it is conceivable that in a relatively hot mantle environment at depths corresponding to 25 - 35 kb. pressure the efficiency of wall-rock reaction might markedly increase as the degree of partial melting increases. Since increased melting of garnet lherzolite at 30 kb. pressure produces primary magmas which become progressively picritic, this hypothetical relationship could be the cause of the observed coherence between MgO and K and associated elements.

Wall-rock reaction, therefore, is a plausible process of enrichment of K and associated elements. It is, however, difficult to assess on a more quantitative basis.

Crystal-Liquid Fractionation

The concentration of K_2O builds up in the residual liquid during the low pressure fractionation of tholeiitic magma. This is because the gabbroic crystalline extract of olivine, clinopyroxene and plagioclase contains very little K_2O. Wager and Brown (1968, Chapter VII) have documented this behaviour in the Skaergaard intrusion. However, the Nuanetsi olivine-rich lavas have primitive picritic compositions (Chapter 5); they have been subjected to minimal low-pressure fraction-ation. Also it will be recalled that K_2O and MgO in these rocks are sympathetically related. Clearly, low pressure fractionation cannot have significantly enhanced the K_2O contents of the olivine-rich rocks. In this respect the Nuantsi Olivine-rich Group almost certainly contrasts with the well-evolved, low-magnesian Upper Basalts.

In their recent papers dealing with basalt origins Green and Ringwood (1967), O'Hara (1968a) and Ito and Kennedy (1967) have demonstrated that during ascent to the Earth's surface the primary magmas generated at depths of up to 130 km. must be modified in composition by means of crystal-liquid fractionation. Hence magmas erupted at the surface are, in general, the end-products of almost continuous processes of fractionation and, as a result, their compositions may be very different from those of the parental primary magmas.

Although the details of the basalt evolutionary schemes proposed by Green and Ringwood and O'Hara vary considerably in detail, there is agreement that the dominant crystalline phases which will fractionate during magmatic ascent are olivine, orthopyroxene and clinopyroxene. These authors also agree that the passive build up of K and associated elements in the liquid, which must accompany such fractionation of mafic

crystalline phases, is insufficient to account for the enrichment factors of these elements recorded in some tholeiites and in most alkali basalts. This led Green and Ringwood to propose that wall-rock reaction (discussed above) makes an important contribution to the content of K and associated elements.   O'Hara, on the other hand, preferring a closed-system evolutionary scheme, considered that petrogenetic models which incorporated varying degrees of high pressure fractionation of eclogite from primary magmas could account for all the observed enrichment factors.

The possibility that eclogite fractionation has played an important role in the evolution of the Nuanetsi olivine-rich rocks is discussed below, as is the fractionation of the K_2O-bearing phases amphibole and mica.

(i) Fractionation of mica.

Bowen (1928) proposed that the fractionation and subsequent resorption of biotite in basic magmas might play an important part in the development of alkali-rich basic rocks, particularly nepheline basalts, leucite basalts, nephelinites and leucitites.

The sympathetic relationship between K_2O and MgO in the Nuanetsi olivine-rich tholeiites first suggested to the author that the fractionation of a phlogopitic mica might be, in part, responsible for the trend of compositional variation.   Typical natural phlogopites contain between 9% and 11% K_2O and 18% to 26% MgO (Carmichael, 1967).

It must be emphasised that fractionation of phlogopite can account only for the variation trend within the suite of rocks and cannot, in itself, account for the richness in K and associated elements of the suite - in fact phlogopite nucleation and precipitation must be a result of the relatively high concentration of K_2O in the magmas.

Recent P and T determinations using the phlogopite composition

(Yoder and Kushiro, 1969) have confirmed that the field of phlogopite stability extends above 30 kb. and have shown that, in the absence of a gas phase, phlogopite is stable to higher temperatures than in the presence of a gas. In the gas-free system the upper stability limit of phlogopite - at which it breaks down to forsterite + liquid - passes through $1270^{\circ}C$ at 5 kb. and $1375^{\circ}C$ at 30 kb.

One result of this increased stability is that, below 25 kb., the upper stability limit of phlogopite is located at temperatures which are up to $150^{\circ}C$ above the solidus of a natural garnet peridotite (Ito and Kennedy, 1967, Fig. 1). It is conceivable, therefore, that, given sufficient H_2O, phlogopitic mica could nucleate in a K_2O-rich basic magma at temperatures above the solidus of a 4-phase peridotite, i.e. in relatively non-evolved magmas which were still capable of producing basaltic magma at the surface (O'Hara, 1968a, Fig. 7).

The upper stability limit of phlogopite is a maximum of $150^{\circ}C$ above the natural 4-phase peridotite solidus in the pressure range 5 - 10 kb. Considering that phlogopitic mica in a natural K_2O-rich basic system will have a stability field which is more restricted, the chances of significant phlogopitic mica crystallisation are highest in this pressure range. An hypothesis of phlogopitic mica fractionation, in addition to olivine and orthopyroxene (Chapter 5), during an inter-mediate pressure fractionation event was, therefore, considered.

This hypothesis of mica + olivine + orthopyroxene fractionation is supported by the positions of the lava compositions relative to the appropriate mineral composition points in the transformed variable variation diagrams (Figures 22 - 24) and by conventional variation diagrams of MgO v. Ba and K_2O (Figures 25 and 26). However, the following facts are all unfavourable to the hypothesis :

FIGURE 25

MgO v. Ba variation diagram

● : represents Nuanetsi olivine-rich lavas
— 44 in number.

In the triangle formed by the plotted positions
of magnesian olivine (OLIV) and orthopyroxene (OPX) and
phlogopite (PHLOG) the heavily shaded area represents the
most likely necessary crystalline extracts if removal of
these three phases is the principal cause of magmatic
variation. The lighter shaded areas represent less
likely, but possible, extracts.

The 25% phlogopite composition is indicated.

FIGURE 26

MgO v. K$_2$O variation diagram

● : represents Nuanetsi olivine-rich lavas
 - 44 in number.

In the triangle formed by the plotted positions of magnesian olivine (OLIV) and orthopyroxene (OPX) and phlogopite (PHLOG) the heavily shaded area represents the most likely necessary crystalline extracts if removal of these three phases is the principal cause of magmatic variation. The lighter shaded areas represent less likely, but possible, extracts.

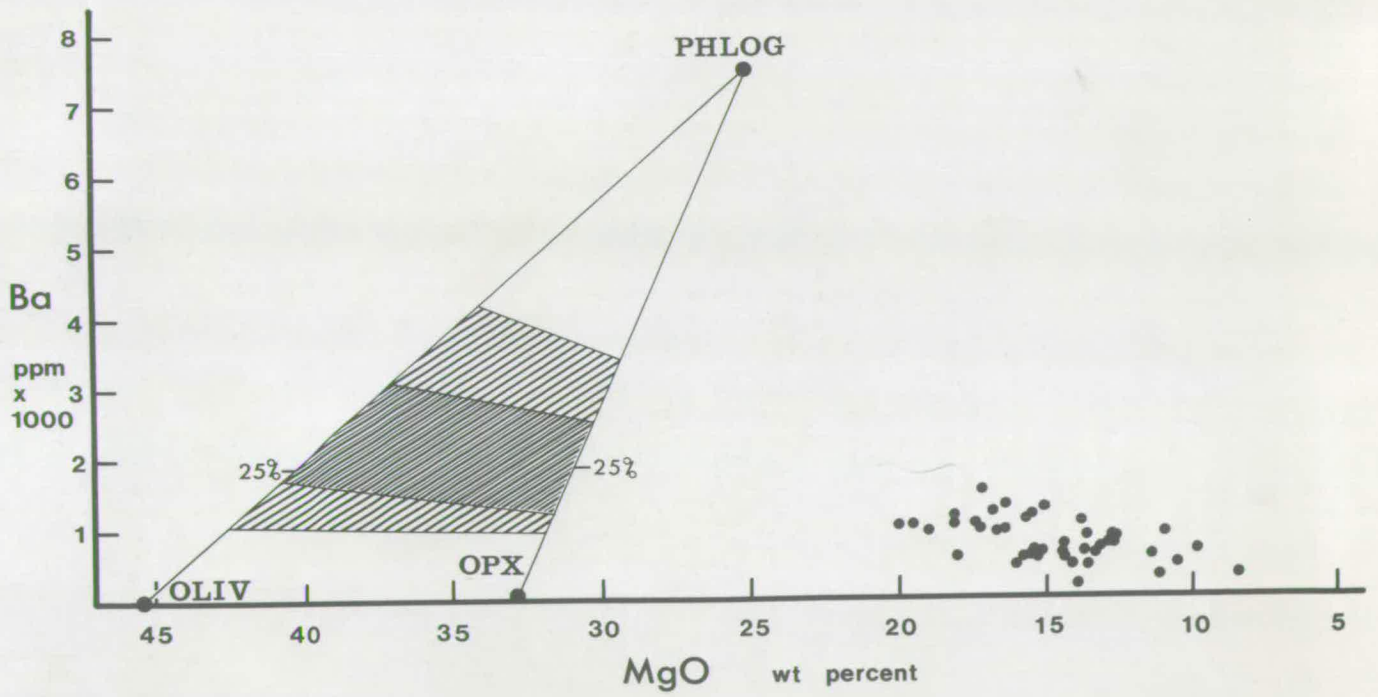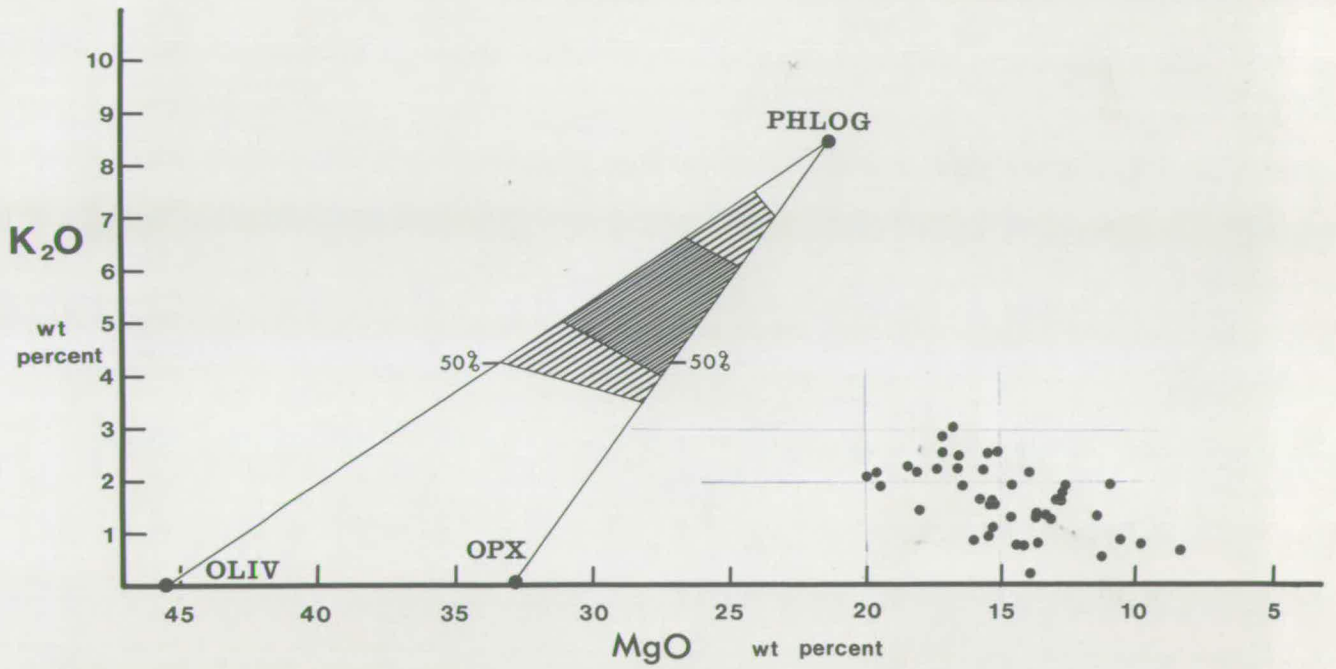The 50% phlogopite composition is indicated.

(a)   A close examination of Figures 25 and 26, especially the latter, reveals that the necessary crystalline extracts must contain large amounts of phlogopite;   the 60% mica harzburgite required to account for the relationship between K_2O and MgO (Fig. 26) seems particularly improbable in view of factor (c), below.

(b)   There is no evidence in the olivine-rich rocks that the magmas contained above-average contents of H_2O.   No primary hydrous minerals were recorded.   The average H_2O content of the lavas is 1.63% but this is closely related to the degree of secondary alteration.   The freshest rocks generally contain less than 0.5% H_2O.   Furthermore, the lavas show no marked vesicularity which might be due to volatile loss on eruption.

(c)   None of the olivine-rich rocks examined in thin section contained mica.   Admittedly, on eruption any phlogopitic mica would be out of its stability field and would break down to olivine + liquid.   Nevertheless, some relict mica or its pseudomorph might be expected.

(d)   Considering the platy crystal form of micas the efficiency of the fractionation of phlogopite in basic magmas is likely to be very low.

It is concluded that the hypothesis of mica fractionation as the cause of some aspects of the variation displayed by the Nuanetsi olivine-rich rocks must be considered to be interesting but improbable.

(ii) Fractionation of amphibole.

Since amphibole is one of the important K_2O-bearing mafic minerals, fractionation of this phase has been considered as a possible cause of the compositional variation in the olivine-rich rocks.   The mineral analyses compiled by Deer et al (1962b) show that while amphiboles can

contain up to 3% K_2O most contain 0.5 - 1.5%.

The preliminary results of Lambert and Wyllie (1968) indicate that amphibole may be stable under upper mantle conditions of modest P and T - i.e. 25 kb. and 1,000°C. Under these conditions relatively H_2O-rich basic magmas might exist.

However, the plotted position of an amphibole - from a hornblende clinopyroxenite inclusion in the lavas of Dreiser Weiher, West Germany (Aoki and Kushiro, 1968) - in the transformed variable variation diagrams (Figs. 22 - 24) is not favourable to amphibole fractionation. The amphibole composition point lies in the middle of the trend of rock composition points, not at one end as would be expected.

Amongst mafic minerals the K_2O/Na_2O ratio of amphiboles is relatively high. However, with only a few exceptions the value of this ratio is less than 1 - generally 0.25 - 1 (Deer et al, 1962b). The concentrations of Ba, Rb and Sr in amphiboles are also relatively high (Deer et al, 1962b). The highest values of these trace elements in amphiboles appear to be those determined by Wood (1968) in pargasite from xenoliths in 4 alkali-rich rocks - Ba 234 - 398 p.p.m., Rb 13 - 77 p.p.m. and Sr 274 - 485 p.p.m.

However, neither the K_2O/Na_2O ratio nor the contents of K_2O, Ba, Rb and Sr in amphibole are sufficiently high to account for the observed trend of rock compositions and it is concluded that the fractionation of amphibole has not played a significant role in the development of the Nuanetsi picritic magmas.

(iii) Fractionation of eclogite at high pressures.

As was pointed out in the introduction to this section on crystal fractionation, at all pressures K (and certain other elements) passively build up in the liquid phase during the evolution of basic magmas by

fractionation of the major mafic silicate phases. Ignoring factors such as wall-rock reaction, the K_2O content is a rough fractionation index of basic magmas.

Because crystal-liquid fractionation of mafic silicates progressively alters the major element concentration, i.e. the bulk composition, of magmas, there must be an upper limit to the degree of fractionation (K_2O enrichment) which an evolving basic magma can sustain and still remain capable of producing tholeiitic magma at the surface. Green and Ringwood (1967) considered this point and concluded that the enrichment factors which could be achieved by partial melting and fractional crystallisation were not high enough to account for the concentrations of K and associated elements observed in alkali and tholeiitic basalts. This logically led these authors to propose the open-system enrichment process of wall-rock reaction which has been discussed above. However, the conclusions of Green and Ringwood have been challenged. O'Hara (1968a) considered that the high pressure fractionation of eclogite (O'Hara and Yoder, 1967) is a process which, if included in a closed-system petrogenetic model, is capable of producing all the enrichment factors displayed by basalts without resorting to open-system processes.

Experimental research has indicated that the partial melt of garnet peridotite at 25 - 40 kb. is a hypersthene-normative picrite with a composition lying close to the garnet-clinopyroxene join. With increasing degrees of melting this liquid becomes progressively enriched in normative olivine and hypersthene (Ito and Kennedy, 1967; O'Hara, 1968, p.82 and Figs. 4 - 6). Because of reaction relationships between crystals and liquid O'Hara and Yoder (1967) have proposed that the fractional crystallisation of a garnet lherzolite partial melt in this pressure range will lead to the precipitation of bimineralic eclogite.

The evidence of the required reaction relationship between orthopyroxene and liquid at the beginning of melting is contained in the results of Tilley and Yoder (1964), Davis and Schairer (1965), Green and Ringwood (1967), Ito and Kennedy (1967) and O'Hara and Yoder (1967). However, the evidence of the necessary reaction relationship between olivine and liquid is less direct. O'Hara and Yoder (pp. 102 - 107) argue that olivine is likely to be resorbed in the equilibrium which involves garnet, olivine, clinopyroxene and liquid. Liquids which fractionate through the 4 solid phase, 'beginning of melting' equilibrium will continue to fractionate, with decreasing temperature, in this equilibrium and according to the proposal of O'Hara and Yoder, garnet and clinopyroxene will be the only precipitating phases.

Perhaps the most important aspect of high pressure eclogite fractionation is a fortuitous near-coincidence of the bulk compositions of the initial partial melt of garnet lherzolite in the pressure range 25 - 40 kb. (the liquid) and the likely garnet-clinopyroxene mixtures which will precipitate from this liquid on cooling (the crystalline extract). As a result, eclogite fractionation can give rise to derivative residual liquids which vary very little in major element concentration from the original liquid or magma. Nevertheless, because an eclogite crystalline extract contains very small concentrations of K and associated elements, there will be a passive build up of these elements in the residual liquids. Therefore, enrichment factors of K and associated elements will change markedly relative to the change of major element concentration.

During a period of high pressure eclogite fractionation the trend of residual liquids is likely to be towards highly-alkaline, nepheline-normative basic compositions. Small amounts of K-rich mafic magma and

magma corresponding to the groundmass of kimberlite are considered by
O'Hara and Yoder (1967) to be possible products of prolonged eclogite
fractionation of hypersthene-normative picritic magma at 30 kb. However,
the attainment of such extreme compositions requires extensive fraction-
ation and is not relevant to tholeiitic basalts. With regard to tholeiites
O'Hara (1968a, p.118) estimates that it might be possible to double
enrichment factors in residual magmas before a nepheline normative
composition was reached.

Because an eclogite crystalline extract contains significant
Na_2O - held in the omphacitic clinopyroxene - this is one of the few
fractionation schemes for basic magmas which efficiently discriminates
between Na and K. In fact, an increasing K_2O/Na_2O ratio is probably
the best index of eclogite fractionation. A much more detailed analysis
of the geochemical aspects of high pressure eclogite fractionation is
given by O'Hara and Yoder (1967, pp. 107 - 114).

Small, but varying, amounts of eclogite fractionation, therefore,
seem to offer an ideal means of enhancing enrichment factors of K and
associated elements in such a way that magmas at the surface with broadly
similar compositions, i.e. tholeiitic basalts, can display greatly
varying concentrations of K and associated elements. Can eclogite
fractionation be invoked to account for the high contents of K and
associated elements, and the high K_2O/Na_2O ratios in the Nuanetsi
olivine-rich rocks ?

From the descriptions above and by O'Hara and Yoder (1967) it
will be obvious that eclogite fractionation in the pressure range of
25 kb. to 40+ kb. cannot commence until a magma has the composition of
the liquid which is in equilibrium with the 4 solid phases of garnet
lherzolite. This composition is, of course, almost immediately achieved

during the partial melting of garnet lherzolite and is also regained if a more advanced partial melt is allowed to cool and to fractionally crystallise. The composition of this 'beginning of melting' liquid exercises an important control over the range of residual magma compositions which can be produced by eclogite fractionation because such residual magmas are likely to become progressively depleted in normative hypersthene, albeit at a slow rate. In other words, at a given elevated pressure a residual magma from which eclogite has been extracted will be poorer in hy than the initial liquid produced by partially melting garnet lherzolite at that pressure.

Because the Nuanetsi olivine-rich lavas have suffered a minimum of low pressure fractionation - which clearly increases hy in tholeiitic compositions - the reasoning above has been applied to this suite in an attempt to define the composition of the 'beginning of melting' liquid, and hence the pressure, from which the Nuanetsi parental magmas might have evolved by eclogite fractionation. The following argument is illustrated by means of a diagram (Figure 27). This is a section $(R_2O_3 - XO.ZO_2 - YO.ZO_2)$ of the pseudoquaternary system $R_2O_3 - XO - YO - ZO_2$, projected from the $2YO.ZO_2$ composition point, which was extensively used in Chapter 5 to present rock compositions and phase relations.

In Figure 27 the curve A B C D is the locus of liquid compositions which are in equilibrium with the solid phases of natural 4-phase peridotites in the pressure range 1 atmosphere to 40 kb. The data, except the 40 kb. composition, have been taken from O'Hara (1968a, Fig. 4). The composition of the 40 kb. 'beginning of melting' liquid was approximately determined by Davis (1964) and Davis and Schairer (1965) in the analogous synthetic system $Al_2O_3 - CaO - MgO - SiO_2$.

It is obvious from an inspection of Figure 27 that the Nuanetsi

FIGURE 27

$2YO.ZO_2$ (Olivine) projection showing the changing
composition of peridotite initial partial melts with
increasing pressure.

A - B - C - D represents the locus of the
composition of the 'beginning of melting' liquid in
equilibrium with 4-phase peridotite in the pressure
range O - 40 kb.

The range of composition of the Nuanetsi olivine-
rich lavas is indicated by stippling (picrites and
cumulus-enriched types having been excluded).

Z represents the possible composition of the
initial eclogite extract from a picritic primary magma
according to the hypothesis of O'Hara and Yoder (1967).
This composition (Z) is derived from a consideration of
likely clinopyroxene and garnet compositions at high
pressure ($\underline{c}$. 40 kb.) and high temperature ($\underline{c}$. $1500^{o}C$)
(O'Hara and Yoder, 1967; O'Hara, 1967).

R_2O_3

60

GARNET

80

B

A

C

D

Z

XO.ZO$_2$

CPX

60

80

OPX

YO.ZO$_2$

27
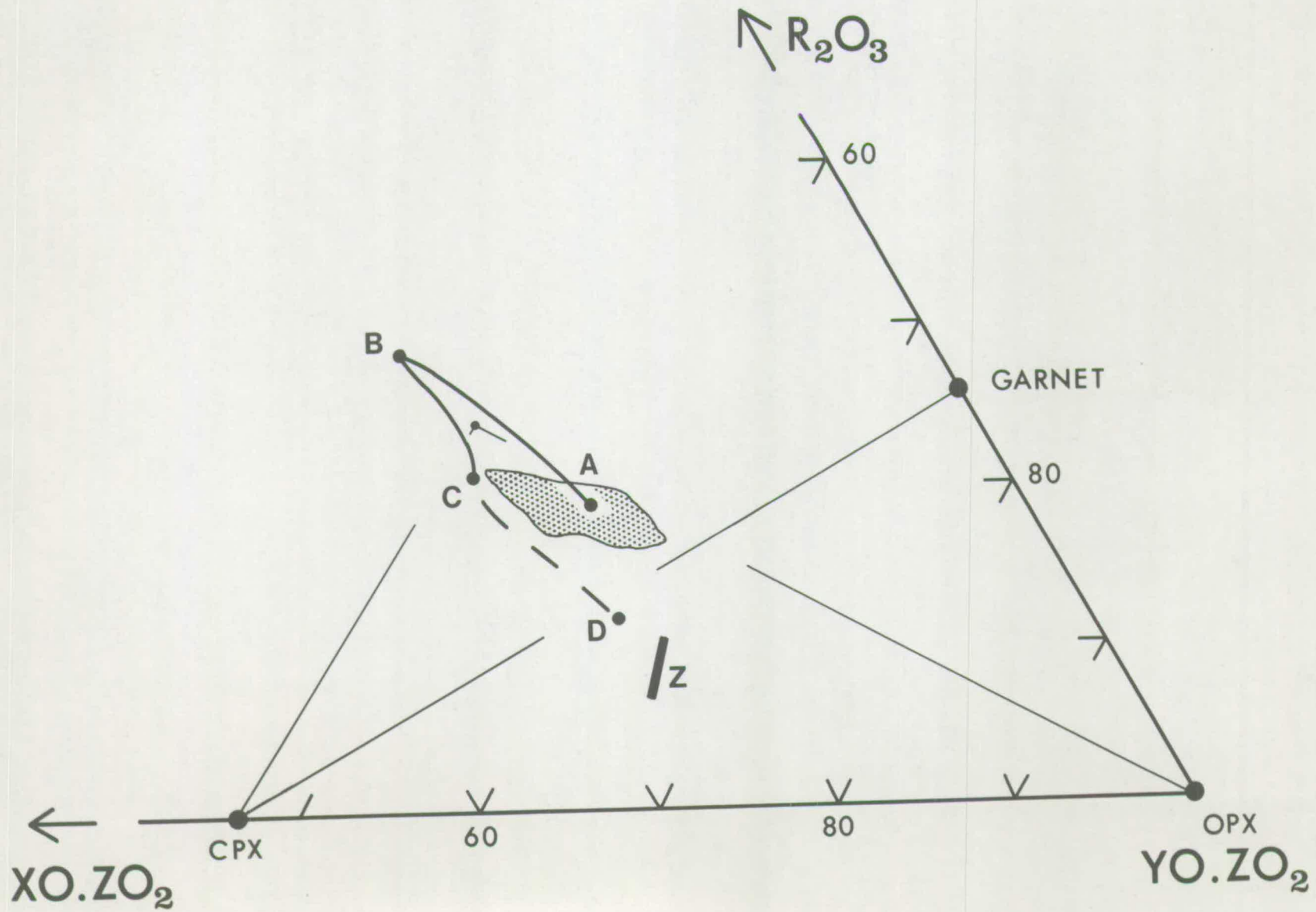
rocks contain more hy than the 30 kb. critical liquid and it is concluded that the parental magmas are unlikely to have undergone eclogite fractionation at this pressure. In contrast, however, at 40 kb. the relative positions in Figure 27 of the Nuanetsi rocks (the residual magmas) and the estimated compositions of the 'beginning of melting' liquid (the initial magma) and bimineralic eclogite (the crystalline extract) are consistent with an eclogite fractionation event.

By referring to Figure 27 the reader may care to confirm that any fractionation of olivine or harzburgite during the ascent of the magmas after eclogite fractionation does not destroy the argument presented above. In fact, the fractionation of an orthopyroxene-bearing assemblage strengthens the argument. Low pressure fractionation of olivine + plagioclase + clinopyroxene does, however, blur the record of high pressure eclogite fractionation.

It is concluded that the compositions of the olivine-rich rocks indicate that any eclogite fractionation which occurred during magmatic evolution must have taken place at pressures of c. 40 kb. - corresponding to depths of about 130 km. This is considerably greater than the depth of magma generation which is generally envisaged and it is certainly greater than the 50 - 60 km. depth of magma generation inferred from seismic data in Hawaii (Eaton and Murata, 1960).

In the transformed variable variation diagrams (Figs. 22-24) the composition points of two eclogite nodules in basalt have been plotted, as have the clinopyroxene and garnet separated from one of the eclogites. Since these compositions lie at one end of the trend of composition points - the low K_2O end - the hypothesis of eclogite fractionation can be considered to receive general support from these diagrams. However, it must be remembered that some of the variation

in the trend of rock compositions is the result of olivine and ortho-
pyroxene fractionation - these minerals plotting beyond the other
end of the trend.

Having demonstrated the plausibility of eclogite fractionation
at 40 kb., it is pertinent to enquire whether this process can account
for the somewhat enigmatic relationship between MgO and K and associated
elements which has previously been described; in Figure 22 the rocks
which have compositions plotting furthest from the two eclogites not
only have high contents of K_2O but have also the highest MgO contents.
The next part of this discussion is, therefore, an attempt to develop
petrogenetic schemes which incorporate eclogite fractionation and which
can account for the sympathetic relationship between MgO and K and
associated elements.

There are two alternative models of magmatic evolution, based on
high pressure eclogite fractionation, which the author believes can
account for the sympathetic relationship between MgO and K and associated
elements. The essential difference between the models is the contrasting
behaviour of MgO in the residual magmas produced by eclogite fractionation .
These models are described with the aid of generalised K_2O $\underline{v}$. MgO
variation diagrams (Figs. 28a and b).

In Model A it is assumed that the initial or primary magma contains
slightly less MgO than the eclogite extract. After eclogite fraction-
ation a trend of residual liquids such as A B will be produced. In order
to derive the observed relationship between MgO and K_2O it is now
necessary to assume that there is an inverse relationship between the
degree of high pressure eclogite fractionation and the degree of the
polybaric fractionation of olivine $\pm$ orthopyroxene which occurs during
the ascent of the magmas from the site of eclogite fractionation. This

FIGURE 28

<u>Hypothetical MgO v. K_2O variation diagrams
illustrating the effects of dual fractionation
schemes involving eclogite fractionation.</u>

A - B and C - D are variation trends
resulting from the fractionation of eclogite (E)
and subsequently olivine (O) from an initial
magma (M).
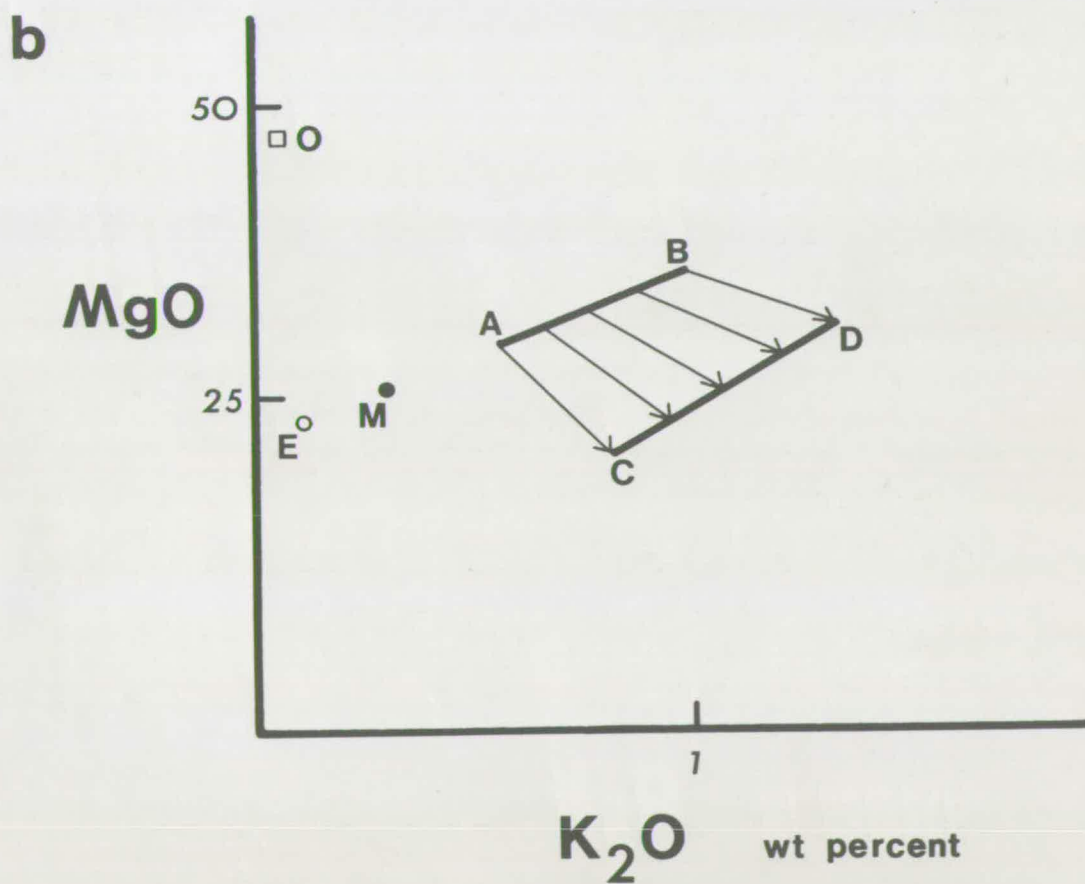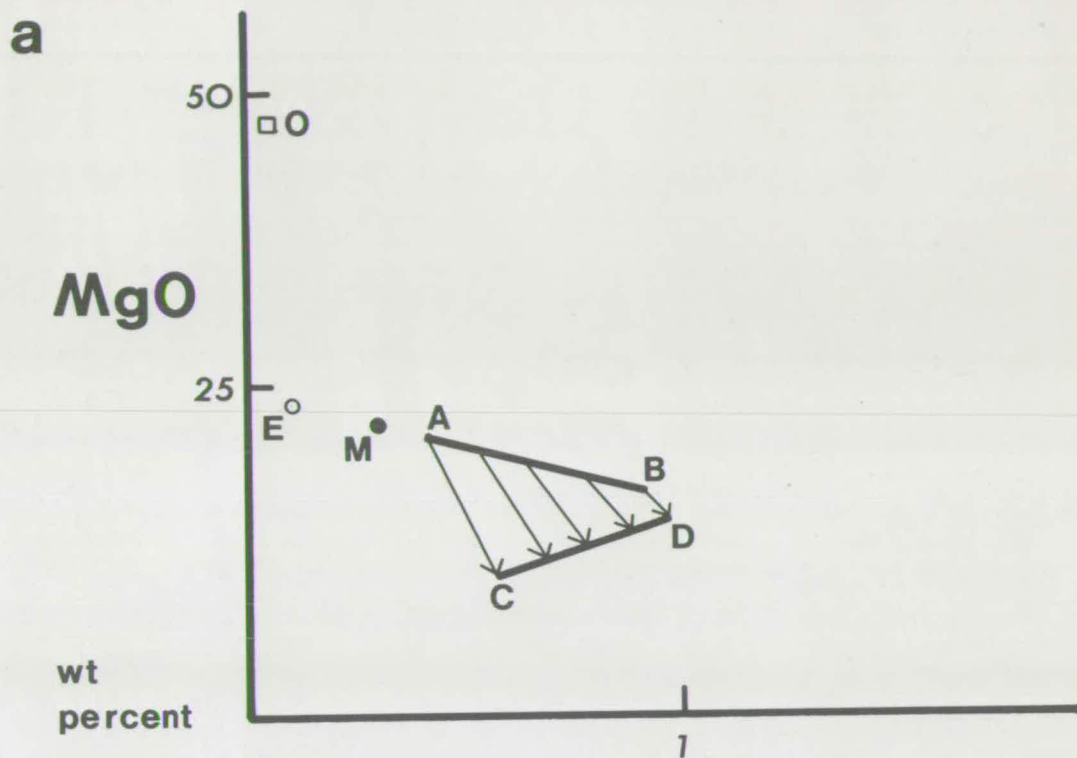
relationship would mean that amongst the range of compositions of magmas which reached the surface those most evolved in terms of high pressure eclogite fractionation (indexed by increasing K_2O and K_2O/Na_2O) would be least evolved in terms of intermediate pressure fractionation of olivine $\pm$ orthopyroxene (indexed by decreasing MgO), and vice versa. In Figure 28a a trend such as C D, which displays the required sympathetic relationship, would be produced by the proposed fractionation of olivine $\pm$ orthopyroxene during magmatic ascent.

The required relationship between high and intermediate pressure fractionation may not be as improbable as it might appear. The two processes could be related to a common factor; the passage of time is an obvious example. The efficiency of eclogite fractionation could wane with time whilst the efficiency of the polybaric fractionation could increase as time passes.

The alternative scheme of magmatic evolution - Model B - is more attractive since it does not rely on an inverse relationship between separate fractionation events. If the primary, or initial, picritic magma, which exists prior to the onset of eclogite fractionation, has an MgO content which is greater than the crystalline extract, MgO will increase in the residual liquids along with K and associated elements. In Figure 28b this situation is depicted and a trend of residual compositions such as A B would be produced by eclogite fractionation. The characteristic Nuanetsi relationship has now been achieved and any amount of further fractionation of K_2O-free mafic phases will not destroy it. Polybaric fractionation of olivine $\pm$ orthopyroxene during ascent would produce in Figure 28b the trend C D, which is similar to the actual trend of compositions recorded.

Because this Model does not rely on a sympathetic or antipathetic

relationship between two different processes to account for the observed
MgO - K and associated elements relationship, as do, for example, Model
A (above) and a scheme involving wall-rock reaction (described in a
previous section), the author finds it the most appealing of the various
schemes considered. Furthermore, it has already been argued that any
eclogite fractionation must have taken place at considerable pressures -
c. 40 kb. Since the initial partial melt of garnet-lherzolite probably
becomes increasingly rich in normative olivine with pressure increase -
because of the expansion of the garnet primary phase volume (O'Hara,
1968a, p.83) - it is quite reasonable to expect that at 40 kb. the
liquid does contain slightly more MgO than the eclogitic extract as is
envisaged in Figure 28b. Therefore the relationship between MgO and
K and associated elements in the Nuanetsi olivine-rich rocks may be an
inevitable result of the fractionation of eclogite at depths of around
130 km.

Finally, before eclogite fractionation is accepted as a plausible
K enrichment mechanism for these rocks, an attempt must be made to semi-
quantitatively assess a petrogenetic scheme which incorporates eclogite
fractionation. Is this process competent to account for the exceptionally
high enrichment factors of K and associated elements in the Nuanetsi
olivine-rich rocks ?

During eclogite fractionation at 40 kb. the near-coincidence of
initial magma and crystalline extract is particularly striking - see
Figure 27. Under these conditions it seems reasonable to propose that
the Nuanetsi primary magmas were subjected to eclogite fractionation
which was much more extensive than was considered possible in the evolution
of tholeiites by O'Hara (1968a, pp. 117-118). The general 2 times
enrichment limit proposed by O'Hara is probably not appropriate to this

case of eclogite fractionation. The closer the coincidence between initial magma and extract compositions, the higher the maximum enrichment values which can be achieved before a nepheline normative residual liquid is produced. Under these circumstances it is difficult to deny that enrichment values of 200 (Ba) might be produced by the combined efforts of 5% partial melting, giving enrichment factors of 15 - 20, followed by extensive eclogite fractionation, giving enrichment factors of 8, and finally polybaric olivine ± orthopyroxene fractionation which might enhance the enrichment factors by 1.3 times. The final enrichment factors in this scheme are 160 - 210.

It is, therefore, concluded that a magmatic evolutionary scheme involving extensive eclogite fractionation under unusually high pressure conditions - c. 40 kb. - can account for the abundances of K and associated elements and the relationship between these elements and MgO which are observed in the Nuanetsi olivine-rich rocks.

Crustal Contamination

Views on the importance of crustal contamination in the development of continental tholeiitic magmas are currently in a considerable state of flux. Although crustal contamination of basic magma has been largely out of favour with most petrologists as a generally significant process, recent determinations of Sr and Pb isotopic ratios in continental basalts have been interpreted as evidence in favour of interaction between magma and the crustal wall-rock.

An extreme stand is taken by Engel et al (1965) who have proposed that sialic contamination plays an important role, along with crystal-liquid fractionation and alkali transfer, in the development of typical continental tholeiites from a low-K_2O primary magma of the composition

of deep oceanic tholeiites. This crustal contamination process was
rather poorly defined by Engel et al. However, since Si was included
amongst the elements (Si, K, Ba, Cs, Rb, Sr, Th and U) which are
'scavenged .... from the walls of crustal conduits' (Engel et al, p.727)
the process is rather different from the selective wall-rock reaction
which was proposed by Green and Ringwood (1967) as an unusual, but
possible, crustal contamination process.

Green and Ringwood envisaged crustal wall-rock reaction as an
extension of mantle wall-rock reaction. However, in the sialic crustal
environment Sr, largely held in plagioclase, does not display
'incompatible' behaviour. Therefore, on the basis of K/Sr and Rb/Sr
ratios Green and Ringwood (Table 21) distinguish between basalts in
which the content of K and associated elements is thought to reflect
mantle wall-rock reaction (low K/Sr and Rb/Sr) and the few tholeiitic
rocks which they consider have been enriched in these elements in the
continental crustal environment by reaction processes (high K/Sr and
Rb/Sr). The best examples of tholeiites with high K/Sr and Rb/Sr
ratios are the petrochemically distinctive Jurassic dolerites of
Tasmania and the Ferrar dolerites of Antarctica of approximately the
same age (Compston et al, 1968). It is of some interest to note
that the K/Sr and Rb/Sr ratios of the average Nuanetsi olivine-rich
tholeiite are 16 and 0.04 respectively. These values are typical of
basalts considered by Green and Ringwood to show only high pressure
mantle enrichment of K and associated elements.

Finally, a more subtle reaction between magma and wall-rock has
been proposed by Pankhurst (1969) on the basis of Sr isotopic studies in
the Caledonian Basic Masses of Insch and Belhelvie in N.E. Scotland.

Pankhurst shows that the Sr^{87}/Sr^{86} ratio of the magma from which these layered intrusions crystallised must have undergone an enrichment in Sr^{87} during differentiation from gabbro to syenite.   In Insch the Sr^{87}/Sr^{86} ratio systematically increases from 0.703 to 0.712.   Since several chemical features of the rocks are claimed to be inconsistent with the progressive extraction of K, Ba, Zr, Rb and Sr from the country rock, Pankhurst concluded that some form of isotopic exchange took place between the Sr in the magma and the country rock and that this exchange did not involve the bulk addition of any element to the magma.

Sr^{87}/Sr^{86} ratios in continental basalts, both alkali basalts and tholeiites, have a slightly higher average than the average in oceanic basalts.   Furthermore, the frequency distribution of Sr^{87}/Sr^{86} ratio in continental basalts has a pronounced positive skew, in contrast to the near-Gaussian distribution in oceanic basalts.   These features have been taken as evidence of contamination of basaltic magma by sialic crustal material (Gast, 1967; Hedge, 1966).   An example of this actually comes from the Nuanetsi Igneous Province.   Seven specimens of basalt, 6 of which are from the Upper Basalts and the basalts inter-bedded with the overlying rhyolite extrusives, have markedly variable, and rather high Sr^{87}/Sr^{86} ratios (0.706 - 0.712) (Manton, 1968).   This feature led Manton to tentatively invoke a 10% contamination of the basalt parent magmas with average upper crustal material.

If of general applicability, the isotopic exchange process proposed by Pankhurst (1969) could account for the above features of Sr^{87}/Sr^{86} ratios in continental basalts, which are taken to imply crustal contamination, without causing any enhancement of K and associated elements.   An isotopic exchange process might also be applicable to the

basic and ultrabasic Tertiary rocks of Skye for which the isotopic studies of Moorbath and Welke (1968) indicate a significant contribution from old crustal material to the total Pb in the rocks.

If the high, and variable Sr^{87}/Sr^{86} ratios detected by Manton (1968) are also present in the Olivine-rich Group, it may be necessary to appeal to an isotopic exchange reaction as envisaged by Pankhurst (1969).   At present there is only one Sr^{87}/Sr^{86} determination for an olivine-rich rock - LM 434 (Table 1, and Manton, 1968, Table 2, no. NB-7) - which gives a measured value of 0.7074.

As for K and associated elements in the olivine-rich rocks, the rapid ascent of the magmas, especially from depths corresponding to c. 7 - 10 kb. pressure, which has previously been considered necessary to account for the primitive picritic compositions of these rocks (Chapter 5), is thought by the author to render unlikely any enhancement of these elements by crustal contamination processes.

Volatile Transfer

Some petrologists have always held that redistribution of the so-called 'pneumatophilic elements' in a magma can occur by solution and upward transport of these elements in a gas phase. This process, termed 'pneumatolytic differentiation' by Rittman (1962), is essentially the same as the gaseous transport differentiation mechanism outlined by Fenner (1926).   Since Na is considered to be more soluble in a gas phase than K, Rittman's hypothesis is that operation of the process will render the upper parts of a differentiating body of basic magma enriched in Na_2O and the middle and lower portions of the magma relatively enriched in K_2O.   Recent experimental work by Luth and Tuttle (1967) has confirmed that in a gas-silicate melt system Na is more soluble than

K in the gas phase.

Pneumatolytic differentiation, crystal-liquid fractionation and limestone assimilation are thought by Rittman (1962) to be the most important processes in the development of the distinctive K-rich basic lavas of the Roman province.

A similar process of 'differentiation by filtration' has recently been proposed by Marinelli and Mittempergher (1966). In this process a volatile-rich magmatic fraction rather than a gas phase is the transporting medium and K is thought to be carried upwards in a magma body more efficiently than Na.

These differentiation processes are envisaged by their proponents as operating when a volatile-rich body of magma is held near the Earth's surface in a tectonically stable region. However, there is no evidence that the Nuanetsi magmas were ever rich in volatiles. This fact, and the evidence of rapid ascent of these magmas, lead the author to conclude that gaseous - volatile transfer differentiation processes have no relevance to Nuanetsi basalt petrogenesis.

Conclusions

Of the processes considered as possible causes of the enrichment of K and associated elements in the Nuanetsi olivine-rich rocks crustal contamination and gaseous - volatile transfer are rejected as being of no significance. This conclusion also applies to the fractionation of the K_2O-bearing mafic phases phlogopite and amphibole.

While chemical inhomogeneity of the mantle cannot be totally rejected the general compositional similarity of basaltic lavas all over the Earth's surface does imply a chemically homogeneous upper mantle. Furthermore, to account for the enrichment in K and associated elements,

the mantle below the Nuanetsi area during the Jurassic would have to
have been enriched in just those radioactive heat-producing elements in
which the sub-continental mantle is predicted to be depleted by many
models.

The degree of melting of the mantle peridotite is clearly a very
important enrichment process. Since high pressure eclogite fractionation
can start only when a primary melt has the composition of a restricted
partial melt - say 5% - a petrogenetic model which involves eclogite
fractionation automatically incorporates the enrichment factors resulting
from limited melting.

Mantle wall-rock reaction is certainly a feasible process of K
enrichment. However, the sympathetic relationship between MgO and K
and associated elements is not an obvious result of this process and
it is necessary to invoke a somewhat speculative increase in the efficiency
of the reaction as the temperature and degree of partial melting increase
during magma genesis.

The high pressure fractionation of eclogite from picritic magmas
is also a rather speculative process. As described by O'Hara and Yoder
(1967) it is potentially a very important mechanism of K enrichment.
O'Hara (1968a and personal communication) believes that such eclogite
fractionation not only plays a key role in the production of variable
contents of K and associated elements in tholeiitic basalts but may
also be a major factor in the generation of mildly nepheline normative
magmas which, in turn, give rise to alkali basalt magmas at the Earth's
surface. In the case of Nuanetsi the rock compositions indicate that
any eclogite fractionation must have taken place at pressures close to
40 kb. However, as a result of eclogite fractionation at this pressure -

corresponding to 130 km. depth - it may be possible to account for both the high enrichment factors of K and associated elements and the relationship between MgO and these elements.

Because of this possibility of accounting for both of these geochemical aspects of the Nuanetsi olivine-rich rocks the author favours a petrogenetic scheme which includes the fractionation of eclogite at 120 - 140 km. depth.

CHAPTER 9

SUMMARY AND CONCLUSIONS

The data presented in this thesis and the main inferences based on these data are summarised. A preferred petrogenetic model for the Nuanetsi olivine-rich rocks is outlined.

Summary

A chemical and mineralogical study of the 6,500 ft. succession of olivine-rich rocks in the Nuanetsi Igneous Province has shown that :

(a) The concentration of MgO in the rocks is high, ranging from 8.3% to 23.3% in 47 lavas and 14.9% to 26.8% in 9 hypabyssal picrites; the average content in the lavas is 15.1%. The rocks are, therefore, picritic, or rich in normative olivine.

(b) All the analysed rocks are silica-saturated; normative hypersthene ranges from 12.1% to 47.2%.

(c) Average contents of K and associated elements in 47 lavas are - K_2O 1.58%, TiO_2 2.64%, P_2O_5 0.41%, Ba 795 p.p.m., Rb 33 p.p.m., Sr 859 p.p.m. and Zr 300 p.p.m. These values, and the K_2O/Na_2O ratio of 0.98, are exceptionally high for tholeiitic rocks.

(d) There are highly significant positive correlations between MgO and each of K_2O, TiO_2, P_2O_5, Ba, Rb, Sr and Zr.

(e) There is a marked compositional gap between the olivine-rich rocks and the overlying Upper Basalts; the former generally have MgO contents in excess of 10%, while

existing analyses of the latter show MgO to be generally
less than 7%.

(f) The rare, but distinctive, orthopyroxene phenocrysts and
the very rare olivine megacrysts are appreciably more
magnesian than the other phenocrysts.

Conclusions

The following major conclusions are made from an interpretation
of these data :

(a) The picritic compositions of the Nuanetsi olivine-rich rocks are
primitive, i.e. the rocks do not represent tholeiitic magmas
enriched in cumulus olivine under low pressure conditions, cf.
Hawaiian picrites. In fact the picritic magmas appear to have
undergone very little differentiation by fractional crystallisation
in the pressure range 0 - 7 kb. The hypabyssal picrites do,
however, show some evidence of limited low pressure fractionation.

(b) It follows from the above conclusion that there is no direct
genetic relationship between the Olivine-rich Group and the
overlying Upper Basalts. However, there is clearly a close
spatial and temporal relationship between the two groups. In
addition the Upper Basalts show, to a lesser degree, the enrich-
ment in K and associated elements which characterises the
Olivine-rich Group.

(c) The orthopyroxene phenocrysts and rare olivine megacrysts cannot
have been in equilibrium with the other phenocrysts in the rocks.
Phase equilibrium considerations indicate that this assemblage
was inherited from a fractionation event at 7 - 9 kb. pressure.

(d) The enrichment of K and associated elements _may_ have resulted, in part, from the fractionation of eclogite from picritic primary magmas at pressures of around 40 kb. - corresponding to depths of 120 - 140 km. The assessment of possible enrichment processes of these elements was very difficult and rather subjective. However, the version of the high pressure eclogite fractionation hypothesis (O'Hara and Yoder, 1967), which has been developed at some length in Chapter 8, has the advantage over other processes of accounting for both the high enrichment factors and the sympathetic relationship between MgO and K and associated elements. For this reason the author favours eclogite fractionation over other plausible processes, for example, wall-rock reaction.

Petrogenetic Model

On the basis of the data and conclusions presented above the following preferred petrogenetic model for the Nuanetsi olivine-rich rocks is offered :

(a) Partial melting at 120 - 140 km. depth of mantle peridotite which has the composition of garnet lherzolite nodules in kimberlite. The primary magma produced from such a mantle composition at this depth is hypersthene normative and picritic.

(b) Cooling and fractional crystallisation of the primary magmas while they are still near the site of generation. This essentially isobaric process will lead to the precipitation of bimineralic eclogite. After extensive eclogite

fractionation - sufficient to reduce the volume of the residual magmas to 15% - 10% of the original magmatic volume - the residual magmas will have compositions which are little different from the initial magmas, except that K and associated elements will be greatly enhanced.

(c) Relatively rapid ascent of these well-fractionated magmas accompanied by the slight polybaric fractionation of olivine. It is anticipated that dT/dP of the magmas during rapid ascent will be considerably less than dT/dP of the relevant phase equilibria. Because of this the magmas will be unable to change their compositions, by fractionation, at a sufficiently fast rate to remain in equilibrium with the 4-phase peridotite wall-rock. The compositions of the magmas under these circumstances will move, relative to the phase relations, into the primary phase volume which under-goes the greatest expansion with pressure drop - the olivine primary phase volume.

(d) A slowing down of the rate of magmatic ascent in the pressure range 7 - 9 kb. - corresponding to 23 - 30 km. depth. This will allow orthopyroxene to join olivine as a frac-tionating phase. This short period of harzburgite frac-tionation is responsible for a further element of the overall magma compositional diversification.

(e) Relatively rapid ascent of the magmas from 23 - 30 km. depth to the surface and either eruption or the formation of minor near-surface intrusions. This stage of magmatic development must be accompanied by very little olivine

polybaric fractionation.

(f) Limited accumulation of olivine, and possibly clinopyroxene, during the crystallisation of the magma which forms the hypabyssal intrusions. This fractionation event represents a further compositional diversification which is, however, largely restricted to the holocrystalline picritic rocks.

According to this model the Nuanetsi olivine-rich rocks combine a high degree of high pressure fractionation with limited fractionation and compositional diversification under intermediate and low pressure conditions. It is because of this limited low pressure fractionation that the chemical and mineralogical evidence of the earlier evolutionary history of the magmas is preserved. From this evidence it has been possible to construct a detailed, but nevertheless speculative, evolutionary model for the Nuanetsi olivine-rich magmas.

The relatively rapid ascent of the magmas after a period of essentially isobaric fractionation at 120 - 140 km., which is required by the model, may seem unlikely. It should be borne in mind, however, that the olivine-rich rocks probably developed in a rather special tectonic environment - just prior to, or during the formation of a major downwarp, the Nuanetsi syncline.

This model adequately accounts for the observed features of the olivine-rich rocks of the Nuanetsi Karroo volcanic succession. However, several aspects of the model are speculative and further developments in petrology, especially high pressure experimental petrology, are likely to cause the model to be modified. In particular it should be possible to prove or disprove the assumptions made about magma generation and crystal-liquid fractionation at pressures of around 40 kb.

ACKNOWLEDGEMENTS

BIBLIOGRAPHY

AOKI, K. and KUSHIRO, I., 1968. Some clinopyroxenes from ultramafic
inclusions in Dreiser Weiher, Eifel. Contr. Mineral.
and Petrol. 18, 326-337.

BOWEN, N.L., 1914. The ternary system : diopside - forsterite -
silica. Am. J. Sci. 38, 207-264.

BOWEN, N.L., 1928. The evolution of the igneous rocks. Princeton :
Princeton University Press.

BOWEN, N.L. and SCHAIRER, J.F., 1935. The system $MgO - FeO - SiO_2$.
Am. J. Sci. 229, 151-217.

BOYD, F.R., ENGLAND, J.L. and DAVIS, B.T.C., 1964. Effects of
pressure on the melting and polymorphism of enstatite,
$MgSiO_3$. J. geophys. Res. 69, 2101-2109.

CARMICHAEL, I.S.E., 1967. The mineralogy and petrology of the volcanic
rocks from the Leucite Hills, Wyoming. Contr. Mineral.
and Petrol. 15, 24-66.

CHAYES, F., 1960. On correlation between variables of constant sum.
J. geophys. Res. 65, 4185-4193.

CHAYES, F., 1962. Numerical correlation and petrographic variation.
J. Geol. 70, 440-452.

CHAYES, F., 1964. Variance - covariance relations in some published
Harker diagrams of volcanic suites. J. Petrology, 5,
219-237.

CLARKE, D.B., 1968. Tertiary basalts of the Baffin Bay area.
Univ. Edinburgh Ph.D. thesis (unpublished).

COMPSTON, W., McDOUGALL, I. and HEIER, K.S., 1968. Geochemical
comparison of the Mesozoic basaltic rocks of Antarctica,
South Africa, South America and Tasmania. Geochim.
cosmochim. Acta, 32, 129-149.

COOLEY, W.W. and LOHNES, P.R., 1962. Multivariate procedures for the
behavioral sciences. New York : John Wiley and Sons, Inc.

COOMBS, D.S., 1963. Trends and affinities of basaltic magmas and
pyroxenes as illustrated on the diopside - olivine -
silica diagram. Spec. Pap. miner. Soc. Am. 1, 227-250.

COX, K.G., JOHNSON, R.L., MONKMAN, L.J., STILLMAN, C.J., VAIL, J.R. and
WOOD, D.N., 1965. The geology of the Nuanetsi Igneous Province.
Phil. Trans. R. Soc., A, 257, 71-218.

COX, K.G., MACDONALD, R. and HORNUNG, G., 1967. Geochemical and
petrographic provinces in the Karroo basalts of Southern
Africa. Am. Miner. 52, 1451-1474.

DAVIS, B.T.C., 1964. The system diopside - forsterite - pyrope at
40 kilobars. Yb. Carnegie Instn Wash. 63, 165-171.

DAVIS, B.T.C. and SCHAIRER, J.F., 1965. Melting relations in the join
diopside - forsterite - pyrope at 40 kilobars and at one
atmosphere. Yb. Carnegie Instn Wash. 64, 123-126.

DEER, W.A., HOWIE, R.A. and ZUSSMAN, J., 1962a. Rock forming minerals,
Volume I. London : Longmans.

DEER, W.A., HOWIE, R.A. and ZUSSMAN, J., 1962b. Rock forming minerals,
Volume II. London : Longmans.

DICKINSON, W.R. and HATHERTON, T., 1967. Andesitic volcanism and
seismicity around the Pacific. Science, N.Y. 157, 801-803.

DREVER, H.I. and JOHNSTON, R., 1957. Crystal growth of forsteritic
olivine in magmas and melts. Trans. R. Soc. Edinb. 63,
289-315.

DU TOIT, A.L., 1954. The geology of South Africa. Edinburgh : Oliver
and Boyd.

EATON, J.P. and MURATA, K.J., 1960. How volcanoes grow. Science, N.Y.
132, 925-938.

ENGEL, A.E.J., ENGEL, C.G. and HAVENS, R.G., 1965. Chemical
characteristics of oceanic basalts and the upper mantle.
Bull. geol. Soc. Am. 76, 719-734.

FENNER, C.N., 1926. The Katmai magmatic province. J. Geol.
34, 673-772.

GAST, P.W., 1967. Isotope geochemistry of volcanic rocks, pp. 325-358 in Basalts : the Poldervaart treatise on rocks of basaltic composition, eds. Hess, H.H. and Poldervaart, A., New York : Interscience.

GAST, P.W., 1968. Trace element fractionation and the origin of tholeiitic and alkaline magma types. Geochim. cosmochim. Acta, 32, 1057-1086.

GREEN, D.H. and RINGWOOD, A.E., 1964. Fractionation of basalt magmas at high pressures. Nature, Lond. 201, 1276-1279.

GREEN, D.H. and RINGWOOD, A.E., 1967. The genesis of basaltic magmas. Contr. Mineral. and Petrol. 15, 103-190.

GRIFFIN, W.L. and MURTHY, V.R., 1968a. Abundances of K, Rb, Sr and Ba in some ultramafic rocks and minerals. Earth planet. Sci. Lett. 4, 497-501.

GRIFFIN, W.L. and MURTHY, V.R., 1968b. Distribution of K, Rb, Sr and Ba in some minerals relevant to basalt genesis. Preprint.

HARRIS, P.G., 1957. Zone-refining and the origin of potassic basalts. Geochim. cosmochim. Acta, 12, 195-208.

HARRIS, P.G., 1967. Segregation processes in the upper mantle, pp. 305-317 in Mantles of the Earth and Terrestrial planets, ed. Runcorn, S.K., New York : Interscience.

HAUGHTON, S.H., 1963. Stratigraphic history of Africa south of the Sahara. Edinburgh and London : Oliver and Boyd.

HEDGE, C.E., 1966. Variations in radiogenic strontium found in volcanic rocks. J. geophys. Res. 71, 6119-6126.

HESS, H.H., 1949. Chemical composition and optical properties of common clinopyroxenes. Part I. Am. Miner. 34, 621-666.

HIGAZY, R.A., 1954. Trace elements of volcanic ultrabasic potassic rocks of southwestern Uganda and adjoining part of the Belgian Congo. Bull. geol. Soc. Am. 65, 39-70.

HOLMES, A., 1920. The nomenclature of petrology. London : Thomas Murby and Co.

HOLMES, A., 1936. A contribution to the petrology of Kimberlite and its inclusions. Trans. geol. Soc. S. Africa, 39, 379-428.

HOLMES, A., 1950. Petrogenesis of Katungite and its associates. Am. Miner. 35, 772-792

HOLMES, A. and HARWOOD, H.F., 1932. Petrology of the volcanic fields east and south-east of Ruwenzori, Uganda. Q. Jl geol. Soc. Lond. 88, 370-442.

HURLEY, P.M., 1968a. Absolute abundance and distribution of Rb, K and Sr in the Earth. Geochim. cosmochim. Acta, 32, 273-283.

HURLEY, P.M., 1968b. Correction to : Absolute abundance and distribution of Rb, K and Sr in the Earth. Geochim. cosmochim. Acta, 32, 1025-1030.

ITO, K. and KENNEDY, G.C., 1967. Melting and phase relations in a natural peridotite to 40 kilobars. Am. J. Sci. 265, 519-538.

JACKSON, E.D., 1960. X-ray determinative curve for natural olivine of composition Fo_{80-90}. Prof. Pap. U.S. geol. Surv. 400-B, 432-434.

JAMIESON, B.G., 1970. Phase relations in some tholeiitic lavas illustrated by the system $R_2O_3 - XO - YO - XO_2$. Mineralog. Mag. in press.

JAMIESON, B.G. and CLARKE, D.B., 1970. Potassium and associated elements in tholeiitic basalts. J. Petrology, in press.

KENDALL, M.G., 1957. Course in multivariate analysis. London : Charles Griffin and Co. Ltd.

KOPECKÝ, L. and VOLDÁN, J., 1959. Crystallisation of melted rocks (in Czech.). Geotechnica, Ústřední ústav geologický, 25, 1-218.

KRETZ, R., 1961. Some applications of thermodynamics to co-existing minerals of variable composition. Examples : orthopyroxene - clinopyroxene and orthopyroxene - garnet. J. Geol. 69, 361-387.

KRETZ, R., 1963. Distribution of magnesium and iron between ortho-
pyroxene and calcic pyroxene in natural mineral assemblages.
J. Geol. 71, 773-785.

KUSHIRO, I., 1964. The system diopside - forsterite - enstatite at
20 kilobars. Yb. Carnegie Instn Wash. 63, 101-108.

KUSHIRO, I., 1965. The liquidus relations in the systems forsterite -
$CaAl_2SiO_6$ - silica and forsterite - nepheline - silica at
high pressures. Yb. Carnegie Instn Wash. 64, 103-108.

KUSHIRO, I., SYONO, Y. and AKIMOTO, S., 1967. Stability of phlogopite
at high pressures and possible presence of phlogopite in
the Earth's upper mantle. Earth planet. Sci. Lett. 3,
197-203.

LAMBERT, I.B. and WYLLIE, P.J., 1968. Stability of hornblende and
a model for the low velocity zone. Nature, Lond. 219,
1240-1241.

LE MAITRE, R.W., 1968. Chemical variation within and between volcanic
rock series - a statistical approach. J. Petrology, 9,
220-252.

LIGHTFOOT, B., 1938. Notes on the south-eastern part of Southern
Rhodesia. Trans. geol. Soc. S. Africa, 41, 193-198.

LUTH, W.C. and TUTTLE, O.F., 1967. The hydrous vapor phase in
equilibrium with granite and granite magmas. Trans. Am.
geophys. Un. 48, 245 (Abstract only).

MACDONALD, G.A., 1944. The 1840 eruption and crystal differentiation
in the Kilauean magma column. Am. J. Sci. 242, 177-189.

MACDONALD, G.A., 1949. Hawaiian petrographic province. Bull. geol.
Soc. Am. 60, 1541-1595.

MACDONALD, G.A. and KATSURA, T., 1964. Chemical composition of
Hawaiian lavas. J. Petrology, 5, 82-133.

MANSON, V., 1967. Geochemistry of basaltic rocks : major elements,
pp. 215-269 in Basalts : the Poldervaart treatise on
rocks of basaltic composition, eds. Hess, H.H. and
Poldervaart, A., New York : Interscience.

MANTON, W.I., 1968. The origin of associated basic and acidic rocks
in the Lebombo - Nuanetsi Igneous Province, Southern
Africa, as implied by strontium isotopes. J. Petrology,
9, 23-39.

MARINELLI, G. and MITTEMPERGHER, M., 1966. On the genesis of some
magmas of typical Mediterranean (potassic) suite.
Bull. volcan. 39, 113-140.

MENNELL, F.P., 1910. An introduction to petrology. London :
Gerrards Ltd.

MERCY, E.L.P. and O'HARA, M.J., 1967. Distribution of Mn, Cr, Ti and
Ni in co-existing minerals of ultramafic rocks.
Geochim. cosmochim. Acta, 31, 2331-2341.

MONKMAN, L.J., 1961. The geology of the Maose - Malibangwe river
basins, with special reference to the Stormberg rhyolitic
volcanicity of Southern Rhodesia. Univ. Leeds Ph.D. thesis
(unpublished).

MOORBATH, S. and WELKE, M., 1968. Lead studies on igneous rocks
from the Isle of Skye, northwest Scotland. Earth
planet. Sci. Lett. 5, 217-230.

MUIR, I.D. and LONG. J.V.P., 1965. Pyroxene relations in two Hawaiian
hypersthene-bearing basalts. Mineralog. Mag. 34, 358-369.

MUIR, I.D. and TILLEY, C.E., 1964. Iron enrichment and pyroxene
fractionation in tholeiites. Geol. J. 4, 143-156.

MUIR, I.D., TILLEY, C.E. and SCOON, J.H., 1957. Contributions to
the petrology of Hawaiian basalts. I. The picrite
basalts of Kilauea. Am. J. Sci. 255, 241-253.

MURATA, K.J. and RICHTER, D.H., 1966a. The settling of olivine in
Kilauean magma as shown by the lavas of the 1959 eruption.
Am. J. Sci. 264, 194-203.

MURATA, K.J. and RICHTER, D.H., 1966b. Chemistry of the lavas of the
1959-60 eruption of Kilauea Volcano, Hawaii. Prof. Pap.
U.S. geol. Surv. 537-A.

NIXON, P.H., VON KNORRING, O. and ROOKE, J.M., 1963. Kimberlites and associated inclusions of Basutoland : A mineralogical and geochemical study. Am. Miner. 48, 1090-1132.

O'HARA, M.J., 1963. Distribution of iron between coexisting olivines and calcium-poor pyroxenes in peridotites, gabbros and other magnesian environments. Am. J. Sci. 261, 32-46.

O'HARA, M.J., 1965. Primary magmas and the origin of basalts. Scott. J. Geol. 1, 19-40.

O'HARA, M.J., 1967. Mineral parageneses in ultrabasic rocks, pp. 393-403 in Ultramafic and related rocks, ed. Wyllie, P.J., New York : John Wiley and Sons, Inc.

O'HARA, M.J., 1968a. The bearing of phase equilibria studies in synthetic and natural systems on the origin and evolution of basic and ultrabasic rocks. Earth-Sci. Rev. 4, 69-133.

O'HARA, M.J., 1968b. Are ocean floor basalts primary magma ? Nature, Lond. 220, 683-686.

O'HARA, M.J. and MERCY, E.L.P., 1963. Petrology and petrogenesis of some garnetiferous peridotites. Trans. R. Soc. Edinb. 65, 251-314.

O'HARA, M.J. and YODER, H.S., Jr., 1967. Formation and fractionation of basic magmas at high pressures. Scott. J. Geol. 3, 67-117.

OSBORN, E.F. and TAIT, D.B., 1952. The system diopside - forsterite - anorthite. Am. J. Sci. Bowen Volume, 413-433.

OXBURGH, E.R., 1964. Petrological evidence for the presence of amphibole in the upper mantle and its petrogenetic and geophysical implications. Geol. Mag. 101, 1-19.

PANKHURST, R.J., 1969. Strontium isotope studies related to petrogenesis in the Caledonian basic igneous province of N.E. Scotland. J. Petrology, 10, 115-143.

POLDERVAART, A. and HESS, H.H., 1951. Pyroxenes in the crystallisation of basaltic magma. J. Geol. 59, 472-489.

POWERS, H.A., 1955. Composition and origin of basaltic magma of
the Hawaiian Islands. Geochim. cosmochim. Acta, 7,
77-107.

PRINZ, M., 1967. Geochemistry of basaltic rocks : trace elements,
pp. 271-323 in Basalts : the Poldervaart treatise on
rocks of basaltic composition, eds. Hess, H.H. and
Poldervaart, A., New York : Interscience.

RAMBERG, H. and DE VORE, G.W., 1951. Distribution of Fe^{++} and Mg^{++}
in co-existing olivines and pyroxenes. J. Geol. 59,
193-210.

RINGWOOD, A.E., 1966. The chemical composition and origin of the
Earth, pp. 287-356 in Advances in Earth Sciences, ed.
Hurley, P.M., Boston : M.I.T. Press.

RITTMAN, A., 1962. Volcanoes and their activity. (English
translation by E.A. Vincent). New York and London :
Interscience.

ROGERS, A.W., 1925. Notes on the north-eastern part of the Zoutpans-
berg district. Trans. geol. Soc. S. Africa, 28, 33-53.

ROSENBUSCH, H., 1872. Petrographische Studien an den Gesteinen des
Kaiserstuhb. Neues Jb. Miner. Geol. Paläont. 35-65.

ROSENBUSCH, H., 1908. Mikroskopische Physiographie der massigen
Gesteine. Part 2, Ergussgesteine. Stuttgart :
E. Schweizerbartsche Verlagshandlung.

SAGGERSON, E.P., 1968. Eclogite nodules associated with alkaline
olivine basalts, Kenya. Geol. Rdsch. 57, 890-903.

SCHMITT, R.A., BINGHAM, E. and CHODOS, A.A., 1964. Zirconium
abundances in meteorites and implications to nucleo-
synthesis. Geochim. cosmochim. Acta, 28, 1961-1979.

SHAW, D.M., 1968. Radioactive elements in the Canadian Precambrian
Shield and the interior of the Earth, pp. 855-870 in
Origin and Distribution of the Elements, ed. Ahrens, L.H.,
Oxford : Pergamon.

SWIFT, W.H., WHITE, W.C., WILES, J.W. and WORST, B.G., 1953. The Geology of the Lower Sabi Coalfield. Bull. geol. Surv. Sth. Rhod. 40.

TATSUMOTO, M., 1966. Genetic relations of oceanic basalts as indicated by lead isotopes. Science, N.Y. 153, 1094-1101.

TATSUMOTO, M., HEDGE, C.E. and ENGEL, A.E.J., 1965. Potassium, rubidium, strontium, thorium, uranium and the ratio of strontium -87 to strontium -86 in oceanic tholeiitic basalt. Science, N.Y. 150, 886-888.

TAYLOR, S.R., 1964a. Chondritic Earth model. Nature, Lond. 202, 281-282.

TAYLOR, S.R., 1964b. Trace element abundances and the chondritic Earth model. Geochim. cosmochim. Acta, 28, 1989-1998.

TILLEY, C.E. and MUIR, I.D., 1967. Tholeiite and tholeiitic series. Geol. Mag. 104, 337-343.

TILLEY, C.E. and YODER, H.S., Jr., 1964. Pyroxene fractionation in mafic magma at high pressures and its bearing on basalt genesis. Yb. Carnegie Instn Wash. 63, 114-121.

TILLEY, C.E., YODER, H.S., Jr. and SCHAIRER, J.F., 1963. Melting relations of basalts. Yb. Carnegie Instn Wash. 62, 77-84.

TURNER, F.J. and VERHOOGEN, J., 1960. Igneous and metamorphic petrology. New York : McGraw-Hill.

VOGT, J.H.L., 1921. The physical chemistry of the crystallisation and magmatic differentiation of igneous rocks. J. Geol. 29, 318-350, 426-443, 515-539, 627-649.

VON HERZEN, R.P., 1967. Surface heat flow and some implications for the mantle, pp. 197-230 in The Earth's Mantle, ed. Gaskell, T.F., London : Academic Press.

VON KNORRING, O. and COX, K.G., 1961. Kennedyite, a new mineral of the pseudobrookite series. Mineralog. Mag. 32, 676-682.

WADE, A. and PRIDER, R.T., 1940. The leucite-bearing rocks of the
West Kimberley area, Western Australia. Q. Jl geol. Soc.
Lond. 96, 39-98.

WAGER, L.R. and BROWN, G.M., 1968. Layered Igneous Rocks. Edinburgh
and London : Oliver and Boyd.

WILLIAMS, H., TURNER, F.J. and GILBERT, C.H., 1954. Petrography.
San Francisco : W.H. Freeman and Co.

WOOD, C.P., 1968. A geochemical study of East African alkaline
lavas and its relevance to the petrogenesis of nephelinites.
Univ. Leeds Ph.D. thesis (unpublished).

YODER, H.S., Jr., 1964. Genesis of principal basalt magmas.
Yb. Carnegie Instn Wash. 63, 97-101.

YODER, H.S., Jr. and KUSHIRO, I., 1969. Melting of a hydrous phase :
phlogopite. Am. J. Sci. Schairer Volume, 267-A, 558-582.

YODER, H.S., Jr. and TILLEY, C.E., 1962. The origin of basalt magmas :
an experimental study of natural and synthetic systems.
J. Petrology, 3, 342-532.

P L A T E S   1 - 18

PLATE 1

N-98 : Ore combs in glassy Olivine Basalt

x 60.

PLATE 2

N-15 : Skeletal plagioclase crystals in glassy
Olivine Basalt.

x 50.
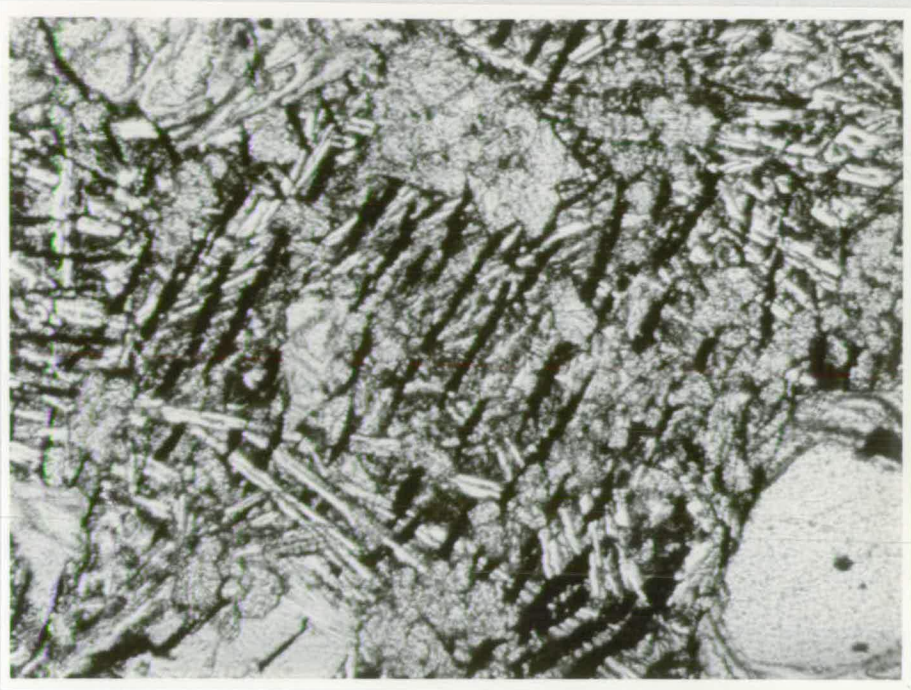
1
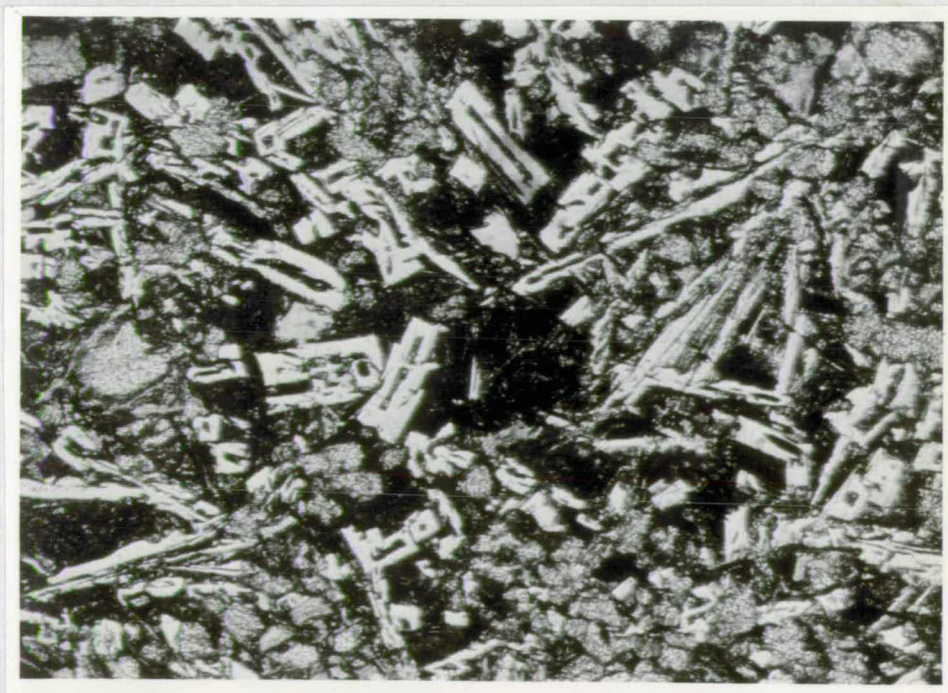
2

PLATE 3

N-400 :   Skeletal clinopyroxene microphenocrysts
          in Limburgite.

x 45.

PLATE 4

N-400 :   Skeletal clinopyroxene microphenocryst
          in Limburgite.

x 70.

3
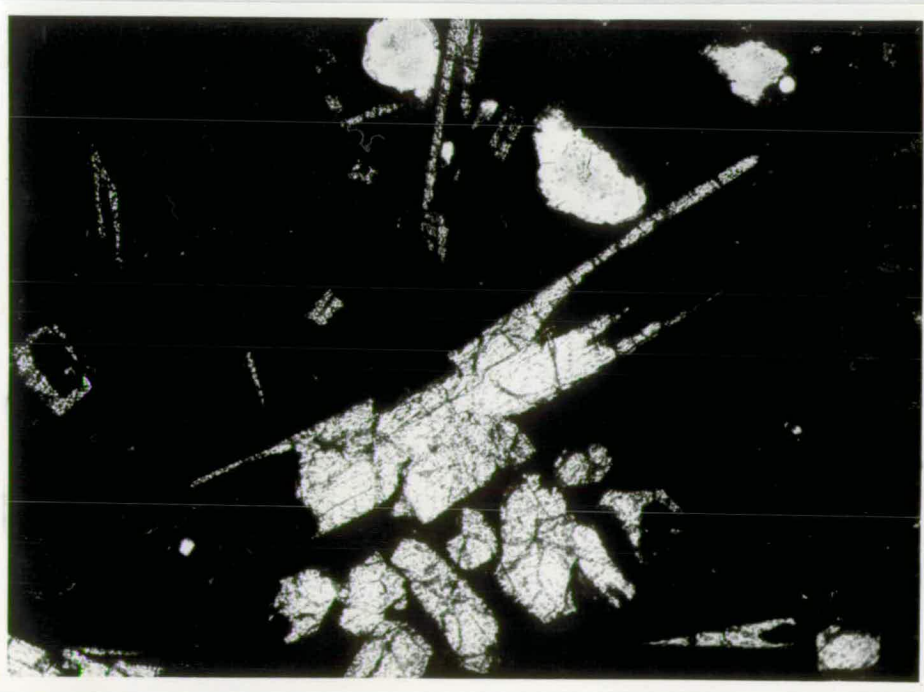
4

PLATE 5

N-190 : Embayed olivine phenocrysts in Limburgite.

x 30.

PLATE 6

N-159 : Orthopyroxene phenocryst in Limburgite.

x 15.
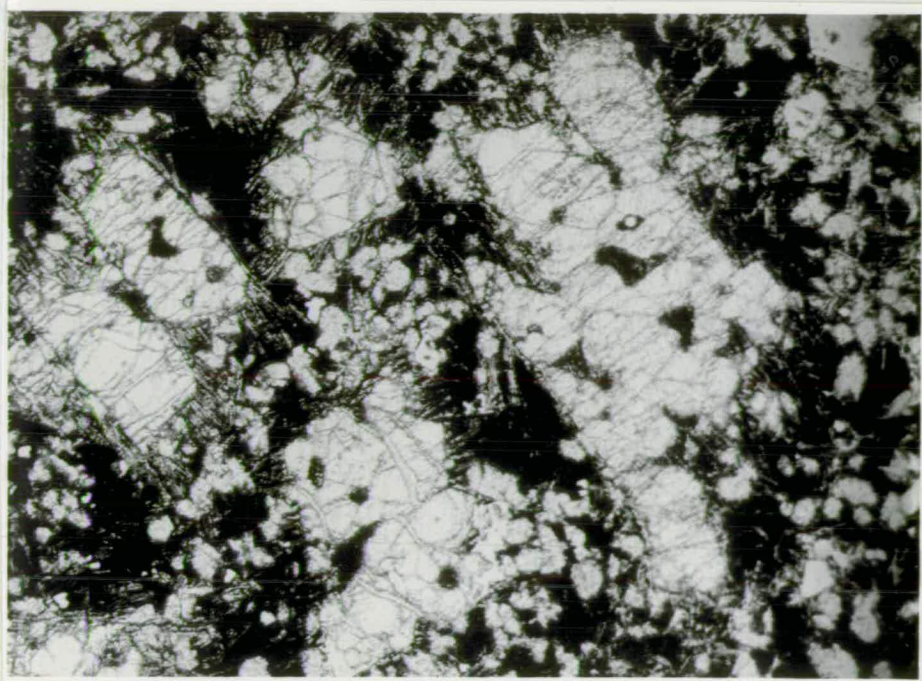
5
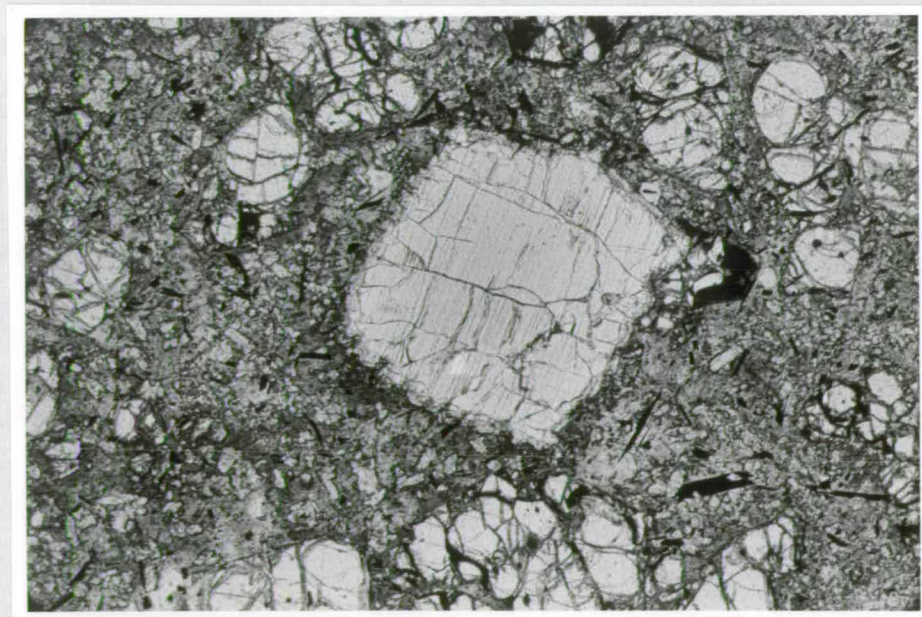
6

PLATE 7

N-88 : Abundant, rounded clusters of orthopyroxene

phenocrysts in Olivine Basalt.

Note rim of clinopyroxene with included,

altered olivine (dark crystals).

x 5.

PLATE 8

N-105 : Small cluster of orthopyroxene phenocrysts

in Limburgite.

Again note rim of clinopyroxene crystals

separating the orthopyroxene from the

remainder of the rock.

x 35.
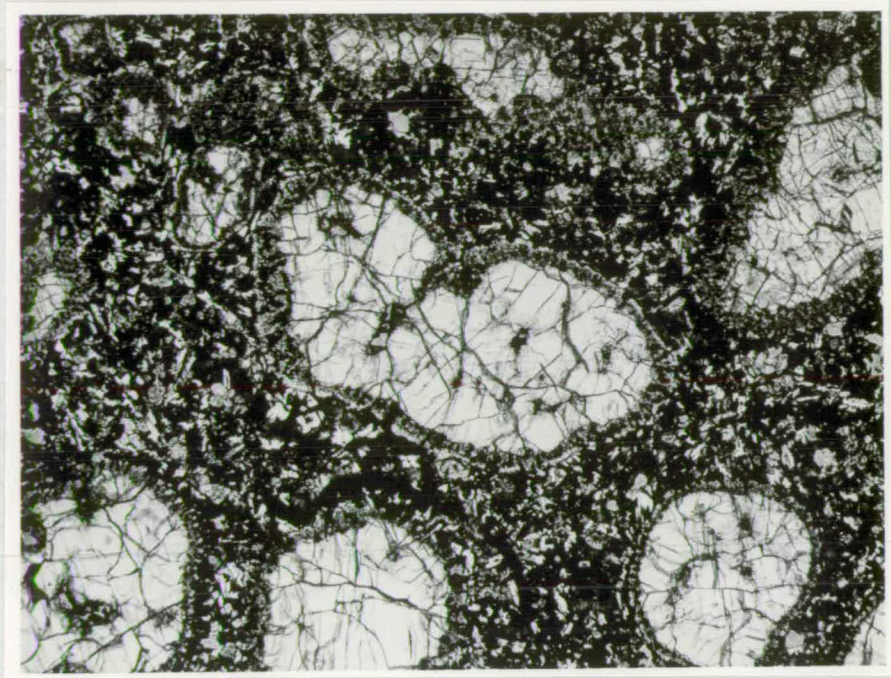
7
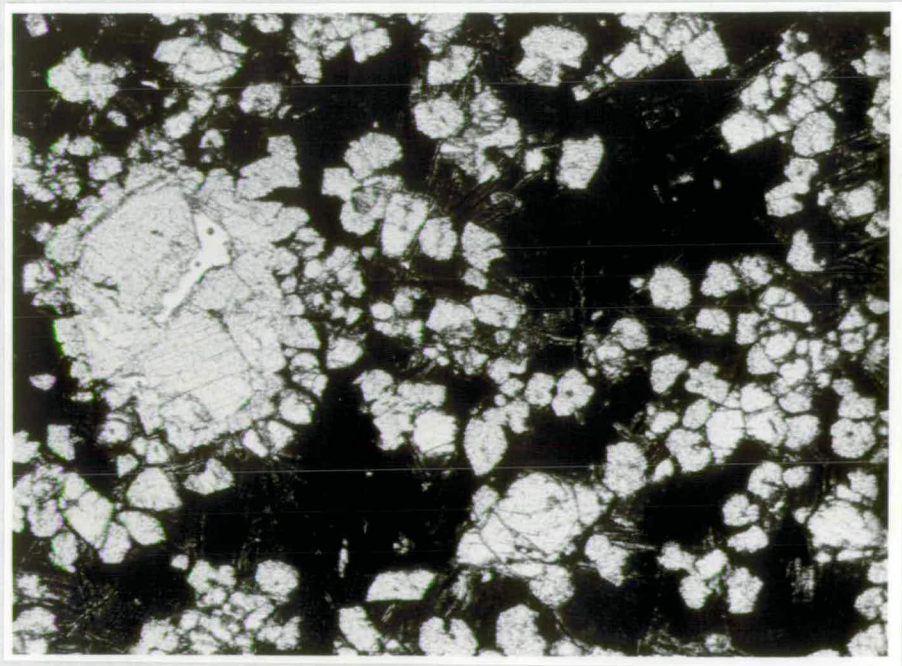
8

PLATE 9

N-26 : Orthopyroxene phenocryst in glassy Olivine
Basalt.

Overgrowth of single clinopyroxene crystal.

x 45.

PLATE 10

Same as Plate 9, but crossed nicols.

Orthopyroxene in extinction position.

9
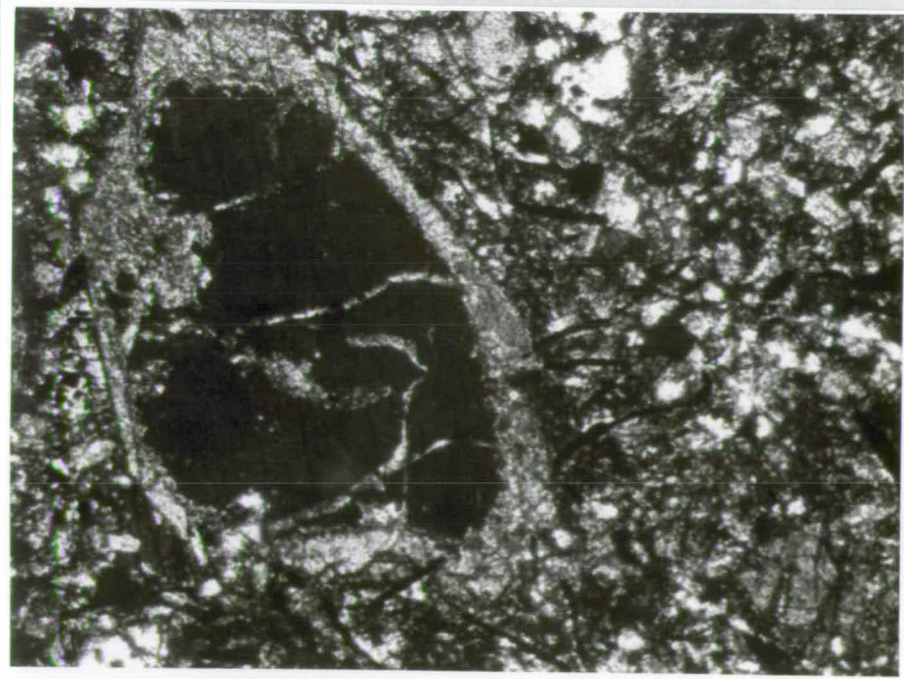
10

PLATE 11

N-88 : Orthopyroxene phenocryst in Olivine Basalt.

Note concentration of small, rounded olivine

crystals (dark) in, and around, the clino-

pyroxene rim.

x 12.

PLATE 12

N-356 : Olivine megacrysts in Limburgite.

x 5.
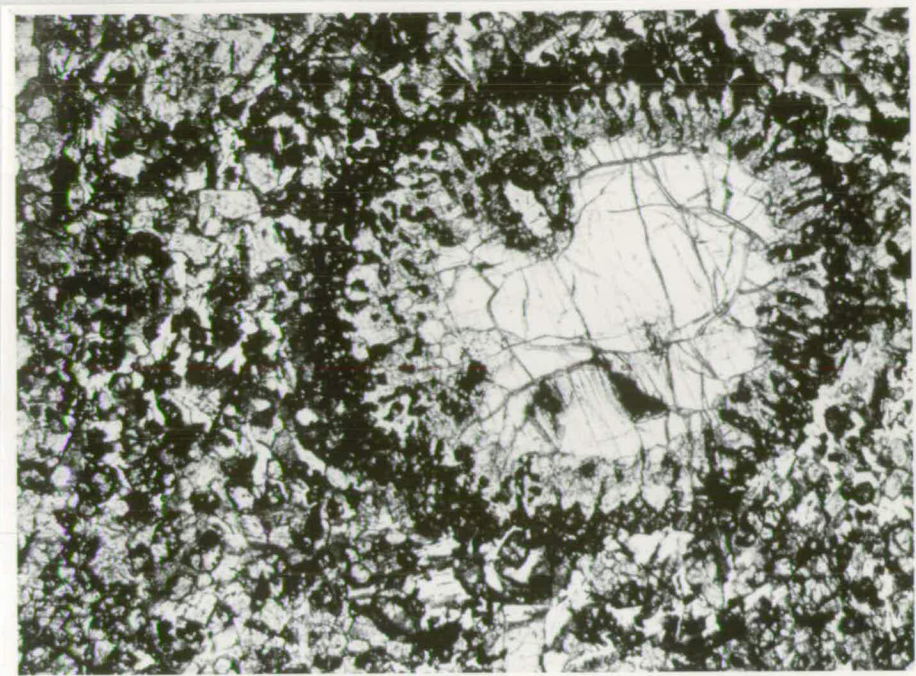
11

12

PLATE 13

N-135 : A 1-phenocryst Limburgite.

Well-developed ore combs.

x 20.

PLATE 14

N-56 : A 1-phenocryst Limburgite.

Clinopyroxene microphenocrysts are generally

skeletal - note axial cavities.

x 13.
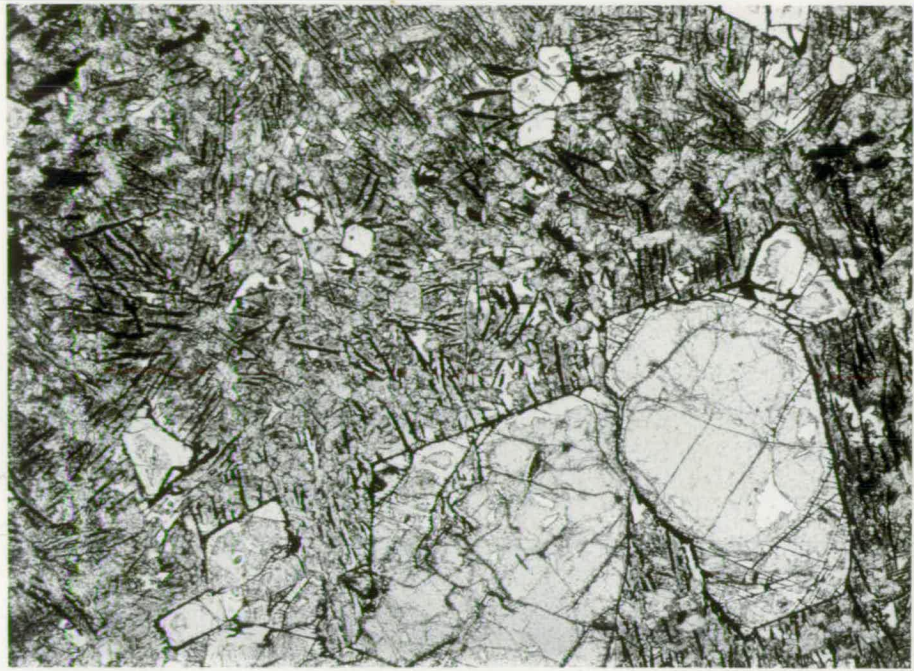
13
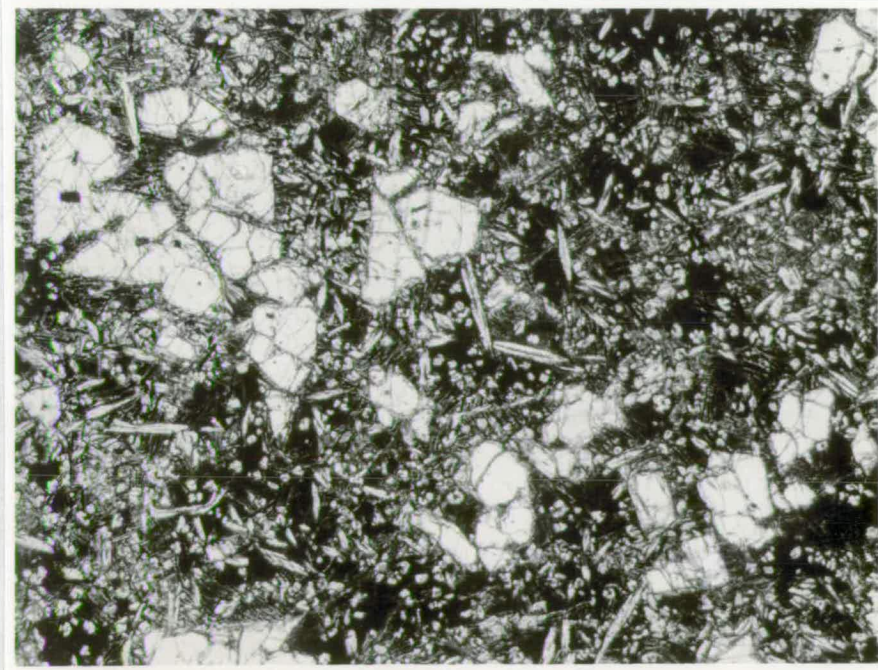
14

PLATE 15

N-37 : A typical 2-phenocryst Limburgite.
Clinopyroxene phenocrysts are smaller than
the olivine phenocrysts.

x 25.

PLATE 16

N-399 : A 2-phenocryst Limburgite.
The size contrast between euhedral olivine
phenocryst and smaller subhedral - anhedral
clinopyroxene phenocrysts is typical of this
group.

x 40.
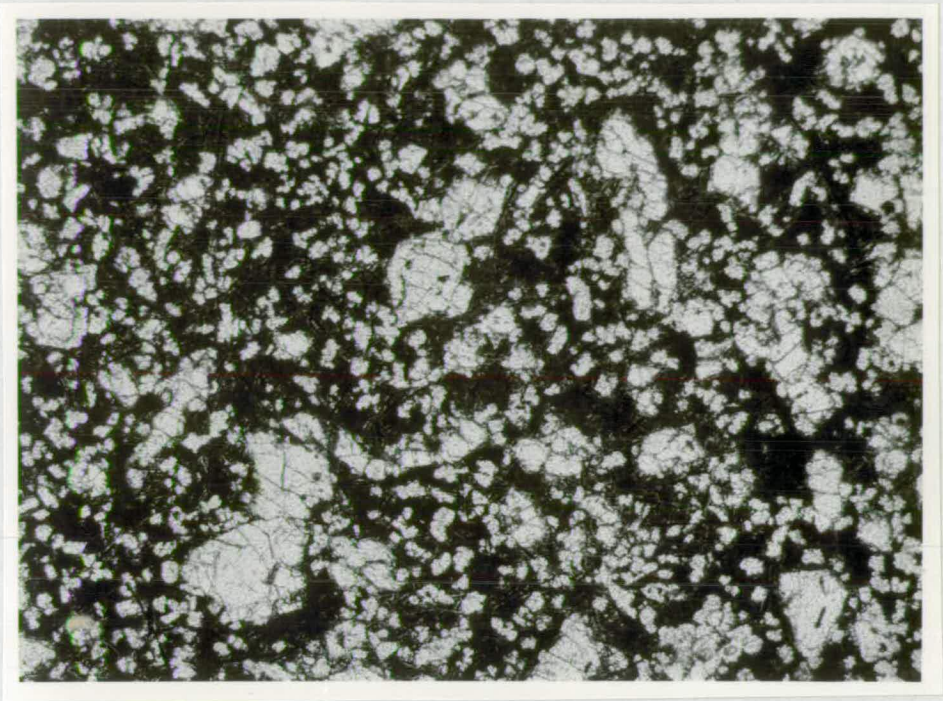
15
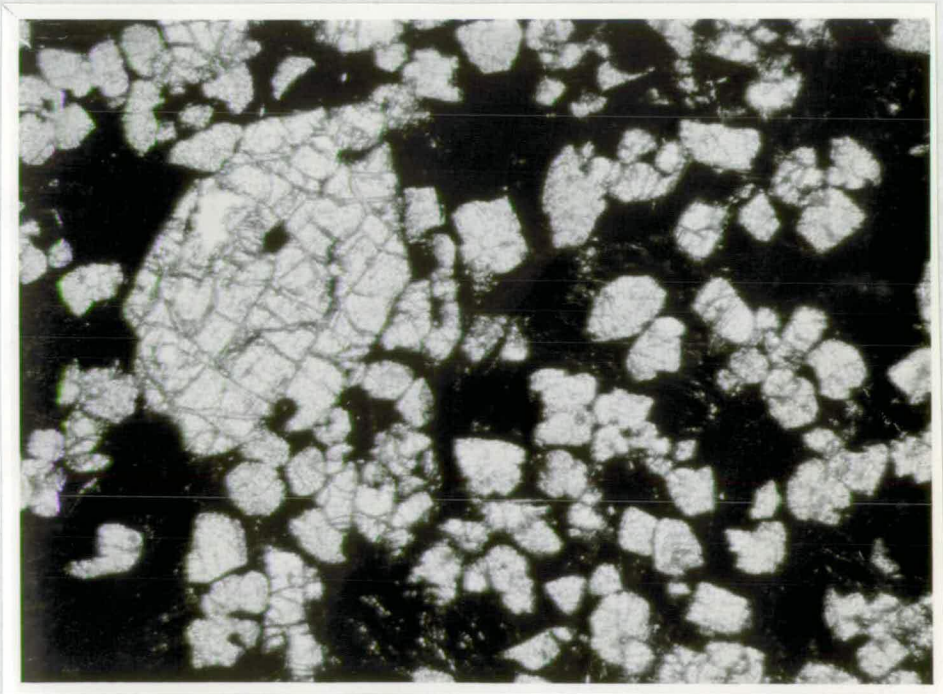
16

PLATE 17

N-13 : 2-phenocryst Limburgite.

A relatively uncommon variety with

clinopyroxene phenocrysts (clear)

equal in size to the olivine phenocrysts.

x 15.

PLATE 18

N-199 : A 1-phenocryst glassy Olivine Basalt.

Groundmass, with dendritic and skeletal

plagioclase crystals and glass, is fairly

typical of this group.   This specimen is

transitional to a Limburgite.

x 35.
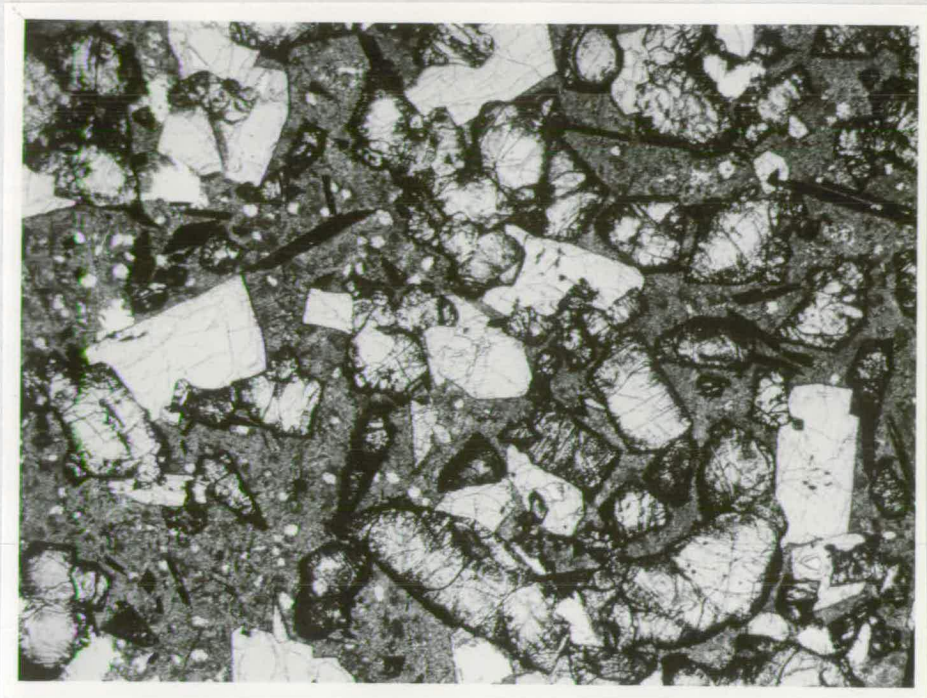
17
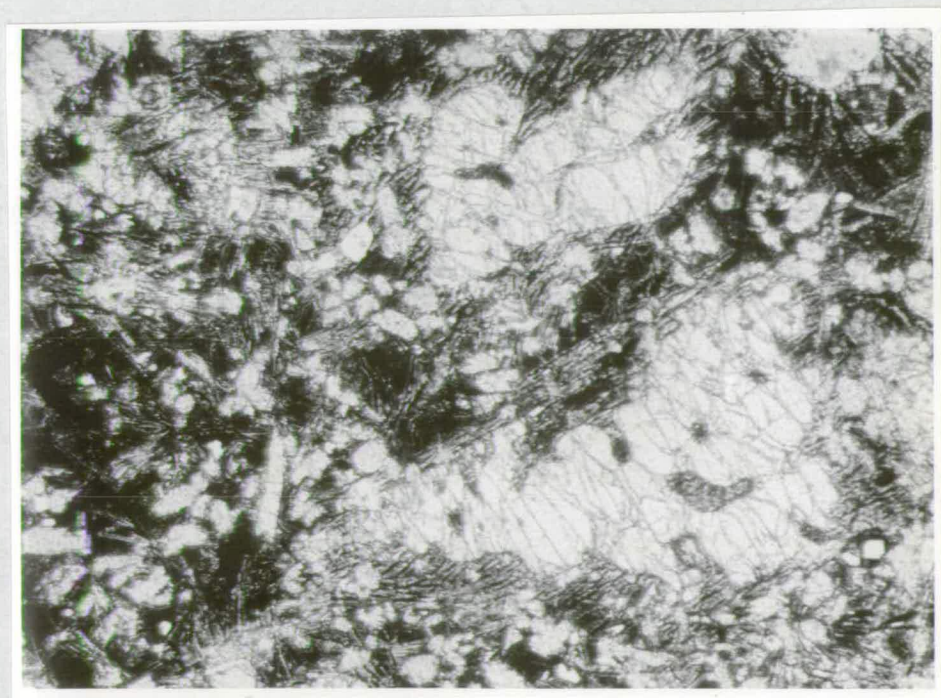
18

A P P E N D I X   A

DESCRIPTIONS OF ANALYSED SPECIMENS

Petrographic notes and the modal mineralogy of the 56 analysed rock specimens are given below.

The modal data were obtained by counting only 700 - 1200 points in one thin section of each specimen and should be considered as approximate estimations of the actual modal mineralogy.   Modal analysis was further complicated by the sparse distribution of large phenocryst phases - principally orthopyroxene - and the medium-fine grain-size of groundmasses. Modal data are expressed as volume per cent.

In the medium-grained holocrystalline rocks a sodium cobaltinitrite stain preparation[1] facilitated the identification of alkali feldspar.

The general locality of each analysed specimen can be obtained from the locality reference, below, and Figure 2.   Unless otherwise stated, the localities are in Nuanetsi District.

N-1 0.42 Km .   2-phenocryst Limburgite

½ mile West of Gomakwe intrusion.

Large, anhedral olivine phenocrysts which are rather spongy;

---

[1] CHAYES, F., 1952.   Am. Miner. 37, 337-340.

microphenocrysts of clinopyroxene and olivine; minute acicular and
granular ore in glass; general appearance suggests the rock has
undergone slight thermal metamorphism.

Phen. oliv.	17
Microph. oliv.	7
Microph. cpx.	23
Ore	11
Glass	42

<u>N-5</u>   0.43 km   <u>1-phenocryst Limburgite</u>

¼ mile West of Gomakwe intrusion.

Subhedral phenocrysts set in a fine-grained, granular matrix; thermally
metamorphosed; probably transitional to 2-phenocryst limburgite.

Oliv.	9
Cpx.	6
Ore	3
Matrix	81
Opx.	1

<u>N-13</u>   0.35   <u>2-phenocryst Limburgite</u>
     Nyasumi

2½ miles South-west of Gomakwe intrusion.

Large phenocrysts — up to 2 mm. in diameter — of olivine (subhedral-
euhedral), clinopyroxene (euhedral) and bladed ore in a glassy matrix
with a few, small, acicular feldspar and apatite crystals; considered
to be enriched in cumulus olivine.

Phen. oliv.	46
Phen. cpx.	17
Phen. ore	3
Glass	30
Mesostasis	4

N-15   1-phenocryst glassy Olivine Basalt

3 miles East-south-east of Beacon.

Sample of a 4 ft. dyke.   Large, subhedral olivine phenocrysts (up
to 3 mm. in diameter) in a groundmass of olivine, clinopyroxene,
skeletal plagioclase laths and interstitial glass;   relatively
coarse grained.

Phen. oliv.	5
Oliv.	14
Cpx.	31
Plag.	34
Glass	14
Ore	2

N-21   Picrite

Beacon sill, Beacon.

Olivine generally large (up to 3 mm. in diameter);   clinopyroxene occurs
as euhedral, prismatic crystals up to 0.75 mm. in diameter;   ore phase
is translucent and has a bladed habit - probably Kennedyite;
abundant alkali feldspar in felsic matrix.

Oliv.		29
Cpx.		27
Alk. Felds.	)	
Plag.	)	38
Glass	)	
Ore		6
Apatite		1

N-22   Picrite

Beacon sill, Beacon.

Holocrystalline rock with all species except interstitital alkali
feldspar and the ore phase forming subhedral grains ca. 1 mm. in
diameter; a few bladed to prismatic ore crystals are up to 4 mm.
long.

Oliv.	38
Cpx.	25
Feldspar	35
Ore	2
Apatite	tr.

N-23   Picrite

Beacon sill, Beacon.

A holocrystalline rock with abundant olivine-rounded, subhedral crystals
up to 2 mm. in diameter; and clinopyroxene, the latter occurring as
prismatic crystals up to 3 mm. long; clinopyroxene tends to form
radiating clusters or rosettes; plagioclase and alkali feldspar are
interstitial; ore blebs thoroughly opaque and probably titaniferous
magnetite -- cf. N-21 and N-22.

Oliv.	42
Cpx.	32
Alk. felds.	19
Plag.	4
Ore	3

N-26   1-phenocryst glassy Olivine Basalt

Beacon.

Sample of a 12 - 15 ft. East - West dyke. Olivine phenocrysts subhedral-
euhedral, up to 3 mm. in diameter; rare orthopyroxene phenocrysts, up
to 2 mm. in length and rimmed by clinopyroxene; clinopyroxene and ore
microphenocrysts all in a matrix of glass, fine-grained plagioclase
and finely comminuted ore granules; has suffered slight thermal
metamorphism - presumably when the Beacon sill was intruded.

Oliv.	21
Cpx.	25
Ore	7
Matrix	46
Opx.	1

N-27   0.05 km.   Picrite

100 yd. North of Beacon.

Large, subhedral olivine crystals - up to 3 mm. in diameter;
euhedral clinopyroxene crystals - also up to 3 mm. in length -
and smaller ore laths and bladed crystals in a fine-grained felsic
groundmass; transitional to a 2-phenocryst Picrite Basalt.

Oliv.	37
Cpx.	21
Ore	4
Matrix	38

N-34   1-phenocryst Limburgite

1 mile North of Beacon.

Olivine phenocrysts are subhedral and up to 1.5 mm. in diameter;
tabular to prismatic ore and clinopyroxene microphenocrysts; abundant
acicular clinopyroxene crystals - up to 0.5 mm. long in a colourless-
faint brown glass; transitional to 2-phenocryst Limburgite.

Oliv.	24
Cpx.	25
Ore	5
Matrix	46
Opx.	tr.

N-35   0.05   1-phenocryst Limburgite
        Km

1 mile North of Beacon.

Olivine phenocrysts are subhedral and up to 2 mm. in diameter; abundant
microphenocrysts of clinopyroxene, generally displaying delicate skeletal
habit; ore dendritic and skeletal, frequently occurring in the parallel
growth habit known as combs; glass colourless - faint brown.

Oliv.	25
Cpx.	22
Ore	13
Matrix	40

N-37   0.19   2-phenocryst Limburgite

2½ miles East of Beacon.

Sample of an 8 ft. East - West dyke. Olivine phenocrysts - frequently

somewhat skeletal, up to 1.5 mm. in diameter - and prismatic, euhedral clinopyroxene microphenocrysts in a brown glass; lathlike - bladed ore microphenocrysts; very rare fine-grained, acicular plagioclase; one cluster of orthopyroxene phenocrysts.

Oliv.	24
Cpx.	26
Ore)	
)	50
Glass)	
Opx	tr.

N-40   O &19   1-phenocryst glassy Olivine Basalt

2½ miles East of Beacon.

Olivine phenocrysts are subhedral and up to 2 mm. in diameter; clino-pyroxene occurs as fine-grained euhedral, crystals; plagioclase laths are subhedral and up to 2.5 mm. long - often with axial holes - and polysynthetic twinning is irregular or absent; interstitial glass.

Oliv.	19
Cpx.	30
Plag.	26
Ore	8
Glass	17
Opx.	tr.

N-41   0·21   Picrite

2½ miles East-North-East of Beacon.

Somewhat rounded olivine crystals up to 3 mm. in diameter; clinopyroxene displays more euhedral habit, and is generally less than 1 mm. long;

ore occurs as bladed crystals which are frequently brown and translucent - probably Kennedyite; felsic groundmass contains alkali feldspar and plagioclase; one large crystal of orthopyroxene with clinopyroxene rim.

Oliv.	33
Cpx.	25
Ore	5
Plag.	22
Alk. felds.	14
Opx.	tr.

N-55   0.51   2-phenocryst Limburgite

½ mile South-East of Gomakwe intrusion.

Large euhedral clinopyroxene phenocrysts - up to 2.5 mm. long - and smaller, rounded olivine phenocrysts, together with prisms and laths of Kennedyite - all in a felsic glassy groundmass; transitional to a picrite or 2-phenocryst glassy Olivine Basalt; one very large orthopyroxene phenocryst (3 mm.).

Oliv.	31
Cpx.	27
Ore	3
Matrix	38
Opx.	1

N-60   0.38   2-phenocryst Limburgite

1½ miles South of Gomakwe intrusion.

A rock very similar to N-55; the fresh, euhedral clinopyroxene phenocrysts contrast with the more rounded, smaller olivine phenocrysts, which show

some alteration to a red iddingsitic product; very fine-grained,
acicular laths of plagioclase, often with a fluxion orientation,
occur in the glassy groundmass; enrichment in cumulus olivine, and
possibly clinopyroxene suspected.

Oliv.	39
Cpx.	16
Ore	4
Matrix	41

N-72 0.32 2-phenocryst glassy Picrite-Basalt

2 miles North-West of Gomakwe intrusion.

Large (up to 3 mm. in diameter) phenocrysts of irregularly shaped
olivine; clinopyroxene phenocrysts much smaller (ca. 0.5 mm. long) and
are prismatic - lathlike; large single crystals of orthopyroxene and
clusters, all with marginal clinopyroxene rim; glassy groundmass with
abundant small plagioclase laths, many of which are acicular.

Oliv.		29
Cpx.		22
Ore		4
Plag.	)	
Matrix	)	43
Opx.	)	
Opx.		2

N-76 0.47 1-phenocryst Limburgite

1 mile South-South-West of Gomakwe intrusion.

Relatively abundant orthopyroxene phenocrysts - one of which is 6 mm.
long - which are invariably rimmed by clinopyroxene; one large

irregular olivine crystal which is 6 mm. by 3 mm., is considered to be an inherited megacryst; the olivine phenocrysts are rounded, up to 1.5 mm. in diameter, and somewhat altered; these, together with small, euhedral clinopyroxene microphenocrysts and bladed ore crystals, up to 1.5 mm. long, are set in a glassy matrix along with considerable acicular plagioclase; transitional to a 1-phenocryst glassy Olivine Basalt.

Oliv.	39
Cpx.	17
Ore	4
Matrix	36
Opx.	4

N-79   0.55   2-phenocryst Olivine Basalt

4 miles South-South-East of Gomakwe intrusion.

Subhedral olivine phenocrysts - up to 1 mm. in diameter - and rare clinopyroxene phenocrysts in a groundmass of granular clinopyroxene and olivine, plagioclase laths, anhedral ore grains and glass; intersertal texture; relatively coarse-grained.

Phen. oliv.	15
Phen. cpx.	tr.
Matrix	85

N-84 0.53   1-phenocryst glassy Olivine Basalt

4 miles South-East of Gomakwe intrusion.

Relatively infrequent subhedral - euhedral olivine phenocrysts - up to 1 mm. in diameter; granular clinopyroxene, skeletal and dendritic ore and elongate, skeletal plagioclase laths, with axial cavities and

which are up to 1.5 mm. long;   all set in a glassy base.

<div style="text-align:center">

Phen. oliv.   7
Matrix   93

</div>

N-88   0·60   1-phenocryst Olivine Basalt

5 miles South-East of Gomakwe intrusion.

A relatively coarse-grained rock with only small patches of interstitial
glass and mesostasis;   abundant large orthopyroxene phenocrysts (up to
7 mm. long), all of which are surrounded by clinopyroxene rims;   altered
olivine microphenocrysts (up to 1 mm. in diameter), smaller olivine
crystals, clinopyroxene prisms, plagioclase laths and laths of ore
constitute the matrix.

<div style="text-align:center">

Phen. oliv.   5
Matrix   74
Opx.   21

</div>

N-89   0·64   1-phenocryst Olivine Basalt

5 miles South-East of Gomakwe intrusion.

A rare basalt type containing occasional microphenocrysts of olivine
and very sparse orthopyroxene phenocrysts in a groundmass of subhedral -
anhedral clinopyroxene, ore and stubby plagioclase laths;   a pronounced
sub-ophitic relationship between clinopyroxene and plagioclase is a
prominent feature;   no modal analysis as distinction between
microphenocrysts and groundmass crystals is very slight.

N-90   Picrite

5 miles South-East of Gomakwe intrusion.

Sample of a prominent East – West dyke, 100 yds. wide. A thoroughly
mafic holocrystalline rock composed of abundant subhedral olivine
(up to 2 mm. in diameter), clinopyroxene, orthopyroxene and ore –
probably Kennedyite – in an interstitial groundmass of plagioclase
laths (up to 1 mm. long) and anhedral alkali feldspar; the ortho-
pyroxene is not rimmed by clinopyroxene and forms subhedral prismatic
crystals up to 3 mm. long.

Oliv.	48
Cpx.	15
Opx.	4
Ore	2
Feldspar	31

N-91   .62   2-phenocryst glassy Olivine Basalt

5 miles South-East of Gomakwe intrusion.

Microphenocrysts of euhedral – subhedral olivine and clinopyroxene
(always less than 1.5 mm. maximum dimension); relatively abundant
small orthopyroxene phenocrysts with characteristic clinopyroxene
rim; clinopyroxene microphenocrysts tend to form clusters; ground-
mass of plagioclase laths, granular clinopyroxene, ore and glass.

Oliv.	19
Cpx.	23
Ore	8
Plag.	26
Glass	21
Opx.	3

N-95   0·51   Picrite

5 miles South-East of Gomakwe intrusion.

A holocrystalline aggregate of rounded - subhedral olivine, subhedral
clinopyroxene and plagioclase, euhedral Kennedyite laths and prisms;
alkali feldspar rare and interstitial; one remnant crystal of ortho-
pyroxene surrounded by a cluster of clinopyroxene prisms was noted.

Oliv.	36
Cpx.	27
Plag.	25
Alk. felds.	8
Ore	3
Opx.	tr.

N-100   0·45   2-phenocryst Limburgite

50 yards South of Gomakwe intrusion.

A thermally metamorphosed assemblage consisting of anhedral, oxidised,
olivine phenocrysts and a few subhedral clinopyroxene and orthopyroxene
phenocrysts all in a dense groundmass with abundant, fine-grained,
granular ore.

Oliv.	9
Cpx.	5
Matrix	84
Opx	2

N-102   0·48   3-phenocryst Olivine Basalt

40 yards South-East of Gomakwe intrusion.

Small (less than 1 mm.) phenocrysts of oxidised olivine, subhedral

clinopyroxene and euhedral plagioclase laths in an extremely fine-grained groundmass of granular ore, felsic material and clinopyroxene ? One prominent cluster of orthopyroxene; has clearly suffered thermal metamorphism.

Oliv.	10
Cpx.	9
Plag.	1
Matrix	77
Opx.	3

N-105   0·17   2-phenocryst Limburgite

2 miles East-South-East of Beacon.

Microphenocrysts of euhedral - subhedral olivine and clinopyroxene and combs of ore in a brown translucent glass; microphenocrysts are always less than 1 mm. in diameter and average 0.3 mm.; rare orthopyroxene phenocrysts.

Oliv.	18
Cpx.	29
Ore	9
Glass	44
Opx.	tr.

N-113   0·86   2-phenocryst glassy Olivine Basalt

6 miles North-West of Chikombedzi.

Subhedral microphenocrysts of olivine and clinopyroxene, skeletal and dendritic ore and rare orthopyroxene phenocrysts in a matrix of long acicular plagioclase crystals (up to 2 mm. long) and glass.

Oliv.	18
Cpx.	25
Ore	6
Matrix	51
Opx.	tr.

N-117   Km
         1.05   1-phenocryst glassy Olivine Basalt

6 miles North-West of Chikombedzi.

Large, subhedral olivine phenocrysts - up to 2.5 mm. in diameter -
in a matrix of granular, subhedral clinopyroxene, quenched plagioclase
crystals - up to 1.5 mm. long and frequently with axial cavities -
ore and glass; relatively abundant large orthopyroxene phenocrysts
with clinopyroxene rims.

Phen. oliv.	5
Matrix	89
Opx.	6

N-126
         0.05   2-phenocryst glassy Olivine Basalt

3½ miles South-South-West of Beacon.

Subhedral phenocrysts of olivine - up to 1.5 mm. in diameter - and
smaller, microphenocrysts of subhedral clinopyroxene; the rare remnants
of orthopyroxene phenocrysts are surrounded by large, euhedral clino-
pyroxene phenocrysts - up to 6 mm. long - displaying polysynthetic
twinning; acicular plagioclase crystals in the glassy groundmass are
up to 2 mm. long.

Oliv.	19
Cpx.	24

Ore		4
Plag.	)	
Glass	)	52
Opx.		1

N-133   0.29   1-phenocryst glassy Picrite-Basalt

4 miles South of Beacon.

Large phenocrysts - up to 2 mm. in diameter - of subhedral -
rounded olivine; bladed crystals of Kennedyite attain lengths of
2 mm.; matrix consists of subhedral clinopyroxene and fine-grained
plagioclase laths in interstitial alkali feldspar; rare acicular
apatite.

Oliv.	34
Cpx.	24
Feldspar	39
Apatite	tr.
Ore	3

N-135   0.23   1-phenocryst Limburgite

4 miles South of Beacon.

Large euhedral phenocrysts of olivine - up to 3 mm. long; granular
microphenocrysts of olivine and clinopyroxene and combs of ore;
reddish-brown glass.

Phen. oliv.		22
Microph. oliv.	)	28
Microph. cpx.	)	
Glass	)	46
Ore	)	
Mesostasis		4

<u>N-149</u> ? 0.15   <u>2-phenocryst Olivine Basalt</u>

3 miles East of Beacon.

Subhedral olivine phenocrysts up to 1.5 mm. in diameter; euhedral
clinopyroxene phenocrysts display polysynthetic twinning and are
associated with the rare orthopyroxene phenocrysts; the groundmass
consists of granular clinopyroxene, ore combs, plagioclase laths
and interstitial glass.

Oliv.	16
Cpx.	6
Matrix	78
Opx.	tr.

<u>N-160</u> 0.48 <u>2-phenocryst glassy Olivine Basalt</u>

2 miles <s>North</s>-West of Gomakwe intrusion.

Probably a sample of a dyke. Subhedral olivine phenocrysts - up to
1.5 mm. in diameter - and euhedral clinopyroxene phenocrysts of
similar dimensions; the clinopyroxenes tend to form clusters around
the remnant cores of orthopyroxene phenocrysts; small, euhedral
plagioclase laths - up to 0.3 mm. long - in a dark brown - black
glass.

Oliv.	22
Cpx.	18
Plag.	14
Glass.	46
Opx.	tr.

N-163   Picrodolerite

Chitea intrusion.

A holocrystalline rock with an average grain-size of 0.3 mm.;
olivine crystals are subhedral and larger than average; plagioclase
forms staut laths and prisms, some of which are totally enclosed in
the relatively abundant orthopyroxene, most of which appears to be
in equilibrium with the rest of the assemblage.

Oliv.	13
Cpx.	28
Opx.	15
Plag.	35
Alk. felds.	3
Ore	5

N-187   Km.   2-phenocryst Olivine Basalt
         1.20

8 miles South-South-West of Chitea intrusion.

Clinopyroxene phenocrysts occur as single euhedral crystals - up
to 1 mm. long - and as aggregates of several crystals which are
surrounding the remnant cores of orthopyroxene phenocrysts; olivine
phenocrysts are smaller and generally are altered to a green product;
the relatively coarse-grained matrix consists of clinopyroxene, ore,
plagioclase laths and some interstitial glass.

Oliv.	19
Phen. cpx.	20
Cpx.	11
Plag.	33
Glass	9
Ore	5
Opx.	3

N-190   *approx*   1-phenocryst Limburgite
         0.25 km.

10 miles South-West of Chilonga's.

Anhedral olivine phenocrysts, many with cavities and amoeboid habit –
up to 1 mm. in diameter; very small clinopyroxene microphenocrysts
and ore combs in a brown glass.

Oliv.		23
Cpx.		21
Glass	)	
	)	56
Ore	)	

N-225   *approx*   1-phenocryst Olivine Basalt
         0.5 km.

4¼ miles South-East of Chilonga's.

Small, rounded olivine phenocrysts in a groundmass of granular clino-
pyroxene, olivine (rather altered), plagioclase laths, ore and glass;
almost aphyric.

Phen. oliv.	4
Oliv.	10
Cpx.	36
Matrix	50

N-231   1-phenocryst glassy Picrite-Basalt
       0.8 km

10 miles South-East of Chilonga's.

Subhedral olivine phenocrysts – somewhat altered – and micro-
phenocrysts of subhedral – anhedral clinopyroxene in matrix of ore
combs, acicular plagioclase with a quenched appearance and brown glass.

Oliv.	29
Cpx.	17
Matrix	54

N-245   1.2 o   **1-phenocryst Olivine Basalt**

4½ miles East-North-East of Chitea intrusion.

Rare, rounded olivine phenocrysts   -   up to 1 mm. in diameter;
even-grained groundmass of granular olivine and clinopyroxene,
plagioclase laths, ore and glass;   intersertal texture.

Phen. oliv.	4
Oliv.	11
Cpx.	20
Rest	65
Opx.	tr.

N-355   Km   0.0   **2-phenocryst glassy Olivine Basalt**

Beside railway at base of volcanic succession.

Abundant small phenocrysts of euhedral clinopyroxene and subhedral
olivine;   maximum phenocryst size 1 mm.;   clinopyroxene phenocrysts
occasionally form clusters;   groundmass of smaller, anhedral olivine
and clinopyroxene crystals, plagioclase laths   -   often with axial
cavities   -   ore and glass.

Oliv.	20
Cpx.	29
Plag.	23
Glass	22
Ore	6
Opx.	tr.

N-356   O.O   <u>1-phenocryst Limburgite</u>

½ mile East of railway at base of volcanic succession.

Large, euhedral olivine megacrysts up to 5 mm. by 4 mm. contrast
with subhedral olivine phenocrysts which are up to 1 mm. in diameter;
subhedral microphenocrysts of clinopyroxene and needles of ore, all
in a clear glass.

Megacryst. oliv.	7
Phen. oliv.	22
Cpx.	17
Glass	48
Ore	6
Opx.	tr.

N-357   O.O   <u>2-phenocryst Limburgite</u>

1 mile North-East of railway at base of volcanic succession.

Subhedral phenocrysts of olivine and clinopyroxene in a dense fine-
grained groundmass; a thermally metamorphosed sample.

Oliv.	14
Cpx.	6
Matrix	80

N-361   1.25 ?   <u>1-phenocryst Olivine Basalt</u>

7 miles North-North-East of Chikombedzi.

Subhedral olivine phenocrysts up to 1 mm. in diameter; groundmass
very fine-grained and consists of granular clinopyroxene and olivine,
ore and elongate plagioclase crystals - many of which have axial

cavities.

Phen. oliv.	5
Rest	95

N-364   Picrodolerite

$6\frac{3}{4}$ miles North-North-East of Chikombedzi.

A relatively coarse-grained, holocrystalline rock consisting of
olivine, clinopyroxene, plagioclase, ore and orthopyroxene;   the
subhedral orthopyroxene crystals lack a clinopyroxene rim and marginally
they poikilitically enclose small plagioclase laths;   they appear,
therefore, to be in equilibrium with the assemblage.

Oliv.	18
Cpx.	26
Opx.	13
Plag.	36
Ore	2
Mesostasis	1

N-399   2-phenocryst Limburgite

3 miles South-West of Chilembeni intrusion.

Euhedral - subhedral olivine phenocrysts - up to 0.7 mm. in diameter;
and smaller subhedral clinopyroxene phenocrysts in a dense brown glass;
imperfect development of ore combs.

Oliv.	20	
Cpx.	26	
Glass)		54
Ore)		

N-400   1-phenocryst   Limburgite

3 miles South-West of Chilembeni intrusion.

Subhedral - euhedral olivine phenocrysts, small clinopyroxene micro-
phenocrysts displaying skeletal habit and ore combs in a dark brown
glass; very rare orthopyroxene phenocrysts surrounded by clinopyroxene.

Oliv.	29
Cpx.	20
Glass)	49
Ore)	
Opx.	tr.

N-405   2-phenocryst glassy Olivine Basalt

2 miles North of Davata.

Phenocrysts of subhedral clinopyroxene (up to 2 mm. long) and olivine
(generally less than 1 mm. in diameter); groundmass consists of
subhedral - anhedral clinopyroxene, rounded olivine, plagioclase laths
with a highly quenched aspect, ore combs and interstitial glass.

Phen. oliv.	4
Phen. cpx.	1
Oliv.	15
Cpx.	28
Plag.	25
Glass	18
Ore	9

N-406   1-phenocryst glassy Olivine Basalt

2 miles North of Davata.

Small, subhedral phenocrysts of olivine (up to 0.8 mm. in diameter);

very sparse small clinopyroxene phenocrysts; groundmass of olivine, clinopyroxene, well developed ore combs, plagioclase with axial cavities and interstitial glass; transitional to 2-phenocryst type.

Phen. oliv.	10
Oliv.	8
Cpx.	27
Plag.	30
Glass	13
Ore	12

N-440   1-phenocryst glassy Picrite-Basalt

Chikwarakwara, Beitbridge District.

Somewhat rounded and marginally altered olivine phenocrysts - up to 1 mm. in diameter; prismatic clinopyroxene microphenocrysts, relatively rare olivine microphenocrysts and elongate blades of ore, all in a matrix of small felted plagioclase laths in glass.

Oliv.	35
Cpx.	20
Matrix	38
Ore	7

N-442   1-phenocryst Olivine Basalt

Chikwarakwara, Beitbridge District.

Subhedral olivine phenocrysts (up to 1 mm. in diameter) in a ground-mass of rounded olivine crystals, laths of clinopyroxene, plagioclase and ore and interstitial brown glass.

Phen. oliv.   12
Rest   88

N-462   2-phenocryst Limburgite

200 yards North-West of Chilembeni intrusion margin.

Phenocrysts of olivine and clinopyroxene (up to 1 mm. in size) and
elongate bladed ore crystals in a groundmass of dendritic ore,
minute felted plagioclase laths and clear glass.

Oliv.   29
Cpx.   20
Matrix   47
Ore   4

N-517   0.33   1-phenocryst Limburgite

Nyasius

2½ miles South-West of Gomakwe intrusion.

Large, euhedral phenocrysts of olivine, which are marginally altered
to a dark brown product, in a groundmass of prismatic and granular
crystals of clinopyroxene, acicular and lathlike ore and glass; rare
orthopyroxene phenocrysts with characteristic clinopyroxene rim.

Phen. oliv.   31
Cpx.   23
Glass   39
Ore   7
Opx.   tr.

N-519   0.20   3-phenocryst Olivine Basalt

3 miles East of Beacon.

A sample of a 12 ft. wide dyke. Subhedral olivine phenocrysts - up to 1 mm. in diameter - smaller clinopyroxene phenocrysts, occurring in clusters, and very rare plagioclase phenocrysts up to 1 mm. in length; groundmass of plagioclase laths, clinopyroxene, ore combs and brown glass.

Phen. oliv.	9
Phen. cpx.	1
Phen. plag.	tr.
Rest	90

KC-204   1-phenocryst glassy Olivine Basalt

Exact locality unknown.

Large phenocrysts of subhedral olivine (up to 3 mm. long); micro-phenocrysts of prismatic clinopyroxene and bladed ore crystals in a groundmass of glass, alkali feldspar and plagioclase; orthopyroxene phenocrysts with distinctive clinopyroxene rim relatively abundant.

Oliv.	21
Cpx.	28
Feldspar }	
Glass }	43
Ore	5
Opx.	3

A P P E N D I X   B

METHODS

The chemical analyses which form the basis of this thesis were
among the first carried out by X-ray emission spectrographic techniques
in the Grant Institute of Geology. Accordingly an attempt has been
made to establish the accuracy and precision of the analytical methods.
After an assessment of the results proposals are made which, if adopted,
should improve the precision of the method.

Crushing and Grinding

Rock samples selected for chemical analysis were first scrubbed
with a hard brush and washed with deionised water. The samples, which
had weights in the range 500 - 2,000 g., were then broken into pieces
of maximum dimension c. 5 cm by a 'Cutrock' hydraulic rock splitter.
Care was taken at this stage to remove, with a hard toothbrush, any
smears of steel from the rock pieces. By using a manually operated
tungsten carbide pestle and plate these pieces were broken down to
smaller pieces of maximum dimension 2 cm. A grab sample of the
smaller pieces, generally weighing c. 400 g., was reduced to - 10 mesh
by passing it through a case-hardened steel roller-mill - similar to
that described and illustrated by Wager and Brown (1960, p.13 and Fig.3).
A random fraction (0.1 - 0.33) of this coarse powder was finally
reduced to - 125 mesh size in an automatic agate mortar and pestle.
Before analysis this powder was dried at 110°C for 24 hours.

During crushing and grinding some contamination of the samples
must have occurred. Fe, Cr and Mn are the main contaminants from

the 'Cutrock' hydraulic splitter and the roller-mill, W and Co from the cemented tungsten carbide pestle and plate and Si from the agate mortar. Initially the roller-mill was considered to be the major source of contamination and the following dual grinding experiment was devised.

Two samples, N-357 and N-190, were each split into two parts after reduction to 2 cm pieces with the tungsten carbide pestle and plate. One part (WC) was broken to - 10 mesh size on the tungsten carbide pestle and plate while the other part (RM) was reduced to - 10 mesh according to the normal procedure. Both the WC and MR samples were reduced to - 125 mesh in the automatic agate mortar and they were analysed as separate unknowns. The results of this experiment (Table B-1) suggest that the level of contamination introduced by the roller-mill is less than the precision of the analytical methods employed.

X-ray Spectrographic Analysis - Major Elements

The general principles of X-ray emission spectrography are described in several recent publications, e.g. Adler (1966) and Jenkins and de Vries (1967).

(i) Sample preparation

The technique adopted for major element analysis is essentially that developed by Rose et al (1963) and involves combined dilution, heavy absorber addition and fusion of the rock powder. Fusion of the sample with $Li_2B_4O_7$ as a flux completely destroys its mineralogical identity and renders it homogenous. The large quantities of $Li_2B_4O_7$ and the heavy absorber, La_2O_3, which are added make a large contribution to, and hence buffer, the total mass absorption coefficient of the glass beads produced on fusion. For Mg Kα1 radiation the mass absorption coefficients of the rock standards G-1 and W-1 differ, after

TABLE B-1

RESULTS OF DUAL GRINDING TEST

	C	N190		N357	
		RM	WC	RM	WC
Fe_2O_3 T	1.83%	11.1	11.3	11.9	12.0
MnO	2.36%	0.132	0.138	0.160	0.154
Cr	7%	1140	1150	890	900
Ni	7%	775	791	570	562

Fe_2O_3 T and MnO as wt. %; Cr and Ni as p.p.m.

C - relative deviation of analytical method -
       taken from Table B-5 and text.

fusion, by only 2%.   This preparation, therefore, practically eliminates effects due to variation of matrix between samples and standards and allows one to produce and use linear calibration curves of intensity v. concentration for all major elements with $Z > 11$.

The following changes were made to the sample preparation scheme of Rose et al (1963, pp. 82-83):

(a)   A sample : La_2O_3 : $Li_2B_4O_7$ ratio of 1:1:8 was adopted. The fusion mixture, therefore, consisted of 0.7500 g. of sample, 0.7500 g. of La_2O_3 and 6.00 g. of anhydrous $Li_2B_4O_7$.

(b)   The mixtures were fused by heating at $1050^\circ C$ for 20 minutes.

(c)   The cracked glass bead was ground for 40 minutes in a tungsten carbide ball mill; the powder was passed through a 200 mesh nylon sieve and finally dried for several hours at $110^\circ C$.

(d)   The powder was pressed against a polished silver steel surface under 15 tons pressure for 1 minute to form a pellet or fusion disc backed by boric acid.

Since the characteristic X-radiation of Mg, Al and Si is relatively soft and non-penetrative - almost all the measured radiation originates at depths less than 5 - 50 μm. below the surface - the surfaces of the fusion discs were treated with great caution.   Nevertheless, deterioration of the fusion discs, indicated by a darkening of the surface and a drastic reduction of light element count-rate, was noticed after a period of several months.   An X-ray diffraction scan, carried out by the Applications Laboratory of M.E.L. indentified crystalline $Li_2B_4O_7$ hydrate.   All fusion discs were subsequently stored

in a warm drying cabinet. This treatment did prolong the useful lives
of the fusion discs. However, all discs more than 6 months old were
liable to have serious deficiencies.

(ii) Operating conditions

A modified Philips single channel spectrometer (PW 1540) was used
for the analyses. Determinative curves for the oxides SiO_2, Al_2O_3,
total Fe_2O_3, MgO, MnO, CaO were set up by using a number of synthetic
and natural standard materials which had been prepared in a manner
identical to that of the unknown rock powders. The standards used
were :

U.S. Geological Survey standard rock powders G-1 and W-1

(Fleischer and Stevens, 1962).

Canadian Association for Applied Spectroscopy standard rock

powder S-1.

(Webber, 1965).

U.S. National Bureau of Standards synthetic standards

NBS 76, 77, 91 and 102, and

Milford Granite standard rock.

Karroo picritic basalts from Nuanetsi, Rhodesia, LM 432,

LM 593

(Cox et al, 1965)

Once calibration had been achieved the samples were analysed
in batches of 3 - the fourth position in the spectrometer sample
holder being used for a standard fusion disc. The intensity of
radiation from this disc was measured with each batch and a correction
made for instrumental drift.

No apparent departure from linearity was noted for any of the
calibration curves. Table B-2 gives the correlation coefficient (r)

TABLE B-2

MAJOR OXIDE CALIBRATION

	Standards Used	r	Date
SiO_2	G-1, W-1, S-1, NBS - 76,77, 91 and 102, Milf. Gr.	0.9991	Oct. 1965
TiO_2	G-1, W-1, S-1, NBS - 76 and 77 Milf. Gr.	0.9998	Dec. 1965
Al_2O_3	G-1, W-1, S-1, NBS - 76 and 91, Milf. Gr., LM 593, LM 432	0.9996	Dec. 1965
Fe_2O_3 T	G-1, W-1, S-1, NBS - 76, 77 and 102, Milf. Gr.	0.9995	Dec. 1965
MnO	G-1, W-1, S-1, Milf. Gr., LM 593, LM 432.	0.9988	Mar. 1966
MgO	G-1, W-1, S-1, LM 593, LM 432	0.9999	Jan. 1966
CaO	G-1, W-1, S-1, NBS - 76, 91 and 102, Milf. Gr., LM 593, LM 432.	0.9995	Feb. 1966

Milf. Gr. - Milford Granite.

r - correlation coefficient between concentration of the oxides and the measured intensities of characteristic fluorescent radiation.

between the intensity of a measured line and the concentration of the oxides in the standards.

In general, standards G-1 and W-1 lay on, or close to, all the calibration curves;   the fit of the synthetic standards was less good. This observation may be the result of two factors :

(a) The analyses of the synthetic standards are less accurate.

(b) Because of the marked chemical contrasts between the rock and the synthetic standard powders, differential mass absorption effects may not have been rendered completely insignificant by the dilution, heavy absorber addition preparation.

In this latter respect it is interesting to note that, despite being single analyses, the two secondary rock standards, LM 432 and LM 593 lay close to all the calibration curves, except that for TiO_2. This feature of the synthetic standards accounts for the MgO correlation coefficient being higher than that for SiO_2 and Al_2O_3 despite the lower number of counts recorded.

Operating conditions for the analysis of each oxide are given in Table B-3.

(iii) Accuracy

Table B-4 gives partial analyses for the rock standards G-1, W-1 and S-1.   The Edinburgh analyses have been calculated from the calibration curves used during the analytical programme, each standard being treated in turn as an unknown.   For each oxide the value represents the mean of 4 - 10 individual determinations on 2 - 4 fusion discs made from one fusion of G-1, W-1 and S-1 powders.   The results for each oxide were collected over two working periods between October 1965 and March 1966.

TABLE B-3

OPERATING CONDITIONS OF X-RAY SPECTROGRAPH

- MAJOR OXIDES

	SiO_2	TiO_2	Al_2O_3	Fe_2O_3 T	MnO	MgO	CaO
Line	Kα1	Kα1	Kα1	Kα1	Kα1	Kα1	Kα1
Tube	Cr	W	Cr	W	W	Cr	W
KV	50	40	45	40	40	50	40
mA	28	20	32	20	28	28	20
Analysing Crystal	Pe	LiF	Pe	LiF	LiF	ADP	LiF
Detector	Flow	Flow	Flow	Scint.	Scint.	Flow	Flow
Vacuum Path?	Yes	Yes	Yes	No	No	Yes	Yes
Collimator	Coarse	Fine	Coarse	Fine	Fine	Coarse	Coarse
Count Time: secs.	60	40	40	40	40	100	40
No. of Counts	1	3	5	3	3	4	3
Count Type	P	P	P	P	P-B	P	P
Background Position	-	-	-	-	$+2.60^{\circ}2\theta$	-	-
Count Rate	40 cps	360 cps	30 cps	260 cps	420 cps	2 cps	690 cps

Count Rate given is rate per 1% of oxide in sample.

Count Type - P = Peak

P-B = Peak-Background

All determinations were duplicated during one working period.

TABLE B-4

STANDARD SAMPLES G-1, W-1 and S-1

G-1

Wt%	*	Edin
SiO_2	72.8	72.7
TiO_2	0.26	0.26
Al_2O_3	14.0	14.5
Fe_2O_3T	1.96	2.06
MnO	0.03	0.028
MgO	0.41	0.37
CaO	1.39	1.38

W-1

Wt%	*	Edin
SiO_2	52.6	52.7
TiO_2	1.07	1.04
Al_2O_3	14.9	15.2
Fe_2O_3T	11.2	11.1
MnO	0.16	0.172
MgO	6.62	6.53
CaO	11.0	11.2

S-1

Wt%	o	Edin
SiO_2	59.45	59.4
TiO_2	0.49	0.49
Al_2O_3	9.58	9.07
Fe_2O_3T	8.32	8.19
MnO	0.40	0.392
MgO	4.07	4.09
CaO	10.32	10.1

* - Preferred values, Fleischer and Stevens, 1962

o - Mean values, Webber, 1965.

Edin. - Edinburgh X-ray spectrographic analyses.

Except for Al_2O_3, agreement between the accepted values and the Edinburgh X-ray values is good and it is concluded that there are no significant systematic errors in the method.   Results presented below indicate that for Al_2O_3 relative deviations greater than 3.2% should occur only in 1% of Al_2O_3 determinations.   Both the G-1 and S-1 discrepancies exceed this value.   It seems probable, therefore, that there is a significant error in the Al_2O_3 determinations and it seems probable that the errors are due to enhancement and absorption of Al Kα1 radiation by the relatively abundant Mg and Si in the fusion discs.

(iv) <u>Precision</u>

In an attempt to measure the precision of the X-ray spectrographic methods adopted in the Grant Institute of Geology 7 samples of N-117 were each treated as unknowns and taken through all stages of the sample preparation and analytical programmes.   The results of this investigation are presented in Table B-5a.   Comparable results obtained by Rose <u>et al</u> (1963), using a very similar X-ray technique, Volborth (1963), using a different X-ray technique, and Gould (1966), using 'rapid' wet chemical methods, are given in Table B-5b.

The overall precision of the present X-ray method is considered to be made up of 3 parts :

(a) random errors during sample preparation - i.e. during the preparation of fusion discs.

(b) a lack of precision due to deterioration of the fusion discs, especially the standards, during the latter stages of the analytical programme.   These may, in part, be systematic errors.   However, because of the accuracy of the method (described above) there cannot be any gross systematic errors.

(c) random instrumental errors.

TABLE B-5a

ANALYTICAL PRECISION

	$\bar{x}$	d	s	C
SiO_2	49.35	1.10	0.32	0.64%
TiO_2	2.31	0.05	0.019	0.82%
Al_2O_3	9.04	0.31	0.097	1.07%
Fe_2O_3T	11.47	0.67	0.13	1.83%
MnO	0.144	0.011	0.003	2.36%
MgO	14.74	0.84	0.28	1.90%
CaO	7.27	0.24	0.078	1.07%

$\bar{x}$ - mean of 7 X-ray spectrographic determinations.

d - range of deviations about the mean

s - standard deviation

C - relative deviation $(100\ s/\bar{x})$

TABLE B-5b

	A		B		C	
	Comp.Range	C	Comp.Range	C	$\bar{x}$	C
SiO_2	50 - 75	0.50%	50 - 80	0.07 - 0.4%	71.78	0.46%
TiO_2	0.1 - 2.0	2.14%	0.2 - 1.6	0.5 - 5.0%	0.59	1.86%
Al_2O_3	10 - 20	1.02%	10 - 20	0.2 - 0.9%	13.12	1.22%
Fe_2O_3T	1 - 12	0.95%	0.4 - 12	0.1 - 1.6%	4.13	0.97%
MnO	0.01- 0.5	3.13%	0.03- 0.18	0.0 - 2.2%	0.073	4.11%
MgO	0.4 - 10	2.07%	0.2 - 6.6	0.1 - 1.2%	0.59	6.27%
CaO	1 - 12	0.97%	0.3 - 11	0.1 - 0.4%	1.48	2.57%

A - precision of X-ray spectrographic analyses by Rose et al (1963)

B - precision of X-ray spectrographic analyses by Volborth (1963)

C - precision of 'rapid' wet chemical analyses by Gould (1966)

The magnitude of random instrumental errors can be readily assessed. There are 3 factors which contribute to the total instrumental error – counting statistics (standard deviation of N counts is $\sqrt{N}$), generator stability or short term drift (always $< 0.1\%$) and other equipment errors, e.g. goniometer setting ($< 0.05\%$) (Jenkins and de Vries, 1967). Ideally generator stability should be the largest, and therefore limiting, factor. However, because of limited time – the longest working period was 30 hours – this was not achieved and the random counting errors for MgO and MnO are considerable. Addition of the 3 instrumental factors for the N-117 analyses according to the equation –

$$\text{error (total)} = \sqrt{(\text{error})^2 \text{ count.} + (\text{error})^2 \text{ gen.stab.} + (\text{error})^2 \text{ equip.}}$$

gives the total instrumental errors. These are listed in Table B-6.

Long term drift is eliminated by ratioing each unknown against the standard fusion disc which was permanently in the sample holder.

A rough estimate of the magnitude of the disc deterioration factor is given in Table B-6. These figures are the average relative deviations of duplicate determinations made on 1 fusion disc of G-1, W-1 and S-1 6 months apart. Along with other standard fusion discs these discs were used to establish calibration curves at the start of analytical working periods.

There are insufficient data to establish the magnitude of the first factor – errors during sample preparation. However, a comparison of the overall precision with the errors attributed to the two factors described above (Table B-6) suggests that it is significant despite the care taken to ensure quantitative transfer of material at all stages of the sample preparation scheme.

TABLE B-6

ANALYTICAL PRECISION

	C instrumental*	C disc deterioration°	C total[x]
SiO_2	0.24%	0.5%	0.64%
TiO_2	0.23%	2.0%	0.82%
Al_2O_3	0.28%	0.6%	1.07%
Fe_2O_3 T	0.16%	1.3%	1.83%
MnO	0.72%	-	2.36%
MgO	0.65%	0.5%	1.90%
CaO	0.14%	1.4%	1.07%

* - based on counting statistics for N-117, generator stability and other equipment errors.

° - estimated errors based on duplicate determinations on G-1, W-1 and S-1 standard discs 6 months apart.

x - from Table B-5a.

(v) Conclusions

During the analytical programme it was realised that the precision of the results could have been improved had a different approach been adopted initially.   Only 1 set of standard fusion discs was prepared and these were used to establish calibration curves for each oxide on separate occasions several months apart.   The tentative results of Table B-6 indicate that the repeatability of the calibration curves was not high.   The factors considered to be responsible for this lack of precision were physical deterioration of the working surface of the discs, possibly chemical changes (see section on sample preparation, above) and a lack of precision in the successive positions of the spectrometer sample holder.

The following improvements are recommended to the method of X-ray spectrographic analysis using a manual, single-channel spectrometer :

    (a) all standard and unknown fusion discs should be prepared before the analytical programme is initiated.

    (b) all fusion discs should be stored in a relatively dry atmosphere - e.g. in a warming cabinet.

    (c) all analyses should be carried out as soon as possible after the preparation of fusion discs.

    (d) all determinations of each oxide should be made in one working period, using one calibration curve.

If implemented, these recommendations should improve the precision of the method.

The analyses produced during this study are, nevertheless, considered satisfactory.   The accuracy of the method, apart, perhaps, for Al_2O_3, has been established.   The precision is similar to that

obtained by the developers of the method - Rose et al (1963). The
precision achieved by Volborth (1963) has not been matched. Volborth's
method involves simplifying the sample preparation procedure and
recording large numbers of counts. However, the accuracy of Volborth's
results has been questioned (Mercy and Saunders, 1966). In view of
the minimal efforts made to reduce matrix effects it is not surprising
that the method adopted by Volborth should give less accurate results.

X-ray Spectrographic Analysis - Trace Elements

Spectrographic trace element analyses were carried out on - 125
mesh rock powder supported by a Mylar film. Ba, Cr, Ni, Rb, Sr and
Zr were determined in all the unknowns; Cu, La, Nb, Pb and Zn only in
a representative sample. The operating conditions are given in Table
B-7.

No attempt was made to calculate the varying mass absorption
coefficients of the standards and unknowns. However, the method of
counting adopted - peak : background ratio - largely compensates
for this variable factor (Andermann and Kemp, 1958).

Correlation coefficients between the concentration of each
element in the standards and the measured peak : background ratios
are given in Table B-8. These are considerably lower than the
calibration correlation coefficients for major oxides (Table B-2).
This is almost certainly a result of the approximate matrix correction
factor and the uncertainty regarding the correct concentrations of
elements in some standards.

Because the Zr $K\alpha 1$ line is subject to interference by the
Sr $K\beta 1$ line an appropriate correction factor was applied to the
measured peak count. The determination of Cr presented a problem.

OPERATING CONDITIONS OF X-RAY SPECTROGRAPH - TRACE ELEMENTS

	Ba	Cr	Cu	La	Nb	Ni	Pb	Rb	Sr	Zn	Zr
Line	Kα1	Kβ1	Kα1	Lα1	Kα1	Kα1	Lα1	Kα1	Kα1	Kα1	Kα1
Tube	W	W	W	W	W	W	W	W	W	W	W
KV	55	50	60	50	50	45	60	60	45	40	45
mA	20	28	20	20	20	20	20	20	20	20	20
Analysing Crystal	Topaz	Topaz	LiF	LiF 200	LiF	LiF 200	LiF 200	LiF	LiF	LiF 200	LiF 200
Detector	Scint.	Flow	Scint.	Flow	Scint.	Scint.	Scint.	Scint.	Scint.	Scint.	Scint.
Vacuum Path ?	No	Yes	No	Yes	No	No	No	No	No	No	No
Collimator	Fine	Fine	Fine	Fine	Fine	Fine	Fine	Fine	Fine	Fine	Fine
Count Time secs. : Peak	2 x 40	2 x 40	2 x 40	3 x 40	1 x 40	2 x 40	2 x 40	2 x 40	2 x 40	2 x 40	2 x 40*
Bckgnd.	2 x 40	4 x 40	2 x 40	3 x 40	2 x 40	1 x 40	2 x 40	2 x 40	1 x 40	2 x 40	2 x 40
Background Position	-1.32°	$+0.50^{\circ}$ -0.65°	$+1.44^{\circ}$	-1.65°	$\pm0.50^{\circ}$	-1.40°	$\pm0.55^{\circ}$	$+0.85^{\circ}$	-2.00°	-1.44°	$+0.75^{\circ}$
Detection Limit p.p.m.	24	65	5	5	6	2	20	3	3.5	2	5

* - Correction applied for Sr Kβ1 interference.

Detection limit given by $\dfrac{3 \times \sqrt{\text{rate background in x secs.}}}{\sqrt{2} \times \text{rate per 1 p.p.m. in x secs.}}$

TABLE B-8

TRACE ELEMENT CALIBRATION

	r
Ba	0.9946
Cr	0.9916
Ni	0.9999
Rb	0.9976
Sr	0.9983
Zr	0.9924

r - correlation coefficient between the concentrations of the elements and the measured peak : background ratios.

V Kβ1 interferes with the Cr Kα1 line, Ti Kβ1 interferes with the V Kα1 line and Mn Kα1 interferes with the Cr Kβ1 line. As the available range of standards displayed a considerable range of MnO content and the Nuanetsi rocks have a small range of MnO, it was decided to determine Cr in several Nuanetsi rocks by a spectrophotometric method (see below) and use these rocks as standards in the X-ray method. The peak : background ratio of the Cr Kβ1 line was measured and a satisfactory calibration was thus established.

As an indication of the accuracy of the X-ray spectrographic determinations the results obtained by Dr. N.B. Price, of the Grant Institute of Geology, for six U.S. Geological Survey standards are given in Table B-9 and compared with the means of all the determinations reported by Flanagan (1969).

The precision of the method has not been fully investigated. Statistical analysis of a few duplicate determinations indicates a repeatability of $\pm$ 5-10% for elements exceeding 100 p.p.m. and $\pm$ 10-20% for elements below the 100 p.p.m. level.

Wet Chemical Analysis

Na$_2$O and K$_2$O were determined using an EEL Model A flame photometer. The sample solutions were diluted to contain 2 - 20 p.p.m. Na$_2$O or K$_2$O and the acid concentration was in the range 0.1 - 1.0% H$_2$SO$_4$. Standard alkali solutions in 0.1% H$_2$SO$_4$ were read at the same time as the unknown solutions.

FeO was determined by the cold solution method of Wilson (1955). PTFE crucibles were used to contain the solutions during the reduction of the metavanadate.

The spectrophotometric method of Baadsgaard and Sandell (1954)

TABLE B-9

ACCURACY OF TRACE ELEMENT ANALYSES

	G-2		GSP-1		AGV-1	
	*	o	*	o	*	o
Ba	1860	1950	1590	1360	1520	1410
Cu	< 2	10.7	30	35.2	60	63.7
Nb	10	16.1	30	28.3	20	21.7
Ni	< 2	6.4	6	10.7	12	17.8
Pb	15	28.7	40	52.4	20	35.4
Rb	170	234	260	343	70	89.4
Sr"	545	463	260	247	745	657
Zn	90	74.9	100	143	80	112
Zr	340	316	580	544	240	227

	PCC-1		DTS-1		BCR-1	
	*	o	*	o	*	o
Ba	-	6.9	-	6.3	970	790
Cu	5	10.4	< 2	7.9	7	22.4
Nb	< 4	1.1	< 4	4	10	34.1
Ni	3300	2430	3200	2330	8	15
Pb	< 4	13.3	< 4	14.9	< 4	18
Rb	< 2	0.5	5	2.8	45	72.8
Sr"	< 2	0.3	< 2	-	340	345
Zn	45	53	40	61	100	132
Zr	< 4	-	< 4	-	180	185

* - Edinburgh values, reported in Flanagan, 1969, Table 3.

o - mean values (Flanagan, 1969, Table 5).

" - determined by thin film technique (Price and Angell, 1968).

All values p.p.m.

was used for the determination of P_2O_5.

H_2O was determined gravimetrically using dried powders. 1 g. of rock powder and 3 g. of PbO and $PbCrO_4$ flux were heated in a Pyrex test tube. The water given off was collected and weighed.

Two spectrophotometric methods were used to determine Cr in 6 samples. These samples were subsequently used as standards in the X-ray spectrographic analysis of Cr. The results obtained by the direct Chromate method (Sandell, 1959, p.398) were in good agreement with those obtained by the second method which used Diphenylcarbazide as a complexing agent (Sandell, p. 399).

Because of spectral interference on both main V X-ray lines this element was determined in 6 samples by the Phosphotungstate spectro-photometric method (Sandell, 1959, p.934). Duplicate determinations were in good agreement and a single determination on W-1 gave a result of 270 p.p.m. - the recommended value is 240 p.p.m. (Fleischer, 1965).

The precision of these methods has been investigated by calculating the standard deviations of all the duplicate pairs of determinations for each oxide or element. If the results of a duplicate determination are x_1 and x_2 then -

$$s = (x_1 - x_2) / \sqrt{2}$$

The relative deviations (C) are given in Table B-10

$$C = 100s / \bar{x}$$

$\bar{x}$ being the average concentration of each oxide or element in all the samples.

X-ray Diffraction

(i) Olivines

Both the method of Yoder and Sahama (1957) - based on the olivine

TABLE B-10

PRECISION OF WET CHEMICAL METHODS

	N	$\bar{x}$	$\bar{d}$	s	C
FeO	72	8.01	0.073	0.052	0.65%
Na_2O	60	1.87	0.036	0.025	1.34%
K_2O	60	1.56	0.031	0.022	1.41%
P_2O_5	7	0.46	0.009	0.006	1.4 %
H_2O	73	1.51	0.051	0.036	2.38%
Cr_2O_3	5	0.136	0.007	0.005	3.7 %
V_2O_3	5	0.031	0.002	0.001	4.2 %

N - number of duplicate determinations

$\bar{x}$ - average wt.%

$\bar{d}$ - mean difference between duplicates

s - standard deviation

C - relative deviation.

(130) reflection - and the method developed by Jackson (1960) -
based on the olivine (062) reflection - were used to determine olivine
compositions.   These methods involve the addition of an internal
standard, Silicon and LiF respectively, to the ground sample. The
values for the (130) and (062) reflection positions are the means of
at least 6 oscillations of each sample.   The results obtained by the
two methods are compared in Table B-11.

(ii) Orthopyroxenes

Hancock (1964) used diffraction techniques to determine ortho-
pyroxene compositions. The absolute position of the (10, 3, 1) and
(060) reflections are sensitive to Mg : Fe substitution and can be used
to determine En content.   The separation between the (10, 3, 1) and
(060) reflections is proportional to the Al_2O_3 content of the ortho-
pyroxene.   A plot of d (10, 3, 1) v. d (060) for standard orthopyroxenes
produces a grid from which the En and Al_2O_3 contents of unknown ortho-
pyroxenes can be read.

Initially it was hoped that X-ray diffraction might be used for
a detailed study of the orthopyroxene phenocrysts in the lavas. However,
preliminary results, using Hancock's grid, gave less than satisfactory
results.   The method indicated 4% Al_2O_3 in N-88 OPX (reported by
Jamieson (1966)); this was shown to be 1.66% Al_2O_3 by X-ray
spectrographic analysis.

Once analyses of 3 Nuanetsi orthopyroxenes were available, a
further attempt was made to use this method.   These 3 samples and a
further analysed orthopyroxene, 10584 (supplied by Dr. M.J. O'Hara) were
used to define a new determinative grid.   The compositional data are
given in Table B-12a.   This new grid differed slightly from that produced

TABLE B-11

OLIVINE COMPOSITIONS

	Jackson	Yoder and Sahama
N-21	75	77
N-22	77	78
N-27	78	78
N-41	76	78
N-55	70	75
N-60	76	77
N-90	82	84
N-95	73	76
N-160 nod	88	86
N-356	86 and 78*	85

* - two olivine compositions detected.

All compositions mol % Fo.

TABLE B-12

ORTHOPYROXENE DATA

a.

	N-88 OPX	N-117 OPX	N-313 OPX	10584
Al_2O_3 wt.%	1.66	1.44	1.49	4.00
En mol.%	90	82.5	84	91

b.

	N-90 OPX	BUCH 4 OPX *
Al_2O_3 wt.%	1.1	0.7
En mol.%	82	88.5

* - chemical analysis of Buch 4 OPX by Dr. E.L.P.
Mercy gives Al_2O_3 0.95% and En 84%.

by Hancock (1964).   Two further samples, Buch-4 (an analysed ortho-
pyroxene) and N-90 (an important Nuanetsi sample which was not sufficiently
abundant for a destructive analysis) were used as unknowns.   The results
obtained by this diffraction technique are in good agreement with the
chemical analysis of Buch-4 (Table B-12b) and it is, therefore,
considered that a reasonable estimate of the Al_2O_3 content and Mg : Fe
ratio of N-90 OPX has been produced.

Electron Probe X-ray Microanalysis

Analyses were carried out at the Department of Geology, University
of Durham through the generosity of Dr. C.H. Emeleus.   A Cambridge
Geoscan microprobe with a dual-channel spectrometer was used.   No
absorption correction was made to the counts as the standards used
were analysed pyroxenes and olivines with compositions very close to
those of the unknown minerals.

Mineral Separation

Mineral separation and purification was achieved by using Franz
electromagnetic separators and heavy liquid techniques.   In general
heavy liquid techniques were adopted only in the later stages.   In
the case of 2 orthopyroxenes - N-117 OPX and N-313 OPX - it proved
impossible to remove all clinopyroxene grains.   Point counting
indicated 2.5% and 5% residual clinopyroxene.   An appropriate
adjustment was made to the chemical analyses of these orthopyroxenes.

References cited

ADLER, I., 1966. X-ray emission spectrography in geology. Elsevier, Amsterdam. 258 pp.

ANDERMANN, G. and KEMP, J.W., 1958. Scattered X-ray as internal standards in X-ray emission spectroscopy. Analyt. Chem., 30, 1306-1309.

BAADSGAARD, H. and SANDELL, E.B., 1954. Photometric determination of phosphorus in silicate rocks. Analytica chim. Acta, 11, 183-187.

COX, K.G., JOHNSON, R.L., MONKMAN, L.J., STILLMAN, C.J., VAIL, J.R. and WOOD, D.N., 1965. The geology of the Nuanetsi igneous province. Phil. Trans. R. Soc., A, 257, 71-218.

FLANAGAN, F.J., 1969. U.S. Geological Survey standards - II. First compilation of data for the new U.S.G.S. rocks. Geochim. cosmochim. Acta, 33, 81-120.

FLEISCHER, M., 1965. Summary of new data on rock samples G-1 and W-1, 1962-1965. Geochim. cosmochim. Acta, 29, 1263-1284.

FLEISCHER, M. and STEVENS, R.E., 1962. Summary of new data on rock samples G-1 and W-1. Geochim. cosmochim. Acta, 26, 525-543.

GOULD, D., 1966. Geochemical and mineralogical studies of the granitic gneiss and associated rocks of Western Ardgour, Argyll. Univ. Edinburgh Ph.D. thesis (unpubl.).

HANCOCK, W.G., 1964. The Mount Tawai peridotite, North Borneo. Univ. Durham Ph.D. thesis (unpubl.).

JACKSON, E.D., 1960. X-ray determinative curve for natural olivine of composition Fo_{80-90}. Prof. Paper U.S. geol. Surv., 400-B, B 432-B 434.

JAMIESON, B.G., 1966. Evidence on the evolution of basaltic magma at elevated pressures. Nature, Lond., 212, 243-246.

JENKINS, R. and de VRIES, J.L., 1967. Practical X-ray spectrometry. Philips Technical Library, Eindhoven. 181 pp.

MERCY, E.L.P. and SAUNDERS, M.J., 1966. Precision and accuracy in the chemical determination of total Fe and Al in silicate rocks. Earth Planet. Sci. Letters, 1, 169-182.

PRICE, N.B. and ANGELL, G.R., 1968. Determination of minor elements in rocks by thin film X-ray fluorescence techniques. Analyt. Chem., 40, 660-663.

ROSE, H.J., ADLER, I. and FLANAGAN, F.J., 1963. X-ray fluorescence analysis of the light elements in rocks and minerals. Appl. Spectrosc., 17, 81-85.

SANDELL, E.B., 1959. Colorimetric determination of traces of metals. Interscience, New York. 1032 pp.

VOLBORTH, A., 1963. Total instrumental analysis of rocks. Nevada Bureau of Mines Report, 6A, 72 pp.

WAGER, L.R. and BROWN, G.M., 1960. Collection and preparation of material for analyses. in Methods in geochemistry, eds. SMALES, A.A. and WAGER, L.R. Interscience, New York and London. 4-32.

WEBBER, G.R., 1965.   Second report of analytical data for C.A.A.S.

     syenite and sulphide standards.   Geochim. cosmochim.

     Acta, 29, 229-248.

WILSON, A.D., 1955.   A new method for the determination of ferrous

     iron in rocks and minerals.   Bull. geol. Surv. Gt. Britain,

     2, 56-58.

YODER, H.S., Jr. and SAHAMA, T.G., 1957.   Olivine X-ray determinative

     curve.   Am. Miner., 42, 475-491.

A P P E N D I X   C

MISCELLANEOUS   ANALYSES

Nephelinites

The alkaline rocks which occur at the base of the volcanic succession in the Bendezi - Chilonga's area consist essentially of nepheline and augite.   Both minerals are present as groundmass and euhedral phenocryst phases.   In N-201 and N-207 the augite phenocrysts and groundmass crystals are zoned to aegerine - augite.   Less common phenocryst phases are olivine (N-207 and N-212), apatite (N-207 and N-222) and biotite (N-222).   The groundmass in the 4 specimens is holocrystalline, consisting mainly of augite laths and interstitial nepheline or its alteration products.   The medium grain size of N-212 suggests it may be a dyke rock.

The analyses are given in Table C-1;   modal and normative data in Table C-2.

N-201 : Nephelinite,   summit of Bendezi, Ndanga District.

N-207 : Olivine nephelinite, northern slopes of Bendezi, Ndanga District.

N-212 : Olivine nephelinite, 2.7 miles south west of Bendezi, Ndanga District.

N-222 : Nephelinite, 1 mile west of Chilonga's.

Upper Basalts

An investigation of the olivine-rich Karroo basic rocks was always the primary objective of this research project.   Nevertheless,

TABLE C-1

NEPHELINITE ANALYSES

Wt.%	N-201	N-207	N-212	N-222
SiO_2	44.2	40.9	44.6	44.2
TiO_2	3.03	3.55	3.11	3.06
Al_2O_3	16.1	14.4	11.6	16.3
Fe_2O_3	7.9	7.7	5.4	6.5
FeO	2.15	4.25	7.95	3.42
MnO	0.20	0.20	0.19	0.21
MgO	3.64	5.19	6.56	2.59
CaO	5.02	8.89	9.90	3.83
Na_2O	10.5	8.02	5.45	10.9
K_2O	2.77	3.00	1.71	2.04
P_2O_5	1.00	1.36	0.54	1.24
F	0.46	0.41	-	-
H_2O	2.54	1.33	1.91	4.23
Total	99.3*	99.0*	98.9	98.5

p.p.m.

Ba	2860	2080	2190	2240
Cr	< 65	< 65	85	< 65
Cu	207	237	-	-
La	66	59	-	-
Ni	7	25	50	< 2
Rb	82	78	41	75
Sr	2019	1700	585	2020
Zn	95	-	-	-
Zr	290	188	150	320

* - includes adjustment for F.

TABLE C-2

NEPHELINITE MODES AND NORMS

Volume %	N-201	N-207	N-212	N-222
Nepheline	34*	12*	32	27*
Clinopyroxene	5*	5*	37	1*
Olivine		tn*	7	
Alk. Feldspar			9	
Apatite		tr.*		0.5*
Ore			9	
Hornblende and Biotite			6	
Groundmass	61	83		72

* - phenocrysts

Wt.%	N-201	N-207	N-212	N-222
or	16.9	2.9	10.4	12.8
ab	1.9	-	14.4	11.5
an	-	-	2.2	-
lc	-	12.0	-	-
ne	36.6	31.8	18.0	35.4
ac	19.5	9.5	-	18.4
di	11.8	26.6	35.9	9.2
ol	2.7	0.6	3.7	2.7
mt	-	4.2	8.1	0.8
hm	1.4	1.7	-	-
il	5.1	6.9	6.1	6.2
pf	0.7	-	-	-
ap	2.4	3.3	1.3	3.1
fr	0.9	0.7	-	-
H_2O	2.5	1.3	1.9	4.2

6 specimens from the thick series of olivine-free and olivine-poor
Upper Basalts were analysed in order to supplement analyses published
by Cox et al (1965).

Five of the new analyses (Table C-3) contain small amounts of
normative Q. The remaining specimen, N-335, is virtually an ankaramite.
However, it does not contain fresh olivine.

1.1 km. N-243 : Chikwedziwa basalt, 4.5 miles east of Chitea intrusion.

1.9   N-285 : Chikombedzi basalt, in Nuanetsi River, 200 yds north
                of causeway.

1.25   N-308 : Chikwedziwa basalt, 2.5 miles north east of Chikombedzi

about 2 km. N-335 : Thermally metamorphosed ankaramitic basalt, 1.7 miles
                west-north-west of Wusaka Pan.

       ✓ N-340 : Interbedded basalt, 1 mile north west of Jordaan's.

       N-497 : Basalt, 1 mile north of Marumbe Complex.

Olivine monzonites

There are 2 olivine monzonite intrusions in the Nuanetsi igneous
province. These are thought to represent differentiates produced
during near-surface, i.e. low pressure, fractionation of the K-rich
parental basic magma. Specimen N-451 is of the leucocratic facies
of the Chilembeni Hill intrusion which has been described by Monkman
(1961) and Cox et al (1965). N-194 is from a small intrusion
discovered during field work in 1964. In terms of both chemistry
and mineralogy, the rocks from this second olivine monzonite body are
strikingly similar to the Caledonian kentallenites of the S.W. Highlands
of Scotland (Westoll, 1968).

Analyses are given in Table C-5; modal and normative data in
Table C-6. Analysis of the brown clinopyroxene separated from N-451

TABLE C-3

UPPER BASALT ANALYSES

Wt.%	N-243	N-285	N-308	N-335	N-340	N-497	Average excluding N.335
SiO_2	52.0	52.2	52.3	48.8	50.6	49.2	51.26
TiO_2	2.97	3.56	1.71	2.30	0.80	3.12	2.43
Al_2O_3	13.4	15.1	15.0	7.65	13.5	13.9	14.18
Fe_2O_3	3.7	4.5	2.5	6.1	5.2	5.6	4.30
FeO	7.73	6.51	8.03	6.28	7.15	7.64	7.4
MnO	0.15	0.13	0.14	0.18	0.22	0.20	0.17
MgO	4.91	2.87	6.27	15.2	6.87	5.17	5.24
CaO	8.91	7.84	9.70	9.70	11.2	10.9	9.70
Na_2O	2.48	2.39	2.72	2.26	2.24	2.13	2.39
K_2O	1.71	2.46	0.88	1.42	0.52	0.50	1.21
P_2O_5	0.39	0.60	0.24	0.29	0.10	0.33	0.33
H_2O	0.89	1.10	0.48	0.15	1.42	1.16	
Total	99.2	99.3	100.0	100.3	99.8	99.9	

p.p.m.	N-243	N-285	N-308	N-335	N-340	N-497	
Ba	735	735	410	735	140	225	419.
Cr	< 65	85	140	1275	220	< 65	
Ni	40	35	135	640	35	45	
Rb	33	38	24	23	52	10	
Sr	745	910	399	515	175	470	540.
Zr	320	–	165	220	32	210	182

TABLE C-4

UPPER BASALT MODES AND NORMS

Volume %	N-243	N-285	N-308	N-335	N-340	N-497
Plagioclase*	1	12	5			6
Clinopyroxene*	1			31		
Orthopyroxene*			2			
Olivine*	0.5					
Groundmass	97.5	88	93	69	100	94

* - phenocrysts

Wt.%	N-243°	N-285°	N-308	N-335°	N-340°	N-497°
Q	5.7	8.3	3.4	-	1.3	4.7
or	10.3	14.8	5.2	8.4	3.1	3.0
ab	21.4	20.6	23.1	19.1	19.3	18.3
an	20.7	23.7	26.2	6.5	25.7	27.3
di	17.9	10.1	16.8	31.9	24.9	21.1
hy	14.0	10.9	17.7	1.3	20.3	15.1
ol	-	-	-	24.1	-	-
mt	3.3	3.1	3.6	3.5	3.5	3.7
il	5.7	6.9	3.3	4.4	1.6	6.0
ap	0.9	1.5	0.6	0.7	0.2	0.8
Rest*	1.0	1.1	0.6	0.5	1.5	1.2

° - $Fe^{+++}/Fe^{++} + Fe^{+++}$ adjusted to 0.18.

* - includes Z, ct and H_2O.

TABLE C-5

OLIVINE MONZONITE ANALYSES

Wt.%	N-194	N-451
SiO_2	48.9	46.8
TiO_2	2.74	3.80
Al_2O_3	11.8	15.8
Fe_2O_3	2.3	2.7
FeO	8.50	7.51
MnO	0.16	0.12
MgO	7.44	3.78
CaO	10.3	9.54
Na_2O	3.15	2.82
K_2O	2.31	3.07
P_2O_5	0.42	1.73
H_2O	0.99	1.08
Total	99.0	98.8

p.p.m.		
Ba	1315	1410
Cr	420	< 65
Ni	115	45
Rb	46	58
Sr	1750	2460
Zr	350	430

TABLE C-6

OLIVINE MONZONITE MODES AND NORMS

Volume %	N-194	N-451
Plagioclase	26	41
Alk. Feldspar	18	37
Clinopyroxene	32	7
Olivine	8	6
Hornblende and Biotite	12	-
Ore	4	6
Apatite	tr.	3

Wt.%	N-194	N-451
or	13.9	18.5
ab	20.6	24.4
an	11.4	21.9
ne	3.6	-
di	30.8	12.4
hy	-	1.8
ol	9.8	5.4
mt	3.4	4.0
il	5.3	7.4
ap	1.0	4.2
Rest*	1.2	1.2

* - includes Z, ct and H_2O.

is given in Table C-9.

   N-194 : Olivine monzonite, 4.5 miles west-south-west of

      Chilonga's, on track to railway.

   N-451 : Olivine monzonite, Chilembeni Hill.

Bezi-type Picrites

  Specimens from 2 bodies of fine-grained picrite, the Bezi dyke
and the Gomakwe intrusion, were analysed. Mineralogically and
texturally these picrites are very different from the relatively coarse-
grained picrites described in the main text. They contain little
or no alkali feldspar and have relatively abundant orthopyroxene which
appears to have been in equilibrium at the time of the final crystalli-
sation.

  Analyses of these picrites (Table C-7) show several marked
contrasts to analyses of the alkaline picrites. In particular, the
lower contents of K_2O, P_2O_5, Ba, Rb and Zr and the higher content of
CaO are distinctive. On this evidence it was concluded that these
post-volcanic Bezi-type picrites were not relevant to the main research
project.

   N-6 : Picrite, Gomakwe intrusion

   N-7 : Picrite, Gomakwe intrusion

   N-106 : Picrite, Bezi dyke.

TABLE C-7

BEZI-TYPE PICRITE ANALYSES

Wt.%	N-6	N-7	N-106
SiO_2	49.1	45.5	46.5
TiO_2	2.20	1.15	2.74
Al_2O_3	10.1	7.92	6.92
Fe_2O_3	2.0	2.1	2.2
FeO	9.68	12.00	10.73
MnO	0.19	0.18	0.18
MgO	14.7	21.6	18.6
CaO	10.4	7.09	9.27
Na_2O	1.48	1.21	0.97
K_2O	0.61	0.54	0.46
P_2O_5	0.14	0.16	0.15
H_2O	0.37	0.40	0.42
Total	101.0	99.9	99.1

p.p.m.			
Ba	330	275	240
Cr	880	1200	1390
Ni	575	1030	765
Rb	10	6	7
Sr	801	406	603
Zr	105	150	120

TABLE C-8

BEZI-TYPE PICRITE MODES AND NORMS

Volume %	N-6	N-7	N-106
Clinopyroxene	47	19	55
Plagioclase	36	30	20
Olivine	4	38	19
Orthopyroxene	9	11	tr.
Ore	4	2	6
Apatite	tr.	tr.	-

Wt.%	N-6	N-7	N-106
or	3.6	3.2	2.8
ab	12.4	10.3	8.3
an	19.0	14.6	13.3
di	25.2	15.8	25.7
hy	20.4	12.0	21.8
ol	12.0	38.3	19.0
mt	2.9	3.1	3.2
il	4.1	2.2	5.3
ap	0.3	0.4	0.4
Rest*	0.6	0.7	0.8

* - includes Z, ct and H_2O.

TABLE C-9

CLINOPYROXENE ANALYSIS

Wt.%	N-451 cpx		
SiO_2	50.1		
TiO_2	1.42		
Al_2O_3	2.92		
Fe_2O_3	0.8	Ca	44.6
FeO	8.44	Mg	40.2
MnO	0.17	Fe	15.3
MgO	13.9		
CaO	21.4		
Na_2O	0.45		
K_2O	0.05		
Total	99.7		

p.p.m.	
Cr	< 65
Ni	100
Sr	220
Zn	88
Zr	274

References cited

COX, K.G., JOHNSON, R.L., MONKMAN, L.J., STILLMAN, C.J., VAIL, J.R. and WOOD, D.N., 1965. The Geology of the Nuanetsi igneous province. Phil. Trans. R. Soc., A, 257, 71-218.

MONKMAN, L.J., 1961. The geology of the Maose - Malibangwe river basins, with special reference to the Stormberg rhyolitic volcanicity of Southern Rhodesia. Univ. Leeds Ph.D. thesis (unpubl.)

WESTOLL, N.D.S., 1968. The petrology of kentallenite. Univ. Edinburgh Ph.D. thesis (unpubl.)